RESEARCH ARTICLE

ZooKeys
A peer-reviewed open-access journal
Launched to accelerate biodiversity research

The diversity of the Baikal lineage of *Hydra oligactis* Pallas, 1766: molecular and morphological evidence

Tatiana E. Peretolchina[1], Igor V. Khanaev[1], Ilya V. Enushchenko[1],
Dmitry Y. Sherbakov[1], Lyubov S. Kravtsova[1]

1 *Limnological Institute SB RAS, Ulan-Batorskaya Str., 3, 664033, Irkutsk, Russia*

Corresponding author: *Lyubov S. Kravtsova* (lk@lin.irk.ru)

Citation: Peretolchina TE, Khanaev IV, Enushchenko IV, Sherbakov DY, Kravtsova LS (2020) The diversity of the Baikal lineage of *Hydra oligactis* Pallas, 1766: molecular and morphological evidence. ZooKeys 912: 1–12. https://doi.org/10.3897/zookeys.912.46898

Abstract

In this paper, molecular analyses of Baikal hydras from the 'oligactis group', based on COI and ITS1–5.8S–ITS2, and morphological analysis of their holotrichous isorhizas, were performed. Low genetic diversity and shared haplotypes were found between *Hydra oligactis* Pallas, 1766 and *Hydra baikalensis* Swarczewsky, 1923 specimens, which is evidence of the mixing of these lineages. Genetic distances among all Baikal hydras (0.006) were less than the interspecific distances of other hydras. The size of hydras and proportions of their holotrichous isorhizas varied depending on microhabitat and environmental conditions. Our combined molecular and morphological approach proves that *H. baikalensis* is synonymous with *H. oligactis*

Keywords

taxonomy, holotrichous isorhizas, phylogeny, Baikal hydras

Introduction

Hydra is a member of the ancient phylum Cnidaria, class Hydrozoa, order Hydroida, family Hydridae. Freshwater representatives of *Hydra* inhabit virtually all zoogeographical regions except the Pacific Ocean Islands and Antarctica (Jankowski et al.

2008), living in lenthic and lothic waters such as ponds, lakes, and rivers, and prefering meso-eutrophic conditions. Lake Baikal is one of the deepest (1642 m) oligotrophic freshwater lakes in the world, but the habitat conditions in its bays are close to meso-eutrophic. Climate warming is currently considered as a key factor capable of stimulating the eutrophication of freshwater ecosystems (Cohen et al. 2016; Paerl and Otten 2013). According to the World Meteorological Organization, 2010 was one of the hottest years in the history of meteorological observations. Global climate changes are affecting the ecosystem of Lake Baikal as well. Structural rearrangements of the phytoplankton community in the pelagic zone of the lake (Bondarenko et al. 2019) and changes in the structure of bottom phytocenoses of the coastal zone (Kravtsova et al. 2014) have been detected. Moreover, the propagation of Palearctic species of invertebrates such as *Lymnaea* mollusks (Gastropoda, Lymnaeidae) and the caddis fly *Apatania majuscula* McLachlan, 1872 (Insecta, Trichoptera, Apataniidae) have been observed in Lake Baikal (Rozhkova et al. 2018). In addition, the mass death of the endemic species of Porifera sponges (Denikina et al. 2016; Khanaev et al. 2018) has also been recently observed. On the contrary, representatives of *Hydra* have begun to play a significant role along the open coasts of Lake Baikal. Previously, representatives of hydras were found in small numbers in the coastal zone of Lake Baikal. The first record of the mass development of *Hydra oligactis* Pallas, 1766 was in the 2000s (Stepanyants et al. 2003). Now, *Hydra* is abundant along the open coasts of all three basins of Lake Baikal (Peretolchina et al. 2018a).

Of the 80 *Hydra* species names described in the world only 12 to 15 are valid (Jankowski et al. 2008). The uncertainty of the position of individual hydra taxa results from the complexity of their identification, due to their primitive structure and limited number of reliable diagnostic features. The species diversity of *Hydra* within the morphological boundaries of Lake Baikal is not high; there are four species of *Hydra* reported from the Baikal Region: *H. oligactis* Pallas, 1766 and *Hydra baikalensis* Swarczewsky 1923, as well as the rare *Hydra circumcincta* Schulze, 1914 and *Hydra oxycnida* Schulze, 1914 (Peretolchina et al. 2018b). *Hydra baikalensis*, *H. oligactis* and *H. oxycnida* belong to the '*oligactis* group' (Hemmrich et al. 2007; Martínez et al. 2010; Schwentner and Bosh 2015). However, the morphological descriptions of *H. baikalensis* and *H. oligactis* are very similar in both polyp morphology and holotrichous isorhiza structure (Swarczewsky 1923; Anokhin 2002).

The aim of our study was to verify the identity of *H. oligactis* and *H. baikalensis* using both morphological and molecular data.

Materials and methods

Hydras were collected by scuba divers along southwestern littoral areas (Bolshie Koty – 51°54.04'N, 105°04.08'E, Sobolev Cape – 51°54.20'N, 105°10.18'E, Listvennichniy Bay – 51°51.24'N, 104°51.61'E) of Lake Baikal at depths of 5 to 18 meters, together

with dying Porifera and *Nitella* algae, and by hand from the eastern shores (Posolskiy Sor – 51°57.21'N, 106°05.65'E, Barguzinskiy Bay – 53°16.65'N, 108°44.01'E, Chivyrkuiskiy Bay – 53°38.43'N, 109°04.03'E) of Lake Baikal at a depth of 1 meter, together with the aquatic plants *Potamogeton perfoliatus* Linnaeus, 1753 and *Potamogeton lucens* Linnaeus, 1753. Typically, representatives of *Hydra* were brought live into the laboratory, but some samples were fixed in 80% ethanol in the field.

Morphological studies of the cnidome (stenoteles, desmonemes, holotrichous and atrichous isorhizas) were carried out using an Olympus CX22 microscope with 1000-fold magnification under oil immersion. Morphometric measurements of holotrichous isorhizas were made with the Image-Pro program. *Hydra* specimens were identified according to keys provided by Schuchert (2010, 2018) and Anokhin (2002).

DNA was extracted from a single live or fixed individual as described by Doyle and Dickson (1987). Gene fragments of mitochondrial cytochrome c oxidase subunit I (COI) were amplified using standard Folmer primers for invertebrates (Folmer et al. 1994), and the internal transcribed spacer 1, 5.8S ribosomal DNA and internal transcribed spacer 2 (ITS1–5.8S–ITS2) were amplified using primers published in White et al. (1990).

All PCR reactions were performed in a final volume of 15 µL using 2-Red PCR mix (10 X PCR buffer, 50 mM MgCI2 and 0.02 unit/ µL Taq DNA polymerase). The PCR amplification conditions were as follows: denaturation at 94 °C for 5 min, 30 cycles at 94 °C for 30 sec, 50 °C for 45 sec, 72 °C for 2 min, and a final elongation step at 72 °C for 10 min. Direct sequencing of forward sequences was performed using an ABI 3130 automated sequencer (Research and Production Company "SYNTOL", Moscow, Russia).

The DNA sequences obtained were aligned using default settings in CLUSTAL W (Thompson et al. 1994), implemented in BIOEDIT v.7.2.5 (Hall 1999) and optimized by eye. The resulting COI alignment was translated to check for the absence of stop codons. To confirm species identity, we compared our sequence dataset to published orthologous sequences from other members of *Hydra* and analyzed genetic distances using MEGA v.6 (Tamura et al. 2013).

Phylogenetic analyses were performed using MRBAYES v.3.2 (Ronquist and Huelsenbeck 2003). The datasets for the COI and ITS1–5.8S–ITS2 fragments (Table 1) consisted of unique haplotypes of Baikal hydras produced for this study and specimens (three species from the '*oligactis* group': *Hydra canadensis* Rowan, 1930, *H. oligactis*, *H. oxycnida*, and a representative of *H. circumcincta*, as outgroup) retrieved from GenBank. To estimate the posterior probabilities of the phylogenetic tree, we used 20,000,000 generations of Metropolis-coupled Markov chain Monte Carlo simulation (two runs with four chains). We used the JMODELTEST v.2.1 (Darriba et al. 2012) to determine the substitution models for the two genes separately. The best-fit model for phylogenetic analysis in the case of COI was HKY, and in the case of ITS1–5.8S–ITS2 it was GTR+I+G. We constructed a majority-rule (50%) consensus tree following 25% burn-in of all sampled trees.

Table 1. List of used specimens with accession numbers provided.

Species name	GeneBank accession numbers	
	COI (reference)	ITS1–5.8S–ITS2 (reference)
H. oligactis	GU722865–GU722875 (Martínez et al. 2010); AB565122, AB565130 (Kawaida et al. 2010); KP895118 (Schwentner and Bosch 2015); MF000491, MF544747, MF135286, MF135293, MF135295, MF135298, MF135299, MF135302, MF135304, MF135305, MF13531 (Schuchert, unpublished)	GU722678–GU722688 (Martínez et al. 2010)
H. robusta	EF059939 (Hemmrich et al. 2007); KP895119 (Schwentner and Bosch 2015); HQ417108 (Wang et al. 2012); AB565143, AB565125, AB565094, AB565093, AB565092 (Kawaida et al. 2010)	
H. oxycnida	GU722876, GU722877 (Martínez et al. 2010); KP895120 (Schwentner and Bosch 2015)	GU722689 (Martínez et al. 2010)
H. canadensis	GU722879–GU722884 (Martínez et al. 2010)	GU722697 (Martínez et al. 2010)
Baikal *H. oligactis*	MH428229–MH428232, MH428234–MH428235, MH428269–MH428270, MH428273, MH428275– MH428276, MH428278– MH428279, MH428281, MH428288, MH428292, MH428294, MH428304, MH428318, MH428338, MH428341, MH428343, MH428347, MH428349–MH428350, MH428354, MH428358–MH428360, MH428363 (Our data)	MH454379, MH454381, MH454383–MH454386, MH454390, MH454393, MH454398, MH454403, MH454407–MH454408, MH454412, MH454419, MH454427–MH454433, MH454437, MH454439, MH454441, MH454443–MH454444, MH454446, MH454450–MH454452, MH454455 (Our data)

Results

Molecular analysis

In total, we produced 30 COI sequences (603 bp long) and 30 ITS1–5.8S–ITS2 sequences (up to 710 bp long). Inspection of the Baikal hydra sequences revealed nine unique haplotypes for the COI gene fragment (shared haplotypes were found in all sampling localities) and three unique haplotypes for the ITS1–5.8S–ITS2 sequences.

The consensus tree topology based on COI (27 unique haplotypes) indicated that Baikal *H. oligactis* and *H. baikalensis* did not form separate clades, but instead were clustered together with representatives of *Hydra robusta* Itô, 1947 from Japan and China and *H. oligactis* from Japan and Europe, forming a neighboring clade with the majority of hydras from Western Europe and North America (Fig. 1A). The consensus phylogenetic tree based on ITS1–5.8S–ITS2 (14 unique haplotypes) showed that differentiation between hydras from Europe + North America and Asia was not evident (Fig. 1B).

Mean pairwise *p*-distances based on COI sequences of *Hydra* species are given in Table 2. Intraspecific genetic distances of *Hydra* varied from 0.010 to 0.040, whereas interspecific distances were about 0.100. The mean genetic distance between Baikal
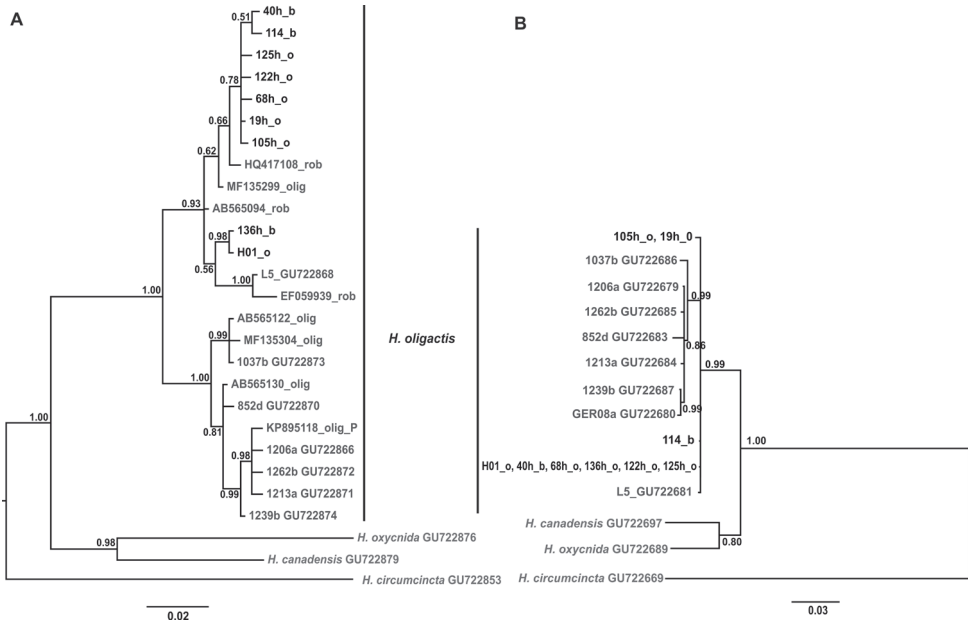
Figure 1. Bayesian phylogenetic tree based on COI (**A**) and ITS1–5.8S–ITS2 unique haplotype sequences. Posterior probabilities (>0.5) are given at nodes. Tip names with '_o' belong to *H. oligactis* specimens and those with '_b' belong to *H. baikalensis* specimens. Tip names marked in grey color indicate nucleotide sequences from GenBank.

Table 2. Pairwise p-distances between COI sequences of different species of the genus Hydra. Within group mean pairwise distances are in bold.

	1	2	3	4	5
1 – *H. oligactis* (Baikal)	**0.006**				
2 – *H. oligactis*	0.030	**0.018**			
3 – *H. robusta*	0.017	0.035	**0.017**		
4 – *H. oxycnida*	0.103	0.101	0.103	**0.040**	
5 – *H. canadensis*	0.101	0.103	0.105	0.105	**0.010**

hydras and *H. oligactis* from Western Europe and North America was 0.030 (min 0.009, max 0.035). The mean *p*-distance for lineages of *H. oligactis*, Baikal hydras and *H. robusta* was 0.024, which corresponds to the intraspecific variability in *Hydra* species (Table 2).

Morphological analysis

In our collections, hydras with a length/width ratio (L:W) of holotrichous isorizas > 2 were identified as *H. oligactis* and hydras with L:W ≤ 2 were identified as *H. baikalensis*, following Schuchert (2010, 2018) and Anokhin (2002). However, morphological analysis of polyps did not reveal specific features between Baikal hydras and *H. oligac-*

tis, and the main diagnostic trait (L:W of holotrichous isorizas) varied from 1.85 to 2.46 (Table 3), depending on the environment, in different sites of Lake Baikal. Hydra specimens with a L:W of holotrichous isorizas ≤ 2.0 were collected at a depth of 15–18 m, where the water temperature was low (6–7 °C, near the bottom). Hydra specimens with holotrichous isorizas ≥ 2.0 were collected in shallow water from 1–5 m, where the water temperature reaches 16–24 °C in summer (Kozhov 1962).

Discussion

According to Schwentner and Bosch (2015), the 'oligactis group' includes *H. oxycnida*, *H. canadensis*, *H. oligactis* and *H. robusta* (possibly synonymous to *H. oligactis*). On the one hand, low genetic distance between the latter two species could be a consequence of shared ancestral polymorphism. On the other hand, the results may be due to population genetic variability of *H. oligactis* (= *H. robusta*). It is known that genetic polymorphism of species with wide geographic distributions is higher than that of species with restricted ranges, where genetic diversity decreases from the center of distribution to range boundaries (Brown 1984; Schuchert 2014). We suppose that *H. oligactis* is a widely distributed species with genetic (population) structure (Figure 1A, B). The "Baikal" clade includes not only regional haplotypes but also haplotypes of *H. oligactis* from Europe, China and Japan (Fig. 1A). We believe that this level of genetic diversity corresponds to population differences, not to interspecific ones. Thus, according to our molecular phylogenetic study, all the haplotypes belong to the same species, *H. oligactis* (*H. oligactis* = *H. robusta* = *H. baikalensis*).

In Lake Baikal, the type locality of the endemic *H. baikalensis* is Chivyrkuyskiy Bay (Swarczewskiy 1923). This species has also been reported from Listvennichniy Bay, the littoral zone near Bolshoy Ushkaniy Island, Bolshie Koty Bay, and in small lakes along the Bolshie Koty River. *Hydra oligactis* occurs in the same areas and was also reported from Dagarskaya Bay, Mukhor Bay (Stepanyants et al. 2006), and Barguzinskiy Bay (Peretolchina et al. 2018a).

Previous researchers (Schulze 1927; Anokhin 2002; Jankowski and Anokhin 2019) distinguished *H. oligactis* from *H. baikalensis* mostly based on differences in the proportions of their holotrichous isorhizas. However, the differences in the length/width ratio of holotrichous isorhizas in *H. baikalensis* and *H. oligactis* are within the range of intraspecific variability (Table 3). Therefore, this morphological feature cannot be used as a diagnostic criterion for *H. baikalensis*. It is known that proportions and relative sizes of the nematocysts vary considerably depending on the stage of development of the nematocysts (Weill 1934) and on environmental factors (Östman 1987; Itô 1951). In our case, the size of the hydras and the proportions of the holotrichous isorhizas varied depending on microhabitat and environmental conditions. That is, specimens sampled in the open littoral of Lake Baikal were larger and their holotrichous isorhizas were shorter and slightly thicker (8–9 µm, length/width ratio ≤ 2), whereas hydras from shallow depths were smaller but their holotrichous isorhizas were longer and

Table 3. Holotrichous isorhizas measuring.

Site	Length, µm	Width, µm	L:W	n
Chivirkuiskiy Bay	9.46±0.17	3.90±0.07	2.44±0.06	17
Barguzinskiy Bay	9.35±0.15	3.81±0.06	2.46±0.04	17
Lystvenichniy	8.26±0.18	4.04±0.08	2.06±0.06	20
Bolshie Koty	8.42±0.10	4.24±0.09	2.02±0.04	42
Sobolev	7.74±0.06	4.19±0.07	1.85±0.03	11
Posolskiy Sor	10.04±0.19	4.24±0.08	2.38±0.05	27

thinner (9–10 µm, length/width ratio > 2) (Table 3). In addition, the packing of sting-ing threads in the holotrichous isorhizas of both Baikal *H. baikalensis* and *H. oligactis* was the same.

Moreover, the species *H. baikalensis* and *H. oligactis* are similar in the number and morphology of chromosomes, in the symmetrical structure of the karyotype, and in C-heterochromatin localization. They only differ in the length ratio of the 1st and 15th pairs of chromosomes (Anokhin 2002). We suppose that the length ratio of chromo-somes is a distinctive feature but may be not sufficient to distinguish *H. baikalensis* as an independent species.

In addition, molecular phylogenetic analyses did not reveal any differences between *H. baikalensis* and *H. oligactis* specimens. Genetic distances among all Baikal hydras (0.006) were less than the interspecific distances of other hydra (Table 2). Moreover, we found shared haplotypes among representatives of Baikal *H. baikalensis* and *H. oligactis*. The sympatric occurrence of *H. oligactis* and *H. baikalensis* and the low level of their genetic distances (revealed using both mitochondrial and nuclear markers) do not allow us to consider these two groups as separate species.

Thus, the morphological characteristics, patterns of haplotype diversity, and the results of phylogenetic analyses lead us to consider *H. baikalensis* as a synonym of *H. oligactis*.

Systematics

Phylum Cnidaria Verrill, 1865
Subphylum Medusozoa Peterson, 1979
Class Hydrozoa Owen, 1843
Subclass Hydroidolina Collins 2000
Order Anthoathecata Cornelius, 1992
Family Hydridae Dana, 1846
    Hydra oligactis Pallas, 1766
    Hydra fusca Linnaeus, 1767
    Hydra roeselii Haacke, 1879
    Hydra rhaetica Asper, 1879
    Hydra rhistica Asper, 1880

? *Hydra monoecia* Downing, 1900
? *Hydra pallida* Beardsley, 1904
? *Hydra corala* Elrod & Ricker, 1902
? *Hydra dioecia* Downing, 1905
Pelmatohydra oligactis (Pallas, 1776)
Hydra baikalensis Swarczewsky, 1923

Diagnosis. The Baikal *Hydra* is large, typically with 5–7 long tentacles, and a more or less distinct peduncle. The cnidome includes four types of nematocysts: stenoteles, holotrichous isorhizas, atrichous isorhizas and desmonemes (Figs. 2, 3). Holotrichous isorhizas are elongated, with a length/width ratio of about 2, and with thread-forming longitudinal, irregular coils inside the capsule. Other types of nematocysts are of a size and shape typical of other hydras. Holotrichous isorhiza measurements are summarized in Table 3, with photographs in Fig. 2.

Distribution. Baikal region: Port Baikal, Ulanovo, Listvennichny Bay, Bolshie Koty, Varnachka, Sobolev Cape, Turali Cape, Elokhin Cape, Mukhor Bay, Posolsky Sor Dagarskaya Bay, littoral zone near Bolshoy Ushkaniy Island, small lakes along the Bolshie Koty River, and Lake Kuzmikhinskoye (Artificial reservoir near the Angara River). This species is also widespread and common on the entire European continent, including the British Isles and Iceland as well as Russia and North America (Hyman 1930; Holstein 1995; Stepanyants et al. 2006).
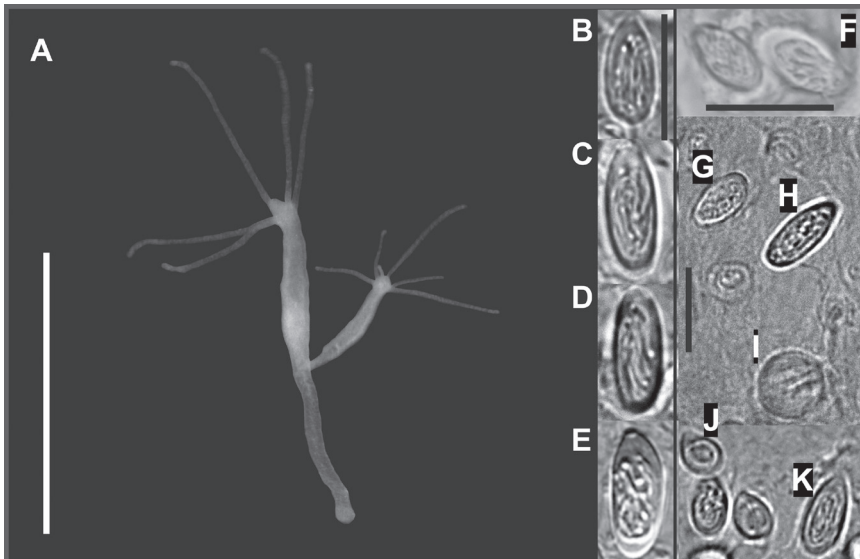

Figure 2. A *H. oligactis*, living polyp from Lake Baikal. **B–F** morphological variability of holotrichous isorhizas **B**, **F** *H. baikalensis*; **C**, **D**, **E** *H. oligactis* (**B** Bolshie Koty **C** Posolskiy Sor **D** Chivyrkuiskiy Bay **F** Sobolev) **E** Photo adapted from Schuchert (2010). **J** desmonemes **F**, **G** atrichous isorhizas **H**, **K** holotrichous isorhizas **I** stenoteles. Scale bars: 5 mm (**A**), 10 μm (**B–K**).
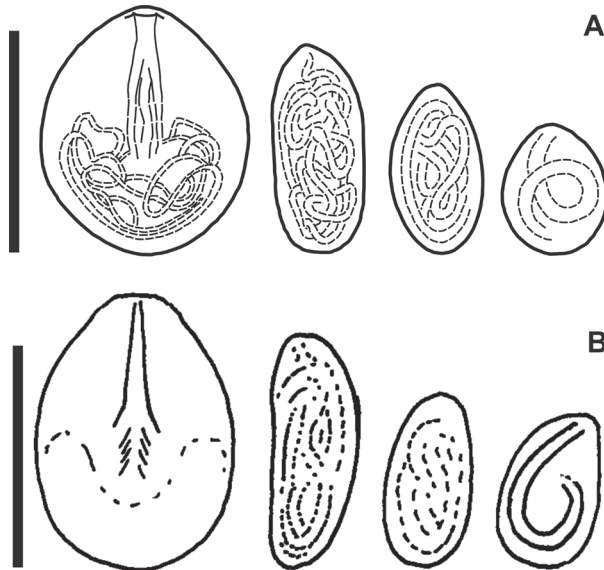
Figure 3. A cnidome of Baikal *H. oligactis* **B** cnidome of *H. oligactis*, figure adapted from Schuchert (2010). From left to right: stenoteles, holotrichous isorhizas, atrichous isorhizas and desmonemes. Scale bars: 10 μm.

Acknowledgements

References

Anokhin B (2002) Redescription of the endemic baikalian species *Pelmatohydra baikalensis* (Cnidaria: Hydrozoa, Hidridae) and assessment of the *Hydra* fauna of Lake Baikal. Annales Zoologici 52(4): 195–200.

Bondarenko NA, Ozersky T, Obolkina LA, Tikhonova IV, Sorokovikova EG, Sakirko MV, Potapov SA, Blinov VV, Zhdanov AA, Belykh OI (2019) Recent changes in the spring microplankton of Lake Baikal, Russia. Limnologica 75: 19–29. https://doi.org/10.1016/j.limno.2019.01.002

Brown JH (1984) On the relationship between abundance and distribution of species. The American Naturalist 124(2): 255–279. https://doi.org/10.1086/284267

Cohen AS, Gergurich EL, Kraemer BM, McGlue MM, McIntyre PB, Russell JM, Simmons JD, Swarzenski PW (2016) Climate warming reduces fish production and benthic habitat

in Lake Tanganyika, one of the most biodiverse freshwater ecosystems. PNAS 113(34): 9563–9568. https://doi.org/10.1073/pnas.1603237113

Darriba D, Taboada GL, Doallo R, Posada D (2012) jModelTest 2: more models, new heuristics and parallel computing. Nature Methods 9(8): 772. https://doi.org/10.1038/nmeth.2109

Denikina NN, Dzyuba EV, Belkova NL, Khanaev IV, Pheranchuk SI, Makarov MM, Granin NG, Belikov SI (2016) The first case of disease of the sponge *Lubomirskia baicalensis*: a study of the microbiome. Proceedings of the Russian Academy of Science, Biological Series 3: 315–322. [in Russian] https://doi.org/10.1134/S106235901603002X

Doyle JJ, Dickson E (1987) Preservation of plant samples for DNA restriction endonuclease analysis. Taxon 36: 715–722. https://doi.org/10.2307/1221122

Folmer O, Black M, Hoeh W, Lutz R, Vrijenhoek R (1994) DNA Primers for Amplification of Mitochondrial Cytochrome c Oxidase Subunit I From Diverse Metazoan Invertebrates. Molecular Marine Biology and Biotechnology 3: 294–299.

Hall TA (1999) "BioEdit: a user-friendly biological sequence alignment editor and analysis program for Windows 95/98/NT". Nucleic Acids Symposium Series 41: 95–98.

Hemmrich G, Anokhin B, Zacharias H, Bosch TCG (2007) Molecular phylogenetics in *Hydra*, a classical model in evolutionary developmental biology. Molecular Phylogenetics and Evolution 44: 281–290. https://doi.org/10.1016/j.ympev.2006.10.031

Itô (1951) Local and seasonal variations of the nematocysts in *Pelmatohydra robusta* (Studies on the nematocysts of the fresh-water polyp. No. III). Memoires Ehime University. Section 2 1: 69–80.

Jankowski T, Anokhin B (2019) Phylum Cnidaria. In: Christopher DR, James H, Thorp HJ (Eds) Thorp and Covich's Freshwater Invertebrates. Academic Press, New York, 93–111. https://doi.org/10.1016/B978-0-12-385024-9.00004-6

Jankowski T, Collins AG, Campbell RD (2008) Global diversity of inland water cnidarians. Hydrobiology 595: 35–40. https://doi.org/10.1007/s10750-007-9001-9

Khanaev IV, Kravtsova LS, Maikova OO, Bukshuk NA, Sakirko MV, Kulakova NV, Butina TV, Nebesnykh IA, Belikov SI (2018) Current state of the sponge fauna (Porifera: Lubomirskiidae) of Lake Baikal: Sponge disease and the problem of conservation of diversity. Journal of Great Lakes Research 44: 77–85. https://doi.org/10.1016/j.jglr.2017.10.004

Kozhov MM (1962) Biology of Lake Baikal. Academy of Science Publishing House, Moscow, 315 pp. [in Russian]

Kravtsova LS, Izhboldina LA, Khanaev IV, Pomazkina GV, Rodionova EV, Domysheva VM, Sakirko MV, Tomberg IV, Kostornova TYa, Kravchenko OS, Kupchinsky AB (2014) Nearshore benthic blooms of filamentous green algae in Lake Baikal. Journal of Great Lakes Research 40: 441–448. https://doi.org/10.1016/j.jglr.2014.02.019

Martínez DE, Iñigues AR, Percell KM, Willner LB, Signorovitch J, Campbell RD (2010) Phylogeny and biogeography of *Hydra* (Cnidaria: Hydridae) using mitochondrial and nuclear DNA sequences. Molecular Phylogenetics and Evolution 57: 403–410. https://doi.org/10.1016/j.ympev.2010.06.016

Östman C (1987) New techniques and old problems in hydrozoan systematics. In: Bouillon J, Boero F, Cigogna FP, Cornelius FS (Eds) Modern Trends in the Systematics, Ecology and Evolution of Hydroids and Hydromedusae. Clarendon Press, Oxford, 67–82.

Paerl HW, Otten TG (2013) Blooms bite the hand that feeds them. Science 342: 433–434. https://doi.org/10.1126/science.1245276

Pallas PS (1766) Elenchus zoophytorum sistens generum adumbrations generaliores et specierum cognitarium succinctas descriptiones cum selectis auctorum synonymis. Hagae, Comitum XIV, Fransiscum Varrentrap, 451 pp. https://doi.org/10.5962/bhl.title.6595

Palumbi SR (1996) Nucleic acids II: the polymerase chain reaction. In: Hillis DM, Moritz C, Mable BK (Eds) Molecular Systematics (2nd edn). Sinauer Associates Inc., Sunderland, 205–247.

Peretolchina TE, Khanaev IV, Kravtsova LS (2018a) The diversity of hydras (Cnidaria: Hydridae) in the Baikal region. Limnology and Freshwater Biology 2: 107–112. https://doi.org/10.31951/2658-3518-2018-A-2-107

Peretolchina TE, Khanaev IV, Kravtsova LS (2018b) Rare species *Hydra oxycnida* Schulze, 1914 (Cnidaria: Hydridae) in Lake Baikal. International Journal of Applied and Basic Research 11: 103–107. [in Russian] https://doi.org/10.17513/mjpfi.12458

Ronquist F, Huelsenbeck JP (2003) MrBayes 3: Bayesian phylogenetic inference under mixed models. Bioinformatics 19(12): 1572–1574. https://doi.org/10.1093/bioinformatics/btg180

Rozhkova NA, Bondarenko NA, Sitnikova TYa (2018) Food Spectrum of Molluscs and Caddisflies under Conditions of *Spirogyra* (Zygnematophyceae, Charophyta) Bloom in Lake Baikal. The bulletin of Irkutsk State University, Series "Biology. Ecology" 25: 91–105. https://doi.org/10.26516/2073-3372.2018.25.91

Schuchert P (2010) The European athecate hydroids and their medusae (Hydrozoa, Cnidaria): Capitata part 2. Revue suisse de Zoologie 3: 440–449. http://www.marinespecies.org/hydrozoa/aphia.php?p=sourcedetails&id=145433

Schuchert P (2014) High genetic diversity in the hydroid *Plumularia setacea*: a multitude of cryptic species or extensive population subdivision? Molecular Phylogenetics and Evolution 76: 1–9. https://doi.org/10.1016/j.ympev.2014.02.020

Schulze P (1927) Zur Kenntnis und geographischen Verbreitung der Süsswasserpolypen. Zoologischer Anzeiger 74(5/6): 129–141.

Schwentner M, Bosch TCG (2015) Revisiting the age, evolutionary history and species level diversity of the genus *Hydra* (Cnidaria: Hydridae). Molecular Phylogenetics and Evolution 91: 41–55. https://doi.org/10.1016/j.ympev.2015.05.013

Stepanyants SD, Anokhin BA, Kuznetsova VG (2006) Cnidarian fauna of relict Lakes Baikal, Biwa and Khubsugul. Hidrobiologia 568(1): 225–232. https://doi.org/10.1007/s10750-006-0310-1

Stepanyants SD, Kuznetsova VG, Anokhin BA (2003) *Hydra*: from Abraam Tramble untill our days. Association of scientific publications KMK, Moscow-Saint-Petersburg, 102 pp. [in Russian]

Swarczewsky B (1923) Sketches about Hydraria. Proceedings of Irkutsk State University 4: 9–102. [in Russian]

Tamura K, Stecher G, Peterson D, Filipski A, Kumar S (2013) MEGA6: Molecular evolutionary genetics analysis, Version 6.0. Molecular Biology and Evolution 30: 2725–2729. https://doi.org/10.1093/molbev/mst197

Thompson JD, Higgins DG, Gibson TJ (1994) ClustalW: improving the sensitivity of progressive multiple sequence alignment through sequence weighting, position-specific gap penalties and weight matrix choice. Nucleic Acids Research 22: 4673–4680. https://doi.org/10.1093/nar/22.22.4673

Weill R (1934) Contribution à l'étude des cnidaires et de leurs nématocystes. I, II. Trav. Stn. zool. Wimereux, 10 and 11: 1–701.

White TJ, Bruns T, Lee S, Taylor JW (1990) Amplification and direct sequencing of fungal ribosomal RNA genes for phylogenetics. In: Innis MA, Gelfand DH, Sninsky JJ, White TJ (Eds) PCR Protocols: A Guide to Methods and Applications. Academic Press, New York, 315–322. https://doi.org/10.1016/B978-0-12-372180-8.50042-1

RESEARCH ARTICLE

A new genus of the tribe Sarimini (Fulgoromorpha, Issidae) from the Guangxi Province of China

Menglin Wang[1], Thierry Bourgoin[2]

1 *Key Laboratory of Southwest China Wildlife Resources Conservation of the Ministry of Education, China West Normal University, Nanchong, Sichuan Province, 637009, China* **2** *Institut de Systématique, Évolution, Biodiversité, ISYEB-UMR 7205 MNHN-CNRS-Sorbonne Université-EPHE, Muséum national d'Histoire naturelle, CP 50, 57 rue Cuvier, F-75005 Paris, France*

Corresponding author: *Menglin Wang* (wangmenglin123@126.com)

Abstract

A new genus with a new species *Eusarimissus hezhouensis* **gen. nov. et sp. nov.** from Guangxi Province of China are described in the tribe Sarimini of the family Issidae. Molecular sequences of 18S, 28S and COXI genes are provided for the new taxon. Phylogenetic analysis places this taxon sister to a previously sequenced but not yet described Sarimini genus 'Eusarima sp. 4'. Taxonomic notes are provided for the genus *Eusarima* Yang, 1994. The species *Eusarima* (*Nepalius*) *iranica* Gnezdilov & Mozaffarian, 2011 is transferred to the genus *Sarima* Melichar 1903.

Keywords

Fulgoroidea, molecular, morphology, new combination, new taxa, oriental, planthopper

Introduction

Without obvious morphological apomorphy, the tribe Sarimini Wang, Zhang & Bourgoin, 2016 was only recently revealed after a molecular phylogenetic analysis of the planthopper family Issidae. It represents an important tribe which is sister to two other emblematic sister tribes in Hemisphaeriinae: the Parahiraciini Cheng & Yang, 1991

and the Hemisphaeriini Melichar, 1906 within the Issidae (Wang et al. 2016, Zhao et al. 2019). Currently, Sarimini includes 26 genera (Bourgoin 2020), plus several other genera already identified but not yet described which were provisionally labelled 'Gen. nov.', '*Eusarima* sp. 1', 'sp. 2', and 'sp. 4' in Wang et al. (2016)'s analysis. The other taxa labelled with 'Gen. nov. *apud Eusarima*' and '*Eusarima* sp. 3' were already described respectively as *Longieusarima* Wang, Zhang & Bourgoin, 2017 (Wang et al. 2017) and *Duplexissus* Wang, Zhang & Bourgoin, 2019 (Wang et al. 2019).

In this paper, we describe an additional new genus, representing a new species from Guangxi Province of China. We also provide taxonomic notes about the genus *Eusarima* Yang, 1994 from which one species, *Eusarima* (*Nepalius*) *iranica* Gnezdilov & Mozaffarian, 2011, is transferred to the genus *Sarima* Melichar, 1903. Finally, the number and the diversity of the taxa, which progressively joined Sarimini since its description, allow now a better understanding of its morphological characteristics.

Materials and methods

The type specimens are deposited in China West Normal University, Nanchong, Sichuan Province, China. The specimens were collected by net capture during daytime. The genitalia were separated from the insect body using micro-scissors under a stereomicroscope Leica M205C, then transferred and boiled in a 5ml beaker with 10% NaOH solution for a few minutes until muscles were completely dissolved leaving only tegumentary structures. After rinsing in distilled water several times to clean the residual NaOH solution, genitalia were subsequently transferred to glycerine for final dissection and observation, and then stored under the specimen in a genitalia vial for final conservation. Photographs for external morphology and genitalia characters were taken using a Leica DFC camera attached to a Leica M205FA stereomicroscope and further refined with LAS X software. Morphological terminologies for male genitalia follow Bourgoin (1987), for female genitalia Bourgoin (1993), and for wing venation Bourgoin et al. (2015).

Total genomic DNA was extracted from the fore and middle legs of the holotype specimen using a Sangon Ezup column animal genomic DNA purification kit. The DNA of the genes (18S rRNA, 28S rRNA, COXI, Cytb) was amplified using the same primers and amplification procedures as in Wang et al. (2016). DNA sequencing was conducted by the Sangon Company (Shanghai, China). Contigs assembly was made using the software Seqman from package DNAstar v5.01 (www.dnastar.com). All sequences were registered in GenBank with accession numbers mentioned below.

MEGA v7.0 (Kumar et al. 2016) was used for performing alignments for a subset of taxa already analysed in Wang et al. (2016) but restricted to Sarimini plus the new genus. Phylogenetic analysis was performed using the software IQTREE v1.4.1 (Nguyen et al. 2015) with 10,000 bootstraps (Minh et al. 2013) and substitution models automatically selected with partitions unlinked. According to the results of Wang et al. (2016), genus *Darwallia* Gnezdilov, 2010 was chosen as an out-group for the analysis. FIGTREE v1.1.2 (Rambaut 2016) was used to visualize the tree.

Taxonomy

Hemisphaeriinae Melichar, 1906 (sec. Wang et al. 2016)
Sarimini Wang, Zhang & Bourgoin, 2016

Eusarimissus gen. nov.
http://zoobank.org/16B6975F-3B6D-4EB7-BF14-3C7FDA91E48C

Type species. *Eusarimissus hezhouensis* sp. nov., here designated.

Diagnosis. This new taxon appears similar to *Eusarima* but differs by: 1) Vertex much longer, around 1.3 times wider than long in midline (Fig. 1), but around 1.6 times wider in *Eusarima* (Chan and Yang 1994, fig. 45A); 2) MP vein forking late in apical 1/3, obviously after CuA (Fig. 4), while MP and CuA fork near middle, almost at the same level in *Eusarima* (Chan and Yang 1994, fig. 45C); 3) A2 lobe on hind wing as wide as Pcu-A1 lobe (Fig. 5), while larger in *Eusarima* (Chan and Yang 1994, fig. 45D); 4) dorsal lobe of periandrium without the posterolateral process (Fig. 9) in *Eusarima* (Chan and Yang 1994, fig. 45H).

From *Longieusarima*, *Eusarimissus* is easily separated by its shorter and wider vertex, the longer sublateral carinae of frons widely surpassing the level of the ventral margin of the antenna, and the general schema of the tegmina with a longer ScP+RA vein and a late-forking MP vein, well after the forking of CuA. Male genitalia also easily differentiated these two genera by the long subapical aedeagus processes in *Longieusarima*, shorter and in the apical 3/4 in *Eusarimissus*.

Description. Head with compound eyes a little wider than pronotum and mesonotum (Fig. 1). Vertex hexagonal, a little wider than long in midline, median carina weakly present or absent on the disc; margins elevated, anterior margin obviously angularly convex at middle, lateral margins nearly straight and parallel, posterior margin angularly concave (Fig. 1). Frons rounded, wider than long, margins elevated; apical margin nearly straight, lateral margins expanding outward below antennae with lateral angles rounded (Fig. 3); median carina apparently elevated from apex extending to frontoclypeal suture (Fig. 3); sublateral carinae obviously elevated from the apex near to the base, but not reaching to the frontoclypeal suture, with lateral ventral angles rounded (Fig. 3). Frons smooth, without any tubercles (Fig. 3). Frontoclypeal suture strongly angularly convex (Fig. 3). Antenna with scape extremely short, pedicel rounded (Fig. 3). Clypeus smooth, without median carina (Fig. 3). Rostrum reaching to midcoxae, apical segment almost the same length with subapical one. Gena in lateral view oblique (Fig. 2). Pronotum triangular, almost same length with vertex in midline; margins elevated, anterior margin angularly protruded, posterior margin straight; median carina very weakly present or absent, with several inconspicuous tubercles on the disc (Fig. 1). Mesonotum triangular, a little wider than pronotum in midline, tricarinated on the disc, anterior margin straight (Fig. 1). Forewings obviously longer than broad, longitudinal veins distinctly elevated (Figs 1, 2, 4); costal area narrow, ScP+R forked at the base, ScP+RA and RP veins parallel, both extremely long,
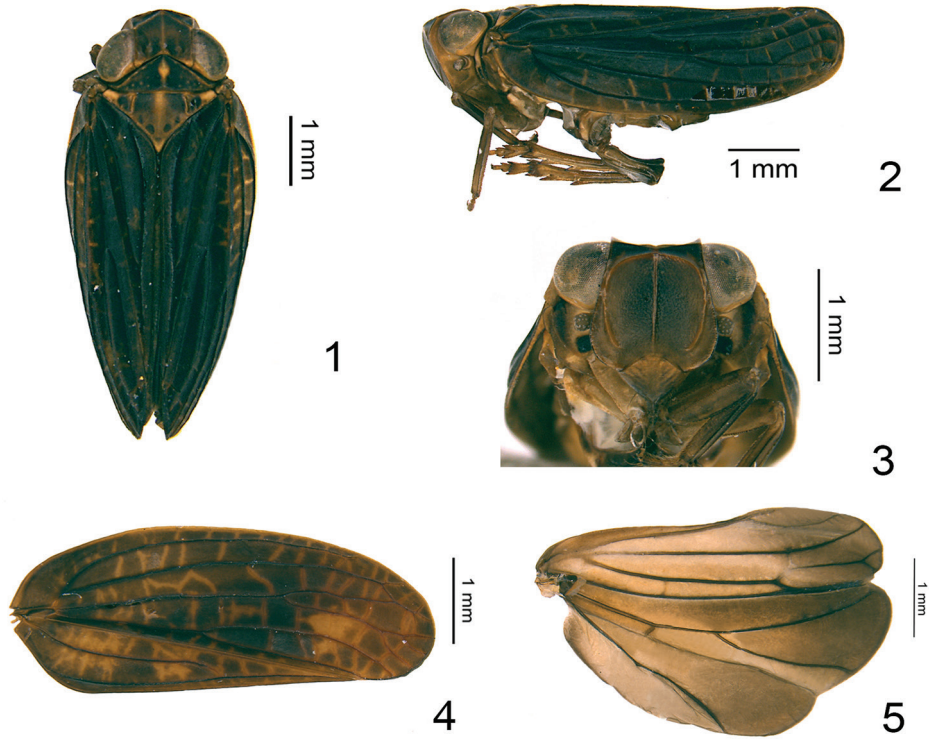
Figures 1–5. *Eusarimissus hezhouensis* sp. nov. **1** adult (holotype), dorsal view **2** adult (holotype), lateral view **3** adult (holotype), frontal view **4** forewing (paratype) **5** hind wing (paratype).

respectively extending to the apical 4/5 of costal margin and the apical margin (Figs 2, 4); MP straight, bifurcated into MP_{1+2} and MP_{3+4} at apical 1/3, forking again or not apically (Figs 2, 4); CuA bifurcated well before MP, slightly before Pcu and A1's junction (Figs 1, 2, 4); clavus closed, CuP long, extending to the same level of ScP+RA, Pcu and A1 fused slightly beyond the middle of clavus (Fig. 4). Hind wings developed, of Sarimini type with 3-lobes (Fig. 5); Pcu-A1 lobe as wide as ScP-R-MP-Cu lobe, Pcu and A1 anastomosing at a medium distance, Pcu, $A1_1$ and $A1_2$ single (Fig. 5); A2 lobe developed, as wide as Pcu-A1 lobe, margin regularly slightly convex, A2 vein simple, non-branched (Fig. 5). Metatibia with two lateral spines on apical half (Fig. 2).

Male genitalia. Anal tube in lateral view long and narrow, reaching to the posterior margin of gonostyli, basal part expanded, ventral margin nearly straight (Fig. 6). Pygofer in lateral view rectangular, obviously longer than broad, dorsal margin nearly straight, posterior margin slightly convex and parallel to anterior margin (Fig. 6). Gonostyli equilateral triangular in side view (Figs 6, 8). Capitulum of gonostylus short and spinous, with an auriform process near base (Figs 6, 8). Periandrium symmetrical (Figs 9, 10), with a dorsal lobe (dl), biforked lateral lobes (ll) and a ventral lobe (vl); dorsal and lateral lobes almost the same length, ventral lobe much shorter. Aedeagus with a pair of processes derived from the apical 3/4 (Figs 9, 10).
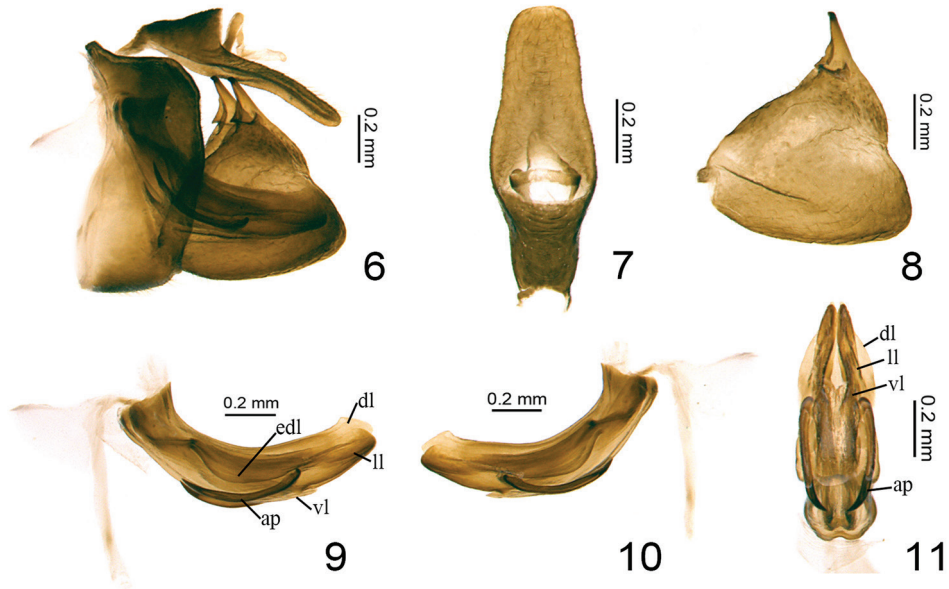
Figures 6–11. *Eusarimissus hezhouensis* sp. nov., holotype. **6** male genitalia, lateral view **7** male anal tube, dorsal view **8** gonostylus, lateral view **9** phallic complex, right lateral view **10** phallic complex, left lateral view **11** phallic complex, ventral view. Abbreviations: dl: dorsal lobe of periandrium; ll: lateral lobe of periandrium; vl: ventral lobe of periandrium; edl: expansion on dorsal lobe of periandrium; ap: aedeagus processes.

Female genitalia. Gonoplacs in dorsal view fused at middle in basal 1/3 (Fig. 13); in lateral view long rectangular, longer than wide (Fig. 14). Gonapophysis IX in lateral view broad, dorsal margin sinuate, basal 1/3 with a needle-like process (Fig. 15); ventral margin concave (Fig. 15). Gonapophysis IX in dorsal view nearly triangular, the basal half broader than the apical half (Fig. 16). Gonospiculum bridge in lateral view rectangular with a short needle-like process at base (Fig. 15). Anterior connective lamina of gonapophysis VIII subtriangular, with teeth at apex and teeth on the outer lateral margin, inner lateral margin without teeth (Fig. 18). Endogonocoxal process membranous (Fig. 18). Gonocoxa VIII long rectangular, posterior and anterior margins parallel and concave (Fig. 18).

Etymology. This name is an arbitrary association between the genera names "*Eusarima*" and "*Issus*" referring to the close relationship of this genus to *Eusarima* in the Issidae tribe Sarimini. The gender is masculine.

Distribution. China (Guangxi Province).

Eusarimissus hezhouensis sp. nov.
http://zoobank.org/41895156-B94F-48B1-A7FC-E82FEFD598F1

Diagnosis. This new species looks similar to the species *Eusarima* (*Eusarima*) *triphylla* (Che, Zhang & Wang, 2012) known also from Guangxi Province, but it differs by: 1) the early bifurcation of CuA before MP (Fig. 4), while almost at the same level in *E.* (*E.*) *triphylla*

(Che et al. 2012, figs 3, 6); 2) the male anal tube widest slightly below middle in dorsal view (Fig. 7), while widest in apical 1/2 in the latter species (Che et al. 2012, fig. 9); 3) the female anal tube shorter, 1.6 times longer in the length at middle than widest part in dorsal view (Fig. 12), while 2.4 times in *E.* (*E.*) *triphylla* (Che et al. 2012, fig. 13); 4) the apical margin of female sternite VII shallowly concave (Fig. 17), while roundly convex medially in *E.* (*E.*) *triphylla* (Che et al. 2012, fig. 14); 5) the single Pcu of the hind wing, while triforked in *E.* (*E.*) *triphylla* (Che et al. 2012, fig. 7).

Type materials. *Holotype*: ♂, China: Guangxi Province, Hezhou, Qichong Nature Reserve, 24°13'6"N, 110°48'34"E, 180 m, 7.viii.2018, coll. Feilong Yang & Kun Zhao. *Paratypes*: 2♂♂, 1♀, same data as holotype.

Description. *Length:* male (including forewings) (N = 3): 6.1–6.3 mm; female (including forewings) (N = 1): 6.4 mm.

Coloration. Vertex almost dark brown, the midline slightly yellow; anterior margin yellow; posterior margin yellow with some black (Fig. 1). Compound eyes silvery white (Figs 1–3). Frons brown, anterior area from apical margin to the middle level of compound eyes darker; median and sublateral carinae tawny (Fig. 3). Antennae brown (Fig. 3). Clypeus dark brown with some yellow (Fig. 3). Rostrum tawny. Gena tawny (Fig. 2). Pronotum dark brown, with yellow midline, some specimens with a yellow ovate marking at middle, the disc scattered with 6–8 yellow tiny nodules on each side; anterior margin yellow, posterior margin black (Fig. 1). Mesonotum mostly dark brown, midline broad yellow, sublateral carinae yellow; the basal median area with four large black spots, the triangular intersection of the anterior and posterior margins yellow (Fig. 1). Forewings dark brown, longitudinal veins black, with irregular pale-yellow transverse veins (Figs 1, 2, 4). Hind wing pale brown, darker apically (Fig. 5). Legs all tawny (Figs 2, 3).

Head and thorax. Vertex 1.3 times wider than long in midline, posterior margin with the protruded level little shallower than anterior margin (Fig. 1). Frons 0.8 times longer in middle than broad at widest part, 1.4 times wider at the widest part than apical margin (Fig. 3); sublateral carinae obviously elevated from apex extending to basal 1/6, not reaching the clypeus (Fig. 3). Pronotum with posterior margin 2.6 times wider than long in midline (Fig. 1). Mesonotum with anterior margin 1.7 times wider than long in midline (Fig. 1). Forewings 2.6 times longer in longest part than widest part, MP vein firstly forked at apical 1/3, MP_{1+2} forked again at apical 1/5 (Fig. 2) or unforked (Fig. 4), MP_{3+4} bifurcate at apical 1/6 (Fig. 4) or unforked (Fig. 2); CuA forked near middle, before the first fork of MP, CuA_1 simple and sinuate, CuA_2 simple and straight (Figs 2, 4). Metatibiotarsal formula: 2–6/8/2.

Male genitalia. Anal tube slender in lateral view, broad in basal 1/3 then gradually narrowing to the apex (Fig. 6); in dorsal view anal tube long cylindrical, broadest below middle, the length in midline 2.7 times longer than the widest part, dorsal margin almost straight (Fig. 7); anal opening located below middle (Fig. 7); epiproct exceeding to the middle of anal tube (Fig. 7). Pygofer with the highest length in midline 2.0 times longer than the width at middle (Fig. 6); dorso-apical angle obtuse and oblique (Fig. 6). Gonostylus in lateral view with dorsal margin oblique and almost straight, posterior margin slightly concaved at middle, ventral margin deeply convex in the apex
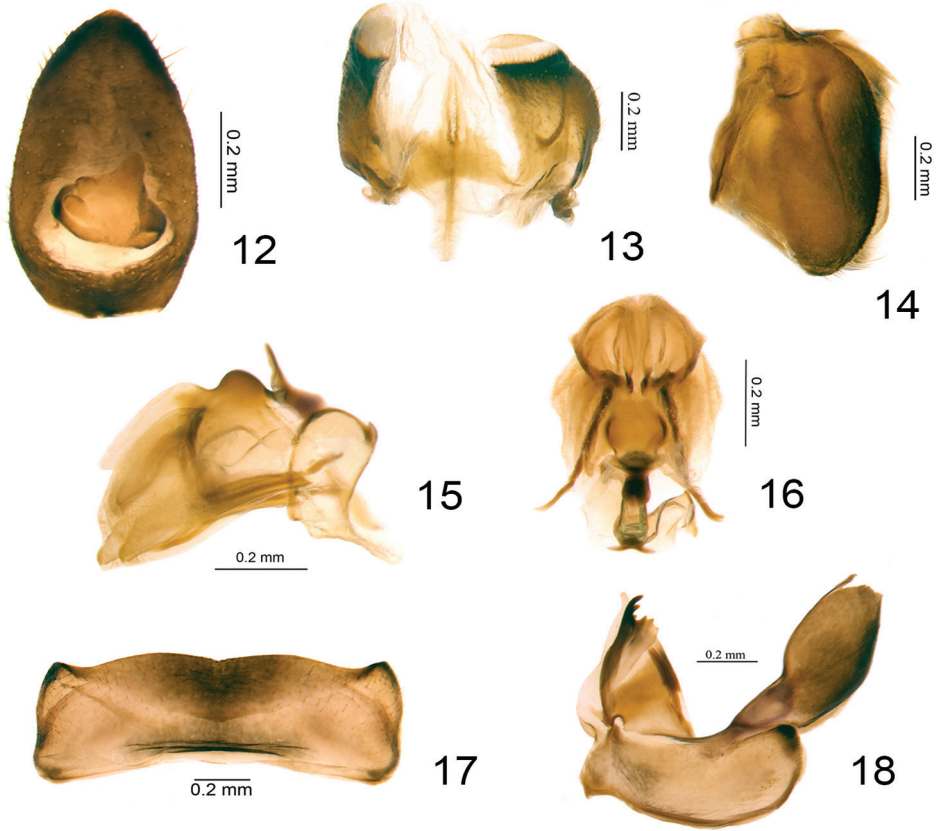
Figures 12–18. *Eusarimissus hezhouensis* sp. nov., paratype. **12** female anal tube, dorsal view **13** gonoplacs, dorsal view **14** gonoplacs, lateral view **15** gonapophysis IX and gonospiculum bridge, lateral view **16** gonapophysis IX and gonospiculum bridge, dorsal view **17** sternite VII, ventral view **18** gonocoxa VIII and gonapophysis VIII, ventral view.

with caudo-ventral angle rounded (Figs 6, 8). Capitulum of gonostylus spiniform, with a small auriform process near base (Figs 6, 8). Periandrium tubular, dorsal lobe with ventral margin expanded (edl) near middle, fused with lateral lobes at basal 1/3 (Figs 9, 10); in ventral view dorsal lobe slightly broaden near the apex, lateral lobes bifurcate at middle near the apex, ventral lobe with dorsal margin slightly concave at middle (Fig. 11); ventral lobe (vl) only reaching the apical 1/3 of periandrium. Aedeagus symmetrical, with a pair of hooked processes (ap) derived from apical 1/3 extending along the ventral margin of periandrium reaching to the basal 1/3 (Figs 9, 10), in ventral view this pair of processes slightly curved inward (Fig. 11).

Female genitalia. Anal tube in dorsal view conical, 1.6 times longer in midline than widest part (Fig. 12); apical margin sharp, lateral margins gradually broadening from apex to basal 1/3 (Fig. 12); anal opening situated at basal 1/3 (Fig. 12). Gonoplacs in dorsal view with outer lateral margins roundly convex, the apical part and

median part membranous (Fig. 13); in lateral view rectangular, 1. 6 times longer in longest part than widest part, the apical margin rounded (Fig. 14). Gonapophysis IX in lateral view broad, dorsal margin elevated and convex at middle, basal 1/3 with a needle-like process (Fig. 15). Gonapophysis IX in dorsal view widest near middle, basal half broader than apical half, outer area concave inward near apical 1/3 (Fig. 16). Anterior connective lamina of gonapophysis VIII with three teeth at apex and three teeth on the outer lateral margin, inner lateral margin without teeth (Fig. 18). Endogonocoxal process reaching to the same level of apex of anterior connective lamina (Fig. 18). Gonocoxa VIII long rectangular, perpendicular the gonapophysis VIII (Fig. 18). Apical margin of sternite VII mostly straight, with middle part very shallowly incised and two prominent dorso-lateral angles in ventral view (Fig. 17).

Etymology. The name refers to the type locality of the species.

Phylogeny. The molecular sequences obtained were registered in GenBank with the following accession numbers: MN955873 (18S, primers: 3F–Bi + A2–9R), MN955872 (28S D3–D5, primers: Ai–D4D5r), MN955852 (28S D6–D7, primers: EE–MM), MN954323 (COXI). Cytb sequence was failed to obtain. Molecular analysis based on available sequences of the 18S rRNA, 28S rRNA, COXI and Cytb genes confirms the morphological data positioning the new taxon in Sarimini. The species takes place as sister to a non-described but already sequenced Sarimini species *Eusarima* sp. 4 in Wang et al. (2016), both being sister taxa to *Longieusarima lunulia* Wang, Bourgoin & Zhang, 2017 (Fig. 19). Barcoding part of COXI gene of *Eusarimissus hezhouensis* sp. nov. differs by 107 bp and 115 bp from *Eusarima* sp. 4 and *L. lunulia* Wang, Bourgoin & Zhang, 2017 respectively over the total length of 681 bp.
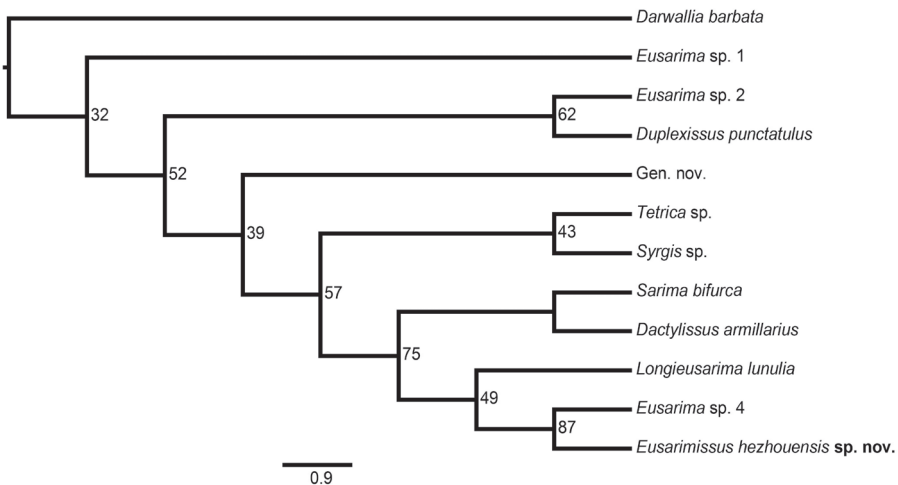

Figure 19. Maximum likelihood tree of Sarimini species based on combined sequences (18S, 28S, COXI, Cytb) with *Darwallia* as outgroup. At each node, values denote ML bootstrap support. The name 'Gen. nov.', '*Eusarima* sp. 1', 'sp. 2', and 'sp. 4' refer to the same taxa as in Wang et al. (2016).

Discussion

Analysis of all Sarimini genera currently available for a molecular phylogeny, places *Eusarimissus* gen. nov. as sister to *Eusarima* sp. 4 which are both sister to the genus *Longieusarima*. Morphologically, *Eusarimissus* gen. nov. resembles the genus *Eusarima* from which it could be easily separated by the forewing venation and the presence of the posterolateral processes of the dorsal lobe of the periandrium in the latter genus.

 Eusarima is a large genus including 37 species (Bourgoin 2020). It was divided into two subgenera: *Eusarima* and *Nepalius* Dlabola, 1997, the latter synonymized with the former by Gnezdilov (2009) before being revalidated as a subgenus by Gnezdilov and Mozaffarian (2011). Subgenus *Nepalius* currently contains three species distributed in the Western Palaearctic area (Nepal, Iran and Pakistan). It represents probably a separated valid independent genus with its type species *Eusarima* (*Nepalius*) *helleriana* (Dlabola, 1997) and *Eusarima* (*Nepalius*) *albifrons* Gnezdilov, 2016. However, according to its forewing conformation (particularly by its short recurved ScP+RA to RP), *Eusarima* (*Nepalius*) *iranica* Gnezdilov & Mozaffarian, 2011 is here transferred in the genus *Sarima* Melichar, 1903 as *Sarima iranica* (Gnezdilov & Mozaffarian, 2011) comb. nov. Because *Sarima* is probably also a composite genus in need of revision, we don't exclude the possibility that *S. iranica* could belong to an independent genus itself. Thirty-one other species in the nominal subgenus *Eusarima* occur in Taiwan, which is regarded as an example of extensive insular diversification (Gnezdilov 2016). Two more species were also described from Japan and another one from Guangxi Province, China. The latter, *Eusarima* (*Eusarima*) *triphylla*, differs from all other *Eusarima* and Sarimini species by several characters that need to be confirmed: a CuA_1 vein apically single, a 3-forked Pcu vein and an incomplete A1 vein. Because the published figure looks rather schematic (Che et al. 2012, fig. 7), this venation needs to be rechecked for confirmation and sequencing this species for comparison with other Sarimini taxa would be of great interest as obviously its generic placement remains dubious. Unfortunately, we don't also know the precise phylogenetic placement of the genus *Eusarima* itself within the Sarimini: all species analysed in Wang et al. (2016) and labelled '*Eusarima* sp.', although quite close to *Eusarima* species, are not true *Eusarima* taxa.

 The diversity of the taxa that progressively joined the Sarimini tribe, allows us now to better clarify the morphological characteristics of the group. Indeed, within the Issidae, Sarimini shares a specific 3-lobed hind wing conformation with an A2 lobe as wide or wider than the other lobes, often notched at the A2 extremity, and with several venation characteristics that seems emerging as a specific combination for the group: lobes with non-reticulated venation, Pcu-A1 lobe usually without transverse veins, cubital band area between CuP and Pcu always much wider than the intra-cubital band area between CuA and CuP, MP single, Pcu anastomosing at some distance with A1 anterior branch, Pcu, $A1_1$, $A1_2$ and A2 single.

Acknowledgements

References

Bourgoin T (1987) A new interpretation of the homologies of the Hemiptera male genitalia, illustrated by the Tettigometridae (Hemiptera, Fulgoromorpha). In: Proceedings of the 6th Auchenorrhyncha Meeting, Turin (Italy), September 1987, 113–120.

Bourgoin T (1993) Female genitalia in Hemiptera Fulgoromorpha, morphological and phylogenetic data. Annales de la Société Entomologique de France 29(3): 225–244.

Bourgoin T (2020) FLOW (Fulgoromorpha Lists On the Web): a world knowledge base dedicated to Fulgoromorpha. Version 8, updated 16 Jan 2020. http://hemiptera-databases.org/flow/ [accessed 17 Jan 2020]

Bourgoin T, Wang RR, Asche M, Hoch H, Soulier-Perkins A, Stroiński A, Yap S, Szwedo J (2015) From micropterism to hyperpterism: recognition strategy and standardized homology-driven terminology of the forewing venation patterns in planthoppers (Hemiptera: Fulgoromorpha). Zoomorphology 134: 63–77. https://doi.org/10.1007/s00435-014-0243-6

Chan ML, Yang CT (1994) Issidae of Taiwan (Homoptera: Fulgoroidea). Chen Chung Book, Taichung, 168 pp.

Che YL, Zhang YL, Wang YL (2012) Review of the issid genus *Parasarima* Yang (Hemiptera: Fulgoroidea: Issidae) with description of one new species from China. Entomotaxonomia 34(3): 533–537.

Gnezdilov VM (2009) Revisionary notes on some tropical Issidae and Nogodinidae (Hemiptera: Fulgoroidea). Acta Entomologica Musei Nationalis Pragae 49(1): 75–92.

Gnezdilov VM (2016) A new species of the genus *Eusarima* Yang (Hemiptera: Fulgoroidea: Issidae) from Pakistan, Entomological Review 96(2): 218–224. [original in Russian published in Entomologicheskoe Obozrenie 2016, 95(1): 176–184]. https://doi.org/10.1134/S0013873816020081

Gnezdilov VM, Mozaffarian F (2011) A new species of the genus *Eusarima* (Hemiptera: Fulgoroidea: Issidae) from Iran. Acta Entomologica Musei Nationalis Pragae 51(2): 457–462.

Kumar S, Stecher G, Tamura K (2016) MEGA7: Molecular evolutionary genetics analysis version 7.0 for bigger datasets. Molecular Biology and Evolution 33(7): 1870–1874. https://doi.org/10.1093/molbev/msw054

Minh BQ, Nguyen MAT, von Haeseler A (2013) Ultrafast approximation for phylogenetic bootstrap. Molecular Biology and Evolution 30: 1188–1195. https://doi.org/10.1093/molbev/mst024

Nguyen LT, Schmidt HA, von Haeseler A, Minh BQ (2015) IQ-TREE: a fast and effective stochastic algorithm for estimating maximum likelihood phylogenies. Molecular Biology and Evolution 32: 268–274. https://doi.org/10.1093/molbev/msu300

Rambaut A (2016) FigTree v1.4.3: Tree figure drawing tool. http://tree.bio.ed.ac.uk/software/figtree/ [Accessed 4 October 2016]

Wang ML, Zhang YL, Bourgoin T (2016) Planthopper family Issidae (Insecta: Hemiptera: Fulgoromorpha): linking molecular phylogeny with classification. Molecular Phylogenetics and Evolution 105: 224–234. https://doi.org/10.1016/j.ympev.2016.08.012

Wang ML, Bourgoin T, Zhang YL (2017) New Oriental genera in the family Issidae (Hemiptera: Fulgoromorpha). Zootaxa 4312(2): 355–367. https://doi.org/10.11646/zootaxa.4312.2.10

Wang ML, Zhang YL, Bourgoin T (2019) On the tribe Sarimini with two new genera from south of China (Hemiptera, Fulgoromorpha, Issidae). Zootaxa 4706(2): 375–383. https://doi.org/10.11646/zootaxa.4706.2.10

Zhao SP, Bourgoin T, Wang ML (2019) The impact of a new genus on the molecular phylogeny of Hemisphaeriini (Hemiptera, Fulgoromorpha, Issidae). Zookeys 880: 61–74. https://doi.org/10.3897/zookeys.880.36828

RESEARCH ARTICLE

Ancyronyx clisteri, a new spider riffle beetle species from Borneo, redescription of *A. sarawacensis* Jäch including a description of the larva and new distribution data for *A. procerus* Jäch using DNA barcodes (Coleoptera, Elmidae)

Ján Kodada[1], Manfred A. Jäch[2], Hendrik Freitag[3,4,5],
Zuzana Čiamporová-Zaťovičová[6], Katarína Goffová[1], Dávid Selnekovič[1],
Fedor Čiampor Jr[6]

1 *Department of Zoology, Faculty of Natural Science, Comenius University, Mlynská dolina B-1, SK-842 15 Bratislava, Slovakia* **2** *Naturhistorisches Museum Wien, Burgring 7, A–1010 Wien, Austria* **3** *Ateneo de Manila University, Biology Department, School of Science and Engineering, Loyola Heights, Quezon City 1101, Philippines* **4** *Universiti Brunei Darussalam, Environmental and Life Sciences, Faculty of Science, Jalan Tungku Link, Gadong, BE1410, Brunei* **5** *Taxon Expeditions, Rembrandtstraat 20, 2311 VW Leiden, Netherlands* **6** *Zoology Lab, Plant Science and Biodiversity Centre, Slovak Academy of Sciences, Dúbravská cesta 9, SK-84523, Bratislava, Slovakia*

Corresponding author: *Ján Kodada* (jan.kodada@uniba.sk)

Citation: Kodada J, Jäch MA, Freitag H, Čiamporová-Zaťovičová Z, Goffová K, Selnekovič D, Čiampor Jr F (2020) *Ancyronyx clisteri*, a new spider riffle beetle species from Borneo, redescription of *A. sarawacensis* Jäch including a description of the larva and new distribution data for *A. procerus* Jäch using DNA barcodes (Coleoptera, Elmidae). ZooKeys 912: 25–64. https://doi.org/10.3897/zookeys.912.47796

Abstract

Ancyronyx clisteri **sp. nov.** (Coleoptera, Elmidae) a new spider riffle beetle discovered from northern Borneo (Brunei; Sabah and Sarawak, Malaysia) and the larva of *Ancyronyx sarawacensis* Jäch are described. Illustrations of the habitus and diagnostic characters of the new species and the similar and highly variable *A. sarawacensis* are presented. Differences to closely related species, based on DNA barcodes and morphological characters, are discussed. Association of the larva and the imago of *A. sarawacensis*, and the occurrence of *Ancyronyx procerus* Jäch in Peninsular Malaysia and Sabah are confirmed by using COI mtDNA sequences.

Keywords

Introduction

The first modern taxonomic review of *Ancyronyx* Erichson was published by Jäch (1994) almost 150 years after the description of the genus. Subsequently, numerous new species and larvae were described from Asia (Jäch 2003, 2004; Freitag and Jäch 2007; Freitag and Balke 2011; Bian et al. 2012; Freitag 2012, 2013; Kodada et al. 2014; Freitag and Kodada 2017a, b). Based on these descriptions, the morphological characteristics of the genus were modified (Freitag 2012, Kodada et al. 2014). A total of 33 described species (including one subspecies) is presently known (Jäch et al. 2016, Freitag and Kodada 2017a).

Six species of *Ancyronyx* were so far recorded from Borneo (Brunei; Sabah and Sarawak, Malaysia), the third largest island of the world. However, only few localities in Brunei, Sabah and Sarawak were sufficiently surveyed so far, and the watercourses of Kalimantan largely remain unexplored. Therefore, it can be expected that the fauna of Borneo is probably much richer than known to date. Only a few species, such as *A. acaroides* Grouvelle, *A. malickyi* Jäch and *A. procerus* Jäch, are considered to be widely distributed in Southeast Asia, however, the published distributional data need confirmation at the molecular level. The distribution of most other species is confined to Sulawesi, Indonesia (12 spp.) and some Philippine islands (11 spp.).

Examination of additional material of *Ancyronyx* from Borneo and a detailed study of *A. sarawacensis* Jäch (including type specimens and freshly collected material) revealed an overlooked new species, which is described below.

The fresh material enabled also the use of DNA barcodes to support species delimitation and to estimate the genetic as well as morphological variability of the two species and to describe the larva of *A. sarawacensis*. Furthermore, we were able to confirm the occurrence of *A. procerus* in Peninsular Malaysia by COI mtDNA comparison.

Material and methods

The material used for study is deposited in the following collections: **BOR/COL** (Borneensis Coleoptera Collection of the Institute for Tropical Biology and Conservation, Universiti Malaysia Sabah, Kota Kinabalu); **CCB** (Collection of Fedor Čiampor Jr, Bratislava, Slovakia); **CFDS** (Collection of Forest Department Sarawak, Kuching, Malaysia); **CFM** (Collection Hendrik Freitag, Manila, currently deposited at the Ateneo de Manila University, Quezon City, Philippines); **CKB** (Collection of Ján Kodada, Bratislava, Slovakia); **NMW** (Naturhistorisches Museum Wien, Austria); **RMNH** (Naturalis Biodiversity Center, Leiden, Netherlands); **UBDM** (Universiti Brunei Darussalam Museum, Brunei).

Dried specimens were soaked in warm water with several drops of concentrated acetic acid and cleaned. Abdomens with genitalia or genitalia only were exposed to lactic acid for one or two days and temporarily mounted onto microscopic slides. Specimens were examined and measured using a Leica M205C stereomicroscope with fusion optics and diffuse lighting at magnifications up to 160 ×. For measurements an eyepiece graticule (5 mm: 100) or the Leica MC190-HD camera attached to microscope and

LAS software were used. The specimens were photographed under a Zeiss Axio-Zoom V-16 stereomicroscope using diffuse LED lighting and a Canon 5D Mark IV camera attached. Dissected genitalia and pregenital segments were studied in a temporary microscope cavity slide covered with a cover glass at magnifications up to 640 × with a Leica DM 1000 microscope. All drawings were made using a Leica drawing device.

Principal component analyses (PCA) was performed separately for male and female specimens using software PAST 3.12 (Hammer et al. 2001) and a variance-covariance matrix with log-transformed variables. PCA plots were subsequently edited in Adobe Illustrator CC.

Metric characters of 108 males and 99 females of *A. sarawacensis* as well as 11 males and 20 females of *A. clisteri* sp. nov. were used for the PCA analyses; all specimens identified by mtDNA characters were included in the dataset measured. Morphometric parameters are provided in tables as range and mean ± standard deviation. The following characters were measured: **BL** (body length without head, length of pronotum and elytra measured along midline); **EL** (elytral length, length measured along suture from level of the most anterior point of elytra to the most posterior tip of elytra) in dorsal view; **EW** (elytral width, maximum width combined); **HW** (head width including eyes); **ID** (interocular distance); **MW** (maximum pronotal width); **PL** (pronotal length along midline).

For scanning electron microscopy, specimens were dehydrated in graded ethanol series and then air dried from absolute ethanol, mounted on a stub, sputter coated with gold and viewed and photographed using a TESCAN microscope.

For the DNA analyses, 32 adults (29 *Ancyronyx* spp.; 3 *Graphelmis* spp.) and one larva were used. The dataset is available on dx.doi.org/10.5883/DS-ELMANC01. DNA was isolated from the whole specimens using DNeasy Blood and Tissue Kit (Qiagen) according to the manufacturer's protocol. Fragment of the 5' end of the mitochondrial gene for cytochrome c oxidase subunit I (COI) was amplified with primers LCO1490, HCO2198 (Folmer et al. 1994). Amplification products were purified by alkaline phosphatase (FastAP) and exonuclease and sequenced from both sides in Macrogen Europe Inc. (Amsterdam, Netherlands). Raw sequences were assembled and edited in Sequencher v5.1. The genetic distances were measured using K2P model, maximum likelihood tree and bootstrap support were performed in MEGA software v7 (Kumar et al. 2016). The best-fitted substitution model (GTR+I+G) was selected by jModelTest 2 (Darriba et al. 2012). Voucher specimens numbers and GenBank numbers are found between square brackets in the lists of specimens below.

The general morphological terminology follows Kodada et al. (2016) and Lawrence and Ślipiński (2013).

Descriptions of the adults holotypes and mature larvae of *Ancyronyx sarawacensis* are completed with SEM figures of specimens from the respective type locality. Using the standard clearing procedure in lactic acid and gentle pressing by a tip of an entomological pin on the aedeagus delivered extruded endophallus in several males, however the form was well preserved in a single specimen only. The endophallic structures were examined and described only from this *A. sarawacensis* male.

Results

DNA analyses

The COI sequences used in the analysis are 661bp long with no ambiguous sites or indels. Maximum likelihood (ML) analysis revealed well-separated clades representing three species of *Ancyronyx* (Fig. 1). The interspecific genetic distance was large, ranging from 9.3–17.9%, the intraspecific diversity within *Ancyronyx sarawacensis* ranged from 1.0–3.0%, and within *A. procerus* from 0.0–1.2% (Tab. 2, Suppl. material 1: Tab. S1). In the latter species two genetic lineages were recovered, which correspond with the geographic distribution of the samples. The COI data clearly confirm the occurrence of *A. procerus* in Peninsular Malaysia, which was previously proposed solely based on the morphology of the genitalia.

The two clades recovered in *A. procerus* differ in color patterns, but their genetic differentiation and the subtle differences in their genital morphology are far too weak to consider them as separate species.

PCA analyses

We examined and quantified the morphometric variations among *Ancyronyx sarawacensis* and *A. clisteri* sp. nov. using PCA (Fig. 2A). First principal component (PC 1) explained 78.18% of variance in males and 76.77% in females. According to loadings (Tab. 3), the strongest correlation was found between body length and elytral length, in both males and females. The second principal component (PC 2) explained 10.15% of variance in males and 9.25% in females and was most strongly correlated with interocular distance, reaching distinctly higher loading compared to other variables in both sexes (Tab. 3).

When assigning the specimens of *Ancyronyx sarawacensis* to three geographically separate groups, i.e., lowlands of Sarawak (40–70 m a.s.l.), uplands of Sabah (170–300 m a.s.l.), and the Kelabit Highlands (around 1000 m a.s.l.), the PCA plot reveals a size gradient related to altitude (Fig. 2A). Specimens from Sarawak lowlands cluster almost separately from those of the Kelabit Highlands. Specimens from Sabah form an intermediate cluster, partly overlapping with both. This gradient corresponds with differences in the actual measurements: elytral length and body length are smallest in the specimens from Sarawak lowlands and largest in the specimens from the Kelabit Highlands (Fig. 2B, Tabs 4, 5).

The cluster of *Ancyronyx clisteri* sp. nov. overlaps with the Kelabit Highlands cluster of *A. sarawacensis* (Fig. 2A, B), but it is clearly separated along the PC 1 axes from clusters of Sarawak lowlands and Sabah uplands. *Ancyronyx clisteri* sp. nov. is also differentiated from *A. sarawacensis* along the PC 2 axes correlating with interocular distance and head width (Fig. 2A) and males of the two species overlap only very marginally in their EL/ID ratios (Fig. 2C).

Table 1. Samples used in the molecular analyses: origin of samples, GenBank and BOLD Data Systems BIN accession numbers (codes after species name refer to the voucher numbers used for DNA extraction).

Sample	Country, state	GenBank no.	BOLD BIN no.
Ancyronyx sarawacensis FZ1634	Malaysia, Sarawak	MK505407	BOLD:ADR1478
Ancyronyx sarawacensis FZ1641	Malaysia, Sarawak	MK505414	BOLD:ADR1478
Ancyronyx sarawacensis FZ1633	Malaysia, Sarawak	MK505406	BOLD:ADR1478
Ancyronyx sarawacensis FZ1631 / Larva	Malaysia, Sarawak	MK505395	BOLD:ADR1478
Ancyronyx sarawacensis 38	Malaysia, Sarawak	MK505398	BOLD:ADR1478
Ancyronyx sarawacensis FZ1642	Malaysia, Sarawak	MK505418	BOLD:ADR1478
Ancyronyx sarawacensis FRElmH39	Brunei	LR735552	BOLD:ADR1478
Ancyronyx sarawacensis 82	Malaysia, Sarawak	MK566773	BOLD:ADR1478
Ancyronyx sarawacensis FZ1643	Malaysia, Sarawak	MK505415	BOLD:ADR1478
Ancyronyx sarawacensis 39	Malaysia, Sarawak	MK505401	BOLD:ADR1478
Ancyronyx sarawacensis 83	Malaysia, Sarawak	MK566771	BOLD:ADR1478
Ancyronyx sarawacensis FZ1635	Malaysia, Sarawak	MK505422	BOLD:ADR1478
Ancyronyx sarawacensis FZ1628	Malaysia, Sarawak	MK505420	BOLD:ADR1478
Ancyronyx sarawacensis 10	Malaysia, Sarawak	MK505409	BOLD:ADR1478
Ancyronyx sarawacensis 36	Malaysia, Sarawak	MK566772	BOLD:ADR1478
Ancyronyx sarawacensis FZ1645	Malaysia, Sarawak	MK505404	BOLD:ADR1478
Ancyronyx sarawacensis FZ1651	Malaysia, Sabah	MK505400	BOLD:ADR1478
Ancyronyx sarawacensis 09	Malaysia, Sarawak	MK505396	BOLD:ADR1478
Ancyronyx sarawacensis 35	Malaysia, Sarawak	MK505399	BOLD:ADR1478
Ancyronyx sarawacensis FZ1636	Malaysia, Sarawak	MK505394	BOLD:ADR1478
Ancyronyx sarawacensis FZ1646	Malaysia, Sarawak	MK505397	BOLD:ADR1478
Ancyronyx clisteri FZ1640	Malaysia, Sarawak	MK505421	BOLD:ADR1475
Ancyronyx clisteri FRElmH44	Brunei	LR735553	BOLD:AEA6347
Ancyronyx procerus FZ1639	Malaysia, Sarawak	MK505411	BOLD:ADR0116
Ancyronyx procerus FZ1644	Malaysia, Sarawak	MK505410	BOLD:ADR0116
Ancyronyx procerus 11	Malaysia, Sarawak	MK505423	BOLD:ADR0116
Ancyronyx procerus 37	Malaysia, Sarawak	MK505417	BOLD:ADR0116
Ancyronyx procerus FZ1660	Malaysia, Sabah	MK505403	BOLD:ADR0116
Ancyronyx procerus FZ1659	Malaysia, Pahang	MK505405	BOLD:ADR0116
Ancyronyx procerus FZ1625	Malaysia, Terengganu	MK505402	BOLD:ADR0116
Ancyronyx procerus FZ1626	Malaysia, Terengganu	MK505412	BOLD:ADR0116
Ancyronyx procerus FZ1623	Malaysia, Terengganu	MK505419	BOLD:ADR0116
Ancyronyx procerus FZ1624	Malaysia, Terengganu	MK505413	BOLD:ADR0116
Graphelmis monticola FZ530	Malaysia, Kelantan	MK505416	BOLD:ADB9822
Graphelmis anulata FZ510	Malaysia, Pahang	MK505424	BOLD:ADC0259
Graphelmis obesa FZ544	Malaysia, Sabah	MK505408	BOLD:ADB9823

Table 2. Estimates of evolutionary divergence over sequence pairs between groups of three *Ancyronyx* species and the genus *Graphelmis* representing the outgroup.

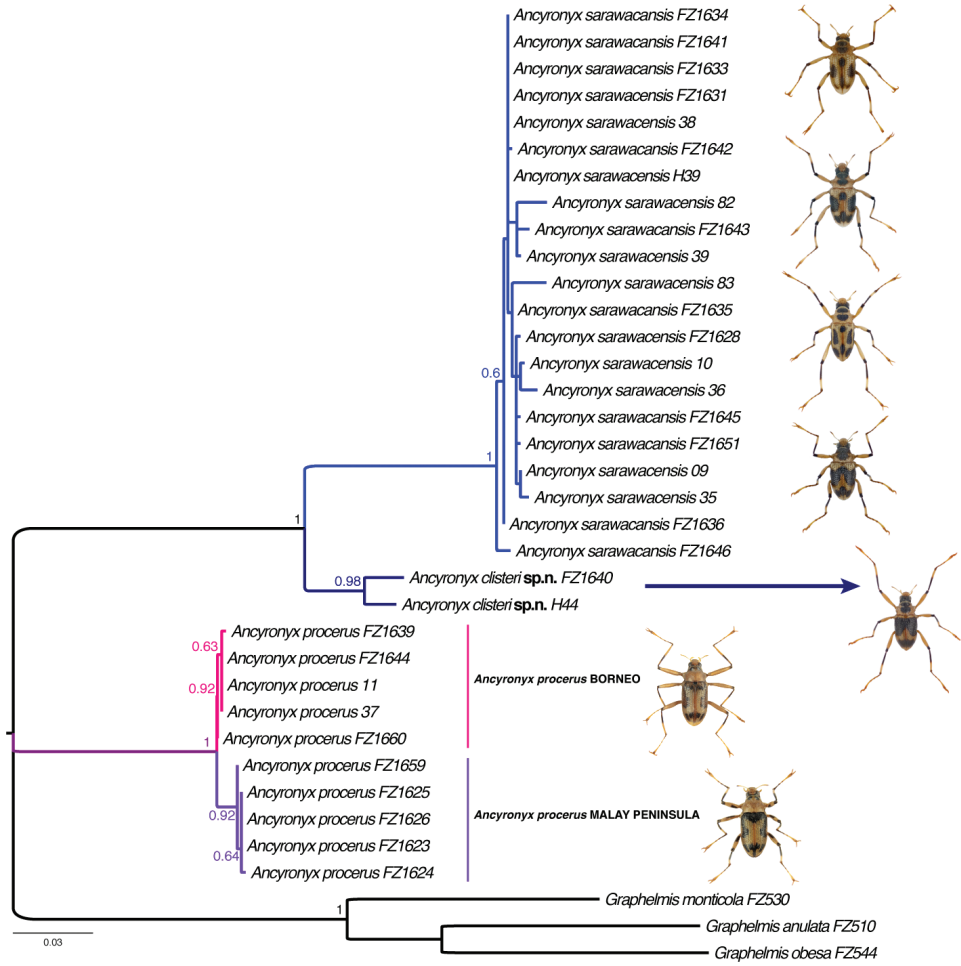|		1	2	3
1	*A. clisteri* sp. nov.			
2	*A. procerus*	17.0%		
3	*A. sarawacensis*	9.9%	20.1%	
4	*Graphelmis* (outgroup)	23.2%	21.2%	23.5%

Figure 1. Results of DNA COI analyses, maximum likelihood tree.

Table 3. The loadings onto the principal components for males and females of *Ancyronyx sarawacensis* and *Ancyronyx clisteri* sp. nov. The first and second highest values for each PC are highlighted in bold.

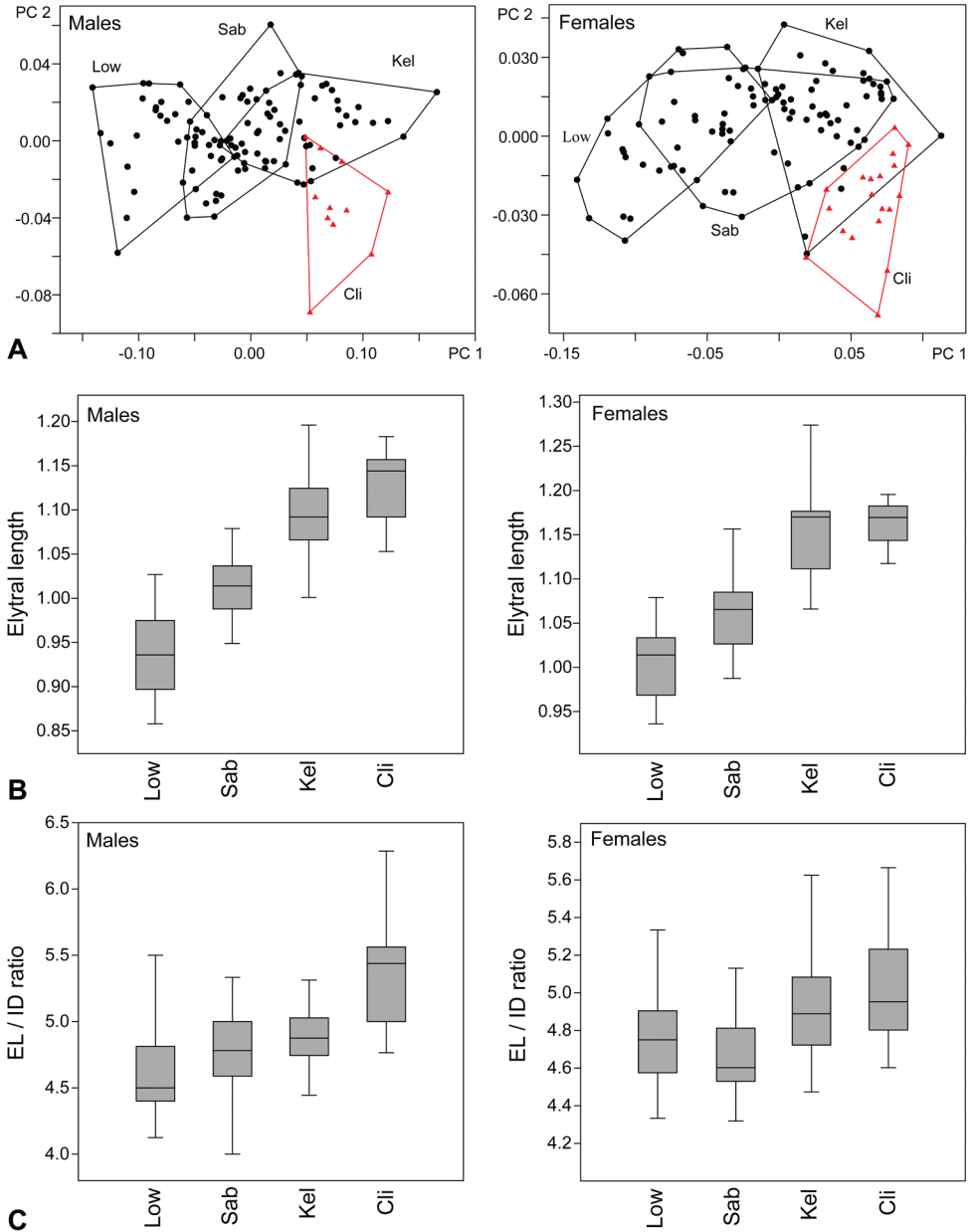|	**Males**			**Females**		
	PC 1	PC 2	PC 3	PC 1	PC 2	PC 3
Explained Variance (%)	78.18	10.15	4.17	76.77	9.25	6.20
Loadings of Variables:						
BL	**0.450**	-0.310	-0.156	**0.454**	-0.222	-0.300
EL	**0.468**	-0.354	-0.481	**0.448**	-0.143	-0.503
EW	0.418	0.021	-0.073	0.374	**0.147**	-0.223
PL	0.353	-0.105	**0.633**	0.385	-0.473	**0.701**
MW	0.317	0.150	**0.507**	0.298	-0.030	0.168
HW	0.322	**0.169**	0.056	0.312	0.052	0.101
ID	0.274	**0.846**	-0.279	0.345	**0.825**	**0.274**

Figure 2. A Results of PCA analyses, black circles: specimens of *Ancyronyx sarawacensis*, red triangles: *A. clisteri* sp. nov. Specimens of *A. sarawacensis* are assigned to three groups representing samples from different localities **B** boxplots showing differences in elytral length between *A. clisteri* sp. nov. and three groups of *A. sarawacensis* **C** Boxplots showing differences of ratio elytral length / interocular distance between *A. clisteri* sp. nov. and three groups of *A. sarawacensis*. Abbreviations: Low: lowlands of Sarawak, Sab: uplands of Sabah, Kel: Kelabit Highlands, Cli: *A. clisteri* sp. nov.

Table 4. Metric characters of *Ancyronyx clisteri* sp. nov. and *Ancyronyx sarawacensis* males. Morphometric parameters are provided as range and mean ± standard deviation.

	A. clisteri sp. nov.	*A. sarawacensis*			
	Aggregated data	Kelabit Highland (*N* = 37)	Sabah uplands (*N* = 44)	Sarawak lowlands (*N* = 27)	Aggregated data
BL: mm	**1.50–1.64** **1.57 ± 0.04**	**1.38–1.64** **1.49 ± 0.06**	**1.32–1.46** **1.40 ± 0.03**	**1.22–1.40** **1.30 ± 0.05**	**1.22–1.64** **1.41 ± 0.09**
EL: mm	1.05–1.18 1.13 ± 0.04	1.00–1.20 1.10 ± 0.05	0.95–1.08 1.01 ± 0.03	0.86–1.03 0.94 ± 0.05	0.86–1.20 1.02 ± 0.07
EW: mm	**0.70–0.71** **0.71 ± 0.01**	**0.66–0.78** **0.72 ± 0.03**	**0.64–0.72** **0.67 ± 0.02**	**0.59–0.65** **0.62 ± 0.02**	**0.59–0.78** **0.67 ± 0.04**
BL/EW	2.14–2.28 2.21 ± 0.04	1.88–2.15 2.07 ± 0.06	1.99–2.20 2.10 ± 0.05	1.99–2.21 2.10 ± 0.06	1.88–2.11 2.09 ± 0.05
EL/EW	**1.50–1.65** **1.59 ± 0.05**	**1.45–1.64** **1.52 ± 0.04**	**1.42–1.61** **1.51 ± 0.04**	**1.40–1.67** **1.52 ± 0.06**	**1.40–1.67** **1.52 ± 0.05**
PL: mm	0.44–0.48 0.45 ± 0.01	0.38–0.48 0.41 ± 0.02	0.38–0.42 0.40 ± 0.01	0.36–0.40 0.38 ± 0.01	0.36–0.48 0.40 ± 0.02
MW: mm	**0.51–0.57** **0.54 ± 0.01**	**0.49–0.62** **0.54 ± 0.02**	**0.47–0.56** **0.52 ± 0.02**	**0.46–0.55** **0.49 ± 0.02**	**0.46–0.62** **0.52 ± 0.03**
PL/MW	0.79–0.83 0.82 ± 0.02	0.70–0.85 0.77 ± 0.03	0.70–0.83 0.77 ± 0.03	0.70–0.83 0.77 ± 0.03	0.70–0.85 0.77 ± 0.03
HW: mm	**0.39–0.40** **0.39 ± 0.00**	**0.36–0.42** **0.39 ± 0.01**	**0.35–0.40** **0.37 ± 0.01**	**0.33–0.36** **0.35 ± 0.01**	**0.33–0.42** **0.37 ± 0.02**
ID: mm	0.18–0.22 0.21 ± 0.01	0.21–0.25 0.22 ± 0.01	0.20–0.25 0.21 ± 0.01	0.18–0.22 0.21 ± 0.01	0.18–0.25 0.21 ± 0.01

Table 5. Metric characters of *Ancyronyx clisteri* sp. nov. and *Ancyronyx sarawacensis* females. Morphometric parameters are provided as range and mean ± standard deviation.

	A. clisteri sp. nov.	*A. sarawacensis*			
	Aggregated data	Kelabit Highland (*N* = 33)	Sabah uplands (*N* = 45)	Sarawak lowlands (*N* = 21)	Aggregated data
BL: mm	**1.60–1.70** **1.64 ± 0.03**	**1.44–1.78** **1.59 ± 0.06**	**1.34–1.64** **1.48 ± 0.06**	**1.32–1.50** **1.39 ± 0.05**	**1.32–1.78** **1.50 ± 0.09**
EL: mm	1.12–1.20 1.16 ± 0.02	1.07–1.27 1.16 ± 0.04	0.99–1.16 1.06 ± 0.05	0.94–1.08 1.00 ± 0.04	0.94–1.27 1.08 ± 0.07
EW: mm	**0.70–0.77** **0.73 ± 0.01**	**0.69–0.79** **0.75 ± 0.02**	**0.66–0.78** **0.71 ± 0.02**	**0.62–0.72** **0.65 ± 0.02**	**0.62–0.79** **0.71 ± 0.04**
BL/EW	2.11–2.38 2.25 ± 0.07	1.94–2.36 2.13 ± 0.07	1.95–2.23 2.08 ± 0.05	2.06–2.24 2.14 ± 0.05	1.94–2.36 2.11 ± 0.06
EL/EW	**1.49–1.67** **1.59 ± 0.04**	**1.47–1.62** **1.54 ± 0.04**	**1.36–1.61** **1.50 ± 0.04**	**1.44–1.65** **1.54 ± 0.05**	**1.36–1.65** **1.52 ± 0.05**
PL: mm	0.45–0.52 0.49 ± 0.02	0.42–0.48 0.44 ± 0.02	0.39–0.47 0.44 ± 0.02	0.39–0.44 0.41 ± 0.01	0.39–0.48 0.43 ± 0.02
MW: mm	**0.55–0.61** **0.58 ± 0.02**	**0.53–0.60** **0.56 ± 0.02**	**0.52–0.61** **0.55 ± 0.02**	**0.49–0.55** **0.52 ± 0.02**	**0.49–0.61** **0.55 ± 0.02**
PL/MW	0.80–0.90 0.85 ± 0.03	0.73–0.86 0.79 ± 0.03	0.73–0.83 0.79 ± 0.02	0.74–0.84 0.80 ± 0.03	0.73–0.86 0.79 ± 0.02
HW: mm	**0.39–0.44** **0.41 ± 0.01**	**0.38–0.43** **0.40 ± 0.01**	**0.36–0.44** **0.39 ± 0.02**	**0.35–0.39** **0.37 ± 0.01**	**0.35–0.44** **0.39 ± 0.02**
ID: mm	0.21–0.25 0.23 ± 0.01	0.21–0.25 0.24 ± 0.01	0.21–0.25 0.23 ± 0.01	0.20–0.23 0.21 ± 0.01	0.20–0.25 0.22 ± 0.01

Ancyronyx clisteri **sp. nov.**
http://zoobank.org/201B4FB8-C588-468F-892A-A6A8F62FFEAF

Type locality (Fig. 11A). River, about 10 m wide (tributary of Kuamut River near Kampung Pisang Pisang), meandering, with submerged wood; Sabah, Malaysia.

Type material. *Holotype* ♂ (NMW): "Malaysia, Sabah, Kuamut river env. near Kampung Pisang Pisang, 3.–4. VII. 1996, 14b: ca 10 m wide tributary of Kuamut River in primary forest". *Paratypes* (BOR/COL, CCB, CFDS, CFM, CKB, NMW, RMNH, UBDM): 1 ♂, 2 ♀♀: same locality data as holotype; 5 ♂♂, 8 ♀♀: "Malaysia, Sabah, (Borneo), Kuamut river env. near Kampung Pisang Pisang, 3.–4. VI. 1996, 14a: shaded stream in primary forest with submerged wood"; 2 ♀♀: "Malaysia, Sabah, Kampung Pisang Pisang env., tributary of Kuamut River, 29. VI. 1998"; 4 ♂♂, 7 ♀♀: "Malaysia, Sabah, Sabalangang river in primary forest ca 25 km SE Sapulut, 26.06.1998"; 1 ♀: "Malaysia, Sabah, ca 5 km S Sapulut, Saliku river,16.V.2001"; 1 ♀: "Malaysia: Sabah: Maliau Basin Studies Center: Kuamut River tributary, road bridge near observation tower; submerged wood, riffle; 4°42'48"N, 116°58'34"E, 280 m a.s.l.; 03.Oct2017, leg. H. Freitag & C.V. Pangantihon / Taxon Expeditions (KRC1f)"; 1 ♀ [FZ1640, MK505421]: "Malaysia, Sarawak, Marudi distr., Gunung Mulu NP, 17.10.2018, (42) 04.0267N, 114.818083E, 60 m a.s.l., river, J. Kodada & D. Selnekovič lgt."; 5 ♂♂ [H44, LR735552], 7 ♀♀: "Brunei: Temburong, Belalong River tributary Sungai Sibut; W of Ashton Trail, submerged wood, run; 4°32'38"N, 115°08'51"E, 170 m a.s.l.; leg. Pangantihon / Taxonexpeditions 29.Sep2018 (SiCf)M".

Diagnosis. *Ancyronyx clisteri* sp. nov. is a medium sized, elongate species with dark head and elytra (Fig. 3A, B). It is morphologically most similar to *Ancyronyx sarawacensis* from which it can be distinguished by: 1) elytra extensively black with a very narrow yellowish band along anterior margin and a moderately wider yellowish portion dividing anterior and posterior black area; 2) ovipositor with longer and narrower distal portion of coxite (2.7–2.9 × as long as wide near middle); 3) proximal portion of coxite ca 0.7–0.8 × as long as distal portion; 4) longitudinal baculum of paraprocts ca 1.04–1.19 × as long as entire coxite length; 5) about 9% divergence of the partial mtDNA for cytochrome c oxidase subunit COI (COI barcodes with 90.7% similarity between *A. clisteri* sp. nov. and *A. sarawacensis*, based upon 661 base pairs). We were unable to find significant differences between the aedeagi of these two species, although in direct comparison the apex of the penis of *A. clisteri* sp. nov. usually appears to be narrower and more pointed than that of *A. sarawacensis*. Some *A. sarawacensis* from Sabah (e.g., Figs 3D, 4A) show darker heads and pronota and wide anterior and posterior elytral spots, their color pattern is very similar to those of *A. clisteri* sp. nov. (see respective comment on variability below). For their correct identification it is best to use the COI barcodes or comparison of ovipositors. It is possible that some of the dark males of *A. sarawacensis* cannot be identified by morphological features without direct comparison with *A. clisteri* sp. nov.

Description of holotype. Body form moderately elongate, elytra moderately convex dorsally, with highest point near midlength; BL: 1.64 mm, EW: 0.74 mm, BL/EW: 2.22.
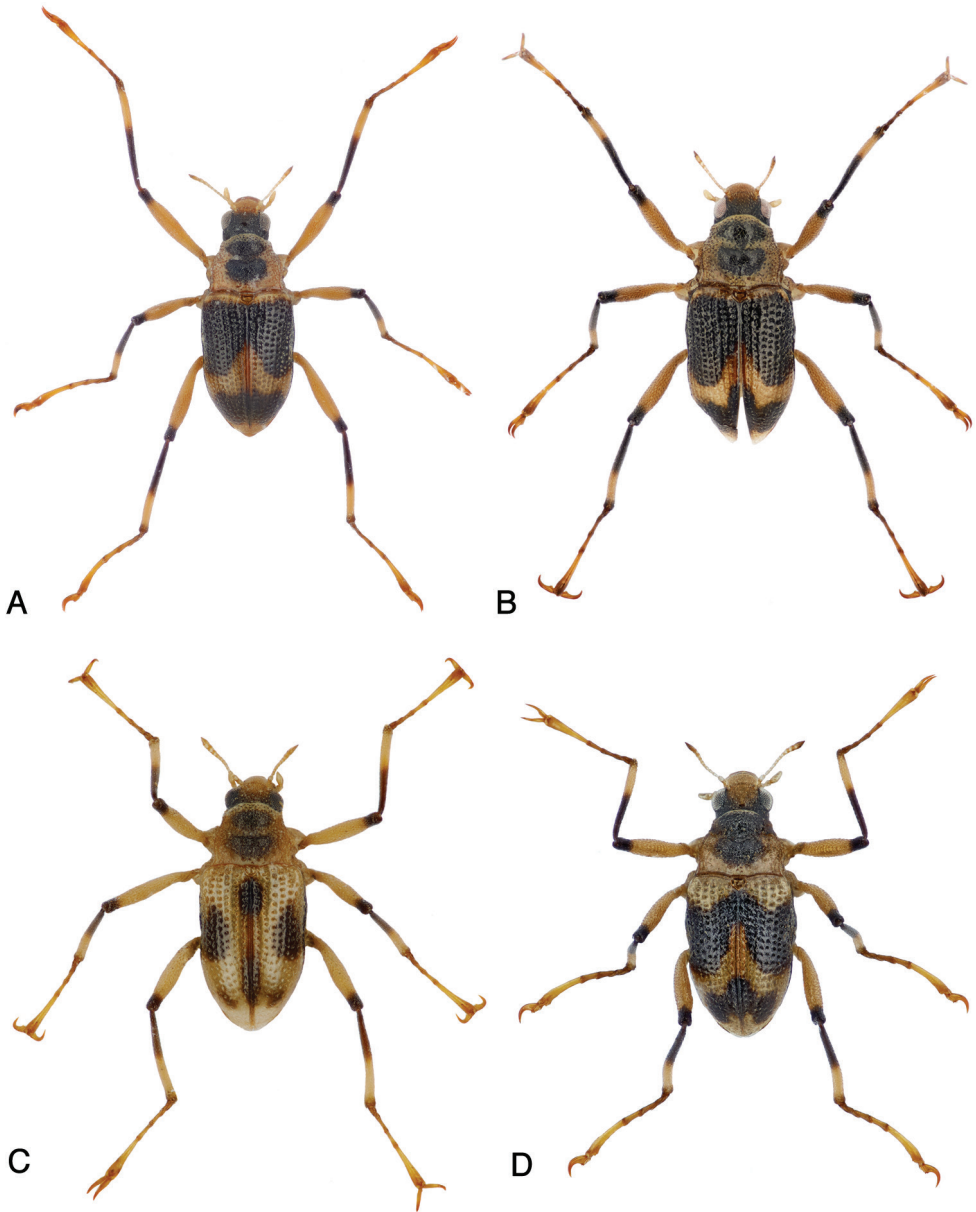
Figure 3. Habitus of: **A** *Ancyronyx clisteri* sp. nov., holotype **B** *A. clisteri* sp. nov., female paratype from Gunung Mulu NP, Sarawak **C** *A. sarawacensis*, holotype **D** *A. sarawacensis*, male from a tributary of Kuamut River "(14a)", Sabah.

Coloration (Fig. 3A, B). Labrum yellowish-brown; mouth parts and antennae yellowish, clypeus and narrow anterior portion of frons yellowish, remaining portions of cranium black dorsally and posteriad of eyes; pronotum yellowish with large mesal
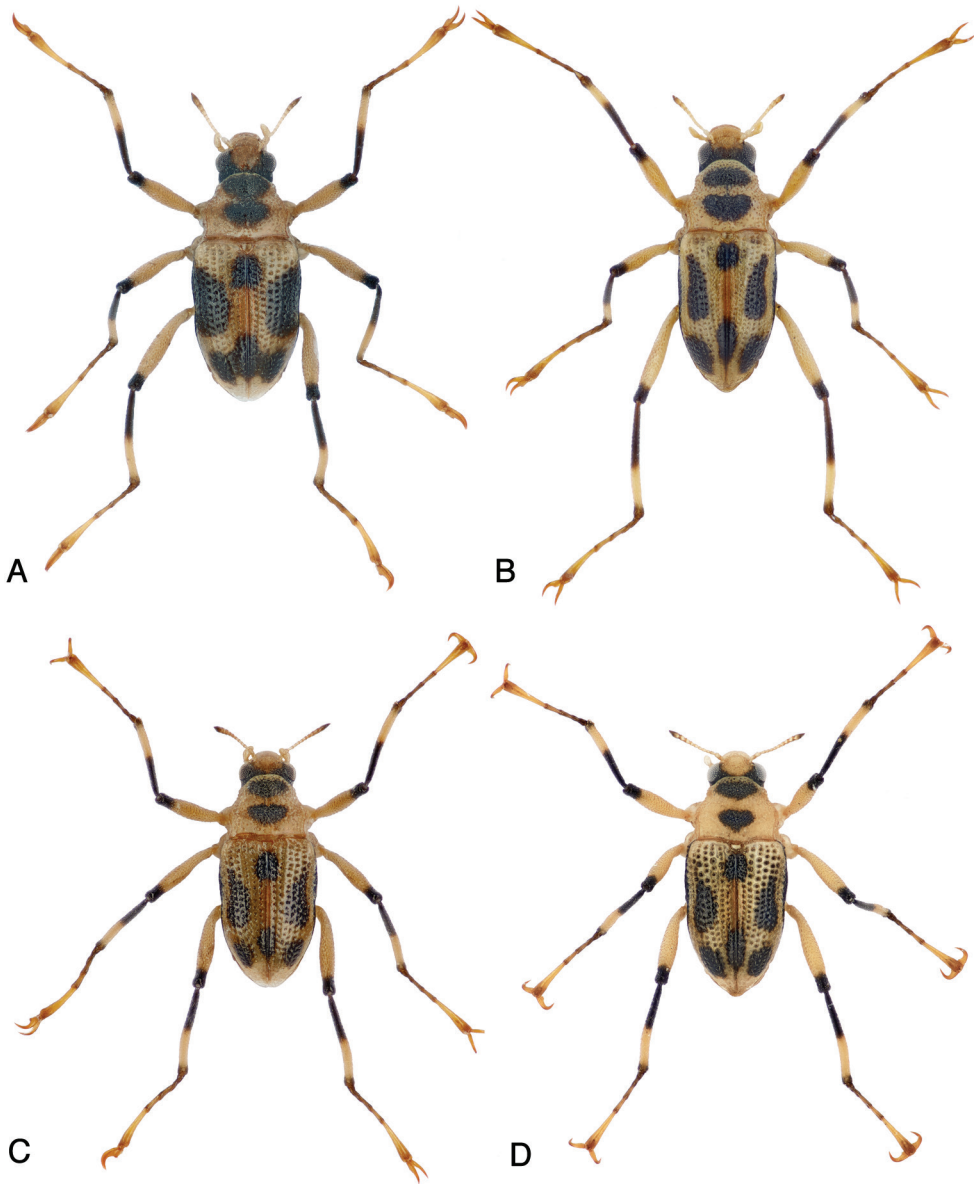
Figure 4. Habitus of: **A** *Ancyronyx sarawacensis*, male from the tributary of Kuamut River "(14a)", Sabah **B** *A. sarawacensis*, male paratype from Kapit area, Sarawak **C** *A. sarawacensis*, female paratype from Gunung Mulu NP, Sarawak **D** *A. sarawacensis*, female from Bayur River near Kampung Bayur, Sarawak.

black spot; spot distinctly narrowed near middle; scutellum brownish; elytra mostly black, with yellowish anterior margin and two oblique yellowish stripes meeting at suture; elytral apices yellowish. Venter yellowish except for almost black mesanepisterna,

metanepisterna, lateral portion of metaventrite and lateral portions of ventrite 1; coxae yellow; femora black on distal one sixth, yellowish on remaining portion; tibiae black on proximal three fourths and near articulation with tarsi, yellowish on distal fourth; tarsomeres 1–2 darker, tarsomeres 3–5 and claws yellowish.

Head. Labrum about as long as clypeus, with anterior margin slightly concave, almost straight; surface with dual punctation; larger punctures deeper with fine setae, smaller punctures very fine and shallow. Clypeus wide, densely punctate and finely reticulate. Frons and vertex densely, finely punctate, appearing reticulated; reticulation more distinct on black portion of vertex; surface with narrow, elongate, hardly discernible granules (Fig. 5C); frontoclypeal suture almost straight, finely impressed. Eyes moderately protruding and large. Antennae 11-segmented, subequal in length with pronotum; each antennomere with a few scattered trichoid setae (sensilla trichoidea); antennomeres 9–11 each with two clusters of peg-like setae near distal margins (Fig. 5D, E); terminal segment with additional different sensilla. Ratio of length of antennomeres 1–11: 0.049 : 0.053 : 0.039 : 0.028 : 0.031 : 0.028 : 0.037 : 0.033 : 0.041 : 0.045 : 0.093 mm. Gena microsculptured; gula narrow, smooth; gular sutures absent; posterior tentorial pits deep and large. HW: 0.39 mm; ID: 0.22 mm.

Thorax. Pronotum distinctly wider than long (PL/MW: 0.84), widest near posterior angles; anteriorly attenuate; anterior margin strongly arcuate; almost entire hypomeral portion visible in dorsal view; anterior transverse groove distinctly impressed, oblique and dividing pronotum; area posteriad of transverse groove strongly gibbous; anterior mesal longitudinal carina absent; posterolateral oblique grooves moderately impressed. Pronotal surface densely punctate and irregularly reticulate on disc; anterior and posterior portion smooth (Fig. 5A, F); flat cordiform granules mainly laterally and anteriorly; PL: 0.48 mm, MW: 0.57 mm. Prosternum irregularly, densely and roughly punctate, very short in front of procoxae; prosternal process distinctly transverse, almost flat; posterior margin widely rounded, feebly protruding posteriad; lateral margins arcuate. Scutellum subpentagonal, smooth and shiny. Elytra elongate; EL: 1.18 mm; slightly narrowed at the level of metacoxae, then gradually convergent towards conjointly rounded apices; with ten more or less regular rows of punctures; six rows between suture and shoulder; accessory scutellary rows absent (Fig. 6A); punctures large, round and deeply impressed on disc and laterally (Fig. 6A, B), smaller and less distinct anteriorly and posteriorly; interstices and intervals wider and flat on disc, narrower and feebly convex laterally and posteriorly; surface very finely sculptured; humeri prominent. Mesoventrite almost flat, approximately half as long as prosternum length; mesoventral cavity shallow and narrow; surface strongly and irregularly punctate; mesoventral discrimen invisible; posterior angles rounded and moderately protruding. Metaventrite along midline distinctly longer than combined length of prosternum and mesoventrite; anterior margin arcuate; disc with shallow longitudinal depression mesally; discrimen strongly depressed (Fig. 5B); surface of disc glabrous with fine scarce punctures; distinct, deep irregular punctures along anterior margin and on lateral portions of metaventrite; punctures coarser and denser laterally. Hind wings fully developed. Forelegs about 1.47 × as long as body length; pro- and mesocoxae large
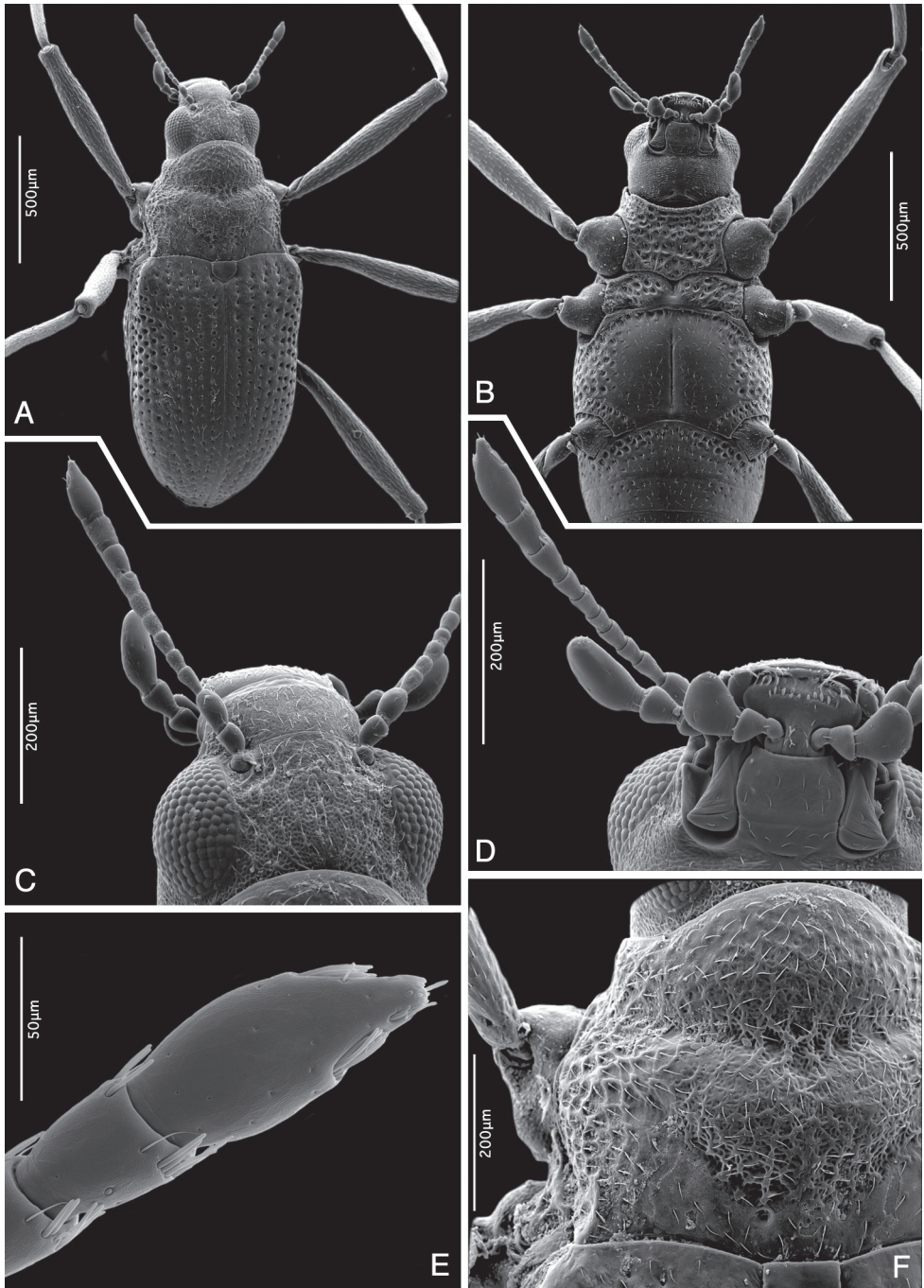
Figure 5. *Ancyronyx clisteri* sp. nov., SEM micrographs, male paratype from the type locality: **A** habitus, dorsal view **B** same specimen, ventral view **C** head, reticulate surface and granules, dorsal view **D** head, detail of mouth parts and antenna, ventral view **E** antennal apex with clusters of sensilla, ventrolateral view **F** pronotum with reticulate surface structure, dorsal view.
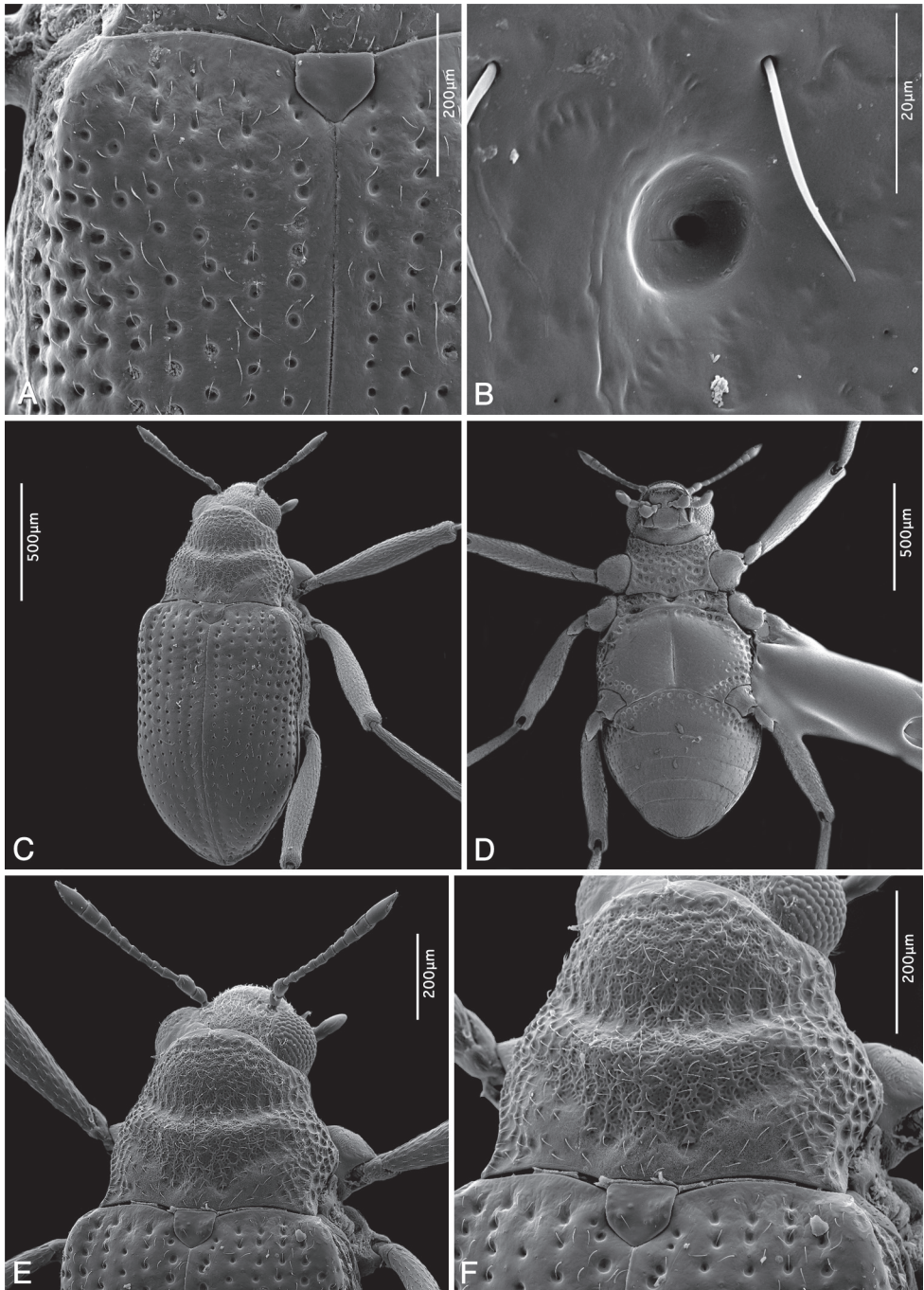
Figure 6. SEM micrographs: **A, B** *Ancyronyx clisteri* sp. nov. (male paratype from the type locality) **C–F** *A. sarawacensis* (female from the type locality). **A** Elytra and scutellum, anterior portion, dorsal view **B** same, detail of elytral surface, dorsal view **C** habitus, dorsal view **D** same, ventral view **E** head, pronotum and anterior portion of elytra, dorsal view **F** pronotum with reticulate surface structure, dorsal view.

and prominent, strongly protruding laterad, bluntly drop-shaped; metacoxae smaller and less protruding laterad; femora, tibiae, and tarsi with short setae; tibiae with a few additional longer setae; distal tarsal segments with several longer setae near apex; claws large, strongly curved, base with two small teeth.

Abdomen. Abdominal intercoxal process moderately longer than length of ventrite 1 posterior of metacoxae, very wide, anteriorly widely arcuate, with rows of deep large punctures along anterior margin; ventrite 1 longest; ventrite 2 ca 0.75 × as long as ventrite 1; ventrite 3 ca 0.88 × as long as ventrite 2; ventrite 4 ca 0.75 × as long as ventrite 3; ventrite 5 as long as combined lengths of ventrites 3 and 4. Surface of ventrites 2–5 with sparse punctures and setigerous flat, more or less cordiform granules; punctures more distinct on mesal portion; granules more prominent and more conspicuous laterally; ventrite 5 granulate. Male sternite IX ca 340 μm long; apical margin arcuately, but distinctly emarginated; lateroapical portion with a few moderately long setae; paraprocts not reaching beyond apical margin. Tergite VIII finely reticulate, with conspicuous median transverse ridge separating posterior and anterior portion; basal half with microtrichial pattern; apical margin hyaline, with subapical fringe of hair-like setae; setae on sublateral portions stronger and longer than those along margin.

Aedeagus (Fig. 13A, B) ca 350 μm long; penis (including lateral basal apophyses) ca 2.85 × as long as phallobase, gradually tapering apicad; apical half moderately curved ventrad (LV), dorsolateral portion with only a few very short setae; apex narrowly rounded; lateral basal apophyses long; ventral sac large; fibula conspicuous, moderately wide; surface of endophallus with spinules; corona indistinct. Phallobase asymmetrical; parameres moderately exceeding middle of penis, widest near base, narrowed to apex; dorsal margin arcuate; ventral margin feebly sinuate; apex narrowed and rounded; mesal and outer surface of parameres with short setae.

Description of ovipositor (Fig. 14A–C)**.** Ovipositor ca 490 μm long; stylus narrow and long, almost straight, ca 0.50 × as long as coxite (compared to the length of distal portion of coxite). Coxite moderately long and stout, rounded at posterolateral angle; distal portion ca 2.70–2.90 × as long as wide near middle, slightly bent, with numerous short stout peg-like setae and with a few thinner peg-like setae; latter mainly at apical portion; inner margin moderately pubescent; proximal portion ca 0.70–0.80 × as long as distal portion, with peg-like and short, fine hair-like setae. Transverse baculum well sclerotised; longitudinal baculum of paraprocts (valvifers) ca 1.04–1.19 × as long as coxite (measured from apical margin of coxite to point where it is joining the transverse baculum).

Secondary sexual dimorphism. Not strongly pronounced. Females on average longer and wider than respective males, with longitudinal depression of metaventrite narrower and shallower. Ventrite 5 in females longer and narrower than in males.

Variability. The specimens vary moderately in size (Tabs 4, 5). The elytral coloration exhibits, in contrast to *Ancyronyx sarawacensis*, only minor variation: some specimens have a larger yellowish anterior margin, oblique yellowish stripes and yellowish apices. In the genitalia, we detected only minor variability in the form of the penis. However, the dataset is too limited for a well supported statistical analysis.

Habitat. The type locality is a shallow meandering river of about 10 m width flowing through primary forest, with stony substrate and plenty of submerged wood (Fig. 11A). Specimens were collected exclusively from submerged wood predominatly in stream reaches with relatively strong current. The specimens from Brunei were collected in a very similar habitat – an upland headwater stream in (slightly disturbed) primary forest (Fig. 12A); the small piece of submerged wood from which the specimens were collected was found in a very shallow, slowly flowing reach (Fig. 12A). A single female was collected from submerged wood in fast flowing, shallow water in a small tributary in primary rainforest (280 m a.s.l.) near the Maliau Basin, Sabah. The altitude of all collection sites ranges from 60–300 m a.s.l. The limited number of collection sites suggests that this species is restricted to rather pristine forest streams at lower altitudes.

Syntopic taxa. At the type locality specimens were collected together with *Ancyronyx acaroides*, *A. procerus* and *A. sarawacensis*, all found on the same submerged tree trunk. Some species of *Graphelmis* Delève (Elmidae), *Elmomorphus* Sharp and *Stenomystax* Kodada, Jäch & Čiampor (Dryopidae) also occurred in the same microhabitat. However, in Temburong, besides *Ancyronyx acaroides*, and *A. sarawacensis*, no other species were collected from exactly the same piece of submerged wood.

Distribution. This species is presently known from a few localities in northern Borneo: Brunei, Sabah and Sarawak.

Etymology. The species is named after Clister V. Pangantihon of the Ateneo de Manila University (Philippines), assistant at Taxon Expeditions, who discovered the new species during the expedition to Brunei. The name was selected by Taxon Expedition participants, instructors and staff of the Kuala Belalong Field Studies Centre in recognition for Clister's discovery and his most appreciated engagement and friendly care for the expedition participants.

Ancyronyx sarawacensis Jäch, 1994

Type locality (Fig. 11C). Small stream, ca 3 m wide, flowing through degraded primary forest above the village of Arur Dalan near Bario, ca 1000 m a.s.l., Kelabit Highlands, northern Sarawak, Borneo, Malaysia.

Material examined. Adults. *Holotype* ♂ (NMW): "Malaysia, Sarawak 1993 Kelabit HL. Umg. Bario, 26.2., ca 1000 m leg. M. Jäch (14)". *Paratypes* (NMW, CKB): 1 ♀, 2 unsexed exs: "Malaysia, Sarawak 1993 Kelabit HL., 5 km E Bario Pa Ukat, 27.2., 1000 m leg. M. Jäch (15)"; 1 ♂, 1 ♀: "MALAYSIA, Sarawak 1993 Kelabit HL., 5 km E Bario Pa Ukat, 1.3., 1000 m leg. M. Jäch (17)"; 1 ♂, 5 unsexed exs: "Malaysia, Sarawak Mulu NP, Long Iman 4.3.1993 leg. M. Jäch (20)"; 4 ♂♂, 2 ♀♀, 8 unsexed exs: "Malaysia – Sarawak 40 km E Kapit III. 1994 leg J. Kodada / Rumah Ugap Ng marating Kapit Sut".

Additional material (BOR/COL, CCB, CFDS, CFM, CKB, NMW, UBDM, RMNH). **SARAWAK:** 1 ♂: "Malaysia, Sarawak, Marudi distr., Gunung Mulu NP, 16.10.2018, (40) 04.0267N, 114.8234E, 55 m a.s.l., small stream, J. Kodada &

D. Selnekovič lgt.”; 1 ♂ [FZ1634, MK505407], 1 ♀ [38, MK505398], 1 ♂ [39, MK505401]: “Malaysia, Sarawak, Miri distr., Bario env., 20.06./24.06.2018, (7) 03.76665N, 115.45371E 1146 m a.s.l., Arur Takang, J. Kodada & D. Selnekovič lgt.”; 1 ♂: “Malaysia, Sarawak, Miri distr., Bario env., 20.06.2018, (8) 03.76567N, 115.45215E 1121 m a.s.l., Arur Takang, J. Kodada & D. Selnekovič lgt.”; 1 ♂ [FZ1641, MK505414], 1 ♀: “Malaysia, Sarawak, Miri distr., Ramudu env., 27.06.2018, (16) 03.56813N, 115.49488E 919 m a.s.l., Pa’Ngaruren riv., J. Kodada & D. Selnekovič lgt.”; 1 ♂ [FZ1633, MK505406], 2 ♀♀: “Malaysia, Sarawak, Miri distr., Bario env., 19.06.2018, (6) 03.74350N, 115.43137E 1131 m a.s.l., Pa’Ramapoh, J. Kodada & D. Selnekovič lgt.”; 1 ♂ [82, MK566773], 1 ♂ [83, MK566771], 9 ♂♂, 9 ♀♀: “Malaysia, Sarawak, Miri distr., Bario env., 5.10.2018, (33) 03.759617N, 115.440233E 1143 m a.s.l., Arur Dalan, J. Kodada & D. Selnekovič lgt.; 1 ♂, 1 ♀: “Malaysia, Sarawak, Miri distr., Bario env., 22.06.2018, (10) 03.76245N, 115.43778E 1167 m a.s.l., Arur Dalan, J. Kodada & D. Selnekovič lgt.”; 7 ♂♂, 7 ♀♀: “Malaysia, Sarawak, Miri distr., Bario env., 21.06.2018, (9) 03.76894N, 115.44592E 1171 m a.s.l., Pa’Marario, J. Kodada & D. Selnekovič lgt.”; 3 ♂♂, 4 ♀♀: “Malaysia, Sarawak, Miri distr., Ramudu env., 26.06.2018, (14) 03.54745N, 115.49052E 921 m a.s.l., Pa’Kasi riv., J. Kodada & D. Selnekovič lgt.”; 1 ♂, 4 ♀♀: “Malaysia, Sarawak, Miri distr., Ramudu env., 28.06.2018, (18) 03.54745N, 115.49052E 921 m a.s.l., Pa’Kasi riv., J. Kodada & D. Selnekovič lgt.”; 1 ♀ [FZ1642, MK505418], 1 ♂ [FZ1643, MK505415], 1 ♀: “Malaysia, Sarawak, Miri distr., Pa’Lungan, 30.06.2018, (20) 03.81132N, 115.50737E 1103 m a.s.l., Petarutun riv., J. Kodada & D. Selnekovič lgt.”; 1 ♂ [FZ1635, MK505422]: “Malaysia, Sarawak, Miri distr., Pa’Ukat, 25.06.2018, (13) 03.77346N, 115.47572E 1118 m a.s.l., J. Kodada & D. Selnekovič lgt.”; 1 ♂ [FZ1628, MK505420], 1 ♀ [9, MK505396], 1 ♂ [10, MK505409], 15 ♂♂, 14 ♀♀: “Malaysia, Sarawak, Kuching distr., Bayur riv. near Kampung Bayur, 20.10.2018, 1°14'42.33"N, 110°17'35.26"E 40 m a.s.l., J. Kodada & D. Selnekovič lgt.”; 1 ♀ [FZ1645, MK505404], 1 ♂ [FZ1646, MK505397], 1 ♂ [35, MK505399], 1 ♀ [36, MK566772]: “Malaysia, Sarawak, Kuching distr., Kampong Jangkar env., 10.7.2018, (29) 01.65911N, 109.70829E 67 m a.s.l., J. Kodada & D. Selnekovič lgt.”; 1 ♂ [FZ1636, MK505394]: “Malaysia, Sarawak, Miri distr., Ramudu env., 26.06.2018, (14) 03.54745N, 115.49052E 921 m a.s.l., Pa’Kasi riv., J. Kodada & D. Selnekovič lgt.”. **SABAH:** 50 ♂♂, 46 ♀♀: “Malaysia, Sabah, (Borneo), Kuamut river env. near Kampung Pisang Pisang, 3.-4. VI. 1996, 14a: shaded stream in primary forest with submerged wood”; 12 ♂♂, 4 ♀♀: “Malaysia, Sabah, Kuamut river env. near Kampung Pisang Pisang, 3.-4. VII. 1996, 14b: ca 10 m wide tributary of Kuamut River in primary forest.”; 2 ♂♂, 1 ♀: “Malaysia, Sabah, ca 7 km S Sapulut, Saupi riv. in primary forest, 15.5.2001, J.F. Kočiam leg.”; 1 ex. (sex not examined) [FZ1651, MK505400]: “Malaysia, Sabah, Tawau Division (Kalabakan), 10.7.2018, (MY16-MAL40) 04.560750N, 117.158367E 210 m a.s.l., Čiampor & Čiamporová-Zaťovičová lgt.”; 1 ♂, 2 ♀♀: “Malaysia: Sabah: Maliau Res. Center.: Belian trail; small Maliau R. tributary; bottom gravel, riffle; ca 4°44'15"N, 116°58'15"E, 220 m a.s.l., 27.Sep2017, leg. H. Freitag, C.V. Pangantihon, I. Njunjić et al. / Taxon Expeditions (MRC2c)M”; 2 ♀♀: “Malaysia: Sabah: Maliau Basin: Aga-

tis River; subm. wood, run; ca 4°41'51"N, 116°54'30"E, 520 m a.s.l., 02.Oct2017, leg. C.V. Pangantihon & I. Njunjić / Taxon Expeditions (AgtR2f)M.". **Brunei:** 1 ♂, 1 ♀: "Brunei: Temburong, Belalong River tributary Sungai Sibut; W of Ashton Trail, root packs, run; 4°32'38"N, 115°08'51"E, 170 m a.s.l.; leg. H. Freitag & W.C. Hayden / Taxon Expeditions 29.Sep2018 (SiCg)M"; 2 ♂♂, 2 ♀♀ [H39, LR735553]: "Brunei: Temburong; Belalong River near UBD field station 4°32'49"N, 115°09'30"E, ca 100 m a.s.l.; primary forest; submerged wood in run; leg. Pangantihon / Taxon Expeditions 28.Sep2018 (BeR1f)M".

Diagnosis. *Ancyronyx sarawacensis* is a moderately large, usually yellowish species with a pronounced variability of coloration and body size (Figs 3C, D, 4A–D; Tabs 4, 5). From the most similar *A. clisteri* sp. nov., *A. sarawacensis* differs mainly in: 1) anterior elytral portion with expanded yellowish area, much larger than in *A. clisteri* sp. nov.; 2) ovipositor with shorter and wider distal portion of coxite which is ca 1.5–1.6 × as long as wide near middle; 3) proximal portion of coxite subequal in length to distal portion; 4) longitudinal baculum of paraprocts ca 1.3–1.4 × as long as entire coxite length; 5) about 9% divergence of the partial mtDNA for cytochrome c oxidase subunit COI. In the direct comparison the apex of the penis appears to be wider and less pointed in *A. sarawacensis.*

Redescription of the holotype. Body form moderately elongate; elytra moderately convex dorsally, shiny, with highest point in 0.45 of elytral length; BL: 1.45 mm, EW: 0.71 mm, BL/EW: 2.04.

Coloration (Fig. 3C). Labrum, mouth parts, antennae, clypeus and anterior half of frons yellowish; remaining portions of cranium black; pronotum yellowish with large mesal black spot, spot narrowed near middle; scutellum brownish. Elytra with lateral margin and epipleura black along anterior half; dorsum extensively yellowish with six black spots: a small elongate sutural spot behind scutellum; a second, elongate narrow sutural spot on elytral declivity; two lateral, suboval spots extending within elytral striae 3–9 from anterior third slightly behind middle length of elytra; two subapical small spots within elytral striae 4–5. Mesanepisterna, metanepisterna, lateral portion of metaventrite and lateral portions of ventrite 1 black; coxae yellow; femora black on distal sixth, yellowish on remaining surface; tibiae dark in proximal half and near articulation with tarsi, yellowish in distal portion; tarsomeres 1–2 darker; tarsomeres 3–5 and claws yellowish.

Head. Labrum shorter than clypeus; anterior margin almost straight; surface with fine irregular punctation, finely setose. Clypeus wide, densely punctate; sides rounded. Frons and vertex densely, finely punctate, reticulate; reticulation more distinct on black portion of vertex; surface with narrow, elongate distinct granules; frontoclypeal suture almost straight, finely impressed. Eyes well protruding, with large facets, semicircular in outline; HW: 0.38 mm, ID: 0.20 mm. Antennae 11-segmented, 0.46 mm long, moderately longer than pronotum; ratio of length of antennomeres 1–11: 0.055 : 0.061 : 0.042 : 0.030 : 0.031 : 0.030 : 0.029 : 0.029 : 0.032 : 0.037 : 0.089 mm. Gena microsculptured; gula narrow, smooth; gular sutures indiscernible; posterior tentorial pits deep and large.

Thorax. Pronotum distinctly wider than long (PL/MW: 0.81), widest near middle; anteriorly attenuate; anterior margin strongly arcuate; most of hypomeral portion visible in dorsal view; anterior transverse groove deep, oblique, dividing pronotum; area anterior and posterior of transverse groove strongly gibbous; anterior mesal longitudinal carina absent; posterolateral oblique grooves strongly impressed (Fig. 6E, F). Pronotal surface densely punctate and irregularly reticulate on disc, with flat cordiform granules mainly in lateral and anterior portion; granules rather irregularly spaced; anterior and posterior portion smooth; prescutellar pits round and deep; PL: 0.42 mm, MW: 0.52 mm. Prosternum densely and roughly punctate; anterior portion very short; prosternal process distinctly transverse, almost flat, slightly protruding posteriad; posterior margin widely rounded. Scutellum subpentagonal; surface smooth and moderately elevated. Elytra elongate; EL: 1.06 mm; sides slightly narrowed at ca anterior 0.4, then gradually convergent to rounded apices; each elytron with ten more or less regular rows of punctures; six rows between suture and shoulder; accessory scutellary rows absent (Fig. 6C); punctures large, round and deeply impressed on disc and laterally, smaller and less distinct anteriorly and posteriorly; interstices and intervals wider and flat on disc, narrower and slightly convex laterally and posteriorly; surface shiny; humeri prominent. Mesoventrite almost flat, less than half as long as prosternum along midline; mesoventral cavity shallow and narrow; surface strongly and irregularly punctate; mesoventral discrimen invisible. Metaventrite along midline distinctly longer than combined length of prosternum and mesoventrite; anterior margin arcuate; disc with large mesal longitudinal depression; discrimen depressed; surface of disc glabrous, with fine, scarce punctures; large, deep irregular punctures along anterior margin and on lateral portions of metaventrite; punctures coarser and denser laterally (Fig. 6D). Hind wings fully developed. Forelegs about 1.54 × as long as body length; claws large and robust, with one small subbasal and one hardly discernible, basal tooth.

Abdomen. Intercoxal process longer than length of ventrite 2, very wide, anteriorly widely arcuate, with rows of deep large punctures along anterior margin; ventrite 1 longest; ventrite 2 ca 0.75 × as long as ventrite 1; ventrite 3 ca 0.88 × as long as ventrite 2; ventrite 4 ca 0.75 × as long as ventrite 3; ventrite 5 ca as long as combined lengths of ventrites 3 and 4. Surface of ventrites 2–5 with sparse punctures and setigerous, flat, more or less cordiform granules; punctures more distinct on mesal portion, granules more prominent and more conspicuous laterally. Male sternite IX ca 340 μm long, asymmetrical; apical margin distinctly arcuately emarginated; lateroapical portion with short setae; paraprocts not reaching beyond apical margin. Tergite VIII finely reticulate, with conspicuous median transverse ridge separating posterior and anterior portion; basal half with microtrichial pattern; apical margin hyaline, with subapical fringe of hair-like setae; setae on sublateral portions stronger and longer than those along margin.

Aedeagus (Figs 15A, B, 16A, B) ca 358 μm long; penis about 2.63 × as long as phallobase; sides subparallel from base to apical fourth then gradually tapering apicad; apical half moderately curved ventrad; dorsolateral portion only with few very short setae; apex narrowly rounded; lateral basal apophyses long; ventral sac large; fibula long and narrow; surface of endophallus with numerous almost regularly arranged, small

spines; corona not discernible in endophallus repose. Entirely extruded endophallus more than twice as long as aedeagus, asymmetrical (description based on one specimen (CKB) from the type locality); most of the following characters of the endophallus, even if it is extruded, are difficult to observe and clearly visible in Fig. 10G: supporting sclerites of endophallus thin; ventral and dorsal bladders bulbous, extending less than half of penis length, with few very fine short thin setae; distal portion of endophallus tubular, very long; apex narrowed and supported by a fine elongate sclerite near gonopore (Fig. 10G). Phallobase asymmetrical; parameres moderately exceeding midlength of penis, widest near base, narrowed to apex; dorsal and ventral margin sinuate; apex narrowed and rounded; outer surface of parameres with short setae.

Description of ovipositor (Fig. 17A–C). Ovipositor in females from the type locality ca 435 μm long; stylus (gonostylus) narrow, straight, about 0.7 × as long as distal portion of coxite. Coxite short and stout; posterolateral angle rounded, not protruding. Distal portion of coxite ca 1.5–1.6 × as long as wide, moderately bent; surface with numerous conspicuous peg-like/spine-like setae; apical area with few moderately long trichoid and few thinner peg-like setae; inner margin moderately pubescent. Proximal portion of coxite about as long as distal portion, with numerous stout peg-like and trichoid setae; transverse baculum well sclerotised; longitudinal baculum of paraprocts ca 1.3–1.4 × as long as coxite length.

Secondary sexual dimorphism. Not strongly pronounced. On average, females are longer and wider than the males (Tabs 4, 5). Females possess narrower and shallower longitudinal depression of the metaventrite, and their terminal ventrite is longer and narrower than in males. All these differences named here refer to syntopic specimens.

Variability. In addition to the metric characters (Tabs 4, 5), adults of *Ancyronyx sarawacensis* vary in color pattern, body form and surface structures. This is obviously dependent on altitude and water temperature. Specimens from the Kelabit Highlands usually exhibit a more extensively black cranium, their pronotal spot is usually not or less distinctly divided, the elytral spots are wide (Fig. 3D). Generally, any fusion of elytral spots is rather rarely seen and if, then only the three posterior spots fuse. The elytral surface appears shinier and smoother; the anterior transverse pronotal groove is deep, and areas anterior and posterior of these grooves are strongly gibbous, and their body form appears generally shorter and more convex. In comparison, the specimens from Sarawak and Brunei lowlands (Gunung Mulu NP, Kapit area, Kampong Bayur, Kampong Jangkar, Temburong) usually have a paler cranium, and their pronotal spots are more distinct, smaller and isolated (Fig. 4B–D). Furthermore, their elytral surface is less shiny, and their interstices are narrower, the pronotum is almost flat and the body appears overall slenderer. Specimens from Sabah uplands (Figs 3D, 4A) tend to have darker heads and pronota and separately fused large anterior and posterior elytral spots, their color pattern is very similar to those of *A. clisteri* sp. nov. Pronota of these specimens are usually more convex, similar to those of the specimens from the Kelabit Highlands.

Material examined. Larva. Nine larvae of three different sizes/instars including the larva used in the DNA analysis (CKB): "Malaysia, Sarawak, Miri distr., Bario env., 5.10.2018, (33) 3.759617N, 115.440233E 1143 m a.s.l., Arur Dalan, J. Kodada &

D. Selnekovič lgt". For the description, the two largest larvae, probably representing last instars, were selected.

Matching of developmental stages. All larvae were collected together with adults at the type locality. One larva [FZ1631, MK505395] was compared with adults of *A. sarawacensis* based on partial COI mtDNA sequences.

Diagnosis of mature larva (Figs 7A, 8A, 9E–G, 10A–F, H). Body elongate, tapered dorsad; length from anterior margin of head to apex of abdomen: 4.43 mm; largest width across metanotum: 1.01 mm; body ventrally almost flat, dorsally convex; dorsal sagittal line present from prothorax up to sixth abdominal segment (Fig. 7A). Ratio of length of thoracic segments and abdominal segment IX: 0.60 : 0.35 : 0.32 : 0.84 mm; lengths of all remaining abdominal segments between 0.21 and 0.26 mm. Thoracic segments II and III with flattened lateral tergal processes (Fig. 7B); abdominal segments I–VIII with conical prominent bent lateral tergal processes (Figs 7A, 9I). All spiracles small and subequal in form and size, biforous, situated at ends of prominent spiracular tubes on mesothorax and abdominal segments I–VIII (Figs 7A, B, 9I). Dorsum densely covered with flat setiferous tubercles except for rugose distal portion of terminal segment (Fig. 7B). Antennae and legs very short (Fig. 8A, B). Prevailing ground color (Fig. 7A) yellowish-brown combined with dark brown patterns on frons, adjacent portion of epicranium, posterior two thirds of pronotum; meso- and metanotum each with four pairs of dark brown signae (Fig. 7B); genae very pale, almost white; abdominal segments I–VIII with two dorsolateral pairs of dark brown signae and with brownish spot near middle, dark coloration increasingly inconspicuous posteriorly (Fig. 7A); segment IX pale brown on anterior portion, dark brown apically (Fig. 7A). In contrast to previous darker patterns, anterior third of pronotum, dorsolateral portions of cranium, middle portion of abdominal segment IX as well as appendages and entire venter paler yellowish.

Head prognathous, partly retractable, distinctly narrower than pronotum (Fig. 9A); maximum head width 0.55 mm. Labrum very short, ca 2.5 × as wide as long, separated from head capsule by complete suture, anterior margin arcuate, middle with transverse row of moderately long, ramified setae (Fig. 9B); clypeus subequal in length with labrum, with a row of pilose setae along posterior margin; frontoclypeal suture complete. Anterior margin of frons arcuate, with a row of moderately long, pilose setae; anterolateral angles form short conical projections, each projection with one distinct peg-like pilose seta. Frontal arms broadly V-shaped, well impressed, epicranial stem absent (Fig. 7B); surface of frons and adjacent area of epicranium with cordiform tubercles, which are distinct, flattened and provided with short scale-like setae (Fig. 9A); anterolateral portion with one moderately long trichoid seta. Setal pattern on epicranial plates: one moderately long trichoid seta near dorsal margin of stemmata; one at 0.6 of cranial length near frontal arm; one ventral near antennal insertion; four long and very conspicuous trichoid setae on lateroventral portion; several simple spine-like setae on lateral/laterodorsal portion, mostly widely spaced, four of them arranged in an oblique laterodorsal row; genae with several spine-like slightly serrate/pilose setae on ventral portion. Antennae (Fig. 9C, D, G) three-segmented, short, approximately 0.25 × as long as maximal head width. Scape (Fig. 9C, D) elongate, moderately longer
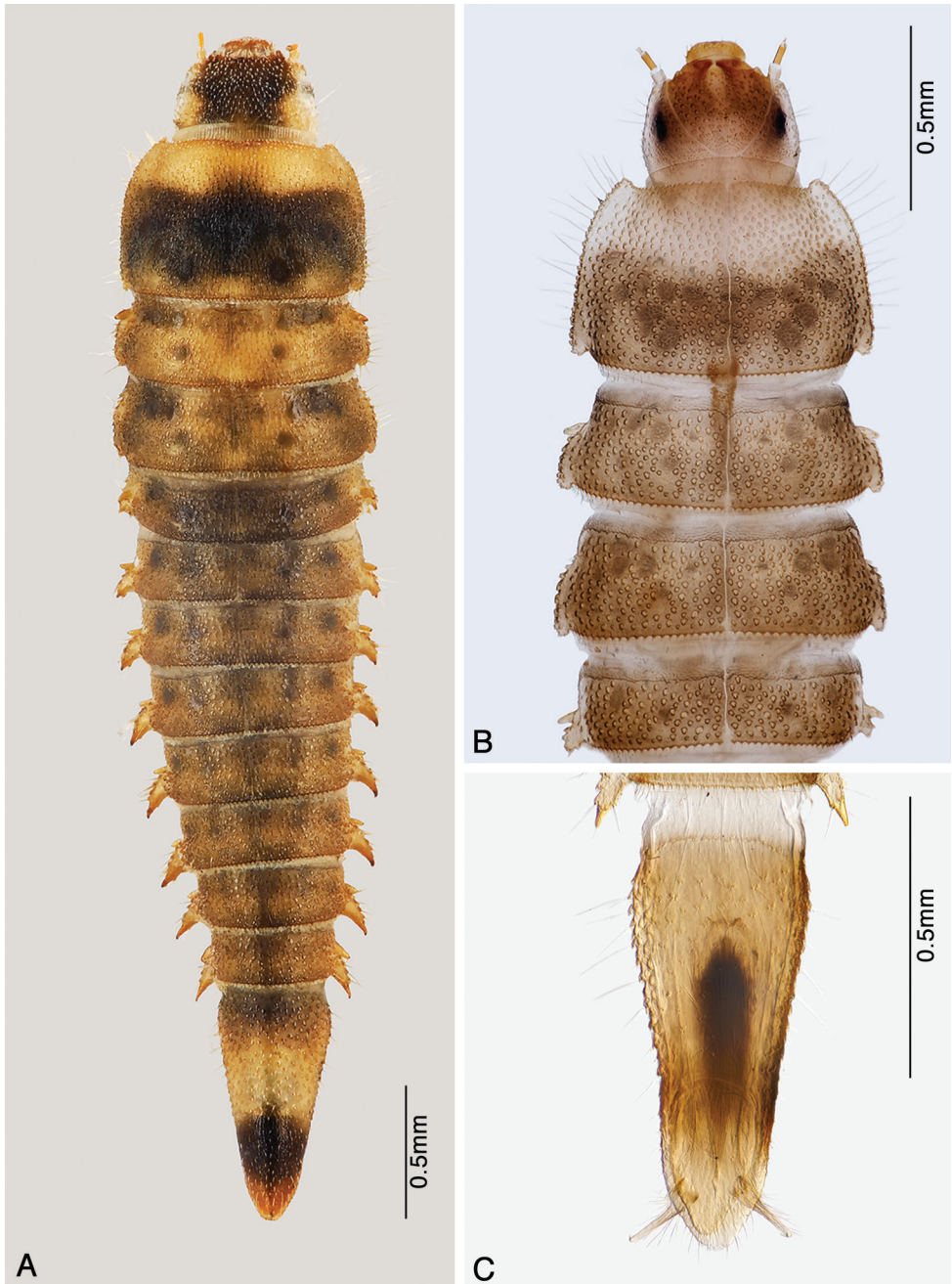
Figure 7. *Ancyronyx sarawacensis*, larvae from the type locality: **A** final instar, dorsal view **B** pre-final instar, cleared specimen mounted on microscopic slide, detail of anterior portion, dorsal view **C** same specimen, terminal abdominal segment showing hooks of operculum, ventral view.

Figure 8. *Ancyronyx sarawacensis*, larvae from the type locality, SEM micrographs: **A** final instar, ventral view **B** pre-final instar, lateral view.

than wide, with three moderately ramified setae around distal margin (two trichoid setae of varying length and a single, moderately long, pointed peg-like seta); pedicel narrow, cylindrical and about 1.5 × as long as scape, distally with two minute peg-like setae (Fig. 9G); flagellum and sensorium subequal in length, both elongate and about 4 × as long as wide; terminal segment with minute setae. Stemmata arranged in a single unified lateral spot, not exposed (Fig. 9A). Mandibles (Fig. 13C) short, distinctly longer than wide, left and right mandible almost symmetrical; apices wide, tridentate, ventral and dorsal teeth continuing in ventral and dorsal carina; right mola convex and prominent, left mola flat, asperities absent; articulated process setose, robust, half as long as mandible. Penicillus with moderately long, thin, setae, densely arranged in a row along mesal portion; outer mandibular edges arcuate, each bearing four conspicuous ramified setae; ventral condyles robust and prominent.

Ventral side of cranium (Fig. 9E) with strong hypostomal ridge extending posteriad into robust hypostomal rods; the latter exceeding middle of cranium; oblique row of 3–5 short stout peg-like setae situated posteriad of hypostomal rods. Posterior tentorial pits small, gular sutures absent. Maxilla elongate, large, almost half as wide as mentum (across stipes); cardo very short, transverse, almost perpendicular to stipes. Stipes elongate, with several different setae (Fig. 9F): one short ramified seta near base; four moderately long, extensively ramified setae in a submarginal row along anterior half; few conspicuous long trichoid setae on anterior fourth; palpifer well sclerotised, short and wider than palpomeres, apical portion with two spine-like setae. Maxillary palp three-segmented (Fig. 9E), distinctly shorter than stipes width; palpomeres with a few short trichoid setae, terminal palpomere with several small peg-like sensilla. Galea undivided, elongate, about 2 × as long as wide; apex narrowed and rounded, with row of several moderately bent spines and numerous short, mesally directed setae; dorsal surface with cluster of dense thin setae. Lacinia subequal to galea in form and length; apex with dense, strong spines. Labium with very short and transverse submentum oriented vertically to mentum. Mentum (Fig. 9E) about 1.6 × as long as wide; widest at anterior third; median portion shallowly impressed, laterally with row of six moderately long, extensively ramified setae in anterior 0.6 and a single moderately long trichoid seta at anterior third; anterolateral portion with one distinct stout peg-like seta on each side; disc of mentum with pair of mesal, longitudinal rows of five trichoid and ramified setae. Ligula with mesal longitudinal line, about as long as lacinia, with four short peg-like setae; anterior margin arcuate and densely setose; labial palp very short; apical segment similar to that of maxillary palp; palpiger undifferentiated.

Pronotum (Fig. 7A, B) 1.5 × as wide as long; posterior half with seven pairs of partly fused small and rather inconspicuous areas (signa) with irregular polygonal reticulation (Fig. 9H); three pairs of erected trichoid setae present on disc and one pair on posterolateral position; lateral margins fringed with long trichoid setae. Meso- and metanotum more than 3 × as wide as long, distinctly shorter than pronotum, each with five pairs of partly fused signa and one posterolateral and two admedian pairs of long erected trichoid setae; sides projected laterally, fringed with long setae; surface with tubercles. Posterior margins of all nota dentate, fringed with row of scale-like setae. Ventral side of prothorax with small triangular presternum (Fig. 8A) and three hardly identifiable
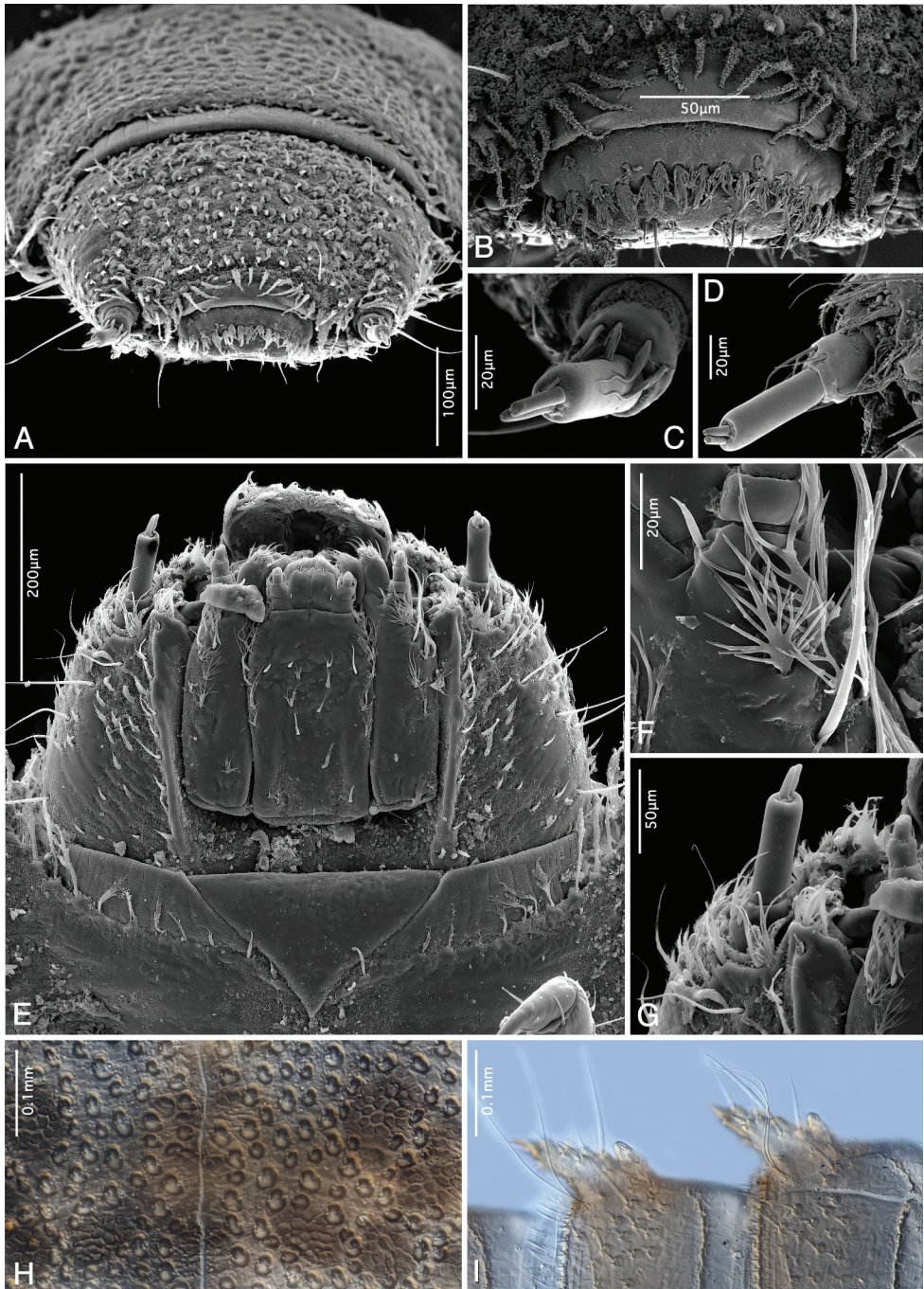
Figure 9. *Ancyronyx sarawacensis*, larvae (pre-final instar) from the type locality, SEM micrographs and cleared microscopic slide mounts: **A** head, frontal view **B** labrum, frontal view **C** left antenna, frontal view **D** right antenna, in rotaded view **E** final instar, head, ventral view **F** detail of ramified setae on anterior portion of stipes, ventral view **G** antenna, ventral view **H** detail of surface structure of prothorax, dorsal view **I** lateral portion of abdominal segments VI and VII, ventral view.

sclerites: one large anterolateral sclerite on each side and one small transverse sclerite on posteromesal portion; sclerites completely surrounding coxae, connate, more or less discernible in cleared specimen only. Ventral portions of both, meso- and metathorax, with six sclerites (Figs 8A, 10A): two large anterior sclerites divided by fine line mesally; each side with one small anterolateral sclerite and one large lateral sclerite; the latter projecting moderately at posteromesal portion; anteromesal sclerites with rows of short spine-like setae along posterior margin. Legs (Figs 8A, B, 10A) stout, five-segmented, about 0.5 × as long as thorax width, all similar in shape and length. Coxae large, distinctly wider than long, subellipsoidal; mesal portion moderately projecting ventrad; surface with a few short setae. Trochanters subconical, each with a single long trichoid seta on distal third. Femora subcylindrical with scattered short peg-like setae, most of them with serrate/setose margins (Fig. 10D, E); largest setae concentrated on inner portion and around distal margins. Tibiotarsi subcylindrical, narrower than femora, subequal in length with trochanters and femora; surface with several different trichoid setae in distal portion and a pair of distinct, very closely set trichoid seta (Fig. 10B, C). Pretarsi elongate, moderately bent, each with a single long trichoid seta.

Abdominal segments I–VIII similar in shape, each distinctly wider than long, subrectangular; sagittal line visible in segments I–VI; lateral tergal processes of segments I–VIII conical, prominent and bent with dorsally directed pointed tip (Figs 7A, 8A); surface with asperities, stout setae and short spines; processes of subsequent segments moderately increase in size. Posterior margins of terga dentate and each fringed with scale-like setae. Ventral portion of segment I–VII with three well differentiated sclerites; median sclerite (sternite) of segment I widest, about 2.8 × as wide as a lateral sclerite (pleurite); sternites moderately narrowed posteriad, pleurites distinctly narrowed posteriad; pleurites of segments VIII–IX completely fused with tergites and sternites. Ventral surface with numerous stout short spines and several longer thinner trichoid setae; the latter concentrated on posterolateral portion; segments I–VIII with a pair of long, very closely set trichoid setae near basis of lateral process (Figs 9I, 10F); posterior margins of segments dentate and fringed with scale-like setae. Terminal segment (Figs 7A, C, 10F) 2.1 × as long as wide, widest at anterior 0.15, subconical; subtriangular in cross-section; apex narrowed. Dorsal surface with flat setiferous tubercles; the latter large and distinct on anterior two thirds, absent or inconspicuous on posterior third; setae on tubercles short; setae along lateral margins long and very distinct; several moderately long erect-trichoid setae intermixed within granules on admedian portion. Ventral side with scattered, short or moderately long trichoid setae. Operculum (Fig. 10F) elongate, subtriangular, almost 2 × as long as wide, slightly impressed medially, rugose; lateral and apical margins with trichoid setae; internally inserted pair of hooks half as long as operculum (Fig. 7C); each hook with two clusters of longitudinally arranged trichoid setae near base.

Variation between larval instars. The pre-final instars are shorter (3.85 mm) with narrower head (HW: 0.43 mm) and exhibit more evenly brown color from the posterior pronotal portion up to the anterior portion of segment IX. The pale anterior portion on the pronotum extends up to half of the pronotal length. Segment IX is relatively slender and 2.3 × as long as wide vs. ratio 2.1 in the final instar. The triangular presternum is not yet clearly delimited.
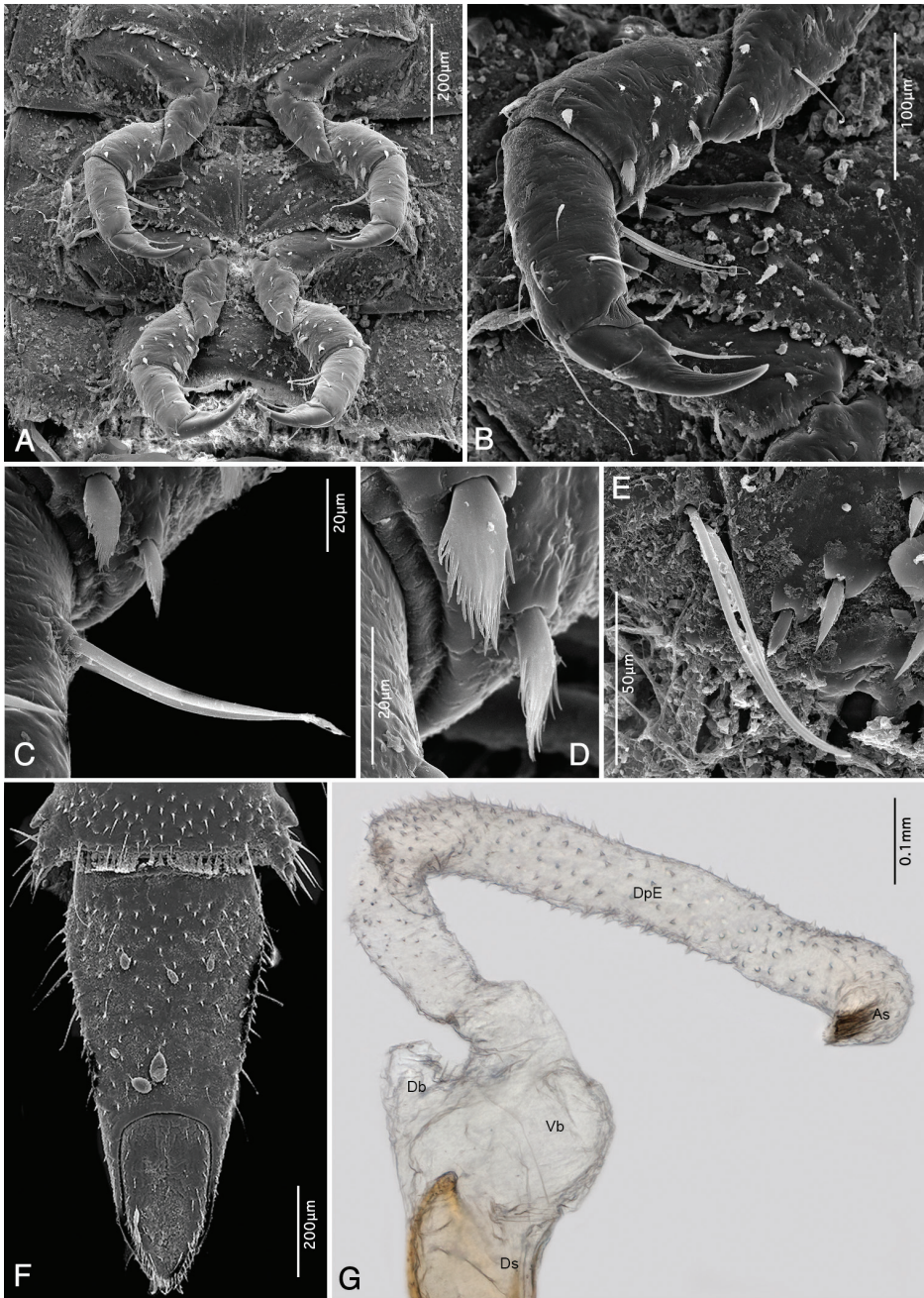
Figure 10. *Ancyronyx sarawacensis* **A–F, H** final instar larvae from the type locality, SEM micrographs and cleared microscopic slide mounts, **G** everted endophallus: **A** meso- and metathorax with legs, ventral view **B** right middle leg, detail, ventral view **C** detail of twin setae on tibiotarsus, ventral view **D** detail of pilose setae on femur, ventral view **E** detail of twin setae on pleurite VI, ventral view **F** terminal abdominal segment, ventral view **G** extruded endophallus, dorsolateral view. Abbreviations: Ds: dorsal sac-supporting sclerite, Vb: ventral bladder, Db: dorsal bladder, DpE: distal portion of endophallus, As: apical sclerite (according to Hayashi and Yoshitomi 2015).

Figure 11. Habitats of *Ancyronyx clisteri* sp. nov. and *A. sarawacensis*: **A** type locality of *A.clisteri* sp. nov., tributary of the Kuamut River near Kampung Pisang Pisang, Sabah **B** atypical locality of *A. sarawacensis*, shaded shallow stream in primary forest, Gunung Mulu NP, Sarawak **C** type locality of *A. sarawacensis*, small stream above Arur Dalan near Bario, Kelabit Highlands, Sarawak.

Figure 12. Habitats of *Ancyronyx clisteri* sp. nov. (**A**) and *A. sarawacensis* (**B, C**) sampled during Taxon Expeditions: **A** Sibut Creek (tributary of Belalong River), Temburong, Brunei, microhabitat (piece of submerged wood from which *A. clisteri* sp. nov. was collected) **B** Belalong River near Kuala Belalong Field Studies Centre, Temburong **C** Agatis River in the vicinity of Maliau Basin, Sabah, Malaysia. All photographs by Clister V. Pangantihon.
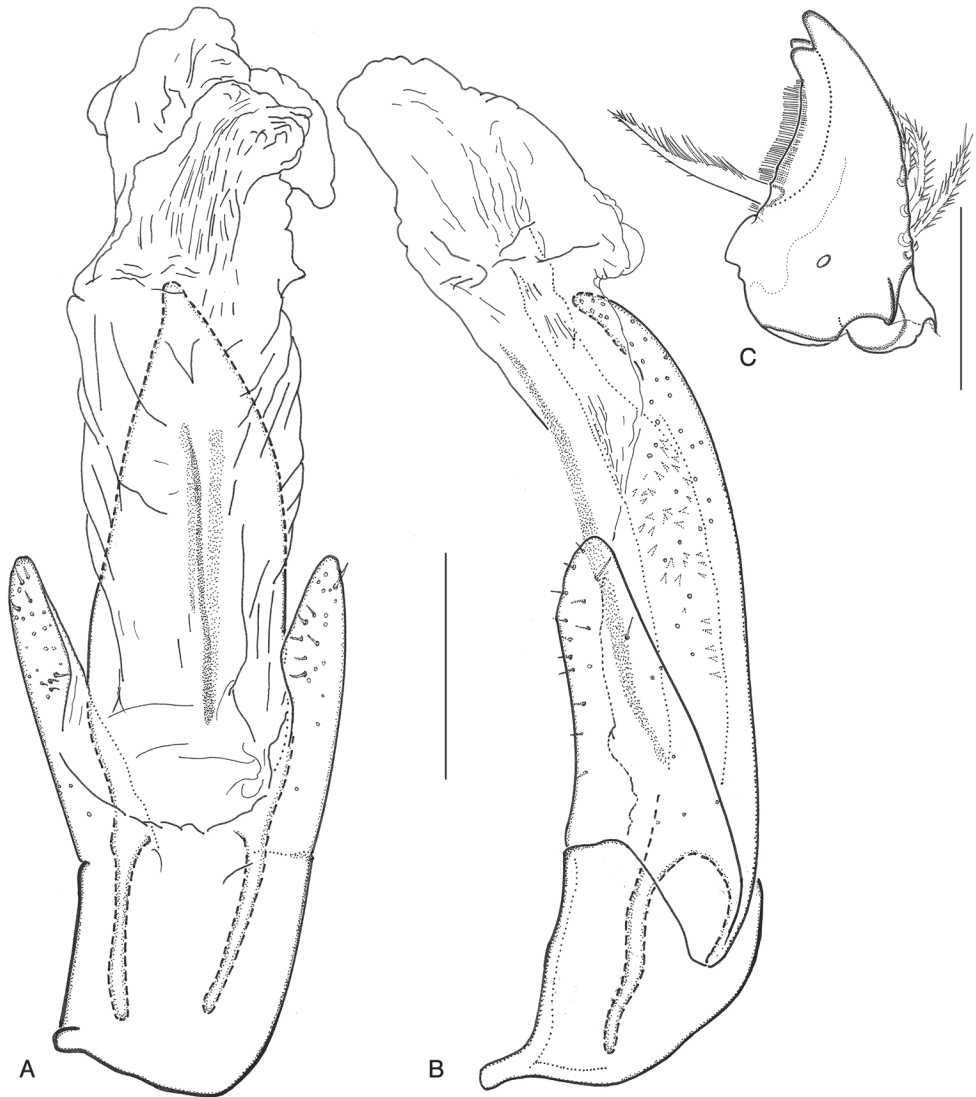
Figure 13. A *Ancyronyx clisteri* sp. nov., aedeagus of holotype with endophallus partly extruded, ventral view **B** same, lateral view **C** *A. sarawacensis*, larval mandible, ventral view.

Comparative remarks. The body shape of the larva is typical for the *Ancyronyx variegatus* (Germar) species group. In this group, larvae were described for *A. helgeschneideri* Freitag & Jäch, *A. procerus*, *A. schillhammeri* Jäch and *A. variegatus* (Brown 1972; Freitag and Balke 2011; Freitag 2013). In contrast to those of the *A. patrolus* species group, these larvae share the comparably large size, dorsoventrally depressed body, stout legs and prominent conical lateral tergal processes (posterolateral appendages). *Ancyronyx sarawacensis* closely resembles *A. helgeschneideri* (comp. Freitag and Balke 2011) in the yellowish-brown color, similar size (final instar HW 0.55 mm vs. 0.50 mm; body length
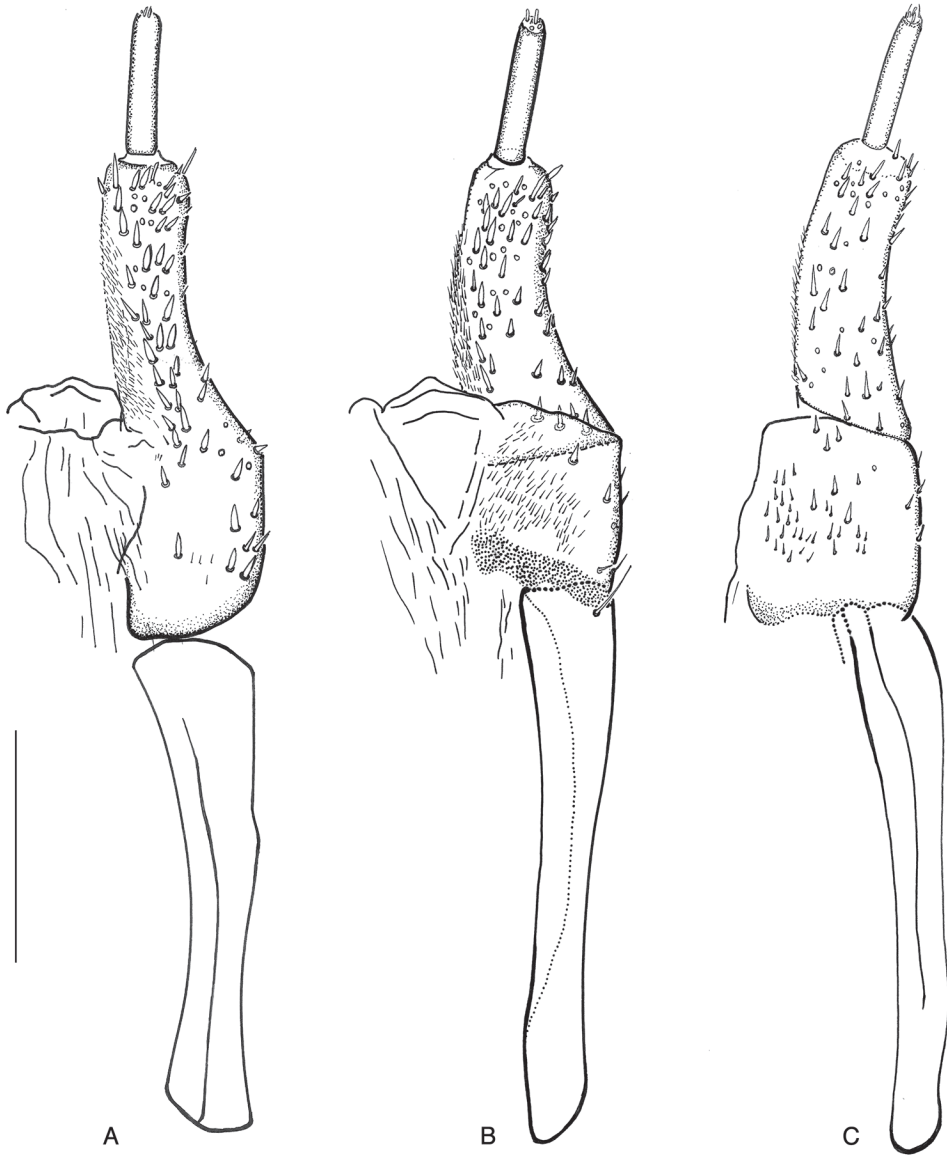
Figure 14. *Ancyronyx clisteri* sp. nov.: **A** ovipositor, paratype from Sarawak, dorsal view **B** same, ventral view **C** ovipositor, paratype from the type locality, ventral view.

4.4 mm vs. 4.5 mm), relatively large spiracles, similar shape and distribution of setae, tubercles and asperities, similar proportions and color pattern of abdominal segment IX, arcuate sides of head, and presence of short anterolateral frontal projections and lack of a median frontal projection. *Ancyronyx sarawacensis* differs from *A. helgeschneideri* in the pale anterior third of pronotum (vs. pale anterior and lateral pronotal margins), labrum with transverse row of ramified setae (vs. tuberculate with rather inconspicuous ramified
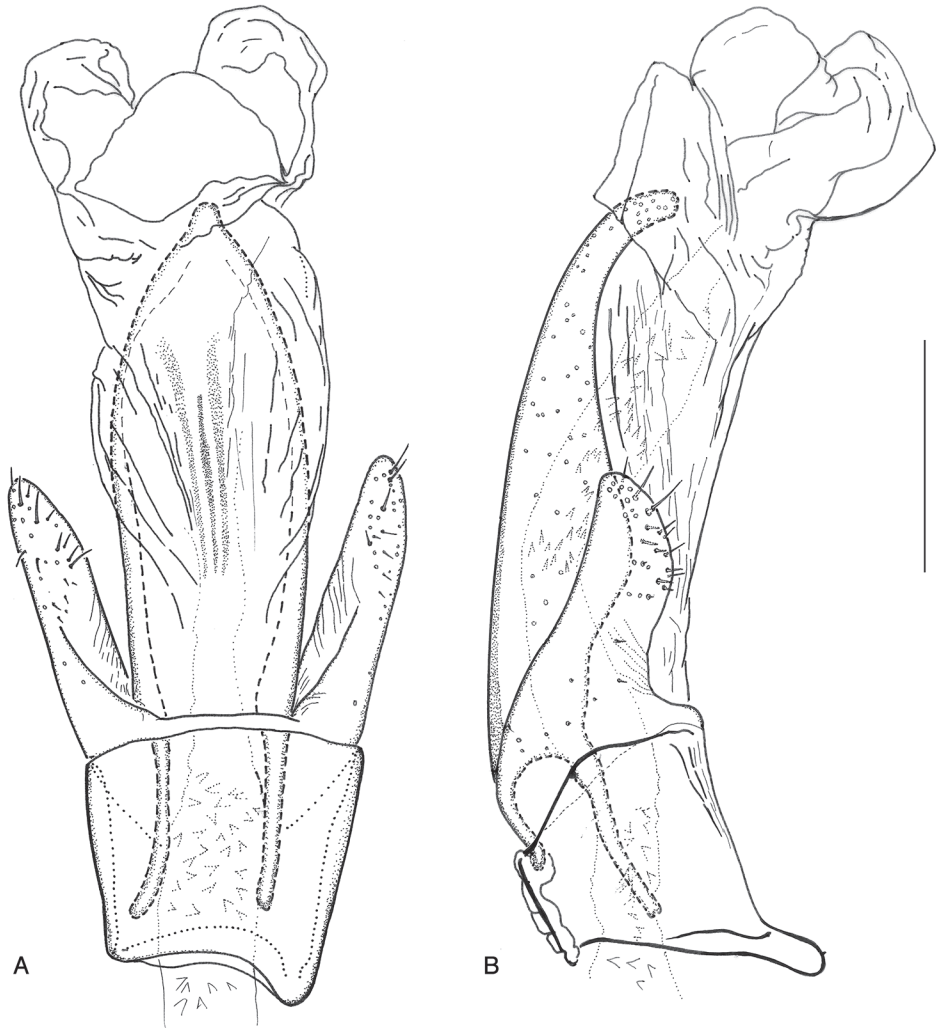
Figure 15. *Ancyronyx sarawacensis*, specimen from the type locality: **A** aedeagus with endophallus partly extruded, ventral view **B** same, lateral view.

and trichoid setae), submentum relatively longer and slenderer (1.6 × as long as wide vs. 1.4 ×) and clearly delimited triangular presternum. Larvae of *Ancyronyx procerus* (comp. Freitag and Balke 2011) can be distinguished by head being almost as wide as pronotum with sides almost straight (vs. head distinctly narrower than pronotum with sides arcuate), presence of a median frontal projection and three prominent frontal projections (vs. short anterolateral frontal projections). Furthermore, *A. sarawacensis* larvae are relatively slenderer than those of *A. procerus* (final instar HW 0.55 mm vs. 0.62 mm, body length 4.4 mm vs. 3.7 mm) and dorsally more densely covered with larger tubercles.

Habitat. The altitude of all collection sites ranges from 40–1200 m a.s.l; the species is described from a small stream near Arur Dalan in the Kelabit Highlands
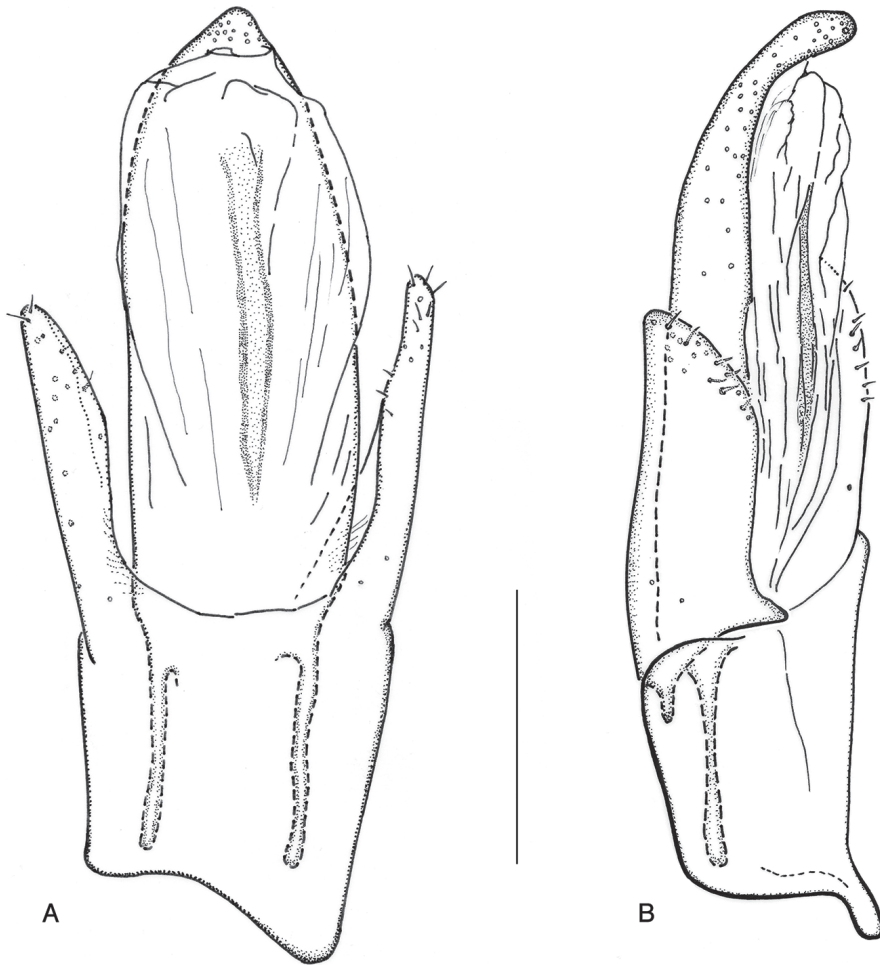
Figure 16. *Ancyronyx sarawacensis*, holotype: **A** aedeagus, ventral view **B** same, lateral view.

(1000–1200 m a.s.l.). It is an upper reach (epirhithron), ca 3 m wide, with boulders and cascades, flowing through degraded primary forest. Water quality is presumably very good since the stream serves as drinking water for the settlements. Current and bottom substrates are heterogeneous; the latter includes mineral and organic deposits. All *Ancyronyx* specimens were collected from submerged wood. The larvae were found together with adults hidden in fissures of the bark of a large, relatively fresh submerged tree branch fully covered with bark. Mountain streams in the Bario area (Pa'Ramapoh, Arur Takang and Pa'Marario) have fewer boulders, fewer cascades and more submerged wood. The river at Pa'Ukat is ca 10 m wide, shallow, slowly flowing, entirely shaded, with stony and sandy substrates and numerous fallen trees. Forest streams near Ramudu, Pa'Ngaruren and Pa'Kasi are ca 4–7 m wide, slowly flowing and meandering, with stones, some cobbles and sand substrates, submerged woods, leaf packs and exposed roots. Specimens were collected mostly from submerged dead wood, however,
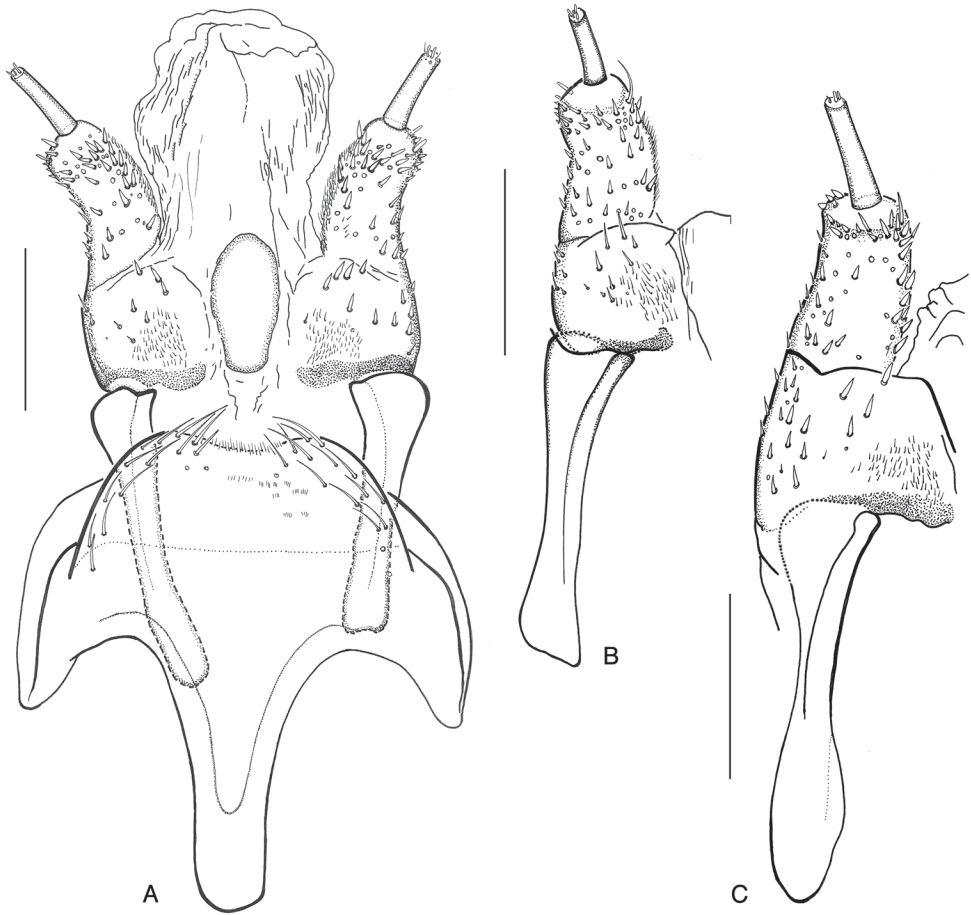
Figure 17. *Ancyronyx sarawacensis*: **A** ovipositor and abdominal segment VIII, specimen from a tributary of Kuamut River, Sabah "(14B)", ventral view **B** ovipositor, paratype from Kapit area, Sarawak, ventral view **C** ovipositor, paratype from the Kelabit Highlands, Sarawak, ventral view.

a few specimens come also from submerged roots of tree or bamboo. The Petarutung River in Pa'Lungan is 7–10 m wide, shallow, meandering, with sandy bottom and represents the only reddish colored river where some specimens were found (water color is probably due to humic substances from a nearby peat swamp forest). Outside the Kelabit Highlands *A. sarawacensis* was collected in small lowland and upland forest streams, which are moderately wide, rather shallow, usually meandering and with sandy or stony substrates, always containing submerged logs, woody debris and leaf packs. The specimens were collected mainly, but not exclusively, in stream reaches with stronger currents. The most atypical stream inhabited by *A. sarawacensis* was a small, slowly flowing, very shallow, meandering creek in Gunung Mulu NP (55 m a.s.l.) with large amounts of accumulated leaves and a sandy bottom, with some gravel and a few

submerged branches (Fig. 11B); specimens were collected together with *Ancyronyx pulcherrimus* Kodada, Jäch & Čiampor and a new species of *Okalia* Kodada & Čiampor.

Syntopic taxa. Usually, the same piece of submerged wood, especially larger pieces can be inhabited by several genera of Elmidae and Dryopidae. *Ancyronyx sarawacensis* was found with specimens of *Graphelmis berbulu* Čiampor, *G. labralis* Čiampor and *G. mumini* Čiampor at the type locality. From lowland and upland Sarawak and Sabah, the following species were found to be syntopic: *Ancyronyx procerus*, *A. acaroides*, *A. pulcherrimus*, *Graphelmis gemuk* Čiampor and several species belonging to the *G. picta* and *G. marshalli* groups. Some species of *Leptelmis* Sharp as well as *Stenomystax montanus* Kodada, Jäch & Čiampor, *S. depressus* Kodada, Jäch & Čiampor and *S. minutus* Kodada, Jäch & Čiampor and some species of *Elmomorphus* Sharp were also found syntopic.

Distribution. This species is widely distributed in northern Borneo (Sarawak, Sabah and Brunei). In Sarawak it was collected in several small tributaries of the Dapur and the Kelapang rivers in the Kelabit Highlands; small tributaries of the Tutoh and the Melinau Paku rivers in and near the Gunung Mulu National Park; tributaries of the Sut River near Kapit, the Jangkar River near Lundu and a small stream near Kampung Bayur (Kuching area). In Sabah, it is known from the tributaries of Sapulut River near Batu Punggul; small tributaries of the Kuamut River as well as the Agatis River and a small tributary of the Maliau River. In Brunei, the species was collected from the Belalong River and from one of its small tributaries.

Ancyronyx procerus Jäch, 1994

Type locality. Tributary of the Tutoh River, near Long Iman, Mulu National Park, northern Sarawak, Borneo, East Malaysia.

Material examined. *Holotype* ♂ (NMW): "Malaysia, Sarawak, Mulu NP, Long Iman 4.3.1993 leg. M. Jäch (20)". *Paratypes*: 5 exs with same data as holotype (NMW), 2 exs (CKB): "Malaysia - Sarawak ca 40 km E Kapit III. 1994 leg. J. Kodada \ Rumah ugap Ng marating Kapit Sut".

Additional material (CCB, CFDS, CKB, NMW). **SARAWAK:** 1 ♀ [37, MK505417], 1 ♀ [FZ1639, MK505411], 2 exs: "Malaysia, Sarawak, Kuching distr., Kampong Jantar env., 10.7.2018, (29) 1.65911N, 109.70829E, 67 m a.s.l., J. Kodada & D. Selnekovič lgt."; 1 ♀ [11, MK505423], 1 ♂ [FZ1644, MK505410], 2 exs: "Malaysia, Sarawak, Kuching distr., Bayur riv. near bridge of jalan Jambur - Bayur, 20.10.2018, 1°14'43.2"N, 110°17'34.8"E, ca 50 m a.s.l., J. Kodada & D. Selnekovič lgt."; 3 exs: "Malaysia, Sarawak, Miri distr., Ramudu env., 5.03.2019, (No. 51), Ramudu riv., 3°32'14.390"N, 115°30'22.456"E, ca 900 m a.s.l., J. Kodada & D. Selnekovič lgt."; 4 exs: "Malaysia, Sarawak, Miri distr., Ramudu env., 6.03.2019, (No. 52), Pa'Masia riv., ca 3°31'57.736"N, 115°30'39.624"E, ca 950 m a.s.l., J. Kodada & D. Selnekovič lgt."; 10 exs: "Malaysia, Sarawak, Miri distr., Dapur riv. near Pa'Umor, 8.03.2019, (No. 54), 3°44'3.49"N, 115°30'56.24"E ca 1070 m a.s.l., J. Ko-

dada & D. Selnekovič lgt.". **SABAH:** 1 ♂: "Malaysia, Sabah, ca 25 km Sapulut, Sabalangang river, 21.V.2001"; 1 ♂, 3 ♀♀, 4 exs: "Malaysia, Sabah, (Borneo), Kuamut river env. near Kampung Pisang Pisang, 3.-4. VI. 1996, 14a: shaded stream in primary forest with submerged wood"; 1 ♂, 1 ex.: "Malaysia, Sabah, Kampung Pisang Pisang env., tributary of Kuamut River, 29.6.1998, J. Kodada & F. Čiampor Lgt."; 1 ex. [FZ1660, MK505403], 1 ♂: "Malaysia, Sabah, Interior Division (Nabawan), Batu Punggul env., 23.5.2001, Čiampor lgt.". **West Malaysia: PAHANG:** 1 ex. [FZ1659, MK505405], 8 ♂♂, 3 ♀♀: "Malaysia, Malaysia, Pahang, Kenong Rimba Park, Kesong River, 5.6.2001, J. Kodada & F. Čiampor". **TERENGGANU:** 4 exs [FZ1623, MK505419; FZ1624, MK505413, FZ1625, MK505402; FZ1626, MK505412]: "Malaysia, Terengganu, Kg. Pancur Merah env., stream ca 7m wide, 5°33'28.86"N, 102°40'47.70"E, 2.8.2016, ca 30 m a.s.l.".

Variability. *Ancyronyx procerus* represents the largest species of the genus (TL 2.4–2.8 mm) with two, more or less distinct color forms. The form with lighter (less black) elytra and sometimes smaller to obsolete femoral spot correspond in habitus to the type specimens from Long Iman, Sarawak (see Jäch 1994: fig. 28). These lighter specimens were found, e.g., in all Sarawak lowland localities and in Sabah, in the Sabalangang River and in the tributary of the Kuamut River. The darker form with extensive black elytra and darker femoral spot were found in Sarawak in the rivers of the Kelabit Highlands, Sabah and in localities from West Malaysia. These color forms do not represent separate taxa, neither according to their genetic differentiation in COI mtDNA sequences, nor according to the fine differences in their genital morphology.

Habitat. All *Ancyronyx procerus* were sampled from submerged wood and seem to prefer larger pieces of fresh wood with bark; so far none of the specimens were found on submerged exposed roots of living trees or bamboo like adults of *A. sarawacensis* or *A. acaroides* (Kodada and Selnekovič pers. obs.). Adults have also not been collected in light traps yet. The larva was described after two specimens, one from type locality and one from Busuanga Island (Philippines); association with adults was corroborated by COI mtDNA sequences (Freitag and Balke 2011).

Specimens were usually found in smaller shallow meandering rivers with low vertical gradient, or – less frequently – in lowlands streams/creeks with a rather slower current, mostly with gravel or sandy substrate (e.g., Kesong River, rivers near Kampung Jalan and Kampung Bayur, Sabalangan River). In mountainous habitats the species is newly recorded from rivers in the Kelabit Higlands: Dapur, Ramudu and Pa'Masia; all these localities are within altitudes of 900–1070 m a.s.l. The largest of these rivers is the Dapur River; at the collecting place near Pa'Umor it is about 10–15 m wide, deep, reddish colored, meandering, with sandy bottom, and contains lot of submerged logs; the water level is strongly fluctuating annually. The partly shaded forest rivers Pa'Ramudu and Pa'Masia are 7–10 m wide, shallow, slowly flowing and meandering, with stones, some cobbles and gravel, and with some submerged wood and a lot of exposed bamboo roots.

Examination of flooded wood in larger rivers at lowland reaches of Sarawak (e.g., the Sarawak River at Kuching, the Rajang River at Kapit, Batang Kayan River near Lundu) did not yield any *Ancyronyx* specimens.

Distribution. *Ancyronyx procerus* was described from a tributary of the Tutoh River near Long Iman in Mulu National Park (Sarawak). The type series contains 12 specimens from the type locality and two specimens from the river Sut near Kapit (Sarawak). Recent collecting activities in northern Borneo showed that *A. procerus* is less abundant than *A. sarawacensis* or *A. acaroides*.

Ancyronyx procerus was recorded from Brunei, Malaysia (Pahang, Sarawak), the Philippines (Busuanga) and Vietnam (Jäch et al. 2016). The distributional data from Sabah and Terengganu represent first records from these states.

Discussion

The species of *Ancyronyx* are usually colorful, showing various color patterns, which were originally considered to be species-specific (e.g., Jäch 1994, 2004, Kodada et al. 2014). In the present study, the use of barcoding confirmed the existence of a cryptic taxon, *A. clisteri* sp. nov., and highlighted the existence of a phenotypic plasticity regarding color patterns and other morphological characters of *A. sarawacensis* and *A. procerus* populations. Generally, in Elmidae, closely related species often replace each other along water courses; remarkably, stenothermic species of cold upper courses are usually larger, more strongly pigmented and smoother than their relatives from the lower courses (e.g., Steffan 1963, 1964; Berthélemy 1967; Jäch 1984). This obviously temperature-related phenomenon has been observed also in different populations of the same species, e.g., in *Elmis maugetii* Latreille (Knie 1977, 1978; Berthélemy 1979), *Ilamelmis foveicollis* (Grouvelle) (Jäch 1984), and it is now confirmed by molecular data for populations of *Ancyronyx sarawacensis*.

The aedeagus of *Ancyronyx* is of a trilobate type, with moderately large parameres and a short phallobase. The form of the penis in most species is simple, with sides more or less straight and narrowed apicad (e.g., *A. sarawacensis*, *A. procerus*, *A. variegatus*), but in some species (*A. acaroides* and *A. johanni* Jäch), the sides of the penis are angular and strongly produced laterad, while they are produced and rounded in *A. patrolus* Freitag & Jäch, *A. pseudopatrolus* Freitag & Jäch and *A. punktii* Freitag & Jäch. The form of the parameres is simple, and their length, setation, and shape are varying between the species.

Hayashi and Yoshitomi (2015) described a technique for endophallus extrusion, which allows a better examination of its internal morphology (bladders and sclerites) and its surface structures, which are difficult to observe when the endophallus is in resting position; in Japanese species of the genus *Zaitzeviaria* Nomura they were able to find characters useful for species identifications. The examination of an extruded endophallus in *A. sarawacensis* revealed a possible diagnostic potential in the form and position of several bladders, microsclerites and different spines. Unfortunately, it is not possible to manually evert the endophallus in all specimens. The success rate of getting the endophallus fully everted was low even when the technique described by Hayashi and Yoshitomi (2015) was used. However, these particular structures are probably of some significance also in *Ancyronyx*.

Acknowledgements

References

Berthélemy C (1967) Description de deux larves de *Limnius* et remarques sur la systématique et la répartition du genre (Coleoptera, Elminthidae). Annales de Limnologie 3(2): 253–266. https://doi.org/10.1051/limn/1967002

Berthélemy C (1979) Elmidae de la region paléarctique occidentale: systématique et répartition (Coleoptera Dryopoidea). Annales de Limnologie 15(1): 1–102. https://doi.org/10.1051/limn/1979014

Bian D, Guo C, Ji L (2012) First record of *Ancyronyx* Erichson (Coleoptera: Elmidae) from China, with description of a new species. Zootaxa 3255(1): 57–61. https://doi.org/10.11646/zootaxa.3255.1.4

Brown HP (1972) Aquatic dryopoid beetles (Coleoptera) of the United States. Biota of freshwater ecosystems identification manual no. 6. Water Pollution Control Research Series, EPA, Washington D.C., 82 pp. https://doi.org/10.5962/bhl.title.4106

Darriba D, Taboada GL, Doallo R, Posada D (2012) jModelTest 2: more models, new heuristics and parallel computing. Nature Methods 9(8): 772. https://doi.org/10.1038/nmeth.2109

Folmer O, Black M, Hoeh W, Lutz R, Vrijenhoek R (1994) DNA primers for amplification of mitochondrial cytochrome c oxidase subunit I from diverse metazoan invertebrates. Molecular Marine Biology and Biotechnology 3: 294–299.

Freitag H (2012) *Ancyronyx jaechi* sp.n. from Sri Lanka, the first record of the genus *Ancyronyx* Erichson, 1847 (Insecta: Coleoptera: Elmidae) from the Indian Subcontinent, and a world checklist of species. Zootaxa 3382(1): 59–65. https://doi.org/10.11646/zootaxa.3382.1.6

Freitag H (2013) *Ancyronyx* Erichson, 1847 (Coleoptera, Elmidae) from Mindoro, Philippines, with description of the larvae and two new species using DNA sequences for the assignment of the developmental stages. ZooKeys 321: 35–64. https://doi.org/10.3897/zookeys.321.5395

Freitag H, Balke M (2011) Larvae and a new species of *Ancyronyx* Erichson, 1847 (Insecta, Coleoptera, Elmidae) from Palawan, Philippines, using DNA sequences for the assignment of the developmental stages. ZooKeys 136: 47–82. https://doi.org/10.3897/zookeys.321.5395

Freitag H, Jäch MA (2007) The genus *Ancyronyx* Erichson, 1847 (Coleoptera, Elmidae) in Palawan and Busuanga, (Philippines) with description of six new species. Zootaxa 1590: 37–59. https://doi.org/10.11646/zootaxa.1590.1.2

Freitag H, Kodada J (2017a) A taxonomic review of the genus *Ancyronyx* Erichson, 1847 from Sulawesi (Insecta: Coleoptera: Elmidae). Journal of Natural History 51(9–10): 561–606. https://doi.org/10.1080/00222933.2017.1285447

Freitag H, Kodada J (2017b) Larvae of *Ancyronyx* Erichson, 1847 (Insecta: Coleoptera: Elmidae) from Sulawesi, using DNA sequences for the assignment of the larval stages. Zootaxa 4299(1): 121–130. https://doi.org/10.11646/zootaxa.4299.1.6

Hammer Ø, Harper DAT, Ryan PD (2001) PAST: Paleontological Statistics software package for education and data analysis. Palaeontologia Electronica 4: 1–9. http://palaeo–electronicaorg/2001_1/past/issue1_01.htm

Hayashi M, Yoshitomi H (2015) Endophallic structure of the genus *Zaitzeviaria* Nomura (Coleoptera, Elmidae, Elminae), with review of Japanese species. Elytra, Tokyo, New Series 5(1): 67–96.

Jäch MA (1984) Die Koleopterenfauna der Bergbäche von Südwest–Ceylon (Col.). Archiv für Hydrobiologie, Supplementum 69(2): 228–332.

Jäch MA (1994) A taxonomic review of the Oriental species of the genus *Ancyronyx* Erichson, 1847 (Coleoptera, Elmidae). Revue suisse de Zoologie 101: 601–622. https://doi.org/10.5962/bhl.part.79919

Jäch MA (2003) *Ancyronyx* Erichson: new faunistic records, and description of a new species from Sulawesi (Indonesia) (Coleoptera: Elmidae). Koleopterologische Rundschau 73: 255–260.

Jäch MA (2004) Descriptions of two new species of *Ancyronyx* Erichson (Insecta: Coleoptera: Elmidae). Annalen des Naturhistorischen Museums in Wien (Ser. B) 105: 389–395.

Jäch MA, Kodada J, Brojer M, Shepard WD, Čiampor Jr F (2016) Coleoptera: Elmidae and Protelmidae. World Catalogue of Insects, Volume 14. Brill, Leiden, XXI + 318 pp. https://doi.org/10.1163/9789004291775

Knie J (1977) Ökologische Untersuchungen der Käferfauna von ausgewählten Fließgewässern des Rheinischen Schiefergebirges (Insecta: Coleoptera). Decheniana. Verhandlungen des Naturhistorischen Vereins der Rheinlande und Westfalens 130: 151–221.

Knie J (1978) Untersuchungen an *Elmis maugetii* var. *hungarica* var.n. und ihre Abgrenzung gegenüber *Elmis maugetii* Latreille, 1798 und *Elmis maugetii* var. *megerlei* (Duftschmid, 1805) (Coleoptera: Dryopoidea). Folia Entomologica Hungarica 31: 61–67.

Kodada J, Jäch MA, Čiampor Jr F (2014) *Ancyronyx reticulatus* and *A. pulcherrimus*, two new riffle beetle species from Borneo, and discussion about elmid plastron structures (Coleoptera: Elmidae). Zootaxa 3760(3): 383–395. https://doi.org/10.11646/zootaxa.3760.3.5

Kodada J, Jäch MA, Čiampor Jr F (2016) 19.2. Elmidae Curtis, 1830. In: Beutel RG, Leschen RAB (Eds) Coleoptera, Beetles. Volume 1: Morphology and Systematics (Archostemata, Adephaga, Myxophaga, Polyphaga partim), Handbook of Zoology, Arthropoda: Insecta (2nd edn). Walter de Gruyter, Berlin, 561–589.

Kumar S, Stecher G, Tamura K (2016) MEGA7: Molecular evolutionary genetics analysis version 7.0 for bigger datasets. Molecular Biology and Evolution 33: 1870–1874. https://doi.org/10.1093/molbev/msw054

Lawrence JF, Ślipiński A (2013) Australian beetles. Volume 1: morphology, classification and keys. CSIRO, Collingwood, 561 pp. https://doi.org/10.1071/9780643097292

Steffan AW (1963) Beziehungen zwischen Lebensraum und Körpergröße bei mitteleuropäischen Elminthidae (Coleoptera: Dryopoidea). Zeitschrift für Morphologie und Ökologie der Tiere 53: 1–21. https://doi.org/10.1007/BF00408496

Steffan AW (1964) Biozönotische Parallelität der Körpergröße bei mitteleuropäischen Elminthidae (Coleoptera: Dryopoidea). Naturwissenschaften 51(1): 20–21. https://doi.org/10.1007/BF00601735

Supplementary material 1

Table S1

Authors: Ján Kodada, Manfred A. Jäch, Hendrik Freitag, Zuzana Čiamporová-Zaťovičová, Katarína Goffová, Dávid Selnekovič, Fedor Čiampor Jr

Data type: measurement.

Explanation note: Pairwise genetic distance among specimens of *Ancyronyx* and *Graphelmis* species (Kimura 2-parameter distance) based on the 661bp barcoding fragment of the COI gene.

Link: https://doi.org/10.3897/zookeys.912.47796.suppl1

RESEARCH ARTICLE

Revision of the *Theopea* genus group (Coleoptera, Chrysomelidae, Galerucinae), part III: Descriptions of two new genera and nine new species

Chi-Feng Lee[1], Jan Bezděk[2]

1 *Applied Zoology Division, Taiwan Agricultural Research Institute, Taichung 413, Taiwan* **2** *Mendel University in Brno, Department of Zoology, Zemědělská 1, 613 00 Brno, Czech Republic*

Corresponding author: *Chi-Feng Lee* (chifeng@tari.gov.tw)

Citation: Lee C-F, Bezděk J (2020) Revision of the *Theopea* genus group (Coleoptera, Chrysomelidae, Galerucinae), part III: Descriptions of two new genera and nine new species. ZooKeys 912: 65–124. https://doi.org/10.3897/zookeys.912.47719

Abstract

This publication treats species within *Theopea* and closely allied genera that were not covered in the previous two revisions. Three species of *Theopea* Baly, 1864 are treated herein, with *T. bicolor* Kimoto, 1989 and *T. mouhoti* Baly, 1864 redescribed, and *T. bicoloroides* **sp. nov.** described. A new genus that we consider closely related to *Theopea*, *Pseudotheopea* **gen. nov.**, is described. This new genus can be recognized with the presence of reticulate microsculpture on the vertex of the head and pronotum and presence of an apical spine on each metatibia. The following species are transferred to *Pseudotheopea* as new combinations: *Theopea aeneipennis* Gressitt & Kimoto, 1963, *T. azurea* Gressitt & Kimoto, 1963, *T. clypealis* Medvedev, 2015, *T. nigrita* Medvedev, 2007, *T. smaragdina* Gressitt & Kimoto, 1963, *T. similis* Kimoto, 1989, and *T. subviridis* Medvedev, 2012. *Theopea subviridis* Medvedev, 2012 is regarded as **new synonym** of *Pseudotheopea similis* (Kimoto, 1989). In addition, six new species of *Pseudotheopea* are described: *P. boreri* **sp. nov.** from India, *P. gressitti* **sp. nov.** from Philippines, *P. hsingtzungi* **sp. nov.** from Laos, *P. kimotoi* **sp. nov.** from Laos, Thailand, and Vietnam, *P. leehsuehae* **sp. nov.** from Laos, and *P. sufangae* **sp. nov.** from Taiwan. A second new genus regarded as closely related to *Pseudotheopea*, *Borneotheopea* **gen. nov.**, can be recognized by possessing uniform antennae in both sexes and lacking an apical spine on each metatibia. Two new species of *Borneotheopea* are described from Borneo: *B. jakli* **sp. nov.** and *B. kalimantanensis* **sp. nov.**

Keywords

Borneotheopea, leaf beetles, *Pseudotheopea*, taxonomic revision

Introduction

Species within the genus *Theopea* Baly, 1864 occur in the Oriental Region from north India to Malaysia and Indonesia (Borneo, Sumatra, and Java) and also in the eastern Palaearctic (China) and the Philippines. *Theopea* includes 32 species and two subspecies (Nie et al. 2017). The genus and presumed closely related genera are currently undergoing revision. The first paper (Lee and Bezděk 2018) was devoted to the east Asian species lacking modified clypeus in males and the *T. sauteri* species group. In total, three species were redescribed, five new species described, and two species transferred from *Hoplosaenidea* Laboissière. The second paper (Lee and Bezděk 2019) treated species from Sundaland and the Philippines and redefined the genus. Seventeen species are recognized and classified into four species groups, including seven new species. Eight species were removed from *Theopea* and regarded as species *incertae sedis*.

This research deals with the remaining species that were not treated in the first two papers, including *Theopea aeneipennis* Gressitt & Kimoto, 1963, *T. azurea* Gressitt & Kimoto, 1963, *T. bicolor* Kimoto, 1989, *T. clypealis* Medvedev, 2015, *T. mouhoti* Baly, 1864, *T. nigrita* Medvedev, 2007, *T. smaragdina* Gressitt & Kimoto, 1963, *T. similis* Kimoto, 1989, and *T. subviridis* Medvedev, 2012. In addition, a number of undescribed species are described based on material deposited at various museums. After evaluating the taxonomic status of all species, two new genera, *Pseudotheopea* gen. nov. and *Borneotheopea* gen. nov., are described that conform to modern phylogenetic genus concepts.

Materials and methods

The abdomens of adults were separated from the bodies and boiled in 10% KOH solution, followed by washing in distilled water to clear and soften genitalia. The genitalia were then dissected from the abdomen, mounted on slides in glycerin, and studied and drawn using a Leica M165 stereomicroscope. For detailed examination a Nikon ECLIPSE 50i microscope was used.

At least two pairs from each species were examined to delimit variability of diagnostic characters. For species collected from more than one locality, at least one pair from each locality was examined. Length was measured from the anterior margin of the eye to the elytral apex, and width at the greatest width of the elytra.

Specimens were available for study and deposited in the following institutions:

NHMUK   The Natural History Museum, London, UK [Michael Geiser];
BPBM   Bernice P. Bishop Museum, Hawaii, USA [James Boone];
CAS   California Academy of Sciences, California, USA [David H. Kavanaugh];
FREY   The collection of Georg Frey, Naturhistorisches Museum, Basel, Switzerland [Matthias Borer];

HNHM   Hungarian Natural History Museum, Budapest, Hungary [Ottó Merkl];

IZAS   Institute of Zoology, Academia Sinica, Beijing, China [Rui-E Nie];

JBCB   Jan Bezděk collection, Brno, Czech Republic;

LMCM   Lev N. Medvedev collection, Moscow, Russia;

MSNG   Museo Civico di Storia Naturale "Giacomo Doria", Genova, Italy [Roberto Poggi];

MNHUB   Museum für Naturkunde, Leibniz-Institut für Evolutions- und Biodiversitätsforschung an der Humboldt-Universität zu Berlin, Berlin, Germany [Johannes Frisch];

NHMB   General collection, Naturhistorisches Museum, Basel, Switzerland [Matthias Borer];

NMNS   National Museum of Natural Science, Taichung, Taiwan [Jing-Fu Tsai];

NMPC   National Museum, Praha, Czech Republic [Lukáš Sekerka];

PAHC   Paul Aston collection, Hong Kong, China;

RBCN   Ron Beenen collection, Nieuwegein, The Netherlands;

SEHU   Laboratory for Systematic Entomology, Hokkaido University, Sapporo, Japan [Masahiro Ohara];

SMNS   Staatliches Museum für Naturkunde Stuttgart, Stuttgart, Germany [Wolfgang Schwaller];

TARI   Applied Zoology Division, Taiwan Agricultural Research Institute, Taichung, Taiwan [Chi-Feng Lee];

USNM   Smithsonian Institution, National Museum of Natural History, Washington, U.S.A. [Alexander S. Konstantinov];

ZSM   Zoologische Staatssammlung München, Munich, Germany [Michael Balke].

Exact label data are cited for all type specimens of previously described species; a double slash (//) divides the data on different labels and a single slash (/) divides the data in different rows. Other comments and remarks are in square brackets: [p] – preceding data are printed, [h] – preceding data are handwritten, [w] – white label, [y] – yellow label, [r] – red label, [y] – yellow label.

Taxonomy

Theopea pulchella group

Remarks. This species group was defined by Lee and Bezděk (2019). Three species are added to this group.

Included species. *Theopea bicolor* Kimoto, *T. elegantula* Baly, *T. fairmairei* Duvivier, *T. houjayi* Lee and Bezděk, *T. kedenburgi* Weise, *T. mouhoti* Baly, *T. pulchella* Baly, *T. tsoui* Lee and Bezděk, *T. yuae* Lee and Bezděk, and *T. bicoloroides* sp. nov.

Theopea bicolor **Kimoto, 1989**
Figs 1A–C, 2

Theopea bicolor: Kimoto 1989: 199 (Vietnam); Mohamedsaid and Costant 2007 (Thailand).

Type. Holotype ♂ (BPBM): "VIET NAM. 20 km / N. of Pleiku / 650m. 9.V.1960 [p, w] // L. W. Quate / Collector [p, w] // Theopea / bicolor / n. sp. [h, w] // HOLO-TYPE [p, r]".

Other material. THAILAND. Chiang Mai: 3♂♂, 2♀♀ (SEHU), Chiang Dao Valley, 2.V.1980, leg. Y. Komiya; 5♀♀ (SEHU), same locality, 24.V.1983, leg. Y. Komiya; 2♀♀ (SEHU), same but with "leg. H. Akiyama; 3♀♀ (SEHU), same locality, 30.V.1983, leg. Y. Komiya; 1♀ (SEHU), same but with "leg. K. Ikeda"; 1♀ (SEHU), same but with "H. Akiyama"; 4♀♀ (NHMB), same locality, 10-16.V.1991, leg. V. Kubáň; 1♂, 7♀♀ (1♂, 6♀♀: NHMB; 1♀: MSNG), same locality, 17-24.V.1991, leg. V. Kubáň; 4♂♂ (SEHU), Doi Pui, 28.IV.-1.V.1980, leg. Y. Komiya; 1♀ (NMPC), Doi Suthep, 19-22.-IV.1991, leg. S. Bílý; 1♂ (JBCB), Doi Suthep to Doi Pui, 18°49N 99°00E, 19.-23.IV.1991, leg. L. Dembický; 1♂ (MSNG), Palong, 19°55'N 99°06'E, 750 m, 26-28.V.1991, leg. V. Kubáň; Kanchanaburi: 1♂, 4♀♀ (SEHU), Ban Nong Bang, 15.V.1985, leg. Y. Komiya; Mae Hong Son: 6♂♂ (JBCB), Ban Huai Po, 19°19N 97°59E, 1600-2000 m, 9.-16.V.1991, leg. L. Dembický; 1♀ (NHMUK), same local-ity, 9-16.V.1992, leg. J. Horák; 33♂♂, 2♀♀ (24♂♂, 2♀♀: NHMUK; 9♂♂: JBCB), Ban Si Lang, 1200 m, 1-8.V.1992, leg. J. Horák; 1♀ (JBCB), Kiwlom-pass near Soppong, 19°26N 98°19E, 1400 m, 23.VI.-2.VII.2002, leg. R. and H. Fouqué; 1♀ (JBCB), SE of Soppong, 19°27N 98°20E, 1500 m, 23.-27.V.1999, leg. M. Řiha; 3♂♂, 1♀ (NHMB), Soppong-Pai, 1800 m, leg. Pacholátko; Nan: 1♂ (JBCB), Ban Huay Kon env., 27.V.-10.VI.2002, leg. P. Průdek, M. Obořil; 1♂ (NHMUK), Doi Phuka N.P., V.2000, leg. local collector; 1♀ (SEHU), Mae Kamme Forest, 17.V.1985, leg. Y. Komiya; 1♂ (SEHU), Nan Watershed Res. Station, 17.V.1985, leg. Y. Komiya; 1♂ (SEHU), Wiang Sa, 15.V.1993, leg. S. Ohmomo; 2♀♀ (SEHU), Wieng Ko Sai N.P., 18.V.1985, leg. Y. Komiya; Prachinburi: 1♀ (HNHM), Sakaerat Ecol. Research Insti-tute, 4.VI.2001, leg. E. Harváth and G. Szirákl; VIETNAM. Daklak: 1♂ (MSNG), 12 km SW of Buon Ma Thout, Lake Eakao, 400 m, 26-27.IV.1986, leg. L. Medvedev.

Redescription. Length 5.8–6.2 mm, width 1.9–2.2 mm. Body color (Fig. 1A–C) dark brown or blackish brown except elytra reddish brown. Antennae filiform in males, but antennomeres VI–VIII slightly swollen (Fig. 2A), length ratios of antennomeres I–XI 1.0: 0.3: 0.8: 1.1: 1.2: 1.2: 1.2: 1.1: 1.1: 1.0: 1.2, length to width ratios of anten-nomeres I–XI 2.8: 1.2: 2.5: 3.3: 3.6: 3.4: 3.4: 3.2: 3.5: 3.4: 4.1; filiform in females (Fig. 2B), length ratios of antennomeres I–XI 1.0: 0.3: 0.8: 1.0: 1.0: 0.9: 0.9: 0.9: 0.9: 0.8: 0.9, length to width ratios of antennomeres I–XI 3.0: 1.4: 3.1: 3.5: 3.5: 3.2: 3.4: 3.4: 3.6: 3.4: 3.7. Elytra elongate, parallel-sided, 2.0× longer than wide; disc with dense,
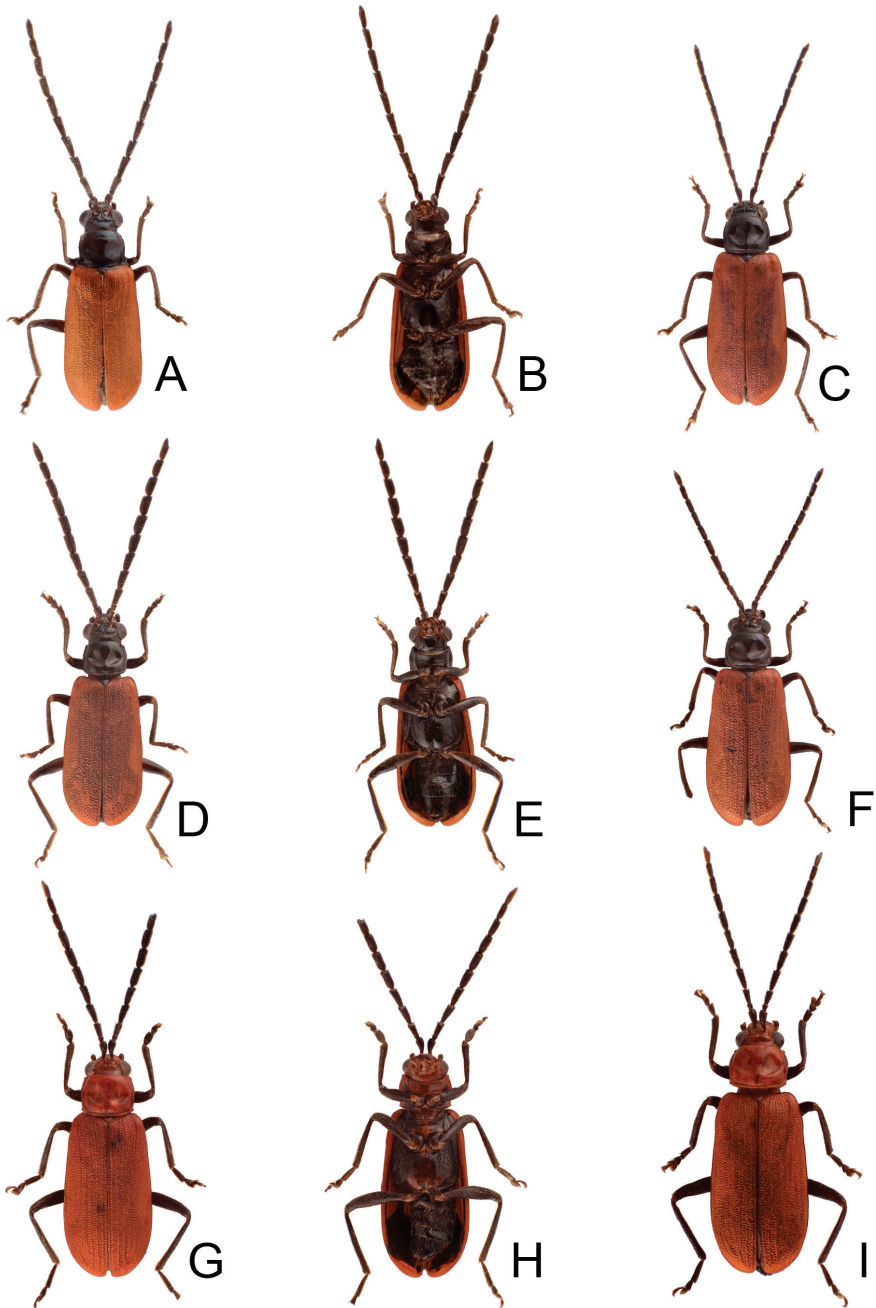
Figure 1. Habitus of *Theopea bicolor*, *T. bicoloroides* sp. nov., and *T. mouhoti*. **A** *T. bicolor*, male, dorsal view **B** Same, ventral view **C** *T. bicolor*, female, dorsal view **D** *T. bicoloroides* sp. nov., male, dorsal view **E** Same, ventral view **F** *T. bicoloroides* sp. nov., female, dorsal view **G** *T. mouhoti*, male **H** Same, ventral view **I** *T. mouhoti*, female, dorsal view.
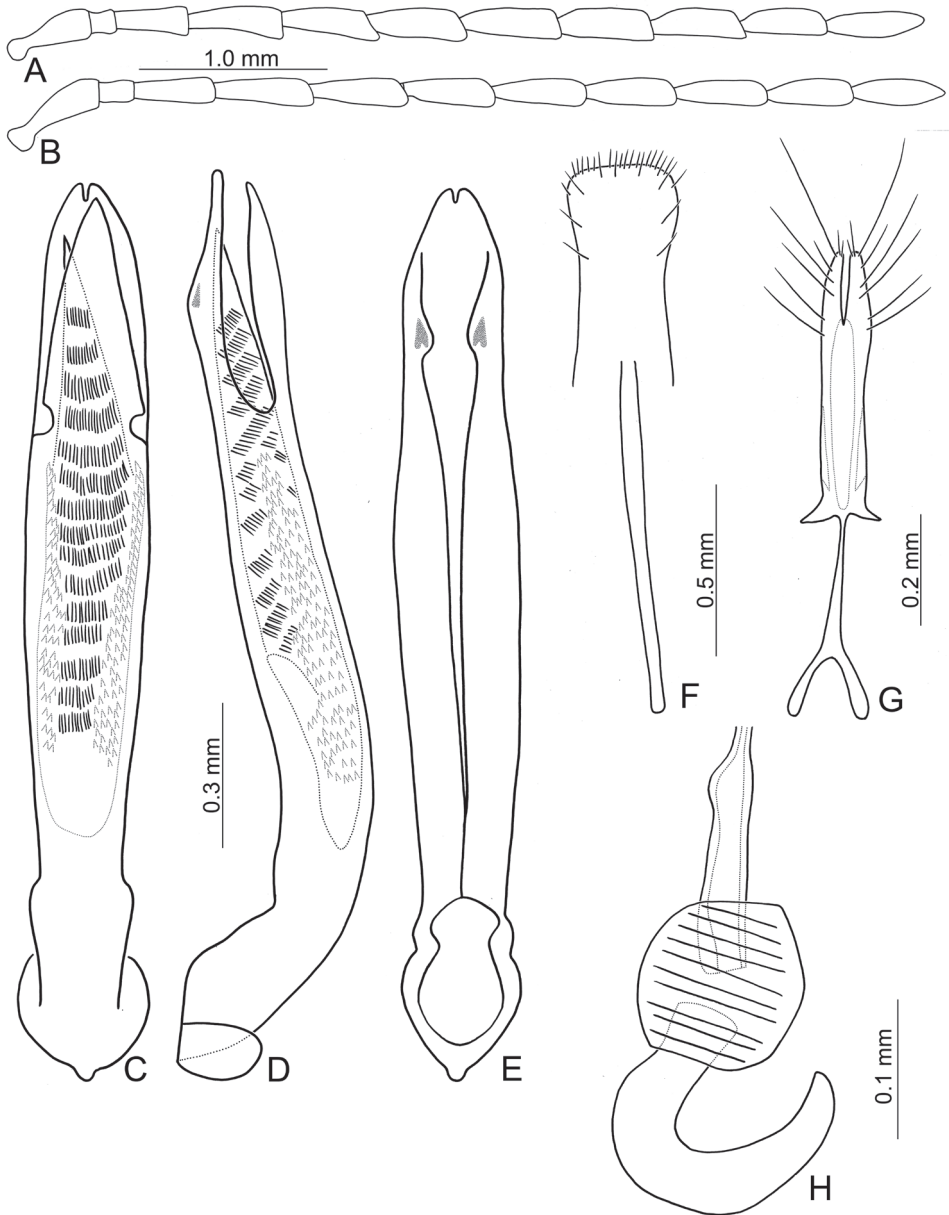
Figure 2. Diagnostic characters of *Theopea bicolor*. **A** Antenna, male **B** Antenna, female **C** Aedeagus, dorsal view **D** Aedeagus, lateral view **E** Aedeagus, ventral view **F** Abdominal ventrite VIII **G** Gonocoxae **H** Spermatheca.

coarse punctures, arranged into longitudinal rows, with one weak longitudinal ridge between two longitudinal rows of punctures, basally abbreviated. Tarsomeres I of front legs slightly swollen in males; subparallel in females. Aedeagus (Fig. 2C–E) slender,

6.5× longer than wide; sides widest at middle, gradually narrowed towards basal 1/4, gradually and apically narrowed towards apical 1/5, parallel between apical 1/5 and 1/12, apex with shallow notch; tectum well sclerotized, basally broadened, as broad as aedeagus, with hollow area behind base of tectum; moderately curved in lateral view; ventral surface with deep notch from near apex, apically extending into basal opening, more approximate at apical 1/5; triangular sclerites small; internal sac with one median, elongate sclerite, 0.7× as long as aedeagus, apically tapering from basal 1/3, apex acute, connected with short broad sclerite at base, disc with dense transverse rows of hair-like setae and with one pair of elongate, longitudinal rows of stout setae at sides. Gonocoxae (Fig. 2G) elongate, widest at apical 1/6, both gonocoxae joined from basal 1/8 to apical 1/7; apices narrowly rounded, each gonocoxa with eight setae along lateral margin from apex to apical 1/6; with one pair of short lateral processes at basal 2/5. Ventrite VIII (Fig. 2F) elongate and well sclerotized; disc with several long setae at sides and near apical margin, and with dense, short setae along apical margin; spiculum extremely slender. Receptacle of spermatheca (Fig. 2H) strongly swollen; pump slender and strongly curved; proximal spermathecal duct deeply inserted into receptacle, narrow and short.

Remarks. Populations from Laos and southwest China were misidentified. They represent *Theopea bicoloroides* sp. nov. (see below).

Diagnosis. *Theopea bicolor* Kimoto, *T. bicoloroides* sp. nov., and *T. mouhoti* Baly are characterized by their reddish brown elytra. *Theopea bicolor* and *T. bicoloroides* sp. nov. (Fig. 1A–F) can be easily separately from *T. mouhoti* (Fig. 1G–I) by the dark brown or blackish brown head, prothorax, and scutellum, and indistinct ridges in the elytra. Besides, males of *T. bicolor* and *T. bicoloroides* sp. nov. possess a median elongate sclerite internally in the aedeagus that is covered with transverse rows of hair-like setae (Figs 2C, D; 3C, D). This differs from those of *T. mouhoti*, which lacks such hair-like setae (Fig. 4C, D). *Theopea bicolor* differs from *T. bicoloroides* sp. nov. by the relatively slender antennae (Fig. 2A) in males (length to width ratios of antennomeres V-X more than 3.0 in *T. bicolor*, relatively broader antenna (Fig. 3A), less than 3.0 in *T. bicoloroides* sp. nov.), the narrowly rounded apex of the ventral surface of the aedeagus (Fig. 2E) (broadly rounded apex of aedeagus in *T. bicoloroides* sp. nov. (Fig. 3E)), endophallic sclerite broad and without longitudinal groove in lateral view (Fig. 2D) (dorso-ventrally flattened and with longitudinal groove in lateral view in *T. bicoloroides* sp. nov. (Fig. 3D)), and slender notch at apex of gonocoxae (Fig. 2G) (broad notch at apex of gonocoxae in *T. bicoloroides* sp. nov. (Fig. 3G)).

Distribution. Thailand, Vietnam.

Theopea bicoloroides sp. nov.

http://zoobank.org/93660DB1-59A6-4C78-A338-A546A6CA2717
Figs 1D–F, 3

Theopea bicolor: Kimoto 1989: 199 (part); Medvedev 2000: 178 (Laos); Bezděk 2012: 401 (China: Yunnan).

Types. Holotype ♂ (NMPC), **LOAS**. 20 km NW Louang Namhta, 21°09.2'N 101°18.7'E, 800-1100 m, 5-11.V.1987, leg. M. Štrba and R. Hergovits; Paratypes. 1♂ (NMPC), same data as holotype; LAOS. Boli Kham Xai: 1♀ (RBCN), Ban Nok env., 18°08.7'N 104°28.1'E, Route no 8, 220 m, 9-14.V.1998, leg. E. Jendek, and O. Sausa; 1♂ (HNHM), Phou Khao Kouay NBCA, Tad Leuk Waterfall, 280 m, 11-12.IV.1998, leg. O. Merkl and G. Csorba (identified as *Theopea bicolor* by Medvedev (2000)); Hua Phan: 3♂♂, 6♀♀ (JBCB), 25km SE Vieng Xai (by road), Ban Kangpabong env., 20°19'N 104°25 E, 14.-18.V.2001, leg. J. Bezděk; **CHINA**. Yunnan: 2♀♀ (TARI), Mohan (磨憨), 14.V.2016, leg. Y.-T. Wang.

Theopea bicolor: one paratype ♂ (ZSM), labeled: "Laos 1963 / Umgeb. Vanky [p, w] // Theopea / bicolor / n. sp. [h, w] // PARATYPE [p, b]".

Description. Length 6.1–6.5 mm, width 2.3–2.5 mm. Body color (Fig. 1D–F) dark brown or blackish brown except elytra reddish brown. Antennae filiform in males, but antennomere VI–IX strongly swollen (Fig. 3A), length ratios of antennomeres I–XI 1.0: 0.3: 0.8: 1.0: 1.0: 1.1: 1.1: 1.1: 1.0: 0.9: 1.0, length to width ratios of antennomeres I–XI 2.8: 1.3: 2.6: 3.2: 3.2: 2.7: 2.7: 2.7: 2.7: 2.8: 3.4; more slender in females (Fig. 3B), length ratios of antennomeres I–XI 1.0: 0.3: 0.8: 0.9: 1.0: 0.9: 0.9: 0.9: 0.9: 0.8: 1.0, length to width ratios of antennomeres I–XI 3.0: 1.5: 2.9: 3.3: 3.1: 3.0: 3.3: 3.2: 3.4: 3.1: 3.5. Elytra elongate, parallel-sided, 1.9× longer than wide; disc with dense, coarse punctures arranged into longitudinal rows, with one weak longitudinal ridge between two longitudinal rows of punctures, basally abbreviated. Tarsomeres I of front legs slightly swollen in males; subparallel in females. Aedeagus (Fig. 3C–E) slender, 6.4× longer than wide; sides strongly narrowed at apical 1/4 in ventral view, apical margin truncate, with shallow notch; tectum well sclerotized, basally broadened, broader than aedeagus, with hollow area at base of tectum; slightly curved in lateral view; ventral surface with deep notch from near apex, apically extending into basal 2/5; triangular sclerites small; internal sac with one median, elongate sclerite, 0.6× as long as aedeagus, dorso-ventrally flattened, apically tapering from basal 1/3, apex acute, connected by short broad sclerite at base, disc with dense, transverse rows of hair-like setae and with one pair of elongate, longitudinal rows of stout setae at sides. Gonocoxae (Fig. 3G) elongate, widest at apical 1/6, gonocoxae combined from basal 1/8 to apical 1/7; apices narrowly rounded, each gonocoxa with eight setae along lateral margin from apex to apical 1/6; with one pair of short lateral processes at basal 2/5. Ventrite VIII (Fig. 3F) elongate and well sclerotized; disc with several long setae at sides and near apical margin, and with dense, short setae along apical margin; spiculum extremely slender. Receptacle of spermatheca (Fig. 3H) strongly swollen; pump slender and strongly curved; proximal spermathecal duct deeply inserted into receptacle, narrow and long.

Diagnosis. *Theopea bicolor* Kimoto, *T. bicoloroides* sp. nov., and *T. mouhoti* Baly are characterized by their reddish brown elytra. *Theopea bicolor* and *T. bicoloroides* sp. nov. (Fig. 1A–F) can be easily separately from *T. mouhoti* by the dark brown or blackish brown head, prothorax, and scutellum, and indistinct ridges on the elytra (Fig. 1G–I). In addition, males of *T. bicolor* and *T. bicoloroides* sp. nov. possess median elongate internal aedeagal sclerites that are covered with transverse rows of hair-like setae (Figs 2C, D; 3C, D). This differs from those of *T. mouhoti* that lack hair-like setae (Fig. 4C,
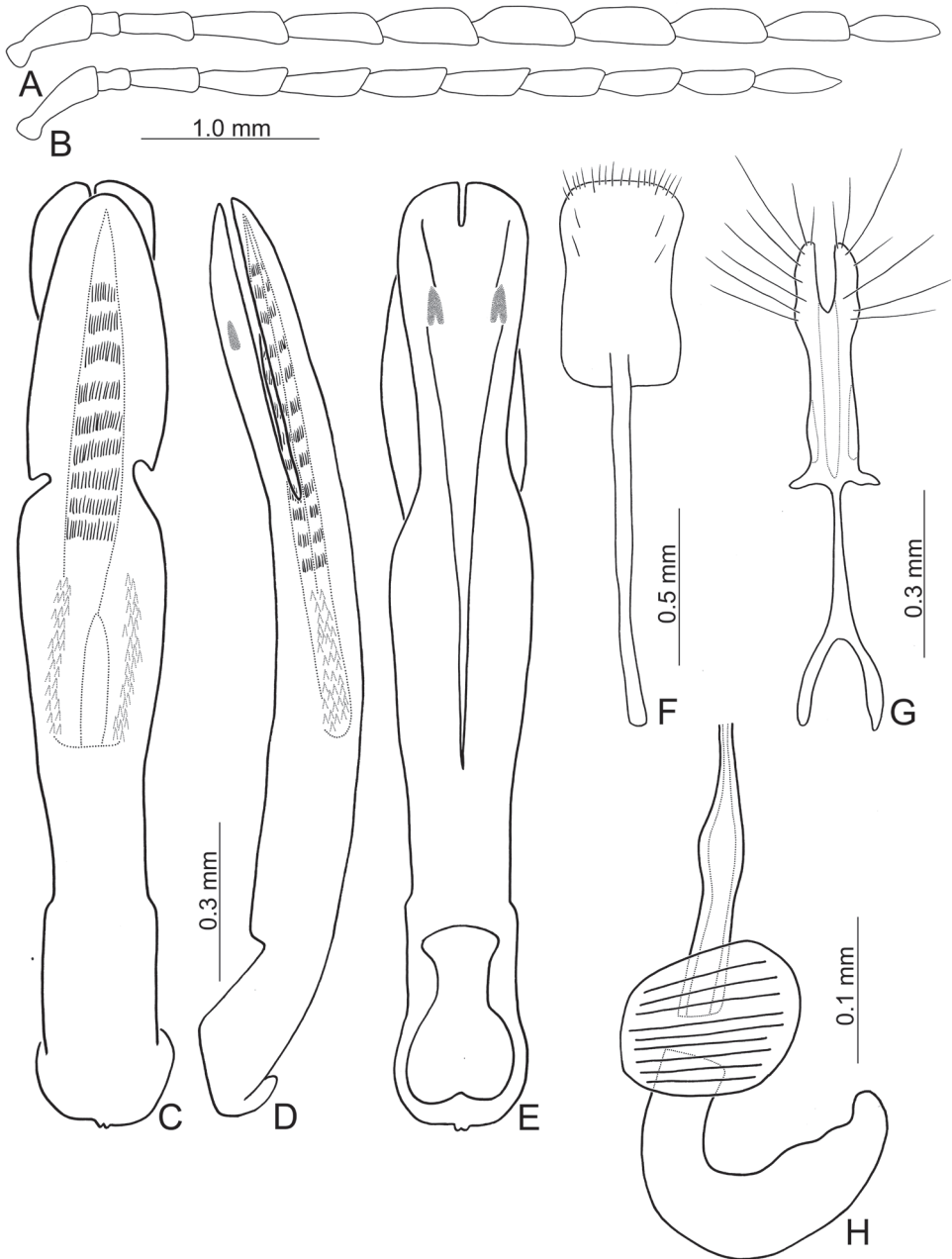
Figure 3. Diagnostic characters of *Theopea bicoloroides* sp. nov. **A** Antenna, male **B** Antenna, female **C** Aedeagus, dorsal view **D** Aedeagus, lateral view **E** Aedeagus, ventral view **F** Abdominal ventrite VIII **G** Gonocoxae **H** Spermatheca.

D). *Theopea bicoloroides* sp. nov. differs from *T. bicolor* by the relatively broader antennae in males (Fig. 3A) (length to width ratios of antennomeres V-X less than 3.0× in *T. bicoloroides* sp. nov. but more than 3.0 in *T. bicolor* (Fig. 2A)), broadly rounded apex

of the ventral surface of the aedeagus (Fig. 3E) (narrowly rounded apex of ventral surface of aedeagus in *T. bicolor* (Fig. 2E)), endophallic sclerite dorso-ventrally flattened and with longitudinal groove in lateral view (Fig. 3D) (broad and lacking longitudinal groove in lateral view in *T. bicolor* (Fig. 2D)); and a broad notch at the apex of the gonocoxae (Fig. 3G) (slender notch at apex of gonocoxae in *T. bicolor* (Fig. 2G)).

Etymology. This new species is named for the similarity with *Theopea bicolor* Kimoto.

Distribution. China: Yunnan; Laos.

Theopea mouhoti **Baly, 1864**
Figs 1G–I, 4

Theopea mouhoti: Baly 1864: 238 (Thailand); Wilcox 1973: 631 (catalogue); Kimoto 1989: 200 (Laos); Staines and Staines 1999: 522 (catalogue).

Types. Holotype ♂ (NHMUK, by monotypy), labeled: "Type [p, w, circle label with red border] // Theopea / Mouhoti / Baly / Siam [h, g] // Baly Coll. [p, w]".

Other specimens examined. CAMBODIA. 1♂ (NHMUK), Chautd; **LAOS**. Attapu: 5♂♂, 2♀♀ (NHMUK), Bolaven Plateau, 15 km SE of Ban Huangkong, Nong Lom (Lake) env., 15°02'N 106°35'E, 800 m, 18-30.IV.1999, leg. E. Jendek and O. Šauša; Boli Kham Xai: 1♂, 3♀♀ (RBCN), Ban Nok env., 18°08.7'N 104°28.1'E, Route no 8, 220 m, 9-14.V.1998, leg. E. Jendek, and O. Šauša; Champasak: 4♀♀ (NHMB), Ban Nong Panouan env., 15°02'N 106°31-34'E, 770-800 m, leg. M. Geiser and D. Hauck; Khammouane: 2♂♂, 8♀♀ (NHMB), Ban Khoun Ngeun, 18°07'N 104°29'E, 200 m, 24-29.IV.2001, leg. Pacholátko; Vientiane: 1♂ (ZSM), III.-VI.1963 (identified by Kimoto (1989); **THAILAND**. 4♂♂ (NHMUK); Loei: 1♀ (RBCN), Phu Rua N.P., 17°30'N 101°21'E, 6-9.IV.1999, leg. M. Říha.

Redescription. Length 6.5–8.0 mm, width 2.4–3.1 mm. Body color (Fig. 1G–I) reddish brown; meso- and metathoracic ventrites, abdomen, and legs dark brown or blackish brown; antenna black but antennomere XI reddish brown. Antennae filiform in males, but antennomere VI–VIII moderately swollen (Fig. 4A), length ratios of antennomeres I–XI 1.0: 0.3: 0.7: 0.9: 1.0: 1.0: 1.0: 1.0: 0.9: 0.8: 1.1, length to width ratios of antennomeres I–XI 3.3: 1.5: 2.8: 3.1: 3.1: 2.8: 2.6: 2.6: 3.0: 3.0: 4.5; filiform in females (Fig. 4B), length ratios of antennomeres I–XI 1.0: 0.3: 0.7: 0.9: 0.9: 0.9: 0.9: 0.9: 0.8: 0.8: 1.0, length to width ratios of antennomeres I–XI 3.2: 1.5: 2.8: 3.7: 3.6: 3.6: 3.6: 3.5: 3.8: 3.9: 4.6. Elytra elongate, parallel-sided, 1.8-2.0× longer than wide; disc with dense, coarse punctures, arranged into longitudinal rows, with one distinct longitudinal ridge between two longitudinal rows of punctures. Tarsomeres I of front legs swollen in males; subparallel in females. Aedeagus (Fig. 4C–E) slender, 8.4× longer than wide; sides widest at middle, gradually narrowed towards basal 1/4, moderately and apically narrowed, apex with shallow notch; tectum well sclerotized, basally broadened, broader than aedeagus, with hollow area behind base of tectum;
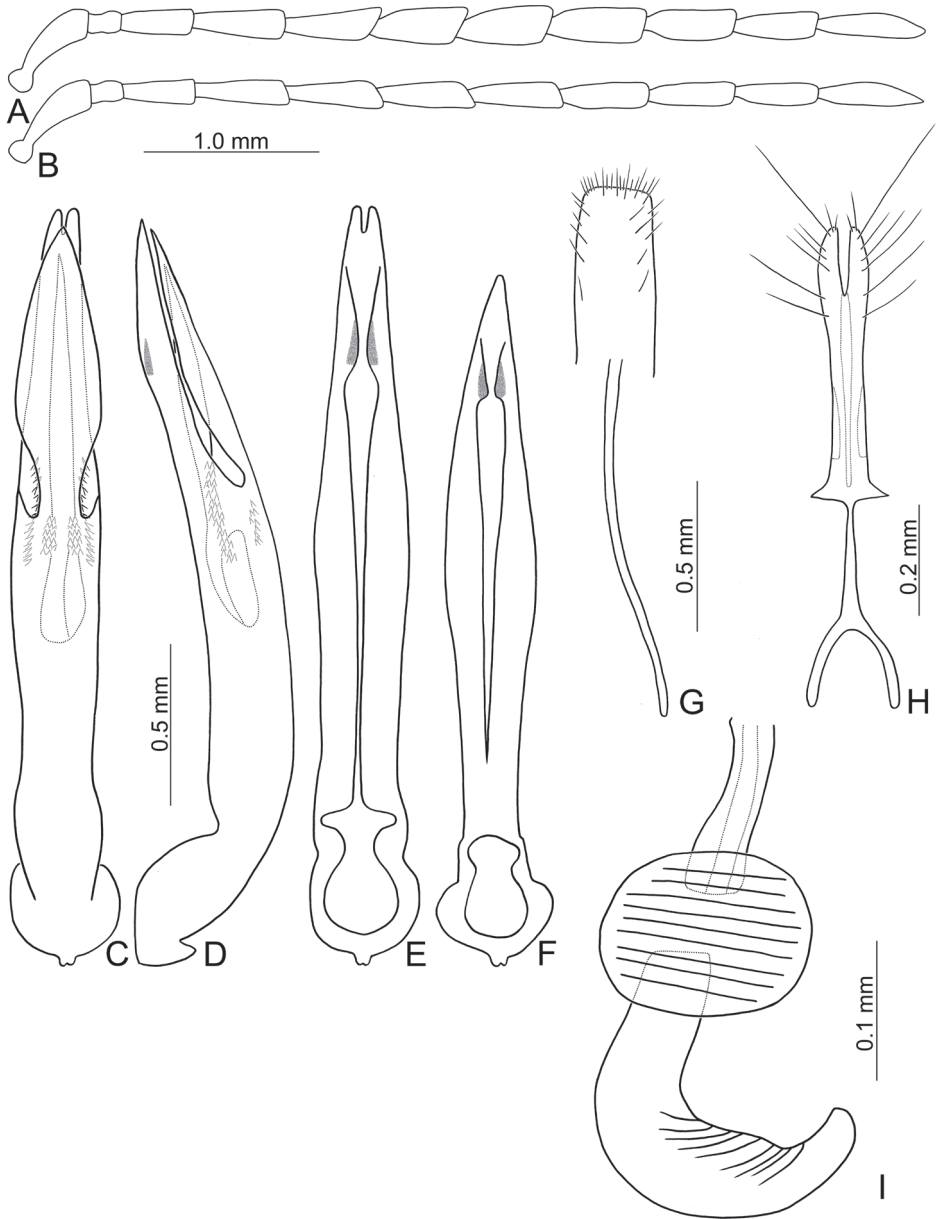
Figure 4. Diagnostic characters of *Theopea mouhoti*. **A** Antenna, male **B** Antenna, female **C** Aedeagus, dorsal view **D** Same, lateral view **E** Same, ventral view **F** Aedeagus, variation, ventral view **G** Abdominal ventrite VIII **H** Gonocoxae **I** Spermatheca.

moderately curved in lateral view; ventral surface with deep notch from near apex, apically extending into basal opening, more approximate in apical 1/5; triangular sclerites small; internal sac with one median, elongate sclerite, 0.5× as long as aedeagus, apically

tapering from basal 1/3, apex acute, connected by short, broad sclerite at base; with one pair of elongate, longitudinal rows of stout setae, and one pair of short, longitudinal rows of stout setae dorsally and basally. Gonocoxae (Fig. 4H) elongate, widest at apical 1/9, both gonocoxae combined from basal 1/7 to apical 1/7; apices narrowly rounded, each gonocoxa with eight setae along lateral margin from apex to apical 1/6; with one pair of short lateral processes at basal 2/5. Ventrite VIII (Fig. 4G) elongate and well sclerotized; disc with several long setae at sides and near apical margin, and with dense, short setae along apical margin; spiculum extremely slender. Receptacle of spermatheca (Fig. 4I) strongly swollen; pump slender and strongly curved; proximal spermathecal duct deeply inserted into receptacle, narrow and short.

Variations. Males of Laos have apically tapering and truncate apex of aedeagus and its ventral surface have median notch not extending into basal opening (Fig. 4F).

Diagnosis. *Theopea mouhoti* Baly, *T. bicolor* Kimoto, and *T. bicoloroides* sp. nov. are characterized by their reddish brown elytra. *Theopea mouhoti* (Fig. 1G–I) can be easily separately from *Theopea bicolor* and *T. bicoloroides* sp. nov. (Fig. 1A–F) by the reddish brown head, prothorax, and scutellum, and distinct and convex ridges on the elytra. Further, males of *T. mouhoti* have median elongate internal aedeagal sclerites without transverse rows of hair-like setae (Fig. 4C, D). This differs from those of *T. bicolor* and *T. bicoloroides* sp. nov., which possess a median elongate internal aedeagal sclerite with hair-like setae in transverse rows (Figs 2C, D; 3C, D).

Distribution. Cambodia, Laos, Thailand.

Pseudotheopea Lee & Bezděk, gen. nov.

http://zoobank.org/94C80C3C-5F26-45CC-B532-AC499817D38D

Type species. *Theopea sauteri* Chûjô, 1935a (here designated)

Description. Body length 4.8–7.2 mm.

Males. Head. Eyes moderately large. Anterior part of head not modified or modified (strongly excavated and modified in *P. costata* group). Frontal tubercles prominent, narrow, usually produced at inner anterior angle. Penultimate maxillary palpomere not greatly swollen, apical palpomere conical. Vertex with reticulate microsculpture.

Antenna 11-segmented, filiform and slender, some antennomeres apically expanded or curved in males; antennomere II very short, III long, 1.7–3.5× longer than II, 0.6–1.0× as long as I, 2.4–3.3× as long as wide.

Pronotum quadrate or transverse, 1.2–1.3× as wide as long, broadest at middle, with pair of discal depressions. Anterior pronotal border absent. Lateral margins rounded or subparallel. Disc with reticulate microsculpture.

Elytra. Surface almost glabrous (with scattered erect setae on apical part only) except *P. similis* (Kimoto); punctate and striate, usually with longitudinal ridges between two longitudinal rows of punctures, sometimes ridges reduced or absent in part. Epipleura gradually narrowed to apex. Disc with reticulate microsculpture.

Legs. Procoxae globular, prosternal process reduced to thin depressed ridge but apically expanded, procoxal cavities closed. Protarsomere I more or less swollen. Metatibia simple, with apical spine. Length of metatarsomere I nearly equal to following tarsomeres combined. Tarsal claws appendiculate with basal tooth small and rounded. Metatarsomere I simple.

Abdomen. Last ventrite apically trilobate.

Aedeagus always ventrally flattened, apex with shallow notch. Ventral surface with wide groove, with a constriction formed by two small triangular sclerites that are elongate in some species. Internal sac with median elongate sclerite, divided into two parts; sometimes with single or paired hook-like or longitudinal and apically tapering sclerites.

Females. Antenna slender, unmodified. Protarsomere I not modified. Posterior margin of last ventrite regularly rounded, without incisions. Spermatheca with small receptacle and C-shaped pump. Gonocoxae bifurcate basally, apically convergent, apical part usually with eight long setae. Ventrite VIII longitudinal, longer setae laterally, shorter setae along apical margin, spiculum 1.6-3.5× as long as ventrite VIII.

Differential diagnosis. This new genus possesses the following characters shared with *Theopea* Baly: the punctures on the elytra are striate, with ridges between two longitudinal rows of punctures; spaces between longitudinal rows of punctures broader when ridges are reduced or absent. But *Pseudotheopea* gen. nov. differs from *Theopea* by the presence of reticulate microsculpture on the vertex and pronotum (lacking reticulations in *Theopea*), with apical spine of metatibia (absent in *Theopea*), and antennomeres III-X usually longer and curved in males (antennomeres III-X usually swollen or modified in males of *Theopea*). Genitalic characters that distinguish males of *Pseudotheopea* from those of *Theopea* include the relatively longer tectum (> 0.5× as long as aedeagus) and divided median elongate endophallic sclerite in *Pseudotheopea* (relative shorter tectum and < 0.5× as long as aedeagus and the intact median elongate endophallic sclerite in *Theopea*). In females, the gonocoxae are convergent apically in *Pseudotheopea* (divergent in *Theopea*).

Remarks. All *Theopea* species (11 species) from East Asia studied by Lee and Bezděk (2018) and *T. costata* (Allard) (Lee and Bezděk 2019) are transferred to this new genus. Twelve additional species are recognized as members of *Pseudotheopea* gen. nov. including five species transferred from *Theopea* and seven new species. Two species groups are proposed here (Table 1).

Etymology. This new genus is named for its similarity with the genus *Theopea* Baly.

Pseudotheopea costata group

Diagnosis. Frontoclypeus modified in males, with concavity between eyes, sometimes with erect processes and setae within concavity.

Included species. *Pseudotheopea aeneipennis* (Gressitt & Kimoto), comb. nov., *P. azurea* (Gressitt & Kimoto), comb. nov., *P. boreri* sp. nov., *P. clypealis* (Medvedev), comb. nov., *P. gressitti* sp. nov., *P. hsingtzungi* sp. nov., *P. kimotoi* sp. nov., *P. leehsuehae* sp. nov., *P. smaragdina* (Gressitt & Kimoto), comb. nov., and *P. sufangae* sp. nov.

Table 1. Definition of species groups and catalogue of *Pseudotheopea* species.

***Pseudotheopea sauteri* species group**	
Frontoclypeus not modified in males; body metallic blue, longitudinal ridges distinct and few setae on the elytra.	
P. coerulea (Gressitt & Kimoto, 1963: 679) (*Theopea*), **comb. nov.**	China
P. geiseri (Lee & Bezděk, 2018: 361) (*Theopea*), **comb. nov.**	India
P. hainanensis (Lee & Bezděk, 2018: 361) (*Theopea*), **comb. nov.**	China
P. laosensis (Lee & Bezděk, 2018: 363) (*Theopea*), **comb. nov.**	China, Laos, Vietnam
P. sauteri (Chûjô, 1935a: 169) (*Theopea*), **comb. nov.**	Taiwan
P. sekerkai (Lee & Bezděk, 2018: 372) (*Theopea*), **comb. nov.**	Laos
***Pseudotheopea costata* species group**	
Frontoclypeus modified in males, with concavity between eyes, sometimes with erect processes and setae inside concavity.	
P. aeneipennis (Gressitt & Kimoto, 1963: 677) (*Theopea*), **comb. nov.**	China
P. azurea (Gressitt & Kimoto, 1963: 677) (*Theopea*), **comb. nov.**	China
P. boreri **sp. nov.**	India
P. clypealis (Medvedev, 2015: 72) (*Theopea*), **comb. nov.**	Vietnam
P. costata (Allard, 1889: 111) (*Ozomena*), **comb. nov.**	Philippines
P. gressitti Lee and Bezděk, **sp. nov.**	Philippines
P. hsingtzungi **sp. nov.**	Laos
P. kimotoi **sp. nov.**	Laos, Thailand, Vietnam
P. leehsuehae **sp. nov.**	Laos
P. smaragdina (Gressitt & Kimoto, 1963: 680) (*Theopea*), **comb. nov.**	China
P. sufangae **sp. nov.**	Taiwan
***Pseudotheopea similis* species group**	
Frontoclypeus not modified in males; longitudinal ridges indistinct and with dense setae on the elytra.	
P. nigrita (Medvedev, 2007: 11) (*Theopea*), **comb. nov.**	Thailand
P. similis (Kimoto, 1989: 201) (*Theopea*), **comb. nov.**	Laos, Vietnam
= *subviridis* Medvedev, 2012: 67 (*Theopea*) **syn. nov.**	
***Pseudotheopea* species current unassigned to any species group**	
P. aureoviridis (Chûjô, 1935b: 85) (*Theopea*), **comb. nov.**	Japan
P. cheni (Lee & Bezděk, 2018: 340) (*Theopea*), **comb. nov.**	Taiwan
P. collaris (Kimoto, 1989: 75) (*Theopea*), **comb. nov.**	Taiwan
P. irregularis (Takizawa, 1978: 129) (*Theopea*), **comb. nov.**	Taiwan
P. kanmiyai (Kimoto, 1984: 53) (*Hoplosaenidea*), **comb. nov.**	Taiwan

Pseudotheopea aeneipennis (Gressitt & Kimoto, 1963), comb. nov.
Figs 5A–C, 6A–C, 7

Theopea aeneipennis: Gressitt and Kimoto 1963: 677 (China: Fujian, Jiangxi, Guandong); Wilcox 1973: 630 (catalogue); Wang et al. 1998: 128 (China: Fujian: Wuyishan); Yang 2002: 656 (China: Fujian); Yang and Yao 2002: 447 (China: Hainan Island); Beenen 2010: 489 (catalogue).

Types. Holotype ♂ (BPBM, by original designation): "Fukian, S. China / Shaowu, TaChuLang / July. 1. 1942 / T. C. Maa [p, w] // HOLOTYPE [P] ♂ / Theopea / aeneipennis [h] / Gressitt and Kimoto [p, r] // Theopea / aeneipennis / holo G and K [h] / J. L. Gressitt det. [p, w]". Paratypes. 1♀ (CAS): "FUKIEN S. China / Shaowu, Tachulan [p] / 24.VIII.[h]194[p]6[h] T. Maa [p, w] // PARATYPE [p] / Theopea / aeneipennis [h] / Gressitt and Kimoto [p, y] // Theopea / aeneipennis / G and K [h] /
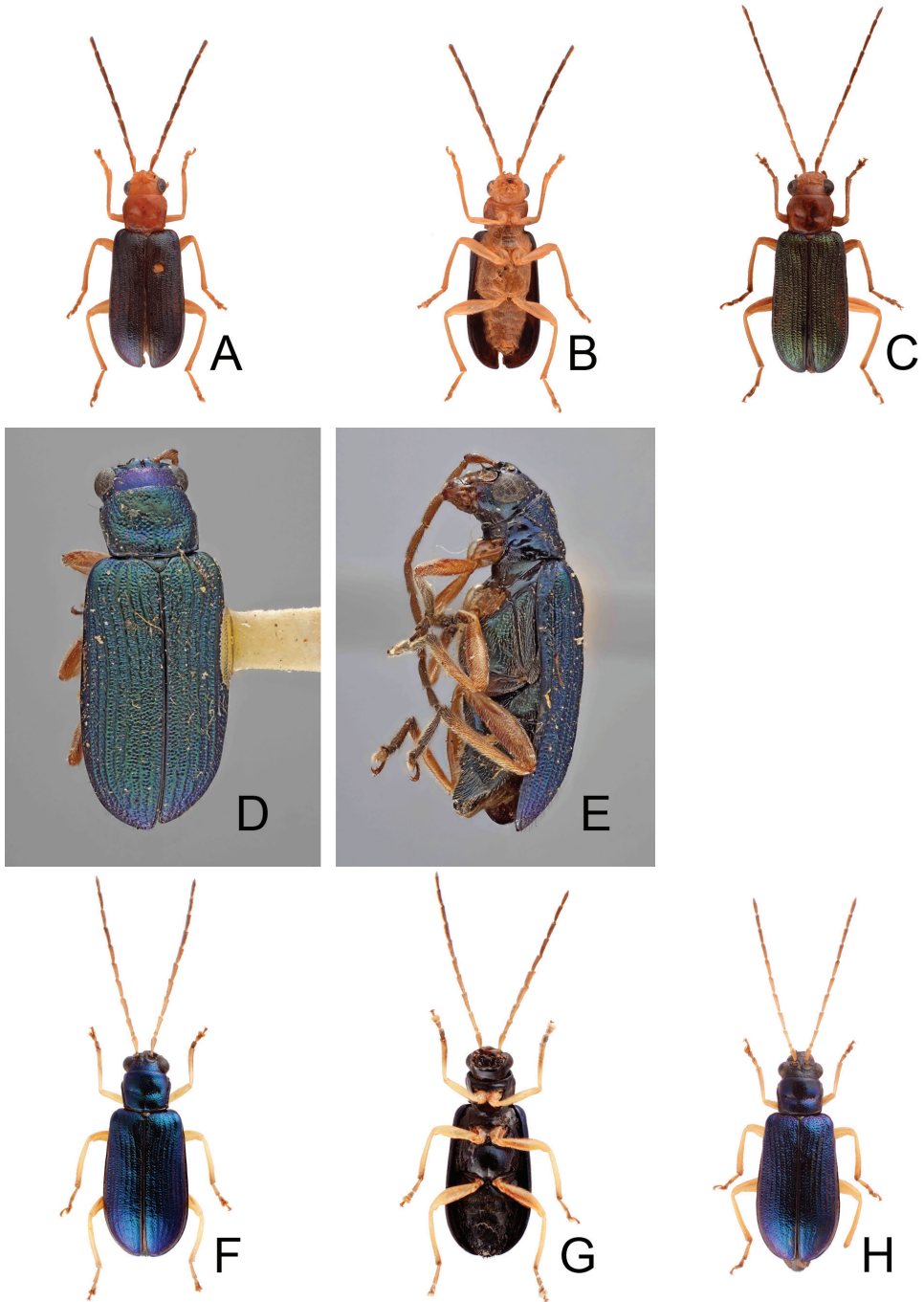
Figure 5. Habitus of *Pseudotheopea aeneipennis*, *P. azurea*, and *P. sufangae* sp. nov. **A** *T. aeneipennis*, male, dorsal view **B** Same, ventral view **C** *P. aeneipennis*, female, dorsal view **D** *P. azurea*, holotype, dorsal view **E** Same, lateral view **F** *P. sufangae* sp. nov., male, dorsal view **G** Same, ventral view **H** *P. sufangae* sp. nov., female, dorsal view.
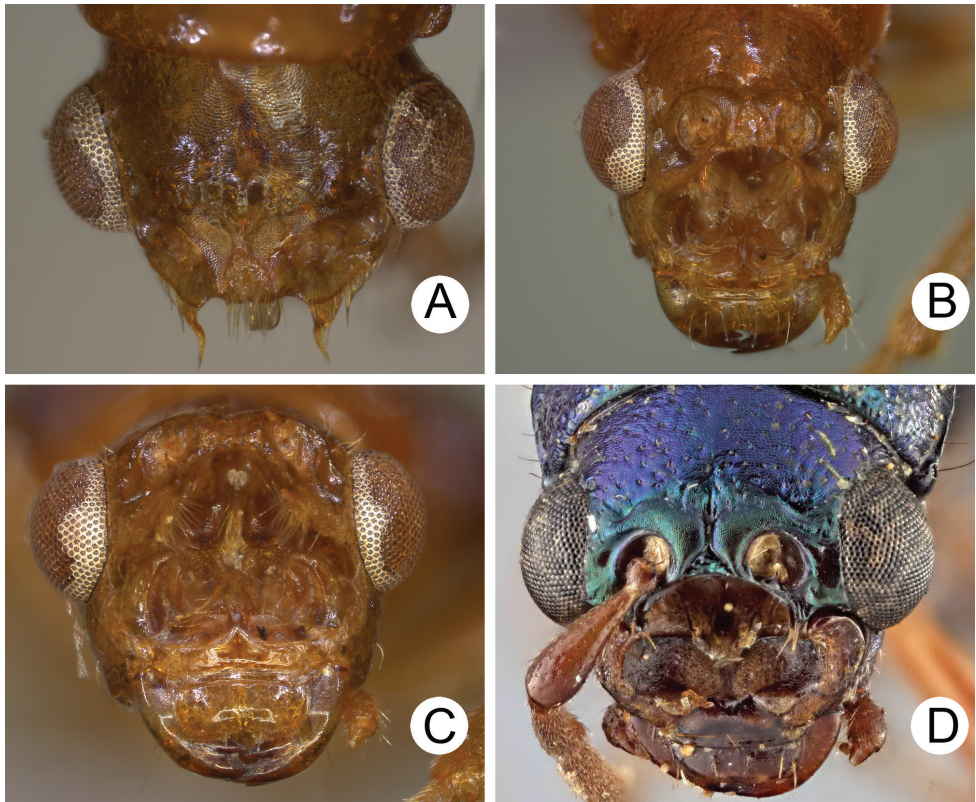
Figure 6. Heads of males of *Pseudotheopea aeneipennis* and *P. azurea*. **A** *P. aeneipennis*, dorsal view **B** Same, dorsofrontal view **C** Same, front view **D** *P. azurea*, holotype, dorsofrontal view.

Gressitt and Kimoto det. 1961 [p, w]"; 1♀ (BPBM): "FUKIEN S. China / Chungan: Upper / Kuatun 1400 m. / T. C. Maa [p, w] // Aug. 6, 1945 [h, w] // ALLOTYPE [p] / Theopea / aeneipennis [h] / J. L. Gressitt [p, pink label] // Theopea / aeneipennis / ♀ G and K [h] / Gressitt and Kimoto det. 1961 [p, w] // Theopea / sp. nov. 4 / allo. [longitudinal] / aeneipennis [h] / Det. S. Kimoto [p] G and K [h, w]"; 1♀ (NHMUK): "Para- / type [p, w, circle label with yellow border] // FUKIEN, S. China / Chungan, Upper / Kuatun, 1400 m, / T. C. Maa [p, w] // Brit. Mus. / 1963-245. [p, w] // Aug. 6, 1945 [h, w] // PARATYPE [p] / Theopea / aeneipennis [h] / Gressitt and Kimoto [p, y] // aeneipennis [h, w]"; 3♀♀ (CAS): "Tai An Tong, S / Kiangsi pr., S / China VII-6-36 [p, w] // L. Gressitt / Collector [p, w] // PARATYPE [p] / Theopea / aeneipennis [h] / Gressitt and Kimoto [p, y]"; 1♀ (CAS): "CHINA: Kiangsi / Tai-an-hong / VII-4-1936 / J.L. Gressitt [p, w] // L. Gressitt / Collector [p, w] // PARATYPE [p] / Theopea / aeneipennis [h] / Gressitt and Kimoto [p, y]".

Other material examined. CHINA. Fujian: 1♂ (IZAS), Chonganxing Village (崇安星村), Sangan (三港), 740 m, 28.VI.1960, leg. Cai Zuo (左采); 1♂, 1♀ (IZAS), same locality, 740-900 m, 6.VII.1960, leg. Yi-Ran Zhang (張毅然); 1♂ (IZAS), Chonganxing Village (崇安星村), Guadun (掛墩), 840-1210 m, 14.VII.1960, leg.
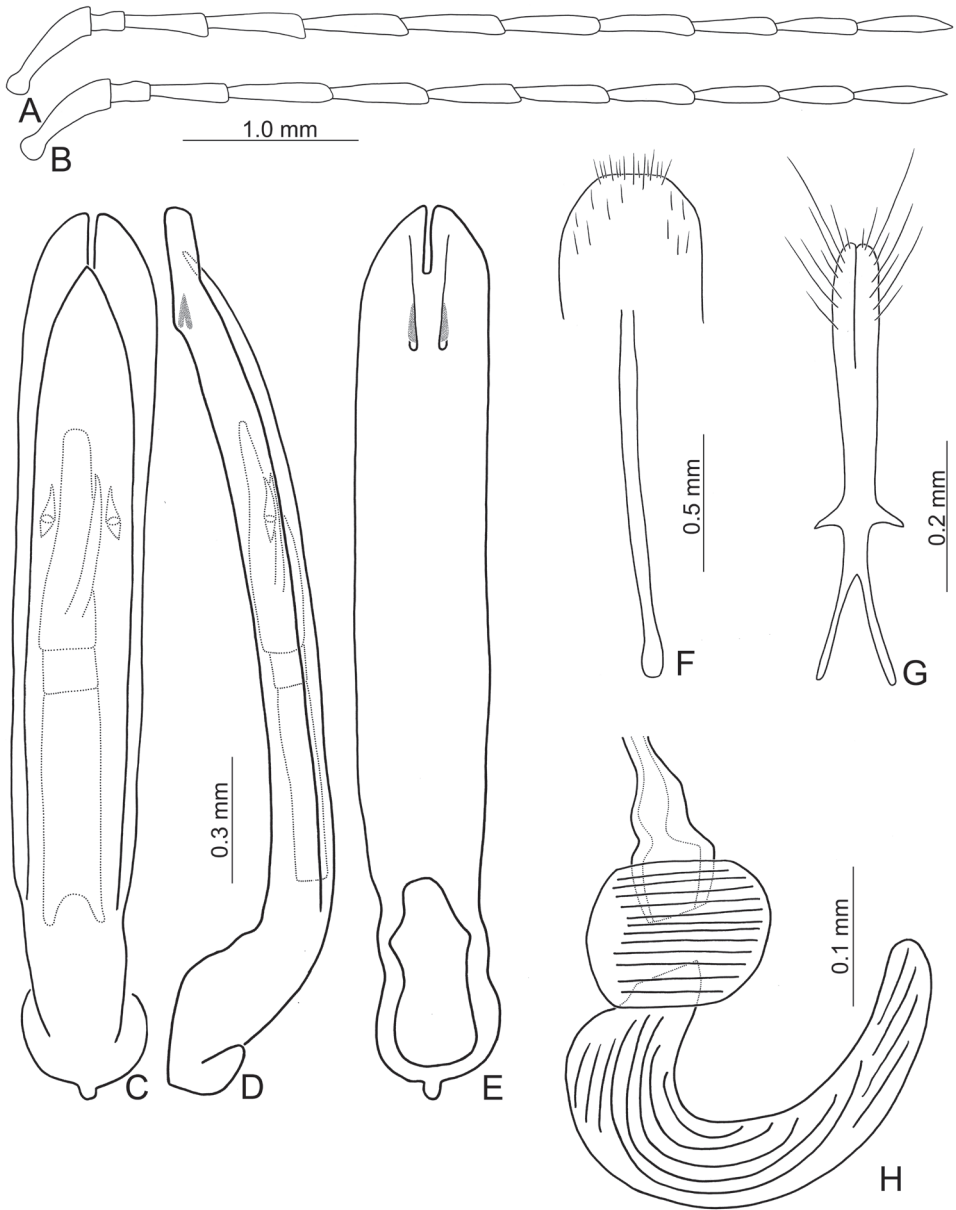
Figure 7. Diagnostic characters of *Pseudotheopea aeneipennis*. **A** Antenna, male **B** Antenna, female **C** Aedeagus, dorsal view **D** Aedeagus, lateral view **E** Aedeagus, ventral view **F** Abdominal ventrite VIII **G** Gonocoxae **H** Spermatheca.

Yi-Ran Zhang (張毅然); 1♀ (IZAS), same locality, 1140 m, 2.VII.1960, leg. Sheng-Qiao Jiang (姜勝巧); 1♀ (IZAS), same locality, 800-1140 m, 22.VII.1960, leg. Fu-Ji Pu (蒲富基); Guangdong: 1♀ (SMNS), Yu-Yueng Nat. Reserve, S Mt. Shi-King-Kong, 24°56'N 112°59'E, 600-1200 m, 28-30.VI.1996, leg. C. Häuser.

Redescription. Length 6.5–6.6 mm, width 2.4-2.5 mm. Body color (Fig. 5A–C) reddish brown or yellowish brown, but antennomeres III-XI more or less darker, elytra greenish bronze. Frontoclypeus (Fig. 6A–C) transverse and deeply excavated between eyes in males, concavity as wide as interspace between eyes; apical margin produced anterior, with clusters of hair-like setae at middle and sides, and convex at sides; with one pair of erect and slender sclerites at center, close to each other, apices rounded; with short, erect, and rounded sclerites insides at middle and sides of basal margin, margined with long hair-like setae and with longitudinal ridges at middle of basal margin. Antennae filiform in males, (Fig. 7A), antennomeres V and VI slightly curved, length ratios of antennomeres I–XI 1.0: 0.3: 0.8: 1.0: 1.0: 1.0: 1.0: 0.9: 0.8: 0.8: 0.9, length to width ratios of antennomeres I–XI 3.7: 1.8: 3.9: 4.4: 5.0: 5.1: 5.3: 5.1: 4.8: 4.6: 5.9; similar in females (Fig. 7B), length ratios of antennomeres I–XI 1.0: 0.4: 0.7: 0.9: 0.9: 0.9: 0.9: 0.8: 0.8: 0.7: 0.9, length to width ratios of antennomeres I–XI 3.7: 1.9: 4.0: 4.7: 4.8: 5.1: 4.9: 4.6: 4,8: 4.2: 5.3. Elytra elongate, parallel-sided, 1.9× longer than wide; disc with dense, coarse punctures, arranged into longitudinal rows, with one indistinct longitudinal ridge between two longitudinal rows of punctures. Tarsomeres I of front legs slightly swollen in males; subparallel in females. Aedeagus (Fig. 7C–E) slender, 7.2× longer than wide; apex with shallow notch; tectum elongate, from apical 1/20 to basal 1/5; dorso-ventrally flattened, slightly curved in lateral view, angular at apical 1/7, straight from apex to apical 1/7; triangular sclerites small; internal sac with elongate, endophallic sclerite complex, 0.5× as long as aedeagus, composed of three sclerites, apical piece as long as basal piece, 0.45× long as entire sclerite; median piece shortest, 0.1× long as entire sclerite; with one elongate, apically sclerite located near base of apical piece; with one pair of short hook-like sclerite at sides. Gonocoxae (Fig. 7G) elongate, both gonocoxae fused from basal 1/4 to apical 1/3; apices convergent and narrowly rounded, each gonocoxa with eight setae along lateral margin from apex to apical 1/6, with lateral processes at basal 2/5. Ventrite VIII (Fig. 7F) elongate and well sclerotized; disc with several long setae at sides and near apical margin, and with dense, short setae along apical margin; spiculum extremely slender. Receptacle of spermatheca (Fig. 7H) tightly joined with pump, pump slender and strongly curved; proximal spermathecal duct deeply inserted into receptacle, narrow and short.

Diagnosis. *Pseudotheopea aeneipennis* (Gressitt and Kimoto) is characterized by its color pattern: reddish brown body with bluish or greenish metallic elytra (Fig. 5A–C). The aedeagus is characterized by its broadly rounded apex, with one additional elongate dorsal sclerite near base of apical piece, and with one pair of small hook-like sclerites at sides near apex of median apical piece (Fig. 7C–E).

Distribution. China (Fujian, Jiangxi, Guandong, Hainan Island).

Pseudotheopea azurea (Gressitt & Kimoto, 1963), comb. nov.
Figs 5D–E, 6D

Theopea azurea: Gressitt and Kimoto, 1963: 677 (China: Guandong); Wilcox 1973: 630 (catalogue); Wang et al. 1998: 128 (China: Fujian); Yang 2002: 656 (China:

Fujian); Yang and Yao 2002: 447 (China: Hainan Island); Beenen 2010: 489 (catalogue).

Type. Holotype ♂ (CAS): "CHINA: Kwang- / tung, Summer / 1950. JL. Gressitt [p, w] // L. Gressitt / Collection [p, w] // HOLOTYPE [p] ♂ / Theopea / azurea [h] / Gressitt and Kimoto [p, r] // Theopea / azurea / holo G and K [h] / J. L. Gressitt det. [p, w] // California Academy / of Sciences / Type / No. [p] 13312 [h, w]".

    Diagnosis (based on photographs)**.** Body color (Fig. 5D, E) bluish metallic, mouth parts and antennae dark brown; legs yellowish brown but tibiae and tarsi dark brown. Frontoclypeus (Fig. 6D) transverse and deeply excavated between eyes in males, concavity as wide as interspace between eyes, apico-lateral angles margined with long hair-like setae except along basal margin; with a pair of erect processes at center, almost reaching level of opening.

    Distribution. China (Fujian and Guandong).

Pseudotheopea boreri sp. nov.

http://zoobank.org/1646E14D-D30C-4144-813C-628D6B014FF8
Figs 8A–C; 9A, B; 10

Types. Holotype ♂ (NHMB), INDIA. Meghalaya, 9 km NW of Jowai, 25°30'N 92°10'E, 1400m, 12.V.1999, leg. Dembický and Pacholátko. Paratypes. 1♂, 2♀♀ (NHMB), same as holotype; **INDIA**. Assam: 1♀ (NMPC), 5 km N of Umrongso, 700 m, 25°27'N 92°43'E, 17.-25.V.1999, leg. J. Rolčík; 1♀ (NHMB), same locality, 21.V.1999, leg. Dembický and Pacholátko"; Meghalaya: 2♀♀ (JBCB), Nokrek N.P., 3km S Daribokgiri, 1400 m, 25°27'N 90°19'E, 26.IV.1999, leg. Rolčík; 1♀ (JBCB), 8 km N of Shillong, 1200 m, 25°38'N 91°54'E, 7.-9.V.2004, leg. R. Businský; 1♂, 1♀ (NHMB), same but with "leg. L. Dembický".

    Description. Length 5.6–6.6 mm, width 2.0–2.6 mm. Body color (Fig. 8A–C) golden green, but legs yellowish brown but apices of tibiae and tarsi darker; mouth parts and antennae dark brown. Frontoclypeus (Fig. 9A, B) transverse and deeply excavated between eyes in males, concavity as wide as interspace between eyes, margined with long hair-like setae except along basal margin; with dense, long hair-like setae at center. Antennae filiform in males, (Fig. 10A), relatively broader than females, antennomeres V and VI slightly curved, length ratios of antennomeres I–XI 1.0: 0.3: 0.9: 1.2: 1.1: 1.1: 1.1: 1.0: 1.0: 0.9: 1.1, length to width ratios of antennomeres I–XI 3.2: 1.3: 3.2: 4.1: 4.4: 4.5: 4.9: 5.1: 5.2: 5.0: 5.8; filiform in females (Fig. 10B), length ratios of antennomeres I–XI 1.0: 0.3: 0.7: 0.9: 0.9: 0.8: 0.8: 0.8: 0.8: 0.8: 0.9, length to width ratios of antennomeres I–XI 3.8: 2.1: 3.7: 4.8: 4.9: 4.4: 4.7: 5.1: 5.3: 4.9: 6.6. Elytra elongate, parallel-sided, 1.8-2.0× longer than wide; disc with dense, coarse punctures, arranged into longitudinal rows, with one indistinct longitudinal ridge between two longitudinal rows of punctures; with distinct convex area behind scutellum in males. Tarsomeres I of front legs swollen in males; subparallel in females. Aedeagus (Fig. 10C–E) extremely slender, 7.7× longer than wide; apex with shallow notch, both
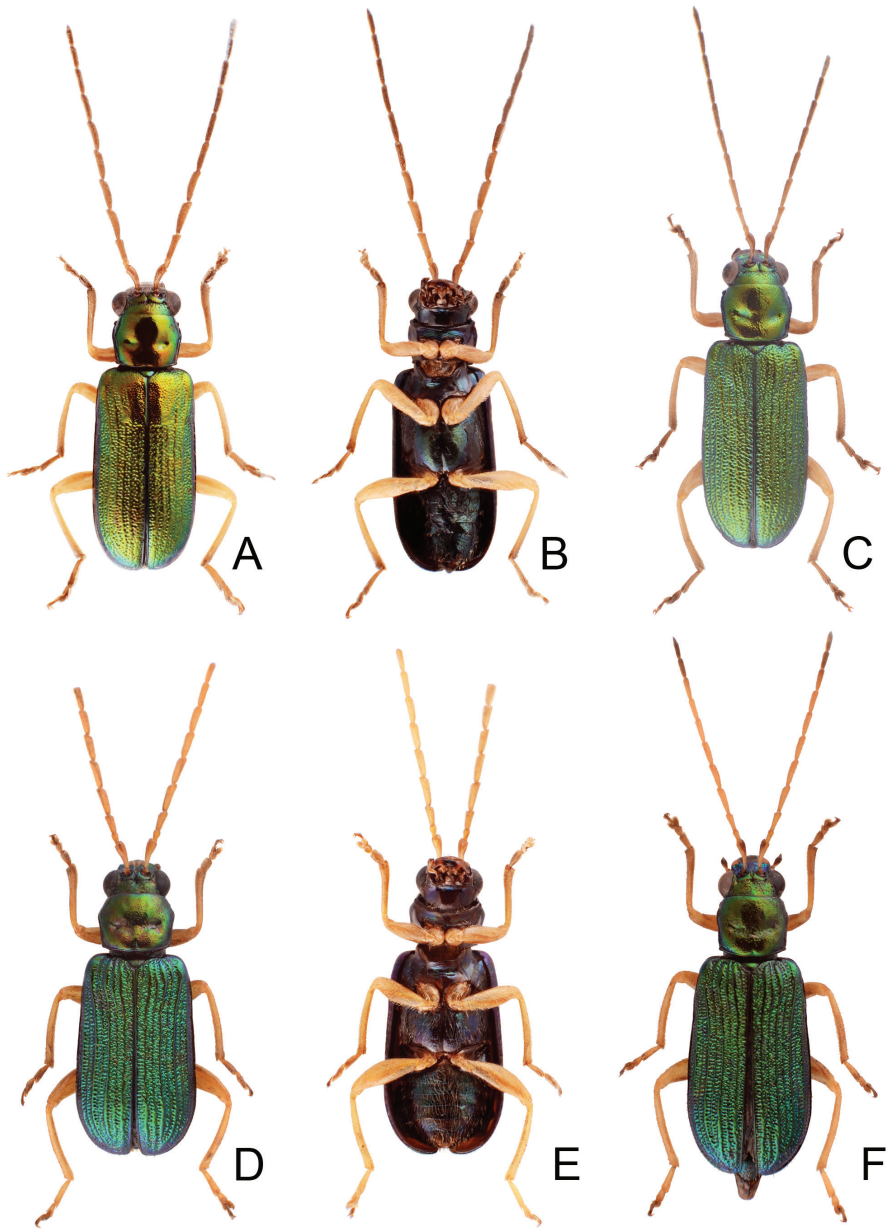
Figure 8. Habitus of *Pseudotheopea boreri* sp. nov. and *P. clypealis*. **A** *P. boreri* sp. nov., male, dorsal view **B** Same, ventral view **C** *P. boreri*, female, dorsal view **D** *P. clypealis*, male, dorsal view **E** Same, ventral view **F** *P. clypealis*, female, dorsal view.

apices equal in length; tectum elongate from apical 1/10 to basal 2/5; moderately curved in lateral view, angular at apical 1/4, straight from apex to apical 1/4; triangular sclerites elongate; internal sac with elongate, endophallic sclerite complex, 0.4× as long as aedeagus, composed of two sclerites, apical piece (0.6×) much shorter than basal
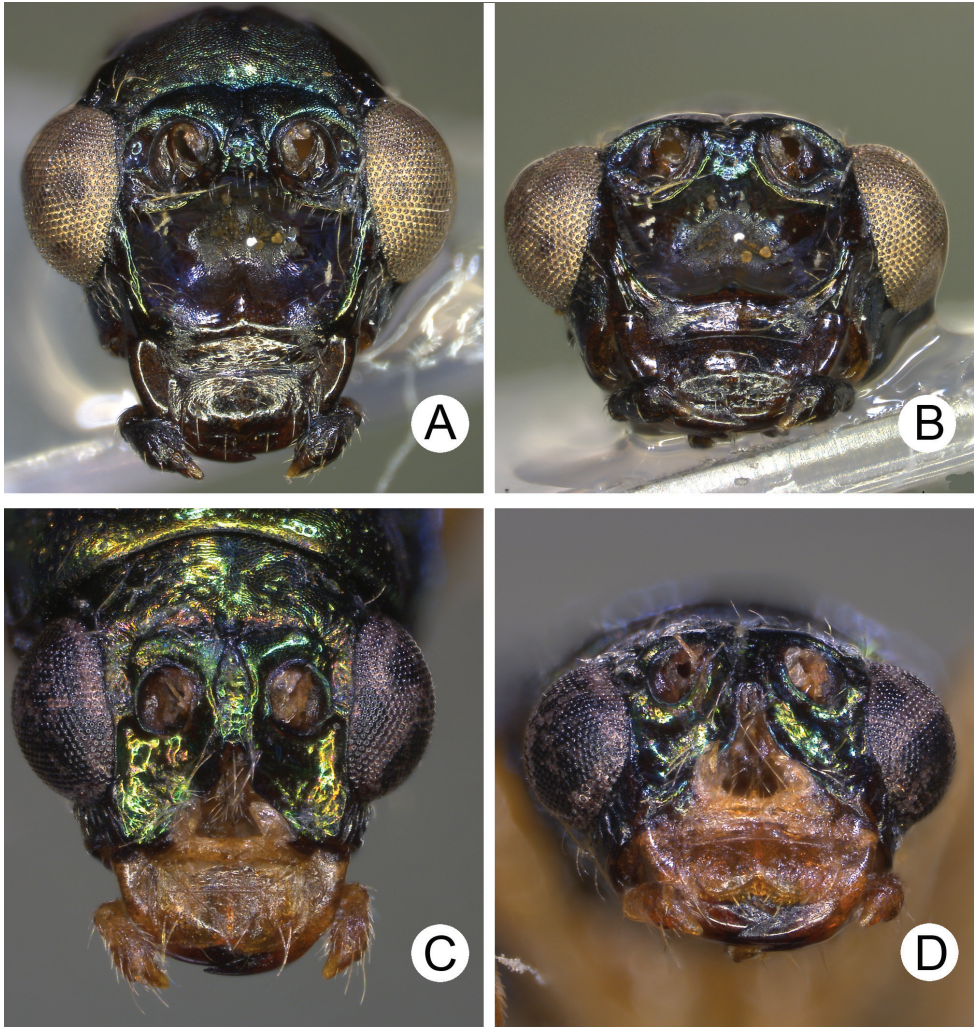
Figure 9. Heads of males of *Pseudotheopea boreri* sp. nov. and *P. clypealis*. **A** *P. boreri* sp. nov., dorsofrontal view **B** Same, front view **C** *P. clypealis*, dorsofrontal view **D** Same, front view.

piece. Gonocoxae (Fig. 10G) elongate, both gonocoxae fused from basal 1/4 to apical 1/5; apices convergent and narrowly rounded, each gonocoxa with eight setae along lateral margin from apex to apical 1/6, some setae extremely short; lateral processes reduced. Ventrite VIII (Fig. 10F) elongate and well sclerotized; disc with several long setae at sides and near apical margin, and with dense, short setae along apical margin; spiculum extremely slender. Receptacle of spermatheca (Fig. 10H) tightly joined with pump, pump slender and strongly curved; proximal spermathecal duct deeply inserted into receptacle, narrow and short.

Diagnosis. *Pseudotheopea boreri* sp. nov. (Fig 8A–C), *P. clypealis* (Medvedev) (Fig. 8D–F), *P. hsingtzungi* sp. nov. (Fig. 15A–C), and *P. smaragdina* (Gressitt and Kimoto)

Figure 10. Diagnostic characters of *Pseudotheopea boreri* sp. nov. **A** Antenna, male **B** Antenna, female **C** Aedeagus, dorsal view **D** Aedeagus, lateral view **E** Aedeagus, ventral view **F** Abdominal ventrite VIII **G** Gonocoxae **H** Spermatheca.

(Fig. 15D–F), are characterized by their golden green coloration. They can be identified based on their distribution: *P. boreri* sp. nov. from India, *P. clypealis* from Vietnam, *P. hsingtzungi* sp. nov. from Laos, and *P. smaragdina* from China. *Pseudotheopea boreri*

sp. nov. (Fig. 8A) is similar to *P. hsingtzungi* sp. nov. (Fig. 15A) and *P. smaragdina* (Fig. 15D) by sharing the indistinct longitudinal ridges on the elytra (convex and distinct longitudinal ridges on the elytra in *P. clypealis* (Fig. 8D)), but differs by the presence of convex area surrounding scutellum and with reduced longitudinal ridges on the elytra in males (Fig. 8A) (without convex area surrounding scutellum on the elytra in those of others (Figs 8D, 15A, D)) and concavity wide between eyes and without erect processes in males (Fig. 9A, B) (concavity wide between eyes with one erect process in those of *P. smaragdina* (Fig. 16C, D); concavity narrowed between eyes and without erect processes in those of *P. hsingtzungi* sp. nov. (Fig. 16A, B)). In males, the internal aedeagal sac of *P. boreri* sp. nov. lacks additional sclerites except the median elongate sclerite (Fig. 10C, D). This structure is shared with males of *P. gressitti* sp. nov. (Fig. 14C, D), and *P. costata* (Allard), *Pseudotheopea boreri* sp. nov. males differ from both species in possessing a dorso-ventrally flattened aedeagus with a sclerotized ventral surface (Fig. 7C–E) (wide aedeagus with membranous ventral surface in *P. gressitti* sp. nov. (Fig. 14C–E)).

Etymology. This new species is dedicated to Matthias Borer (Curator, NHMB), who encouraged the first author to focus his research on leaf beetles.

Distribution. India.

Pseudotheopea clypealis (Medvedev, 2015), comb. nov.
Figs 8D–F; 9C, D; 11

Theopea clypealis : Medvedev 2015: 72 (South Vietnam)

Type. Holotype ♂ (LMCM, based on photographs): "Vietnam Dongnai Pr. / Cat Tien V.99 / leg. A. Polilov [p, w] // HOLOTYPUS / Theopea / clypealis / L. Medvedev [p, r]".

Other specimens examined. VIETNAM. Kien Giang: 2♂♂, 3♀♀ (TARI), Phu Quoc island, 12-14.IV.2013, leg. Y.-T. Wang; 2♂♂, 1♀ (NMNS), same island, Ding Ba Rd. + Banh Dan Rd., 14.IV.2013, leg. M.-L. Jeng.

Redescription. Length 5.9–6.8 mm, width 2.3–2.6 mm. Body color (Figs 8D–F, 11) golden green, but antennae, mouth parts, and legs yellowish brown, two or three apical antennomeres darker. Frontoclypeus (Fig. 9C, D) transverse and deeply excavated between eyes in males, concavity 0.5× as wide as interspace between eyes, anteriorly narrowed, margined with long hair-like setae and with one erect process at center, margined with hair-like setae; baso-lateral angles covered by rounded membranous sclerites. Antennae filiform in males, (Fig. 11A), antennomeres III-IX slightly curved, length ratios of antennomeres I–XI 1.0: 0.3: 0.7: 0.8: 0.8: 0.8: 0.8: 0.7: 0.7: 0.6: 0.7, length to width ratios of antennomeres I–XI 3.6: 2.0: 3.2: 3.8: 3.8: 3.8: 4.2: 4.3: 3.9: 4.4: 5.3; filiform in females (Fig. 11B), similar to males, length ratios of antennomeres I–XI 1.0: 0.3: 0.6: 0.8: 0.8: 0.7: 0.7: 0.7: 0.6: 0.6: 0.7, length to width ratios of antennomeres I–XI 4.0: 2.0: 3.3: 4.8: 4.9: 4.4: 4.8: 4.7: 4.3: 3.9: 4.5. Elytra elongate, parallel-sided, 1.8× longer than wide; disc with dense, coarse punctures, arranged into longitudinal rows, with one longitudinal ridge between two longitudinal rows of
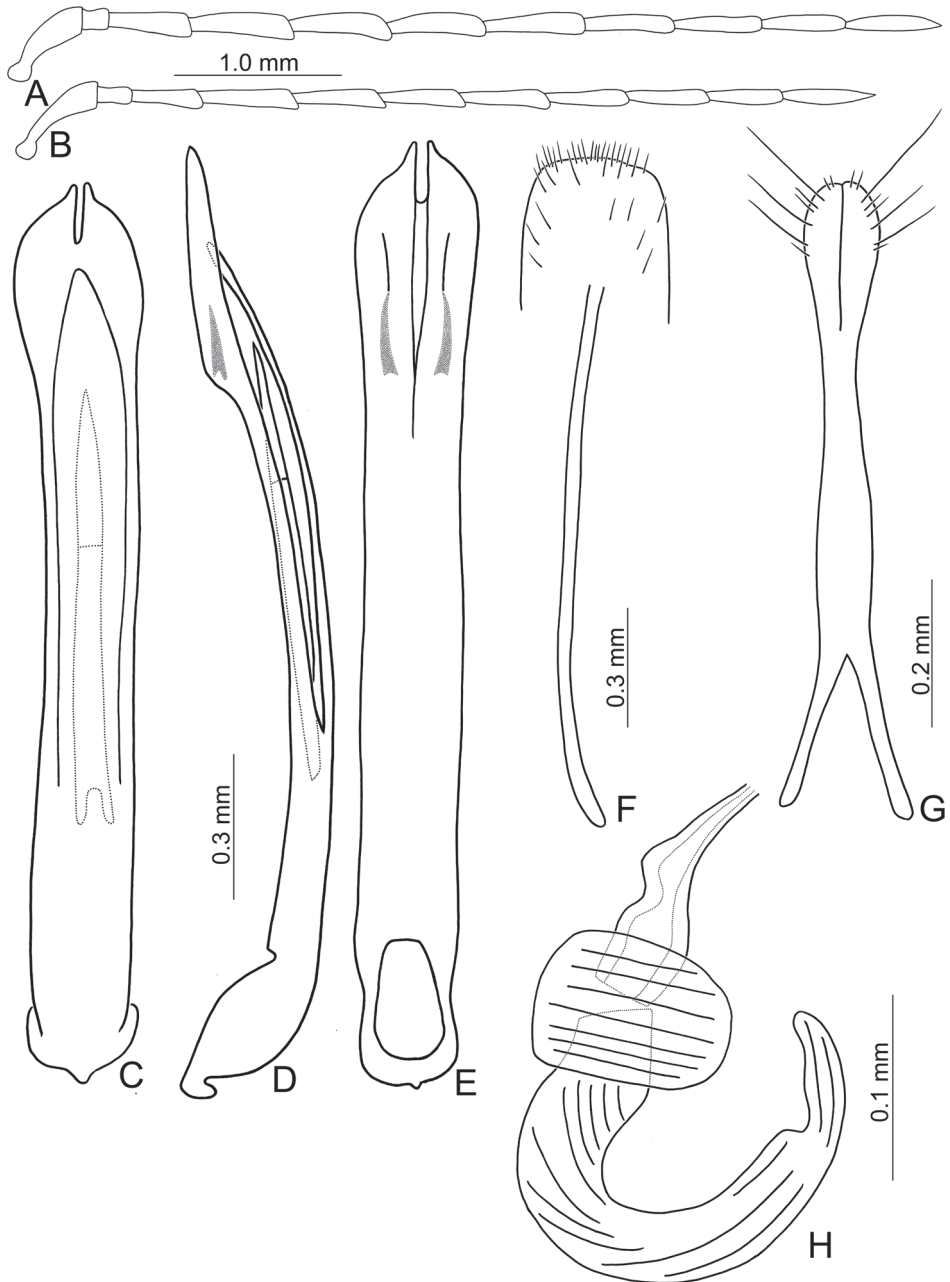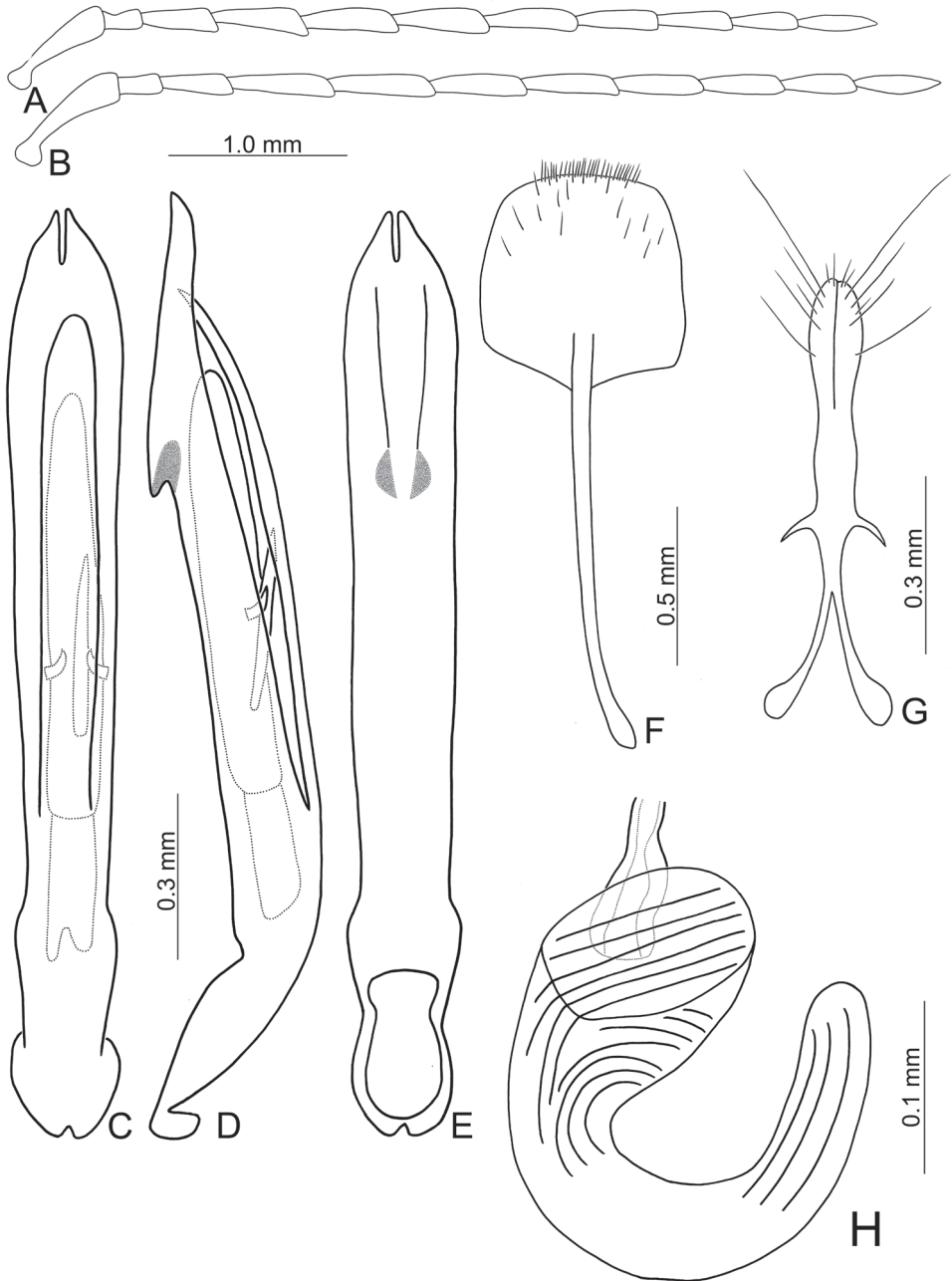
Figure 11. Diagnostic characters of *Pseudotheopea clypealis*. **A** Antenna, male **B** Antenna, female **C** Aedeagus, dorsal view **D** Aedeagus, lateral view **E** Aedeagus, ventral view **F** Abdominal ventrite VIII **G** Gonocoxae **H** Spermatheca.

punctures with convex, with distinct and indistinct ridges intertwined. Tarsomeres I of front legs swollen in males; subparallel in females. Aedeagus (Fig. 11C–E) extremely slender, 10.0× longer than wide; apex with shallow notch, both apices equal in length;

tectum elongate, from apical 1/10 to basal 2/5; almost straight but moderately curved at basal 1/5 in lateral view, apically curved, angular at apical 1/3; triangular sclerites small; internal sac with elongate, endophallic sclerite complex, 0.6× as long as aedeagus, composed of two sclerites, apical piece (4.0×) much longer than basal piece, one dorsal sclerite slender, 0.3× as long as endophallic sclerite; ventral sclerites absent but one additional pair of hook-like sclerites present. Gonocoxae (Fig. 11G) elongate, both gonocoxae fused from basal 1/3 to apical 1/4; apices convergent and narrowly rounded, each gonocoxa with seven setae along lateral margin from apex to apical 1/6; with one pair of short lateral processes at basal 2/5. Ventrite VIII (Fig. 11F) elongate and well sclerotized; disc with several long setae at sides and near apical margin, and with dense, short setae along apical margin; spiculum extremely slender. Receptacle of spermatheca (Fig. 11H) tightly joined with pump, pump slender and strongly curved; proximal spermathecal duct deeply inserted into receptacle, narrow and short.

Diagnosis. *Pseudotheopea clypealis* (Medvedev) (Fig. 8D–F), *P. boreri* sp. nov. (Fig. 8A–C), *P. hsingtzungi* sp. nov. (Fig. 15A–C), and *P. smaragdina* (Gressitt and Kimoto) (Fig. 15D–F), are characterized by their golden green coloration. They can be identified based on their distribution: *P. boreri* sp. nov. from India, *P. clypealis* from Vietnam, *P. hsingtzungi* sp. nov. from Laos, and *P. smaragdina* from China. *Pseudotheopea clypealis* can be separated from the others by the convex and distinct longitudinal ridges on the elytra (Fig. 8D, F) (indistinct longitudinal ridges on the elytra in others (Figs 8A, C; 15A, B, D, E), and the narrower anterior concavity between eyes (Fig. 9C, D) (broadly rounded anterior margin of concavity between eyes in others (Figs 9A, B; 16A–D). Males of *P. clypealis* are similar to those of *P. smaragdina* in possessing one additional elongate dorsal sclerite and one pair of small lateral hook-like sclerites inside the internal sac (Figs 11C, D; 22D, E). They differ in possessing symmetrical aedeagal apices and a relatively longer apical piece (4.0× longer than basal piece, Fig. 11C, D) (asymmetrical apices and relatively shorter apical piece, as long as basal piece in *P. smaragdina* (Fig. 22D, E)).

Distribution. Vietnam.

Pseudotheopea gressitti **sp. nov.**
http://zoobank.org/B7FF7AC0-9480-4998-8E34-A83824BE7C8D
Figs 12A–C; 13A, B; 14

Types. Holotype ♂ (USNM), PHILIPPINES, Mindanao: Zamboanga, 1927, leg. Baker. Paratypes. 3♀♀ (USNM), same data as holotype.

Description. Length 5.0-5.7 mm, width 1.8-2.0 mm. Body color (Fig. 12A–C) dark brown; elytra metallic purple, vertex and pronotum with metallic purple reflection, prosternite, mesoventrite, and legs yellowish brown, but tibiae and tarsi darker. Frontoclypeus (Fig. 13A, B) with semi-circular excavation between eyes in males, concavity 0.5× as wide as interspace between eyes, with erect process at center and one pair small processes at baso-lateral angles. Antennae filiform in males (Fig. 14A), with apico-lateral process on antennomere I, length ratios of antennomeres I–XI 1.0: 0.2:
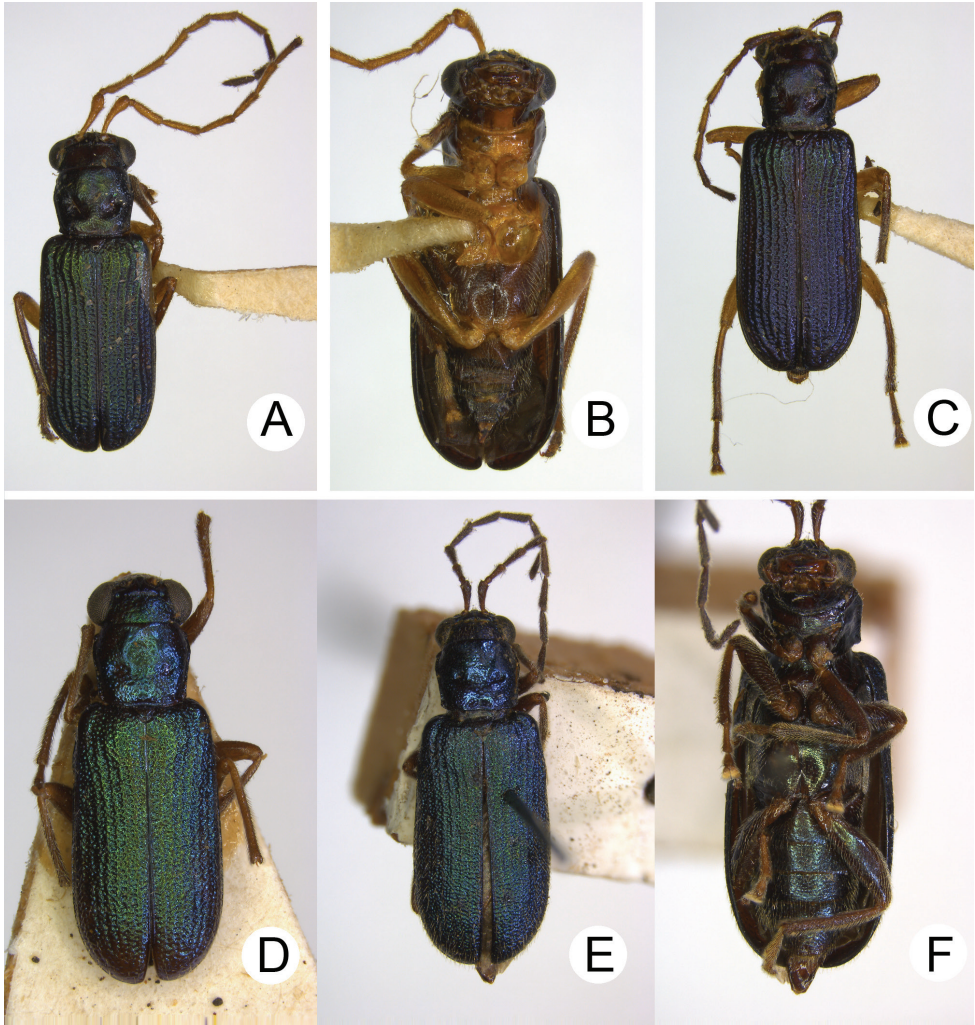
Figure 12. Habitus of *Pseudotheopea gressitti* sp. nov. and *P. similis*. **A** *P. gressitti* sp. nov., male, dorsal view **B** Same, ventral view **C** *P. gressitti* sp. nov., female, dorsal view **D** *P. similis*, male, dorsal view **E** *P. similis*, female, dorsal view **F** Same, ventral view.

0.7: 0.8: 0.7: 0.7: 0.7: 0.7: 0.7: 0.6: 0.7, length to width ratios of antennomeres I–XI 4.8: 1.6: 4.6: 5.2: 4.9: 4.5: 4.8: 4.9: 4.8: 4.8: 4.5; without apico-lateral process of antennomere I in females (Fig. 14B), relatively shorter than males, length ratios of antennomeres I–VIII (IX-XI lost) 1.0: 0.2: 0.6: 0.7: 0.8: 0.7: 0.7: 0.7, length to width ratios of antennomeres I–XI 4.0: 1.3: 3.7: 4.5: 5.1: 4.7: 4.8: 4.9. Elytra elongate, parallel-sided, 1.9-2.0× longer than wide; disc with dense, coarse punctures, arranged into longitudinal rows, with one distinct longitudinal ridge between two longitudinal rows of punctures. Tarsomeres I of front legs swollen in males; subparallel in females. Aedeagus (Fig. 14C–E) slender, 8.1× longer than wide; apex with shallow notch; tec-

Figure 13. Heads of males of *Pseudotheopea gressitti* sp. nov. and *P. leehsuehae* sp. nov. **A** *P. gressitti* sp. nov., dorsofrontal view **B** Same, front view **C** *P. leehsuehae* sp. nov., dorsofrontal view **D** Same, front view.

tum elongate, from apical 1/7 to basal 1/3; straight from apex to apical 2/5 in lateral view, angular at apical 2/5; ventral surface membranous from apex to basal 2/5, triangular sclerites small; internal sac with elongate endophallic sclerite, 0.8× as long as aedeagus, composed of two sclerites, apical piece (0.9×) a little shorter than basal piece. Gonocoxae (Fig. 14G) elongate, both gonocoxae fused from basal 1/4 to apical 2/5; apices convergent and narrowly rounded, each gonocoxa with eight setae along lateral margin from apex to apical 1/6, four much longer than others; lateral processes reduced. Ventrite VIII (Fig. 14F) elongate and well sclerotized; disc with several long setae at sides and near apical margin, and with dense, short setae along apical margin; spiculum extremely slender. Receptacle of spermatheca (Fig. 14H) strongly swollen; pump slender and strongly curved; proximal spermathecal duct deeply inserted into receptacle, narrow and short.
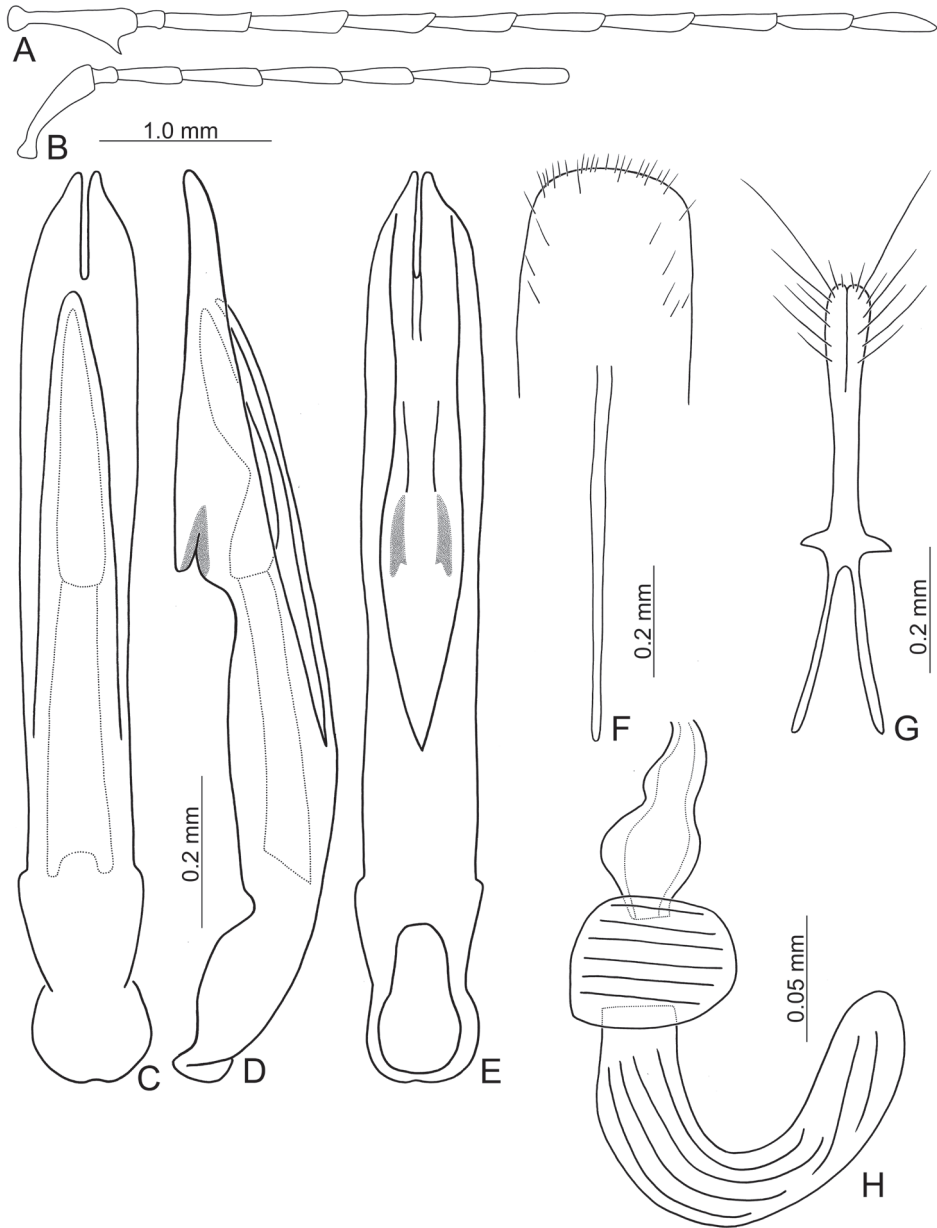
Figure 14. Diagnostic characters of *Pseudotheopea gressitti* sp. nov. **A** Antenna, male **B** Antenna, female **C** Aedeagus, dorsal view **D** Aedeagus, lateral view **E** Aedeagus, ventral view **F** Abdominal ventrite VIII **G** Gonocoxae **H** Spermatheca.

Diagnosis. *Pseudotheopea gressitti* sp. nov. is similar to *P. costata* (Allard) in possessing a semi-circular concavity between the eyes in males that includes one erect process at center and one pair of small processes at the baso-lateral angles of the concavity

(Fig. 13A, B). However, *P. gressitti* sp. nov. can be recognized by the small body sizes (5.0–5.7 mm long, 7.0–7.2 mm in P. *costata*), metallic purple dorsum (Fig. 12A, C) (reddish brown dorsum in *P. costata*), and a lateral apical process of antennomere I in males (Fig. 14A) (without the lateral process on apex of antennomere I in those of *P. costata*). Males of *P. gressitti* sp. nov. are similar to those of *P. costata* and *P. boreri* sp. nov. based on a median elongate sclerite of the internal sac (Figs 10C, D; 14C, D). Males of *P. gressitti* sp. nov. are similar to those of *P. costata*, based on the broad aedeagi in lateral view (Fig. 14D) (dorso-ventrally flattened in lateral view in those of *P. boreri* sp. nov. (Fig. 10D)). But males differ from those of *P. costata* in possessing smaller triangular sclerites and membranous areas on the ventral surface of the aedeagus extending into basal 1/3 (Fig. 10E) (larger triangular sclerites and membranous areas on the ventral surface of aedeagus only reaching basal 1/2 in *P. costata*).

Etymology. This new species is dedicated to late Dr. J. Linsley Gressitt for his great contribution to the taxonomy of oriental Cerambycidae and Chrysomelidae.

Distribution. Philippines: Mindanao.

Pseudotheopea hsingtzungi sp. nov.
http://zoobank.org/B0707A1E-F90D-45C7-B578-33344BB022D3
Figs 15A–C; 16A, B; 17

Theopea sauteri: Medvedev 2000: 178 (part, misidentification).

Types. Holotype ♂ (NHMUK), LAOS. Hua Phan: Ban Saluei, Phou Pane (Mt.), 20°12'N 104°01'E, 1300-1900 m, 3-30.IV.2014, leg. C. Holzschuh. Paratypes. **LAOS**. Champassak: 1♀ (HNHM), Dong Hua Xao NBCA, bank of Nam Phak river, 15°59'N 105°55'E, 280 m, 28-29.III.1998, leg. O. Merkl and G. Csorba (identified as *Theopea sauteri* by Medvedev (2000)); Hua Pan: 1♀ (JBCB), Ban Kangpabong env., 25km SE Vieng Xai (by road), 20°19'N 104°25'E, 14-18.V.2001, leg. J. Bezděk; 1♀ (NHMB), Phou Pane Mt., 20°13'N 104°00'E, 1350-1500 m, 1-16.VI.2009, leg. M. Brancucci; Oudomxai: 1♀ (NHMB), Oudom Xai (17 km NEE), 20°45'N 102°09'E, 1100 m, 1-9.V.2002, leg. V. Kubáň.

Description. Length 5.8–6.2 mm, width 2.1–2.4 mm. Body color (Fig. 15A–C) golden green, but mouthparts and legs yellowish brown, antennae dark brown. Frontoclypeus (Figs 16A–16B) with transverse deep groove between eyes in males, concavity 0.5× as wide as interspace between eyes. Antennae filiform in males (Fig. 17A), antennomere I smaller than others, length ratios of antennomeres I–XI 1.0: 0.3: 1.0: 1.2: 1.2: 1.2: 1.2: 1.1: 1.1: 1.0: 1.1, length to width ratios of antennomeres I–XI 3.3: 1.2: 3.8: 4.8: 5.7: 5.5: 5.5: 5.4: 6.1: 5.6: 6.2; similar but slightly shorter in females (Fig. 17B), length ratios of antennomeres I–XI 1.0: 0.3: 0.8: 0.9: 0.9: 0.9: 0.9: 0.9: 0.9: 0.8: 0.9, length to width ratios of antennomeres I–XI 3.6: 1.7: 4.0: 4.9: 5.3: 5.3: 5.1: 5.4: 5.3: 4.9: 4.7. Elytra elongate, parallel-sided, 1.8-1.9× longer than wide; disc with dense, coarse punctures, arranged into longitudinal rows, with one distinct

Figure 15. Habitus of *Pseudotheopea hsingtzungi* sp. nov. and *P. smaragdina*. **A** *P. hsingtzungi* sp. nov., male, dorsal view **B** *P. hsingtzungi* sp. nov., female, dorsal view **C** Same, ventral view **D** *P. smaragdina*, male, dorsal view **E** *P. smaragdina*, female, dorsal view **F** Same, ventral view.

longitudinal ridge between two longitudinal rows of punctures. Tarsomeres I of front legs swollen in males; subparallel in females. Aedeagus (Fig. 17C–E) extremely slender, 7.2× longer than wide; apex with deep notch; tectum elongate, from apical 1/9 to mid-

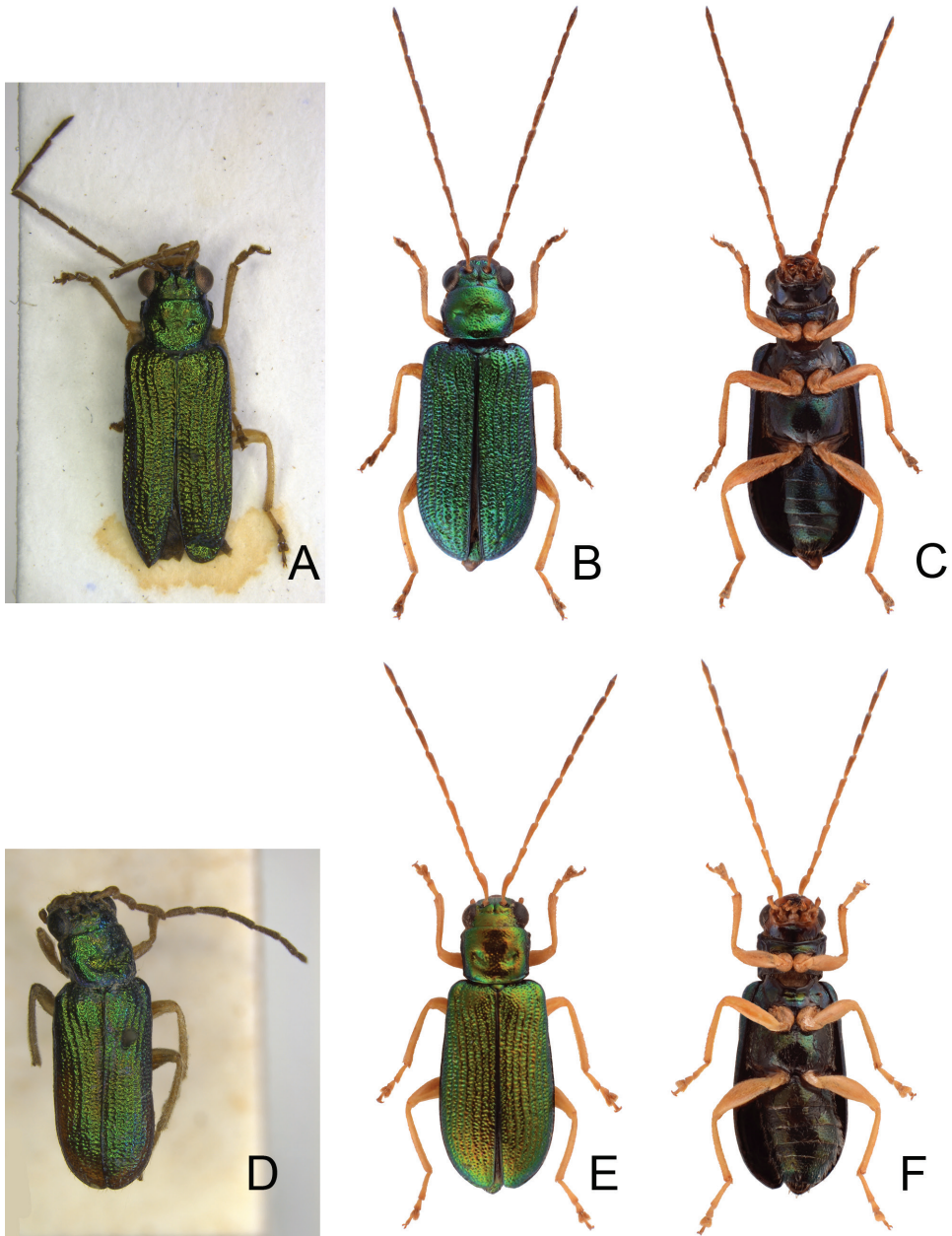**Figure 16.** Heads of males of *Pseudotheopea hsingtzungi* sp. nov. and *P. smaragdina*. **A** *P. hsingtzungi* sp. nov., dorsofrontal view **B** Same, front view **C** *P. smaragdina*, dorsofrontal view **D** Same, front view.

dle; almost straight in lateral view, moderately curved near base, angular at apical 2/5; triangular sclerites elongate; internal sac with elongate, endophallic sclerite complex, 0.5× as long as aedeagus, composed of two sclerites, apical piece as long as basal piece, one pair of dorsal sclerite hook-like, connected near base of apical piece; ventral sclerites absent. Gonocoxae (Fig. 17G) elongate, both gonocoxae fused from basal 1/4 to apical 1/4; apices convergent and narrowly rounded, each gonocoxa with eight setae along lateral margin from apex to apical 1/6; with one pair of short lateral processes at basal 2/5. Ventrite VIII (Fig. 17F) elongate and well sclerotized; disc with several long setae at sides and near apical margin, and with dense, short setae along apical margin; spiculum extremely slender. Receptacle of spermatheca (Fig. 17H) strongly swollen; pump slender and strongly curved; proximal spermathecal duct shallowly inserted into receptacle, narrow and short.

Diagnosis. *Pseudotheopea hsingtzungi* sp. nov. (Fig. 15A–C), *P. boreri* sp. nov. (Fig. 8A–C), *P. clypealis* (Medvedev) (Fig. 8D–F), and *P. smaragdina* (Gressitt and Kimoto)
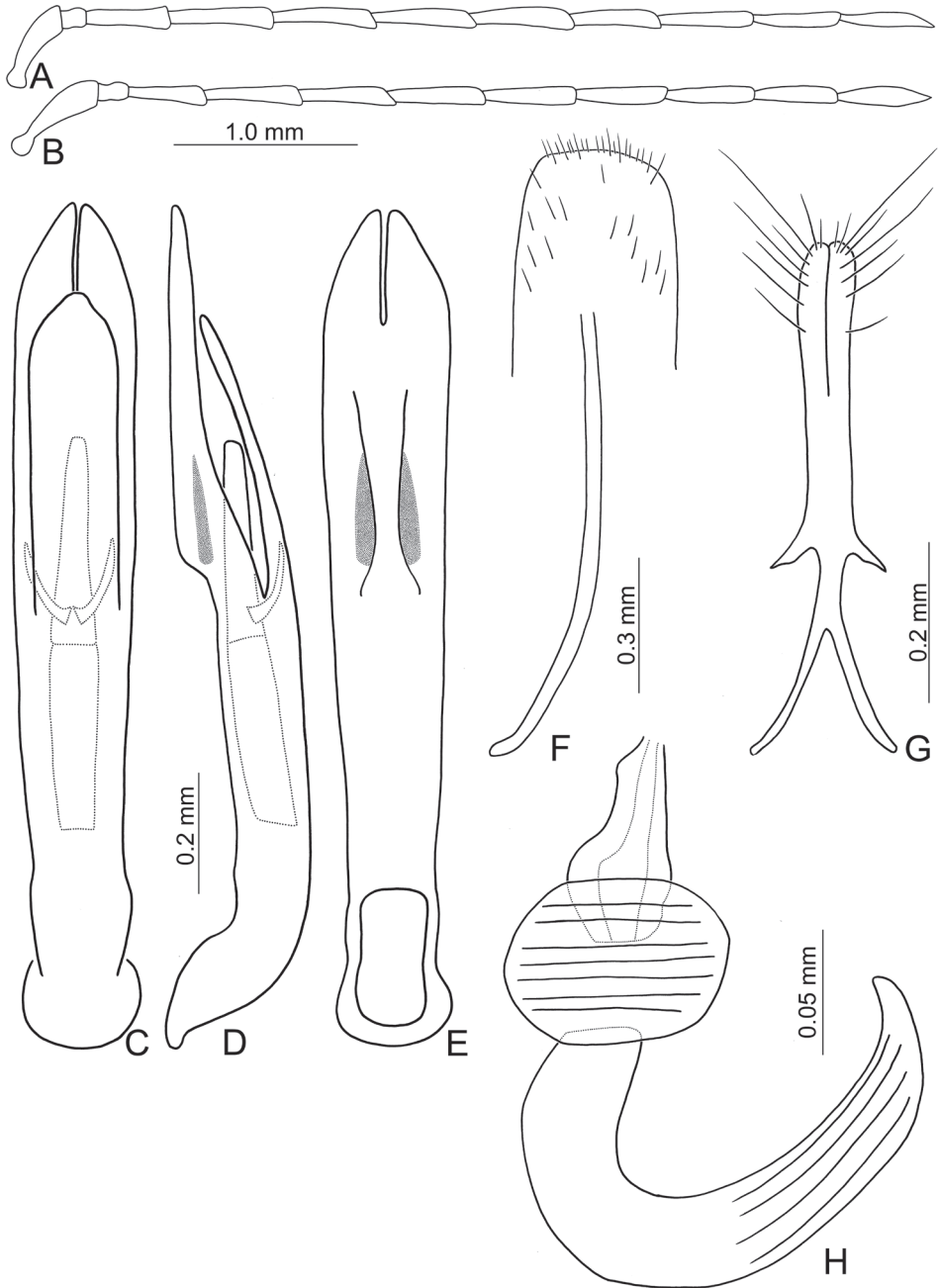
Figure 17. Diagnostic characters of *Pseudotheopea hsingtzungi* sp. nov. **A** Antenna, male **B** Antenna, female **C** Aedeagus, dorsal view **D** Aedeagus, lateral view **E** Aedeagus, ventral view **F** Abdominal ventrite VIII **G** Gonocoxae **H** Spermatheca.

(Fig. 15D–F), are characterized by their golden green coloration. They can be identified based on their distribution: *P. boreri* sp. nov. from India, *P. clypealis* from Vietnam, *P. hsingtzungi* sp. nov. from Laos, and *P. smaragdina* from China. *Pseudotheopea hsingtzungi* sp. nov. (Fig. 15A, B) is similar to *P. boreri* sp. nov. (Fig. 8A, C) and *P. smaragdina* (Fig. 15D, E) based on the shared indistinct longitudinal ridges on the elytra (convex and distinct longitudinal ridges on the elytra in *P. clypealis* (Fig. 8D, F)), but differs by having the concavity narrower between the eyes in males (Fig. 16A, B) (concavity wide between eyes in others (Figs 9A, B; 16C, D)). Males of *P. hsingtzungi* sp. nov. are similar to those of *P. kimotoi* sp. nov. in possessing elongate triangular aedeagal sclerites (Figs 17D, E; 20E, F) but differ in the presence of one pair of long hook-like lateral sclerites of the median elongate sclerite, lacking small spines near the apex of the median elongate sclerite, and the median division (Fig. 17C, D) (lacking hook-like sclerites at sides of median elongate sclerite, with small spines near apex of median elongate sclerite, and undivided in those of *P. kimotoi* sp. nov. (Fig. 20D, E)).

Etymology. The new species is dedicated to Mr. Hsing-Tzung Cheng, who is a member of the Taiwan Chrysomelid Research Team (TCRT) for inventorying leaf beetles.

Distribution. Laos.

Pseudotheopea kimotoi sp. nov.
http://zoobank.org/5A493FF3-7DD0-4DCB-81FF-893F6FCA9420
Figs 18A–D; 19A, B; 20

Theopea sauteri: Kimoto 1989: 200 (part); Medvedev 2000: 178 (part).

Types. Holotype ♂ (BPBM): "VIET NAM: 7km SE / of Dilinh (Djiring) / 990m, 2.V.1960 [p, w] // ♂ [p, w] // R. E. Leech / Collector / BISHOP [p, w] // Theopea / sauteri / Chujo [h] / Det. S. Kimoto, 19 [p] 87 [h, w]". This specimen was misidentified as *Theopea sauteri* by Kimoto (1989). Paratypes. **LAOS**. Boli Kham Xai: 1♀ (JBCB), Ban Nape (8km NE), ~600 m, 18°21'N 105°08'E, 1-18.V.2001, leg. C. L. Peša; Champassak: 1♂, 5♀♀ (HNHM), Dong Hua Xao NBCA, 2 km S of Ban Nong Luang, bank of Touay-Guai Stream, 15°04'N 106°13'E, 800 m, 1-5.IV.1998, leg. O. Merkl and G. Csorba (identified as *Theopea sauteri* by Medvedev (2000)); Hua Pan: 3♀♀ (JBCB), Ban Kangpabong env., 25km SE Vieng Xai (by road), 20°19'N 104°25'E, 14-18.V.2001, leg. J. Bezděk; Khammouane: 2♀♀ (RBCN), Nakai env., Rout no 8, 17°42.8'N 105°09.1'E, 560 m, 4-8.V.1998, leg. E. Jendek and O. Šauša; Louangphrabang: 4♀♀ (NHMB), Thong Khan, 19°33'N 101°58'E, 750 m, 11-21.V.2002, leg. V. Kubáň; **THAILAND**. Loei: 1♀ (NMPC), Phu Kradung N.P., 16-17.V.1999, leg. D. Hauck; **VIETNAM**. 1♀ (ZSM), Tam Dao, 1982, leg. L. Medvedev; Cao Bang: 1♂ (NMPC), Bao-Lac; Lam Dong: 1♂, 1♀ (BPBM), 6 km S Dalat, 1400-1500 m, 6.VI.-7.VII.1961, leg. N. R. Spencer, identified as *Theopea sauteri* by Kimoto (1989); Ninh Binh: 1♀ (NHMB), Cuc Phuong N.P., 21-27.V.1996, leg. Pacholátko and Dembický.
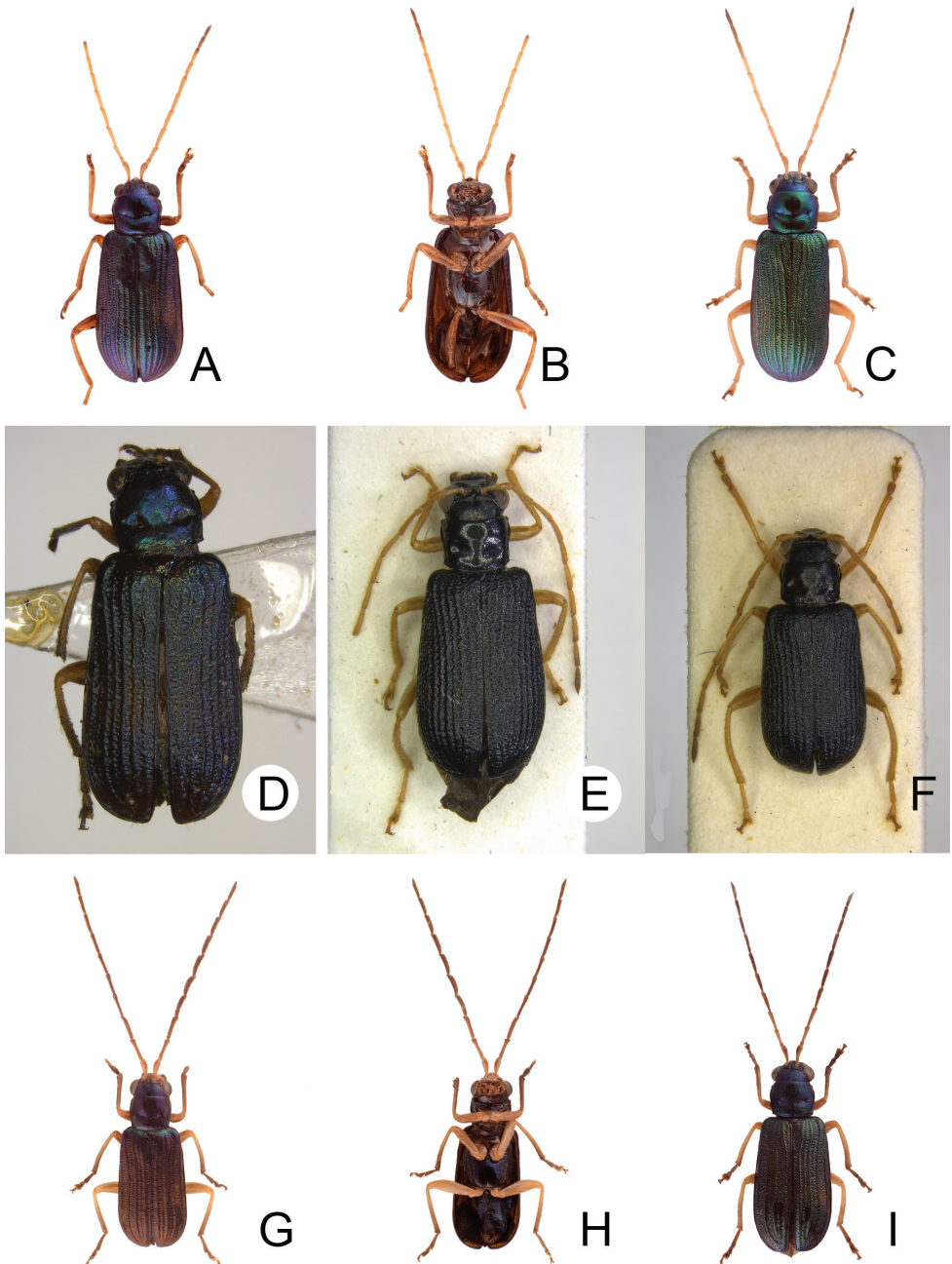
Figure 18. Habitus of *Pseudotheopea kimotoi* sp. nov., *P. nigrita*, and *P. leehsuehae* sp. nov. **A** *P. kimotoi* sp. nov., male, dorsal view **B** Same, ventral view **C** *P. kimotoi* sp. nov., female, dorsal view **D** *P. kimotoi* sp. nov., male, from Dalat **E** *P. nigrita*, holotype, dorsal view **F** *P. nigrita*, male, dorsal view **G** *P. leehsuehae* sp. nov., male, dorsal view **H** Same, ventral view **I** *P. leehsuehae* sp. nov., female, dorsal view.
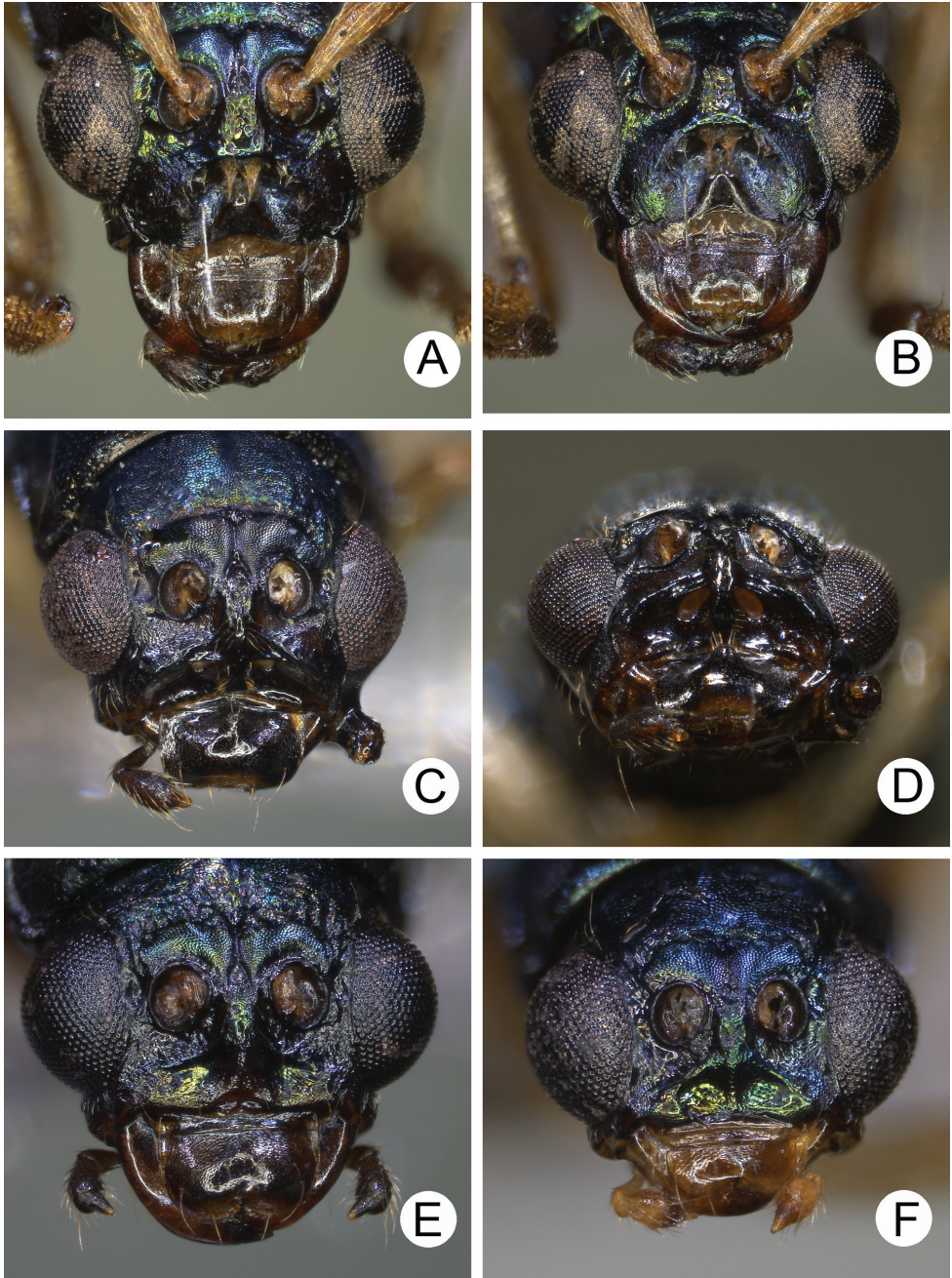
Figure 19. Heads of *Pseudotheopea kimotoi* sp. nov., *P. sufangae* sp. nov., and *P. sauteri*. **A** *P. kimotoi* sp. nov., male, dorsofrontal view **B** Same, front view **C** *P. sufangae* sp. nov., male, dorsofrontal view **D** Same, front view **E** *P. sufangae* sp. nov., female, dorsofrontal view **F** *P. sauteri*, female, dorsofrontal view.
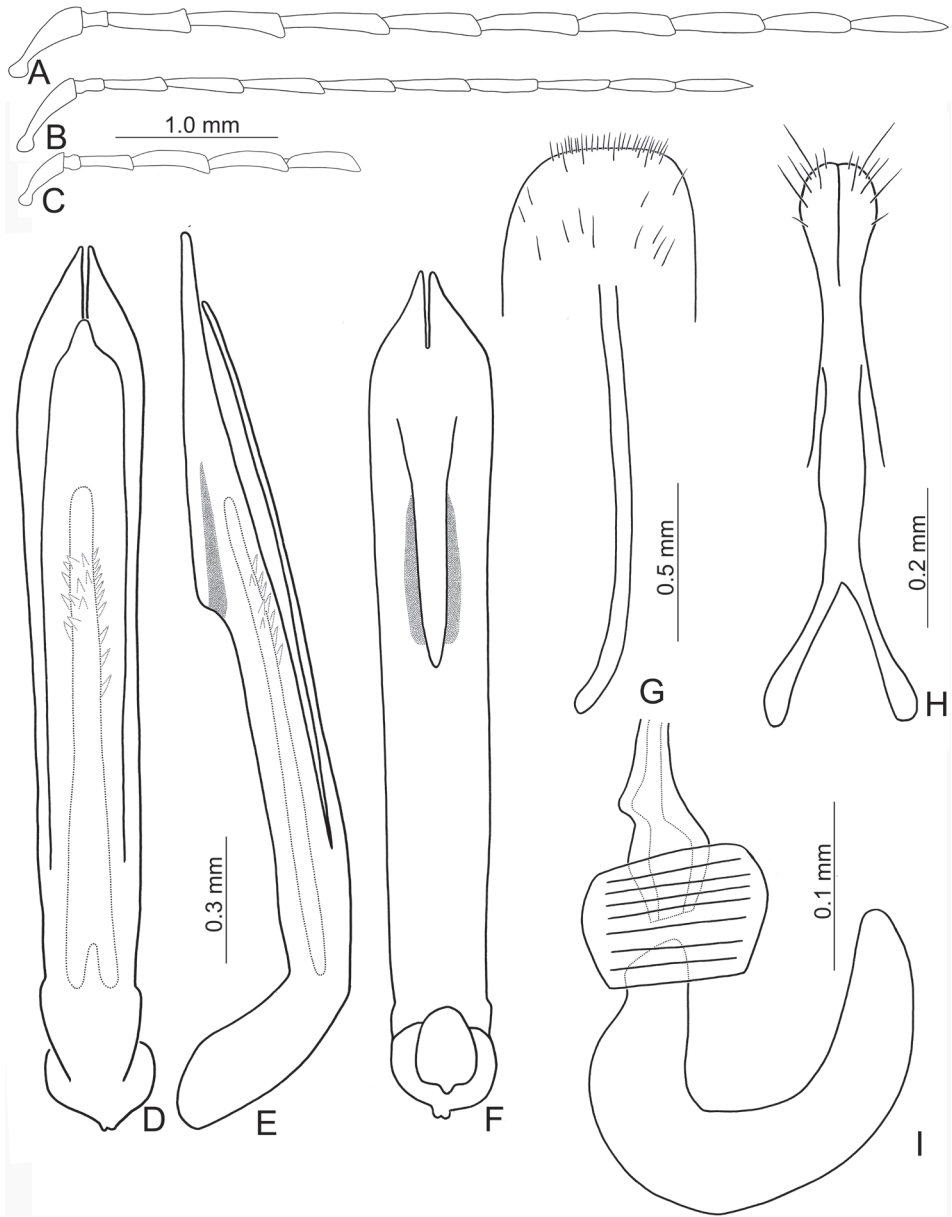
Figure 20. Diagnostic characters of *Pseudotheopea kimotoi* sp. nov. **A** Antenna, male **B** Antenna, female **C** Antenna, male, from Dalat **D** Aedeagus, dorsal view **E** Aedeagus, lateral view **F** Aedeagus, ventral view **G** Abdominal ventrite VIII **H** Gonocoxae **I** Spermatheca.

Description. Length 6.6-7.5 mm, width 2.6-3.2 mm. Body color (Fig. 18A–D) metallic blue or purple, but antennae and legs yellowish brown, mouth parts dark brown. Frontoclypeus (Fig. 19A, B) transverse and weakly excavated between eyes in males, semi-circular, the annular concavity 0.8× as wide as interspace between eyes, with cluster of long setae near middle of anterior margin, some shorter setae scattered

along anterior margin. Antennae filiform in males (Fig. 20A), but relatively broader than those of females (Fig. 15A), length ratios of antennomeres I–XI 1.0: 0.3: 0.9: 1.1: 1.2: 1.0: 1.1: 1.0: 1.0: 0.9: 1.1, length to width ratios of antennomeres I–XI 3.3: 1.6: 3.4: 4.4: 4.9: 4.2: 4.8: 4.5: 4.7: 4.8: 4.7; filiform in females (Fig. 20B), length ratios of antennomeres I–XI 1.0: 0.3: 0.7: 0.9: 1.0: 0.9: 0.9: 0.8: 0.8: 0.8: 0.9, length to width ratios of antennomeres I–XI 4.2: 2.2: 4.1: 5.1: 5.6: 5.4: 5.7: 5.1: 5.5: 5.2: 6.2. Elytra elongate, parallel-sided, 1.7-1.9× longer than wide; disc with dense, coarse punctures, arranged into longitudinal rows, with one distinct and convex longitudinal ridge between two longitudinal rows of punctures, with convex area behind scutellum, ridges reduced at convex area. Tarsomeres I of front legs strongly swollen in males; subparallel in females. Aedeagus (Fig. 20D–F) slender, 8.4× longer than wide; apex with shallow notch; tectum elongate, from apical 1/13 to basal 1/3; almost straight in lateral view, angular at apical 2/5, moderately curved near base; triangular sclerites elongate; internal sac covered with stout teeth, with elongate endophallic sclerite, 0.5× as long as aedeagus, some small, stout teeth at apical 1/8 to 2/5. Gonocoxae (Fig. 20H) elongate, both gonocoxae fused from basal 1/4 to apical 1/5; apices convergent and narrowly rounded, each gonocoxa with eight setae along lateral margin from apex to apical 1/6, four much longer than others; lateral processes reduced. Ventrite VIII (Fig. 20G) elongate and well sclerotized; disc with several long setae at sides and near apical margin, and with dense, short setae along apical margin; spiculum extremely slender. Receptacle of spermatheca (Fig. 20I) strongly swollen; pump slender and strongly curved; proximal spermathecal duct deeply inserted into receptacle, narrow and short.

Variation. One male collected from Dalat has a smaller body (5.3 mm long, 2.2 mm wide) and the convex area on the elytra is indistinct and with longitudinal ridges (Fig. 20D), antennomeres IV-VI are curved (VII-XI lost, Fig. 20C), and the frontoclypeus lacks a concavity.

Diagnosis. *Pseudotheopea kimotoi* sp. nov. is similar to *P. clypealis* (Medvedev) and *P. leehsuehae* sp. nov. based on the convex and distinct longitudinal ridges on the elytra but differs in having all longitudinal ridges convex and distinct (Fig. 18A, C, D) (intertwined with convex distinct ridges and weak indistinct ones in others (Figs 8D, F; 18F, H), with a convex area surrounding the scutellum and longitudinal ridges reduced on the convex area in males (Fig. 18A) (without convex area surrounding scutellum in those of others (Figs 8D, 18F)) and the shallow concavity between it in males (Fig. 19A, B) (deep concavity in others (Figs 9C, D; 13C, D)). Males of *P. kimotoi* sp. nov. (Fig. 20E, F) are similar to those of *P. hsingtzungi* sp. nov. (Fig. 17D, E) in possessing elongate triangular aedeagal sclerites but differ in the absence of lateral sclerites attached to the median elongate sclerite, with small spines near apex of median elongate sclerite, which is undivided (Fig. 20D, E) (with one pair of hook-like sclerites at sides of median elongate sclerite, without small spines near apex of median elongate sclerite, and divided at middle in those of *P. hsingtzungi* sp. nov. Fig. 17C, D)).

Etymology. This new species is dedicated to late Dr. Shinsaku Kimoto for his great contribution to taxonomy of oriental and Palaearctic Chrysomelidae.

Distribution. Laos, Thailand, Vietnam.

Pseudotheopea leehsuehae sp. nov.

http://zoobank.org/4A9146B2-EDC1-4E51-9C51-5109CA37CB18
Figs 13C, D; 18F–H; 21

Types. Holotype ♂ (NHMB), LAOS, Louang Namtha, Namtha → Muang Sing, 21°09'N 101°19'E, 900-1200 m, 5-31.V.1997, leg. V. Kubáň. Paratypes. 5♂♂ (NHMB), same as holotype; **LAOS**. Houa Phan: 1♂ (NHMB), Ban Saluei → Phou Pane Mt., 20°12-13.5'N 103°59.5'-104°01'E, 1340-1870 m, 10.V.-16.VI.2009, leg. M. Brancucci and local coll.; Louang Namtha: 1♂ (NMPC), 20 km BW Louang Namtha, 21°09.2'N 101°18.7'E, 800-1100 m, 5.-11.V.1987, leg. M. Štrba and Hergovits; Phongsali: 1♂ (JBCB), Boun Tai (10km SE), 16-25.V.2004, leg. Lao collector; Xaisomboun: 1♀ (NMPC), Phou Khao Khouay N.P., Tad Leuk, 18°23'N 103°04'E, 150-200 m, 15.-21.V.2001, leg. E. Jendek and O. Šauša

Description. Length 4.8–5.9 mm, width 1.8–2.4 mm. Body color metallic purple (Fig. 18F–H), legs yellowish brown, tarsi darker; mouth parts and antennae dark brown or blackish brown. Frontoclypeus (Fig. 13C, D) transverse and deeply excavated between eyes in males, concavity transverse and as wide as interspace between eyes; with small membranous sclerite covering sides; membranous sclerite covering most shallow areas of concavity, also with one pair of erect membranous sclerites, concavity with short hair-like setae along margin. Antennae filiform in males (Fig. 21A), relatively broader than females, antennomeres III-X slightly curved, length ratios of antennomeres I–XI 1.0: 0.2: 1.0: 1.1: 1.2: 1.1: 1.1: 1.1: 1.0: 1.0: 1.0, length to width ratios of antennomeres I–XI 3.3: 1.3: 4.0: 4.8: 4.9: 4.8: 5.0: 5.1: 5.1: 4.9: 5.5; slender and straight in females (Fig. 21B) length ratios of antennomeres I–XI 1.0: 0.3: 0.8: 1.0: 1.0: 1.0: 1.0: 1.0: 1.0: 1.0: 1.0, length to width ratios of antennomeres I–XI 3.4: 1.5: 3.9: 5.5: 5.7: 5.4: 5.9: 6.5: 6.2: 5.4: 6.5. Elytra elongate, parallel-sided, 1.7–1.9× longer than wide; disc with dense, coarse punctures arranged into longitudinal rows, with convex longitudinal ridges between rows of punctures, distinct and indistinct ridges intertwined. Tarsomeres I of front legs swollen in males; subparallel in females. Aedeagus (Fig. 21C–E) extremely slender, 11.9× longer than wide; parallel-sided; apex with shallow notch, both apices equal in length; tectum elongate, from apical 1/9 to basal 1/4; slightly curved in lateral view, angular at apical 1/5; triangular sclerites small; internal sac with elongate, endophallic sclerite complex, 0.3× as long as aedeagus, composed of two sclerites, apical piece as long as basal piece, with one pair of hook-like sclerites combined at base of apical piece ventrally. Gonocoxae (Fig. 21G) elongate; apices convergent and narrowly rounded, each gonocoxa with six setae along lateral margin from apex to apical 1/6, three much longer than others; lateral processes reduced, with one or two setae near base; base membranous. Ventrite VIII (Fig. 21F) elongate and well sclerotized; disc with several long lateral setae, and with dense, short setae along apical margin; spiculum extremely slender. Receptacle of spermatheca (Fig. 21H) strongly swollen; pump slender and strongly curved; proximal spermathecal duct deeply inserted into receptacle, narrow and short.
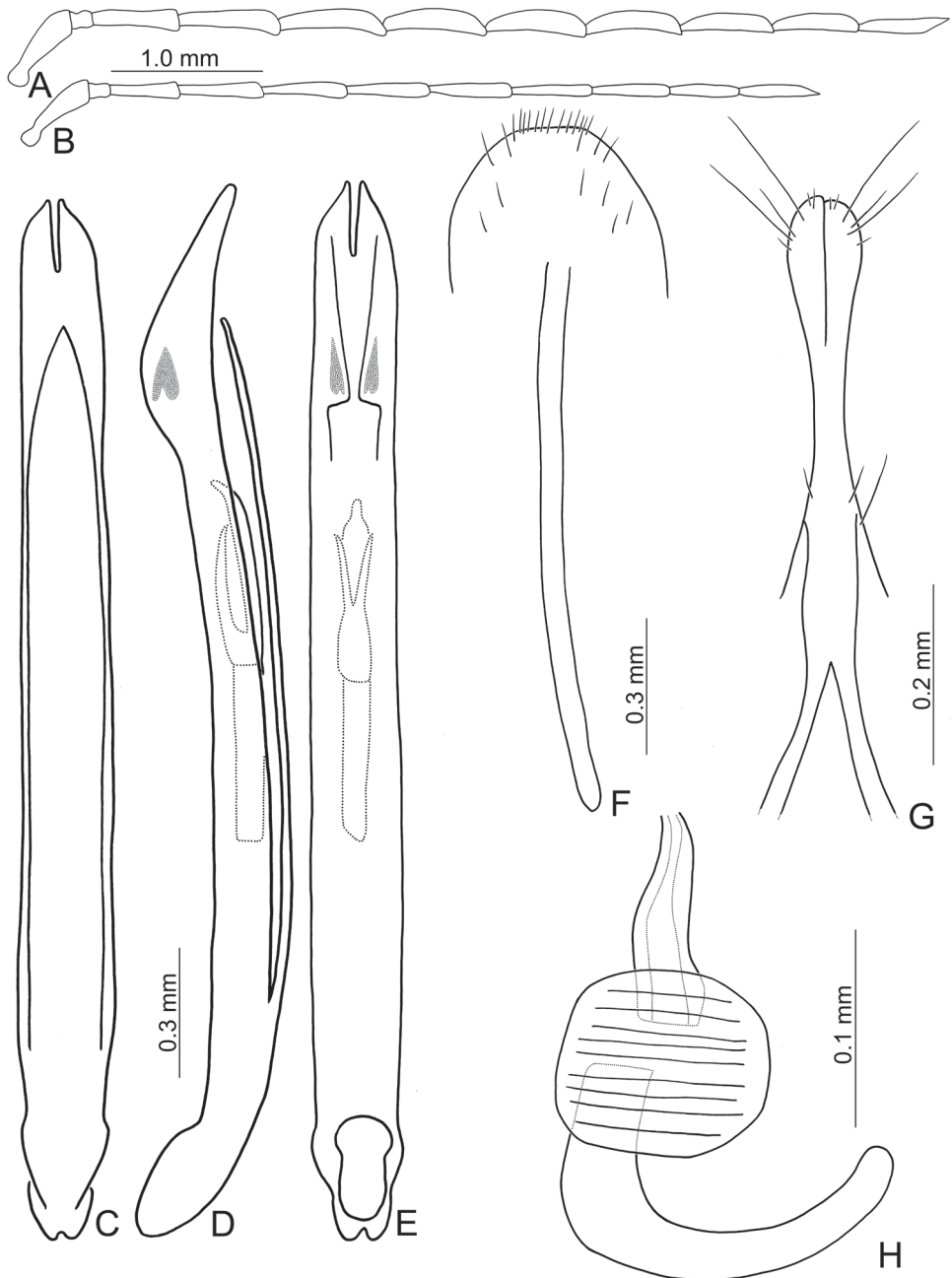
Figure 21. Diagnostic characters of *Pseudotheopea leehsuehae* sp. nov. **A** Antenna, male **B** Antenna, female **C** Aedeagus, dorsal view **D** Aedeagus, lateral view **E** Aedeagus, ventral view **F** Abdominal ventrite VIII **G** Gonocoxae **H** Spermatheca.

Diagnosis. *Pseudotheopea leehsuehae* sp. nov. (Fig. 18F, H) is similar to *P. clypealis* (Medvedev) (Fig. 8D, F) based on the convex, distinct ridges and weak indistinct ridges intertwined on the elytra, but *P. leehsuehae* sp. nov. can be separated from *P. clypealis* by its metallic purple body (Fig. 18F, H) (golden green body in *P. clypealis* (Fig. 8D, F)), and concavity covered with a membranous sclerite and with one pair of erect rounded sclerites (Fig. 13C, D) (without such structures in *P. clypealis* (Fig. 9C, D)). Males of *P. leehsuehae* sp. nov. are characterized by their extremely elongate aedeagi (11.7× longer than wide) and one pair of hook-like sclerites arising from the middle of the ventral surface of the apical piece of the endophallic sclerite complex (Fig. 21C–E).

Etymology. The new species is dedicated to Mrs. Hueh Lee, who is a member of the Taiwan Chrysomelid Research Team (TCRT) for inventorying leaf beetles.

Distribution. Laos.

Pseudotheopea smaragdina (Gressitt & Kimoto, 1963), comb. nov.
Figs 15D–F; 16C, D; 22

Theopea smaragdina: Gressitt and Kimoto 1963: 680 (China: Hainan Island, Guandong); Wilcox 1973: 631 (catalogue); Wang et al. 1998: 129 (China: Fujian: Wuyishan); Yang 2002: 656 (China: Fujian); Yang and Yao 2002: 447 (China: Hainan Island); Aston 2009: 24 (Hong Kong); Beenen 2010, 489 (catalogue).

Types. Holotype ♂ (CAS): "HAINAN I. China / Tahau VIII [p] 6 [h] 1935 / L. Gressitt [p, w] // L. Gressitt / Collection [p, w] // HOLOTYPE [p] ♂ / Theopea / smaragdina [h] / Gressitt and Kimoto [p, r] // Theopea holo- / sp. nov. 2 / smaragdina [h] / Det. S. Kimoto [p] G and K [h, w]" // California Academy / of Sciences / Type / No. [p] 12422 [h, w]". Paratypes. 1♀ (NHMUK): "Para- / type [p, w, circle label with yellowish border] // CHINA: Kwang- / tung [= Guangdong], Fei-ha-fei- / loi. VII-1-1956 / J. L. Gressitt [p, w] // Brit. Mus. / 1963-245. [p, w] // L. Gressitt / Collection [p, w] // PARATYPE [p] / Theopea / smaragdina [h] / Gressitt and Kimoto [p, y] // Theopea / smaragdina / G and K [h] / Gressitt and Kimoto det. 196[p] 2[h]"; 1♂ (MNHUB): "China, Canton, [p] / Fati 10.V.10 [h] / Mell S. V. [p, y] // PARATYPE [p] / Theopea / smaragdina [h] / Gressitt and Kimoto [p, y]"; 1♀ (CAS): "HAINAN I. China / Tahau. VII[p] 6[h] 1935 / L. Gressitt [p, w] // L. Gressitt / Collection [p, w] // PARATYPE [p] / Theopea / smaragdina [h] / Gressitt and Kimoto [p, y] // Theopea / smaragdina / G and K [h] / Gressitt and Kimoto det. 196[p]2 [h, w]".

Other specimens examined. CHINA. Guangdong: 1♂ (SEHU), 廣州 (Guangzhou), 16.IV.1983, leg. A. Tanaka; 6♀♀ (NMPC), Guangzhou, Baiyunshan vill., 23°09'47"-10'30"N 113°13'27"-17'44"E, 50-250 m, 27.VI.2014, leg. J. Hájek, J. Růžička and M. Tkoč; Hong Kong: 1♀ (PAHC), Nam Chung, 8.V.2009, leg. P. Aston; 9♀♀ (BPBM), Soko island, Tai-A-Chan, 23-25.V.1988, coll. C. O'Connell; 2♂♂, 1♀ (PAHC), Sha Lo Tung, 10.V.2012, leg. P. Aston; 1♀ (PAHC), same but with "3.V.2014".

Redescription. Length 5.7–6.7 mm, width 2.2–2.4 mm. Body color (Fig. 15D–F) golden green, but antennae, mouth parts, and legs yellowish brown, five or six
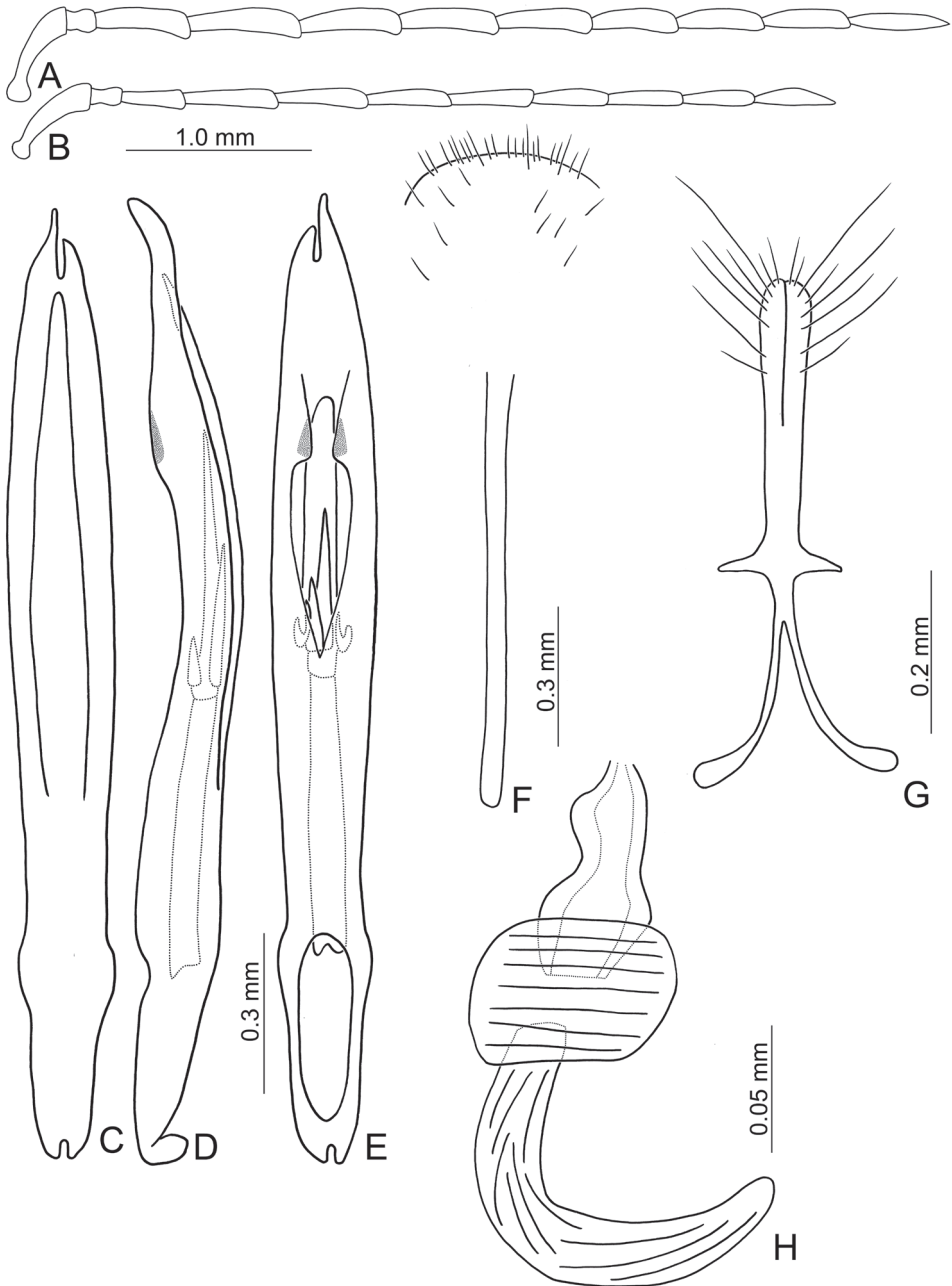
Figure 22. Diagnostic characters of *Pseudotheopea smaragdina*. **A** Antenna, male **B** Antenna, female **C** Aedeagus, dorsal view **D** Aedeagus, lateral view **E** Aedeagus, ventral view **F** Abdominal ventrite VIII **G** Gonocoxae **H** Spermatheca.

apical antennomeres darker. Frontoclypeus (Fig. 16C, D) transverse and deeply excavated between eyes in males, concavity as wide as interspace between eyes; with one erect process at center, apically tapering; one pair of membranous areas surrounding

erect process, mesally connected; with several erect hair-like setae at sides of anterior margin. Antennae filiform in males, but relatively broader than those of female (Fig. 22A), antennomeres III-IX slightly curved, length ratios of antennomeres I–XI 1.0: 0.3: 0.9: 1.1: 1.0: 0.9: 0.9: 0.8: 0.8: 0.8: 1.0, length to width ratios of antennomeres I–XI 3.8: 1.3: 3.4: 4.1: 4.5: 4.2: 4.1: 4.1: 4.3: 4.6: 6.4; filiform in females (Fig. 22B), length ratios of antennomeres I–XI 1.0: 0.3: 0.6: 1.0: 1.0: 0.9: 0.9: 0.8: 0.8: 0.7: 0.9, length to width ratios of antennomeres I–XI 3.4: 1.7: 3.1: 4.7: 4.6: 5.0: 4.8: 4.9: 4.9: 4.6: 5.3. Elytra elongate, parallel-sided, 1.8-1.9× longer than wide; disc with dense, coarse punctures, arranged into longitudinal rows, with distinct longitudinal ridge between two longitudinal rows of punctures. Tarsomeres I of front legs swollen in males; subparallel in females. Aedeagus (Fig. 22C–E) extremely slender, 9.4× longer than wide; apex with shallow notch, both apices not equal in length; tectum elongate, from apical 1/12 to basal 2/5; almost straight in lateral view, apically curved, angular at apical 1/4; triangular sclerites small; internal sac with elongate, endophallic sclerite complex, 0.6× as long as aedeagus, composed of two sclerites, apical piece as long as basal piece, two dorsal sclerites unequal in length; ventral sclerites present. Gonocoxae (Fig. 22G) elongate, both gonocoxae fused from basal 1/4 to apical 1/3; apices convergent and narrowly rounded, each gonocoxa with eight setae along lateral margin from apex to apical 1/6; with one pair of short lateral processes at basal 2/5. Ventrite VIII (Fig. 22F) longitudinal and well sclerotized; disc with several long setae at sides and near apical margin, and with dense, short setae along apical margin; spiculum extremely slender. Receptacle of spermatheca (Fig. 22H) strongly swollen; pump slender and strongly curved; proximal spermathecal duct deeply inserted into receptacle, narrow and short.

Diagnosis. *Pseudotheopea smaragdina* (Gressitt and Kimoto) (Fig. 15D–F), *P. boreri* sp. nov. (Fig. 8A–C), *P. clypealis* (Medvedev) (Fig. 8D–F), and *P. hsingtzungi* sp. nov. (Fig. 15A–C), are characterized by their golden green coloration. They can be identified based on their distribution: *P. boreri* sp. nov. from India, *P. clypealis* from Vietnam, *P. hsingtzungi* sp. nov. from Laos, and *P. smaragdina* from China. *Pseudotheopea smaragdina* (Fig. 15D, E) is similar to *P. hsingtzungi* sp. nov. (Fig. 15A, B) and *P. boreri* sp. nov. (Fig. 8A, 8C) in sharing the indistinct longitudinal ridges on the elytra (convex and distinct longitudinal ridges on the elytra in males *P. clypealis*), but it differs by having a wider concavity between the eyes bearing one erect process in males (Fig. 16C, D) (concavity wide between eyes without erect processes in males of *P. boreri* sp. nov. (Fig. 9A, B); concavity narrowed between eyes and without erect processes in males of *P. hsingtzungi* sp. nov. (Fig. 16A, B)). Males of *P. smaragdina* are similar to those of *P. clypealis* with one additional elongate aedeagal sclerite and one pair of small lateral hook-like sclerites inside the internal sac (Figs 11C, D; 22D, E). They differ in having asymmetrical apices of the aedeagus and a relatively shorter apical piece (as long as basal piece) of the median elongate sclerite (Fig. 22C–E) (symmetric apices and relatively longer apical piece, 4.0× as long as basal piece in *P. clypealis* (Fig. 11C–E)).

Distribution. China (Hainan Island, Fujian, Hong Kong).

Pseudotheopea sufangae **sp. nov.**

http://zoobank.org/E2AAABD6-8244-4AAB-A48D-BE4AF1E1E9B2
Figs 5F–H; 19C–E; 23

Theopea sauteri: Chûjô 1962: 158 (misidentification).

Types. Holotype ♂ (TARI), **TAIWAN**, Pingtung, Tahanshan (大漢山), 30.V.2014, leg. Y.-T. Chung; Paratypes. **TAIWAN**. Chiayi: 1♂ (TARI), Fenchihu (奮起湖), 25.V.2013, leg. W.-C. Liao; Hualien: 1♀ (NMPC), 15 km W of Yuli (玉里), 475 m, 7.VI.2008, leg. F. and L. Kantner; Ilan: 5♂♂ (HNHM), Fushan Botanical Garden (福山植物園), 8-11.IV.2002, leg. O. Merkl; 1♂, 8♀♀ (TARI), same locality, 3-9.VII.2013, leg. Y.-T. Wang; 1♀ (TARI), Songluoshan (松蘿山), 4.VI.2017, leg. Y.-T. Wang; Kaohsiung: 3♀♀ (NMNS), Shanping (扇平), 1.VI.1987, leg. C. W. and L. B. O'Brien; 1♂ (TARI), same locality, 11.IV.2015, leg. W.-C. Liao; 1♀ (TARI), Tengchih (藤枝), 7.IX.2012, leg. W.-C. Liao; 1♀ (TARI), same locality, 6.VIII.2013, leg. B.-X. Guo; 1♀ (TARI), same locality, 10.VIII.2013, leg. W.-C. Liao; Nantou: 1♀ (HNHM), Fuhosho (茅埔庄, = Wucheng 五城), VI.1909, leg. Sauter; 1♂ (NMNS), Howang (合望), 14-16.VIII.2002, leg. W.-T. Yang; 5♂♂, 7♀♀ (SEHU), Lienhwachih (蓮花池), 5-7.V.1978, leg. Y. Komiya; 4♀♀ (TARI), same locality, 23-26.V.1980, leg. K. S. Lin and B. H. Chen; 8♂♂, 11♀♀ (NMNS), same locality, 9.IV.-19.V.1998, leg. C. S. Lin and W. T. Wang; 2♀♀ (NMNS), same but with "6.VII.-12.VIII.1998"; 1♂ (NMNS), same but with "26.II.-21.III.2001"; 2♂♂ (NMNS), same but with "21.III.-9.IV.2001"; 10♂♂ (NMNS), same but with "2.V.-12.VI.2001"; 2♂♂ (NMNS), same but with "5.V.-10.VI.2002"; 1♂, 1♀ (NMNS), same but with "10.VI.-9.VII.2002"; 8♂♂, 2♀♀ (NMNS), same but with "4.III.-6.V.2003"; 4♀♀ (NMNS), same but with "6.V.-10.VI.2003"; 1♂, 1♀ (NMNS), same but with "10.VI.-7.VII.2003"; 1♂, 1♀ (NMNS), same but with "7.VII.-4.VIII.2003"; 1♀ (NMNS), same but with "4.VIII.-8.IX.2003"; 7♂♂, 8♀♀ (NMNS), same but with "10.V.-12.VII.2004"; 2♂♂ (NMNS), same but with "13.XII.2004-10.I.2005"; 1♀ (NMNS), same but with "7.III.-11.IV.2005"; 4♂♂, 2♀♀ (NMNS), same but with "11.IV.-2.V.2005"; 1♂, 1♀ (NMNS), same but with "2.V.-6.VI.2005"; 1♀ (NMNS), same but with "6.VI.-4.VII.2005"; 1♀ (TARI), same locality, 10.III.2013, leg. W.-C. Liao; 1♂ (SEHU), Nanshanchi (南山溪), 12.V.1977, leg. J. Ito; 3♂♂ (SEHU), same locality, 8.V.1978, leg. Y. Komiya; Pingtung: 1♂ (TARI), Lanren River (欖仁溪), 7.IV.2012, leg. Y.-H. Peng and Y.-C. Lan; 1♂ (TARI), Nanjenshan (南仁山), 4.III.2010, M.-L. Jeng; 1♂, 1♀ (TARI), same locality, 27.III.-5.IV.2010, leg. M.-L. Jeng; 1♀ (TARI), same locality, 18.IV.2010, leg. M.-L. Jeng; 1♂ (TARI), Tahanshan (大漢山), 14.VIII.2011, leg. Y.-T. Wang; 1♀ (TARI), same locality, 25.V.2013, leg. Y.-T. Chung; 1♂, 1♀ (TARI), same locality, 30.V.2013, leg. Y.-T. Chung; 1♂ (TARI), same locality, 9.VI.2013, leg. Y.-T. Chung; 1♀ (TARI), same locality, 3.VII.2013, leg. B.-X. Guo; 1♂ (TARI), same locality, 23.V.2014, leg. Y.-T. Chung; 1♀ (TARI), same locality, 30.V.2014, leg. Y.-T. Chung; Taipei: 3♂♂, 2♀♀ (HNHM), Neitong Forest Recreation Area (內洞森林遊憩區), 6 km S of Wulai (烏來), 7.IV.2002, leg. G. Fábián and O. Merkl; 1♀
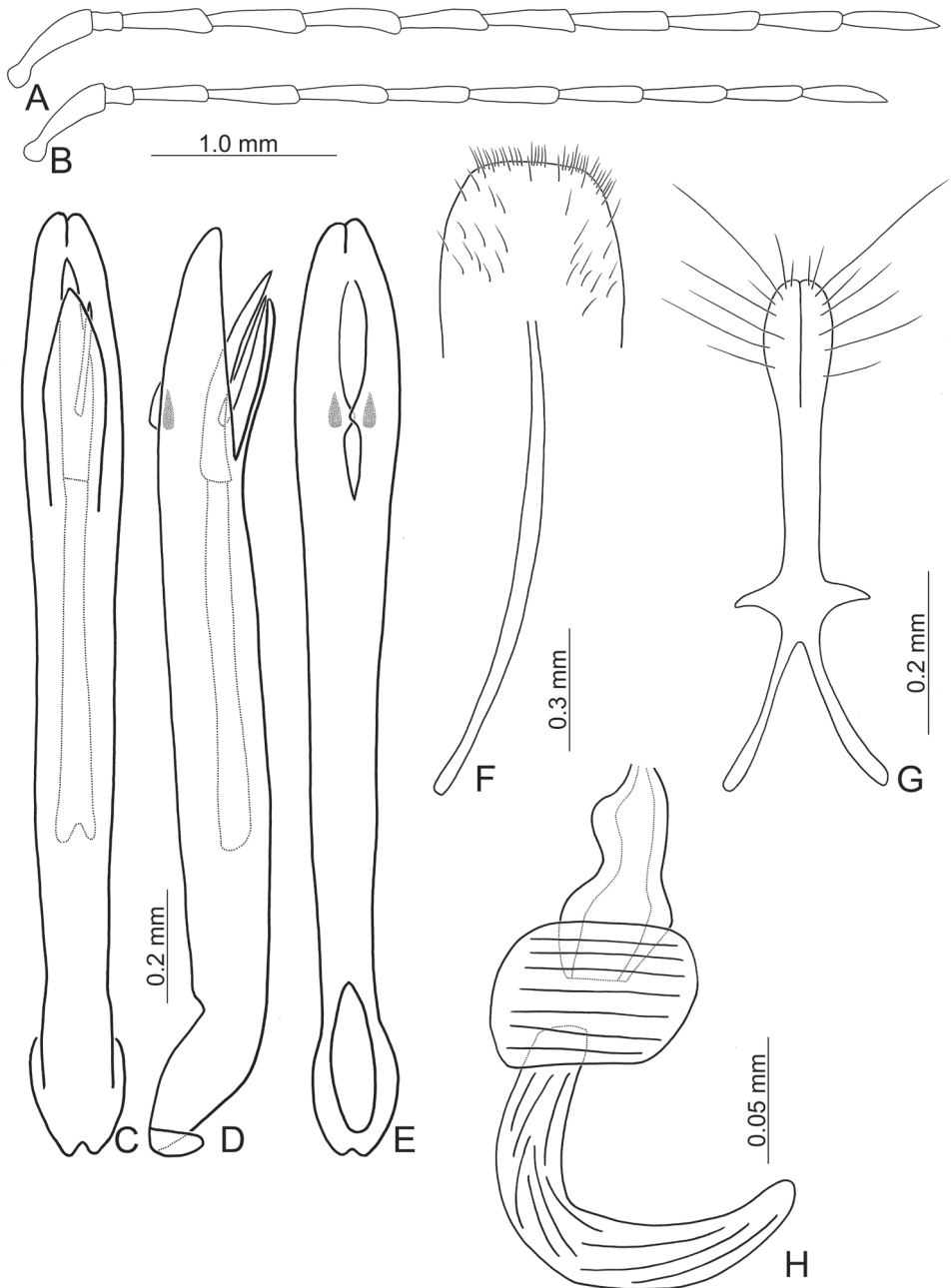
Figure 23. Diagnostic characters of *Pseudotheopea sufangae* sp. nov. **A** Antenna, male **B** Antenna, female **C** Aedeagus, dorsal view **D** Aedeagus, lateral view **E** Aedeagus, ventral view **F** Abdominal ventrite VIII **G** Gonocoxae **H** Spermatheca.

(TARI), Pinglin (坪林), 6.V.2007, leg. S.-F. Yu; Taitung: 1♂, 1♀ (TARI), Chihpen (知本), 24.V.2013, leg. J.-C. Chen; 1♂ (TARI), Shouka (壽卡), 19.IV.2015, leg. W.-C. Liao; 1♀ (NMNS), Tyokakurai (= Chaochia, 紹家), 28.VII.1936, identified as

Theopea sauteri by Chûjô (1962); Taoyuan: 1♂ (FREY), Monte Rara (= Lalashan, 拉拉山), VI.1939, leg. Arakawa.

Description. Length 5.3–6.7 mm, width 2.3–2.8 mm. Body color (Fig. 5F–H) metallic blue or purple, antennae and legs yellowish brown, mouthparts dark brown. Frontoclypeus (Fig. 19C, D) transversely deeply excavated between eyes, concavity 0.8× as wide as interspace between eyes; with one longitudinal ridge from middle of anterior margin to basal 1/3, with hair-like setae along lateral margins of longitudinal ridge; one pair of membranous areas near sides of longitudinal ridge and anterior margin; with one small rounded process at center of labrum, disc with several hair-like setae. Antennae filiform in males, but relatively broader than those of females (Fig. 23A), length ratios of antennomeres I–XI 1.0: 0.3: 0.8: 0.9: 0.9: 0.9: 0.9: 0.9: 0.9: 0.8: 1.0, length to width ratios of antennomeres I–XI 4.2: 1.2: 3.6: 3.9: 4.2: 4.2: 4.2: 4.9: 4.6: 4.2: 5.8; filiform in females (Fig. 23B), length ratios of antennomeres I–XI 1.0: 0.3: 0.7: 0.9: 0.9: 0.8: 0.9: 0.8: 0.8: 0.7: 0.8, length to width ratios of antennomeres I–XI 3.6: 1.7: 3.9: 4.9: 5.3: 5.0: 5.3: 5.0: 4.8: 4.9: 5.5. Elytra elongate, parallel-sided, 1.7× longer than wide; disc with dense, coarse punctures, arranged into longitudinal rows, with one distinct longitudinal ridge between two longitudinal rows of punctures. Tarsomeres I of front legs slightly swollen in males; subparallel in females. Aedeagus (Fig. 23C–E) extremely slender, 9.7× longer than wide; apex with shallow incision; tectum short, from apical 1/12 to 1/4; almost straight in lateral view, slightly curved at base; triangular sclerites small; internal sac with elongate, endophallic sclerite complex, 0.6× as long as aedeagus, composed of two sclerites, apical piece (0.7×) much shorter than basal piece, dorsal sclerite well developed, 0.5× as long as apical piece. Gonocoxae (Fig. 23G) elongate, both goncoxae fused from basal 1/4 to apical 1/4; apices convergent and narrowly rounded, each gonocoxa with eight setae along lateral margin from apex to apical 1/6; with one pair of short lateral processes at basal 2/5. Ventrite VIII (Fig. 23F) elongate and well sclerotized; disc with several long setae at sides and near apical margin, and with dense, short setae along apical margin; spiculum extremely slender. Receptacle of spermatheca (Fig. 23H) strongly swollen; pump slender and strongly curved; proximal spermathecal duct deeply inserted into receptacle, narrow and short.

Diagnosis. *Pseudotheopea sufangae* sp. nov. (Fig. 5F–H) is similar to *P. azurea* (Gressitt and Kimoto) (Fig. 5D, E) based on distinct but not convex ridges on the elytra. It differs by possessing a broad concavity between the eye with a median ridge (Fig. 19C, D) (narrow concavity between eyes and without ridge in *P. azurea* (Fig. 6A)). Males of *P. sufangae* sp. nov. are characterized by its incised aedeagal apex (with notch in other species), and presence of only one additional elongate dorsal sclerite near the base of the apical piece of the aedeagus (Fig. 23C–E). Females of *P. sufangae* sp. nov. are similar to those of the sympatric species, *P. sauteri*. Both lack sexually dimorphic characters but female *P. sufangae* differ in having the frons elevated above the clypeus (Fig. 19E) (frons as same height as clypeus in females of *P. sauteri* (Fig. 19F)).

Etymology. The new species is dedicated to Mrs. Su-Fang Yu, who is a member of the Taiwan Chrysomelid Research Team (TCRT) for her contribution to the diversity of leaf beetles.

Distribution. Taiwan.

Pseudotheopea similis group

Diagnosis. Frontoclypeus not modified in males, elytra with short dense hair.

Included species. *Pseudotheopea nigrita* (Medvedev), comb. nov. and *P. similis* (Kimoto), comb. nov.

Pseudotheopea nigrita (Medvedev, 2007), comb. nov.
Figs 18D, E; 24

Theopea nigrita: Medvedev 2007: 11 (Thailand).

Type. Holotype ♀ (SMNS): "W-THAILAND, Klong / Lan NP, 50 km SW / Kamphaeng Phet, 2.-5. / VII.1997, leg. J. REJSEK // HOLOTYPUS [p] / Theopea / nigrita m. [h] / L. Medvedev det. [p] 2006 [h, w]".

Other specimens examined. THAILAND. Mae Hong Son: 1♂, 1♀ (JBCB), Ban Huai Po, 19°19N 97°59E, 1600-2200 m, 17.-23.V.1991, leg. L. Dembický; 3♂♂ (JBCB), Kiwlom-pass near Soppong, 19°26N 98°19E, 1400 m, 23.VI.-2.VII.2002, leg. R. and H. Fouqué.

Redescription. Length 5.6–5.9 mm, width 2.3–2.5 mm. Body color (Fig. 18D, E) black, antennae and legs pale yellow, two or three apical antennomeres, and one or two apical tarsomeres darker. Antennae filiform in male, antennomeres VII-XI slightly curved (Fig. 24A), length ratios of antennomeres I–XI 1.0: 0.3: 0.8: 1.2: 1.3: 1.1: 1.2: 1.1: 1.0: 0.9: 1.0, length to width ratios of antennomeres I–XI 3.4: 1.6: 3.5: 4.9: 5.2: 4.8: 4.9: 4.8: 4.4: 4.1: 4.4; filiform and shorter in females (Fig. 24B), length ratios of antennomeres I–XI 1.0: 0.3: 0.8: 0.9: 1.0: 0.9: 1.0: 1.0: 0.9: 0.8: 1.0, length to width ratios of antennomeres I–XI 3.6: 1.8: 3.8: 4.2: 4.7: 4.3: 5.0: 4.9: 4.4: 4.3: 5.5. Elytra elongate, parallel-sided, 1.6-1.7× longer than wide; disc with dense, coarse punctures, arranged into longitudinal rows, with one indistinct longitudinal ridge between two longitudinal rows of punctures, with dense, short setae along ridges. Tarsomeres I of front legs slightly swollen in males; subparallel in females. Aedeagus (Fig. 24C–E) slender, 7.8× longer than wide; apex with shallow, broad notch, with a pair of small processes forming circular cavity; tectum short, from apex to apical 1/3, as broad as aedeagus; almost straight in lateral view, strongly curved at base, moderately curved near apex; triangular sclerites absent; internal sac with elongate, endophallic sclerite complex, 0.4× as long as aedeagus, undivided; with one ventral sclerite elongate, 0.85× as long as elongate, endophallic sclerite complex, with lateral expansion at apical 1/3, composed of dense short setae, apically tapering. Gonocoxae (Fig. 24G) elongate, both gonocoxae fused from basal 1/3 to near apex; apices convergent and narrowly rounded, each gonocoxa with eight setae along lateral margin from apex to apical 1/6; with one pair of short lateral processes at basal 2/5, recurved and combined, extending to apex.
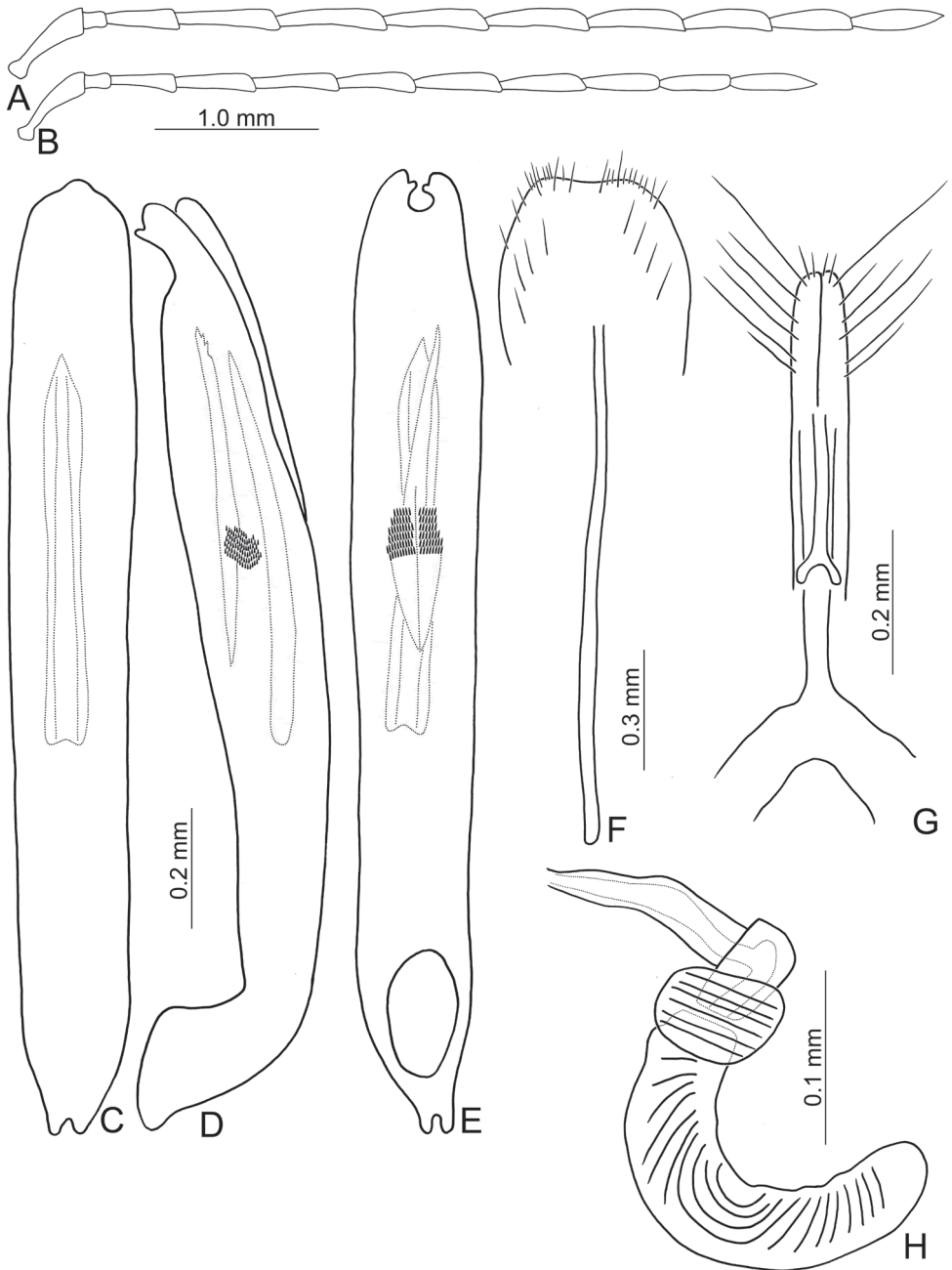
Figure 24. Diagnostic characters of *Pseudotheopea nigrita*. **A** Antenna, male **B** Antenna, female **C** Aedeagus, dorsal view **D** Aedeagus, lateral view **E** Aedeagus, ventral view **F** Abdominal ventrite VIII **G** Gonocoxae **H** Spermatheca.

Ventrite VIII (Fig. 24F) elongate and well sclerotized; disc with several long setae at sides and near apical margin, and with dense, short setae along apical margin; spiculum extremely slender. Receptacle of spermatheca (Fig. 24H) strongly swollen; pump slender and strongly curved; proximal spermathecal duct deeply inserted into receptacle, broad and short, strongly curved near base.

Diagnosis. *Pseudotheopea nigrita* (Medvedev) is easily recognized by its characteristic black color and dense setae on the elytra. In addition, a number of autapomorphic characters among genitalic structures are diagnostic, including the circular notch of the aedeagal apex; broad tectum, characteristic shape of the ventral sclerite, the recurved and combined lateral processes of the gonocoxae, and strongly curved proximal spermathecal duct of spermatheca.

Remarks. Most setae are missing from the elytra of the holotype (Fig. 18E), but these setae are dense on the elytra (Fig. 18F) of other specimens examined.

Distribution. Thailand.

Pseudotheopea similis (Kimoto, 1989), comb. nov.
Figs 12D–F; 25

Theopea similis: Kimoto 1989: 201.
Theopea sauteri: Kimoto 1989: 200 (part, misidentification).
Theopea subviridis: Medvedev 2012: 67. syn. nov.

Types. *Theopea similis*. Holotype ♀ (BPBM): "LAOS. Vientiane / 31.V-3.VI.1960 [p, w] // S. Quate and / L. Quate / Collectors [p, w] // Theopea / similis / n. sp. [h, w] // HOLOTYPE [p, r]".

Theopea subviridis. Holotype ♂ (LMCM, based on photographs): "S Vietnam, N. Dongnai Pr. / Nam Cat Tien Nat. Park / Exped. Russ.-Vietnamese / Tropical Centre / at light HLQ450 / leg. D. Fedorenko .X.2004 [p, w] // HOLOTYPUS / Theopea / subvidiridis / L. Medvedev [p, r]".

Other specimens examined. LAOS. 1♂ (BPBM), Umgeb. Vanky, 1963, identified as *Theopea sauteri* by Kimoto (1989).

Redescription. Length 5.0–6.4 mm, width 1.8–2.3 mm. Body color (Fig. 12D–F) metallic blue or purple, but antennae, legs, and mouth parts dark brown. Antennae filiform in females (Fig. 25A, lost in males), length ratios of antennomeres I–XI 1.0: 0.3: 0.7: 1.0: 1.0: 1.0: 1.0: 1.0: 1.0: 0.8: 1.0, length to width ratios of antennomeres I–XI 3.3: 1.6: 2.9: 4.0: 4.1: 3.9: 4.0: 4.6: 4.8: 4.4: 5.0. Elytra elongate, parallel-sided, 1.9-2.0× longer than wide; disc with dense, coarse punctures, arranged into longitudinal rows, with one indistinct longitudinal ridge between two longitudinal rows of punctures, with dense, short setae along ridges. Tarsomeres I of front legs slightly swollen in males; subparallel in females. Aedeagus (Fig. 25B–D) slender, 9.0× longer than wide; apex with shallow incision; tectum long, from apical 1/7 to basal 2/5; almost straight in lateral view, strongly curved at base; triangular sclerites small; internal
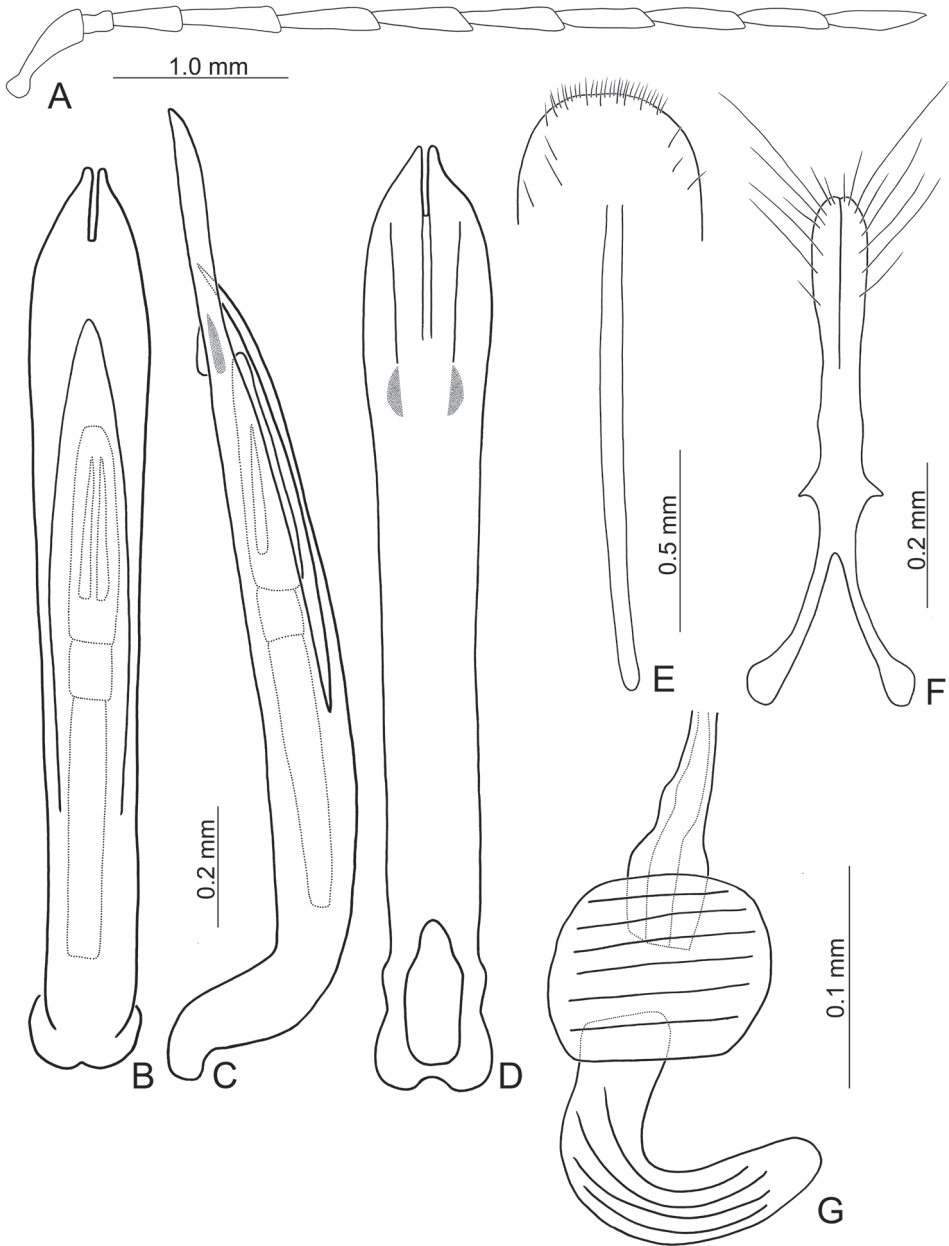
Figure 25. Diagnostic characters of *Pseudotheopea similis*. **A** Antenna, female **B** Aedeagus, dorsal view **C** Aedeagus, lateral view **D** Aedeagus, ventral view **E** Abdominal ventrite VIII **F** Gonocoxae **G** Spermatheca.

sac with elongate, endophallic sclerite complex, 0.5× as long as aedeagus, composed of three sclerites, basal piece longest, 0.5× long as entire sclerite, apical piece a little shorter than basal piece, 0.4× long as entire sclerite, median piece shortest, 0.1× long as entire sclerite; with one pair of dorsal sclerites elongate, 0.5× as long as apical piece.

Gonocoxae (Fig. 25F) elongate, both gonocoxae fused from basal 1/3 to apical 1/3; apices convergent and narrowly rounded, each gonocoxa with eight setae along lateral margin from apex to apical 1/6; with one pair of short lateral processes at basal 2/5. Ventrite VIII (Fig. 25E) elongate and well sclerotized; disc with several long setae at sides and near apical margin, and with dense, short setae along apical margin; spiculum extremely slender. Receptacle of spermatheca (Fig. 25G) strongly swollen; pump slender and strongly curved; proximal spermathecal duct deeply inserted into receptacle, narrow and short.

Variation. Reticulate microsculpture on pronotum is more or less reduced on specimens from Vietnam. A specimen from South Vietnam is metallic green in colour.

Diagnosis. *Pseudotheopea similis* (Kimoto) is similar to *P. irregularis* (Takizawa) based on the indistinct ridges on the elytra and metallic blue body. This species is characterized by the presence of dense, short erect setae on the elytra. Males of *P. similis* are similar to those of *P. collaris* in the presence of paired dorsal aedeagal sclerites, but differ in the bifurcate and symmetrical apices (Fig. 25B–D) (apices obliquely truncate apex in those of *P. collaris*).

Remarks. *Pseudotheopea similis* is easily recognized by the presence of dense erect setae on the elytra, which is also found on the holotype of *Theopea subviridis*. Such a characteristic feature supports their synonymy.

Distribution. Laos, Vietnam.

***Borneotheopea* Lee & Bezděk, gen. nov.**
http://zoobank.org/91CB6F48-EF54-4B12-881C-19CFADB1877E

Type species. *Borneotheopea jakli* sp. nov. (here designated)

Redescription. Body length 4.6–5.8 mm.

Males. Head. Eyes moderately large. Anterior part of head not modified. Frontal tubercles prominent, narrow, usually produced at inner anterior angle. Penultimate maxillary palpomere not greatly swollen, apical palpomere conical. Vertex with reticulate microsculpture. Antenna 11-segmented, filiform and slender, uniform in both sexes; antennomere II very short, III long, 2.0–3.5× longer than II, 0.6–0.8× as long as I, 2.8–3.4× as long as wide. Pronotum square or transverse, 1.1–1.2× as wide as long, broadest at middle, with pair of discal depressions. Anterior pronotal border absent. Lateral margins rounded or subparallel. Disc with reticulate microsculpture.

Elytra. Surface almost glabrous (with scattered erect setae on apical part only); punctate and striate, usually with longitudinal ridges between two longitudinal rows of punctures, sometimes ridges reduced or absent in part. Epipleura gradually narrowed to apex. Disc with reticulate microsculpture.

Legs. Procoxae globular, prosternal process apically expanded, procoxal cavities closed. Protarsomere I more or less swollen. Metatibia simple, without apical spine. Length of metatarsomere I nearly equal to following tarsomeres combined. Tarsal claws appendiculate with basal tooth small and rounded. Metatarsomere I simple.

Abdomen. Last ventrite apically trilobate.

Aedeagus always ventrally flattened, apex with shallow notch. Ventral surface entirely sclerotized. Internal sac with median elongate sclerite, undivided; with single pair of large lateral sclerites.

Females. Antennae slender, unmodified. Protarsomere I not modified. Posterior margin of last ventrite regularly rounded, without incisions. Spermatheca with small receptacle and C-shaped pump. Gonocoxae with split and convergent apex, apical part usually with eight long setae, base bifurcate. Ventrite VIII longitudinal, with long setae at sides and short setae along apical margin, spiculum 2.4× as long as ventrite VIII.

Differential diagnosis. This new genus possesses the following characters shared with *Theopea* and *Pseudotheopea* gen. nov.: the punctures on the elytra are striate and ridges are present between two longitudinal rows of punctures; the spaces between two longitudinal rows of punctures are broader when ridges are reduced or absent. *Borneotheopea* gen. nov. is similar to *Pseudotheopea* gen. nov. based on the presence of reticulate microsculpture on the vertex and pronotum (lacking reticulate microsculpture in *Theopea*) and convergent apices of the gonocoxae in females (diverge apices in those of *Theopea*). However, *Borneotheopea* gen. nov. can be separated from other genera by the antennomeres III-X not modified in males (antennomeres III-X usually longer and curved in those of *Pseudotheopea* gen. nov.); absence of an apical spine on the metatibia (presence of apical spine on the metatibia in *Pseudotheopea* gen. nov.; swollen or modified in those of *Theopea*); broader aedeagus, < 6.0× longer than wide (> 7.0× longer than wide in *Pseudotheopea* gen. nov. and > 6.0× longer than wide in *Theopea*); the ventral surface entirely sclerotized and unmodified (with deep groove, short hollow area, hollow area in *Theopea*, or wide groove in *Pseudotheopea* gen. nov.); and with the undivided median elongate endophallic sclerite in males (divided median elongate sclerite in *Pseudotheopea* gen. nov.).

Etymology. This new genus is named for its distribution combined with the genus *Theopea*.

Included species. Two new species are found in Borneo: *Borneotheopea jakli* sp. nov. and *B. kalimantanensis* sp. nov.

Borneotheopea jakli sp. nov.

http://zoobank.org/5A45681E-5605-4790-8732-5BDA28138BB0

Figs 26A–C; 27

Types. Holotype ♂ (NMPC), **INDONESIA**. South Kalimantan: Kandagan distr., 17 km NE of Laksado vill., 900 m, 3-22.IX.1997, leg. S. Jákl. Paratypes. 16♂♂, 2♀♀ (JBCB), same data as holotype.

Description. Length 4.6–5.0 mm, width 1.7–1.8 mm. Body color (Fig. 26A–C) metallic blue or green; ventral part, mouth parts, and antennae dark brown to black. Antennae filiform in males (Fig. 27A), length ratios of antennomeres I–XI 1.0: 0.3: 0.6: 0.7: 0.7: 0.7: 0.7: 0.7: 0.6: 0.7, length to width ratios of antennomeres I–XI
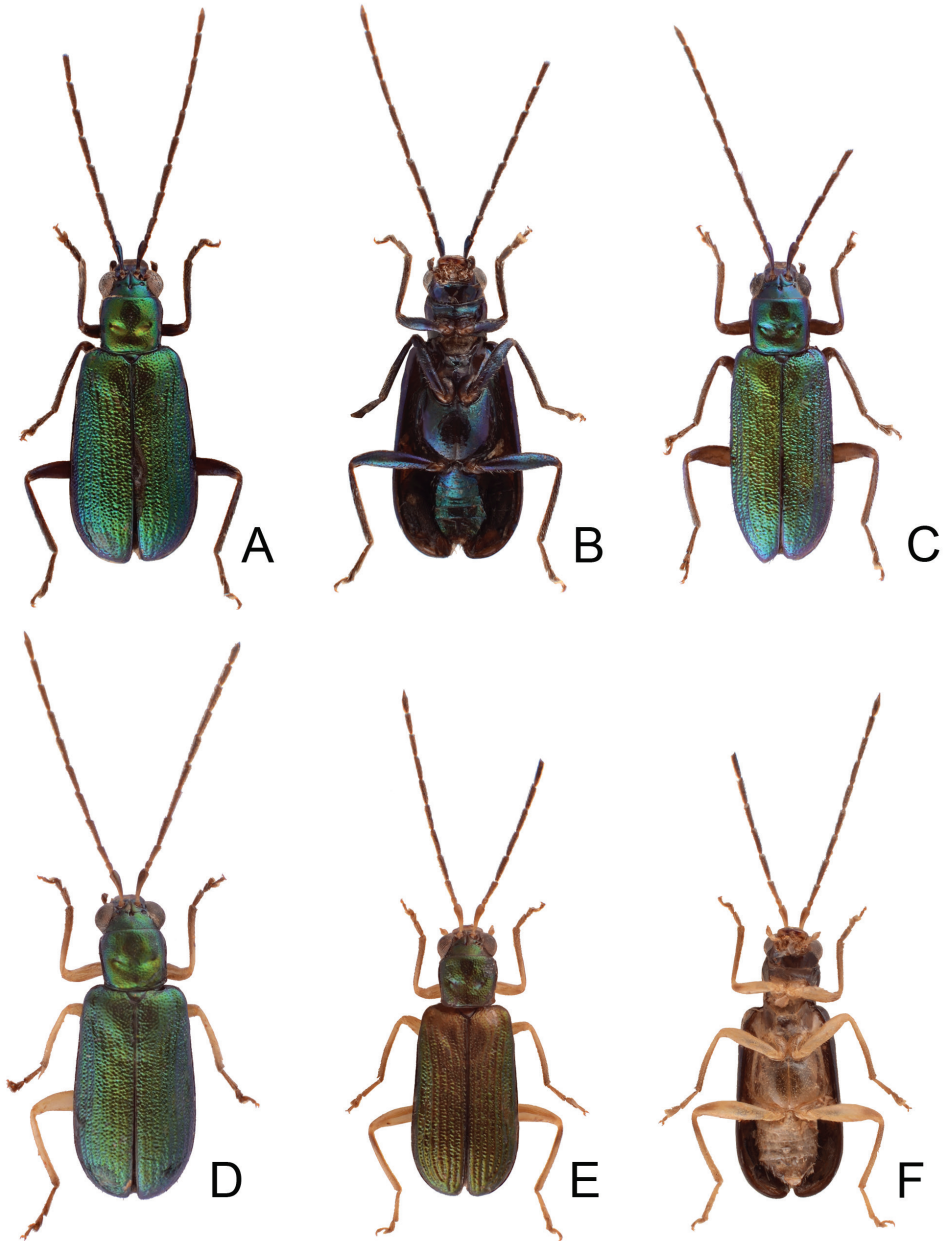
Figure 26. Habitus of *Borneotheopea jakli* sp. nov. and *B. kalimantanensis* sp. nov. **A** *B. jakli* sp. nov., male, dorsal view **B** Same, ventral view **C** *B. jakli* sp. nov., female, dorsal view **D** *B. jakli* sp. nov., male, color variation, dorsal view **E** *B. kalimantanensis* sp. nov., male, dorsal view **F** Same, ventral view.

4.0: 1.9: 3.4: 4.5: 4.6: 4.3: 4.7: 4.6: 4.8: 4.6: 4.5; similar in females (Fig. 27B), length ratios of antennomeres I–XI 1.0: 0.3: 0.6: 0.9: 0.9: 0.8: 0.8: 0.8: 0.8: 0.7: 0.8, length to width ratios of antennomeres I–XI 3.2: 1.8: 2.8: 4.2: 4.5: 4.3: 4.3: 4.6: 5.0: 5.1:

5.2. Elytra elongate, parallel-sided, 1.8-2.0× longer than wide; disc with dense, coarse punctures, arranged into longitudinal rows, with one indistinct longitudinal ridge between two longitudinal rows of punctures, with dense, short setae along ridges. Tarsomeres I of front legs slightly swollen in males. Aedeagus (Fig. 27C–E) slender, 5.5× longer than wide, parallel from apical 1/3 to near base, narrowed towards apex, apical margin medially depressed; tectum short, from near apex to middle; almost straight in lateral view, apically curved; ventral surface entirely sclerotized, triangular sclerites absent; internal sac with elongate endophallic sclerite, 0.8× as long as aedeagus, one pair of lateral sclerites elongate and hook-like, strongly recurved basally, left sclerite much longer than right sclerite. Gonocoxae (Fig. 27G) elongate, both gonocoxae fused from basal 1/3 to apical 1/3; apices convergent and narrowly rounded, each gonocoxa with eight setae along lateral margin from apex to apical 1/6; with one pair of short lateral processes at basal 2/5. Ventrite VIII (Fig. 27F) elongate and well sclerotized; disc with several long setae at sides and near apical margin, and with dense, short setae along apical margin; spiculum extremely slender. Receptacle of spermatheca (Fig. 27H) strongly swollen; pump slender and strongly curved; proximal spermathecal duct deeply inserted into receptacle, elongate and narrow.

Diagnosis. *Borneotheopea jakli* sp. nov. is easily distinguished from the other member of the genus, *B. kalimantanensis* sp. nov., based on the indistinct ridges on the elytra and metallic blue ventral surface (Fig. 26A–D) (distinct ridges on the elytra and yellowish brown ventral surface in *B. kalimantanensis* sp. nov. (Fig. 26E, F)). Males of *B. jakli* sp. nov. are also easily separated from those of *B. kalimantanensis* sp. nov. by the aedeagal apex directed ventrally and lacking angular processes (Fig. 27D) (the apex directed anteriorly and with angular process at apical 1/6 of aedeagus in *B. kalimantanensis* sp. nov. (Fig. 28C)), short, broad tectum (Fig. 27C) (extremely slender tectum in *B. kalimantanensis* sp. nov. (Fig. 28B)), absence of setae at apex of median elongate sclerite (Fig. 27C–E) (presence of clustered setae at apex of median elongate sclerite in *B. kalimantanensis* sp. nov. (Fig. 28B, C)).

Etymology. The new species is dedicated to the Czech specialist Stanislav Jákl who collected the type specimens.

Distribution. Indonesia: South Kalimantan.

Borneotheopea kalimantanensis sp. nov.

http://zoobank.org/C492882F-D6C3-4939-8F11-DE2C27F16A9F
Figs 26D–F; 28

Types. Holotype ♂ (NMPC), **INDONESIA**. South Kalimantan: Kandagan distr., 17 km NE of Laksado vill., 900 m, 3-22.IX.1997, leg. S. Jákl. Paratypes. 11♂♂ (JBCB), same data as holotype; **MALAYSIA**. Sabah: 2♂♂ (TARI), Trusmadi, 1.X.2014, leg. Y.-T. Wang; 2♂♂ (TARI), same but with "2.X.2014".

Description. Length 5.1–5.8 mm, width 1.8–2.3 mm. Body color (Fig. 26D–F) yellowish brown, head and pronotum metallic green, prosternite dark brown, elytra

Figure 27. Diagnostic characters of *Borneotheopea jakli* sp. nov. **A** Antenna, male **B** Antenna, female **C** Aedeagus, dorsal view **D** Aedeagus, lateral view **E** Aedeagus, ventral view **F** Abdominal ventrite VIII **G** Gonocoxae **H** Spermatheca.

yellowish but laterally and apically metallic green, antenna black except three basal antennomeres paler. Antennae filiform in males (Fig. 28A), length ratios of antennomeres I–XI 1.0: 0.3: 0.8: 0.9: 0.8: 0.8: 0.8: 0.8: 0.8: 0.7: 0.8, length to width ratios of
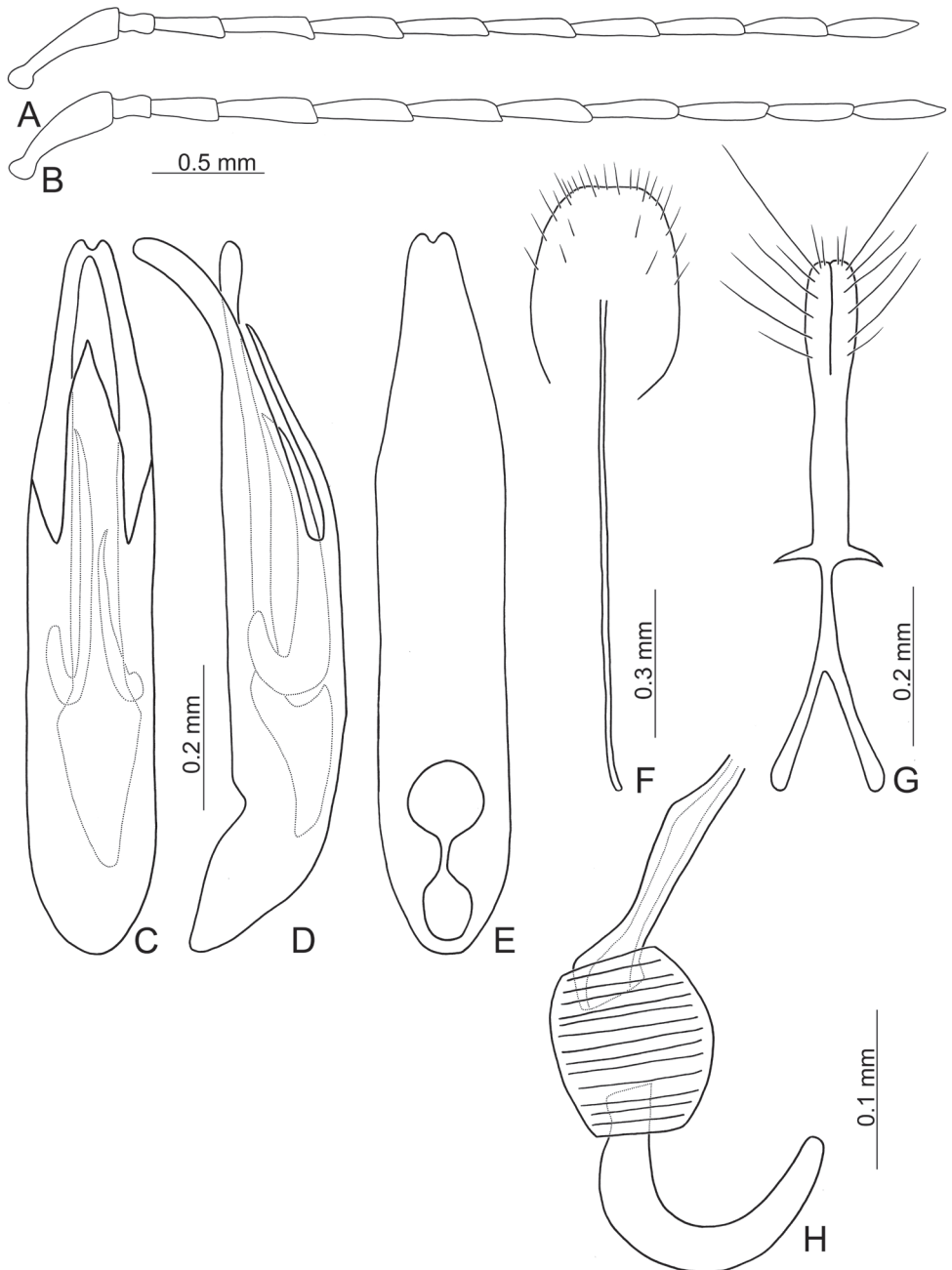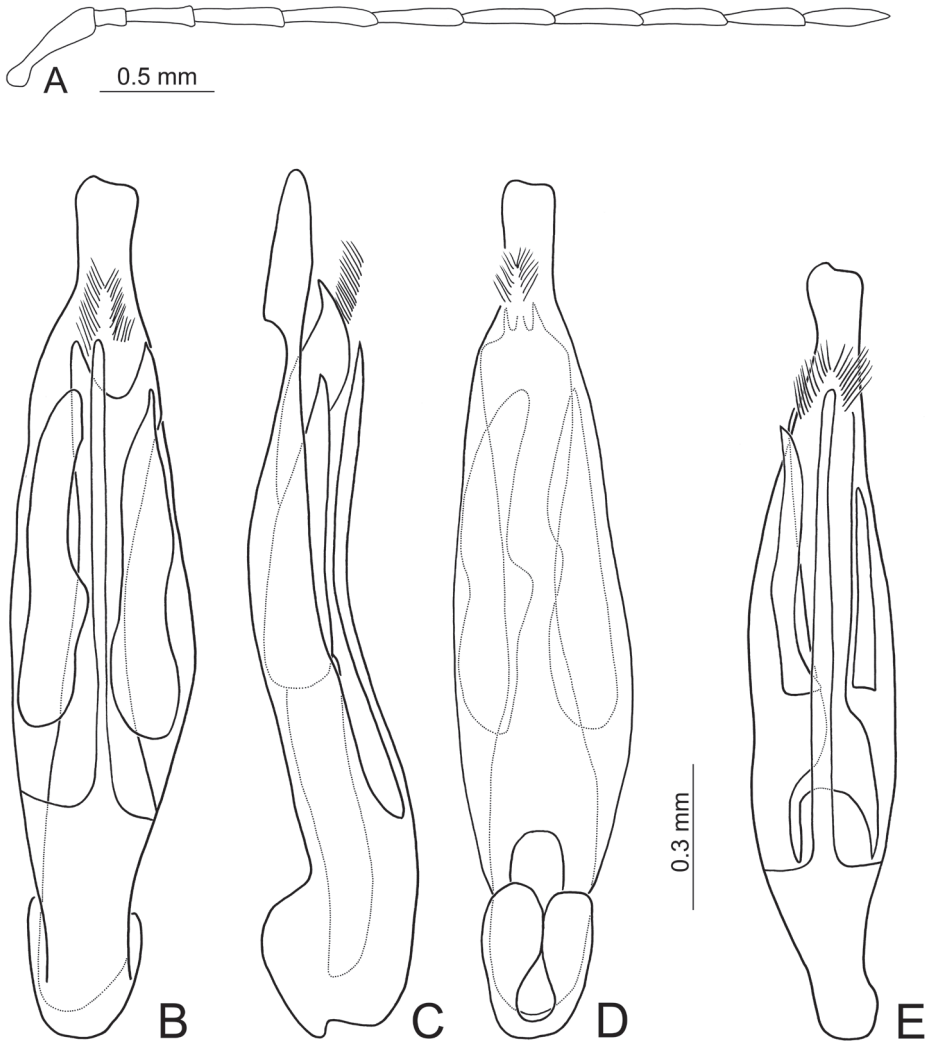
Figure 28. Diagnostic characters of *Borneotheopea kalimantanensis* sp. nov. **A** Antenna, male **B** Aedeagus, dorsal view **C** Aedeagus, lateral view **D** Aedeagus, ventral view **E** Aedeagus, dorsal view, from Sabah.

antennomeres I–XI 3.9: 1.8: 3.4: 4.4: 5.2: 5.3: 5.9: 5.8: 5.6: 4.6: 4.6. Elytra elongate, parallel-sided, 1.9-2.0× longer than wide; disc with dense, coarse punctures, arranged into longitudinal rows, with one indistinct longitudinal ridge between two longitudinal rows of punctures, with dense, short setae along ridges. Tarsomeres I of front legs slightly swollen in males. Aedeagus (Fig. 28B–D) slender, 4.7× longer than wide; widest at basal 2/5, narrowed towards apical 1/7 and basal 1/5, parallel from apical 1/7 to apex, apical margin truncate, slightly depressed medially; tectum extremely slender, from apical 1/5 to basal 1/4; recurved in lateral view, angular at apical 1/6, straight from apical 1/6 to apex; ventral surface entirely sclerotized, triangular sclerites absent; internal sac with elongate endophallic sclerite, 0.9× as long as aedeagus, apex with one pair of small processes directed ventrally, one pair of longitudinal rows of hair-like

setae basally connected with apex of endophallic sclerite, one pair of lateral sclerites large and hook-like, subequal in length but with different apical shapes; basal opening medially closed.

Female unknown.

Variation. Specimens from Sabah have slender lateral sclerites of the internal sac (Fig. 28E).

Diagnosis. *Borneotheopea kalimantanensis* sp. nov. is easily distinguished from the other member of the genus, *B. jakli* sp. nov., based on the distinct ridges on the elytra and yellowish brown ventral surface (Fig. 26E, F) (indistinct ridges on the elytra and metallic blue ventral surface in *B. jakli* sp. nov. (Fig. 26A–D). Males of B. *kalimantanensis* sp. nov. are also easily separated from those of *B. jakli* sp. nov. by the anterior directed apex and angular process at apical 1/6 of the aedeagus (Fig. 28C) (the apex of aedeagus directed ventrally and without angular processes in *B. jakli* sp. nov. (Fig. 27D)), extremely slender tectum (Fig. 28B) (short and wide tectum in *B. jakli* sp. nov. (Fig. 27C)), presence of clustered setae at apex of median elongate sclerite (Fig. 28B, C) (without setae at apex of median elongate sclerite in *B. jakli* sp. nov. (Fig. 27C–E)).

Etymology. The new species is named for its type locality.

Distribution. Indonesia: South Kalimantan; Malaysia: Sabah.

Key to the species of *Pseudotheopea* gen. nov. and *Borneotheopea* gen. nov.

1   Some antennomeres curved or apically broadened in male; metatibia with apical spine; aedeagus with median elongate sclerite divided, with small lateral sclerites present or absent, triangular sclerites present..........(***Pseudotheopea* gen. nov.) 2**

–   Antennomeres filiform, uniform in both sexes; metatibia without apical spines; aedeagus with median elongate sclerites undivided, with large lateral sclerites, triangular sclerites absent .... (***Borneotheopea* gen. nov.) 25**

2   Frontoclypeus modified in males, with concavity between eyes ....
     .... (*P. costata* group) **3**

–   Frontoclypeus not modified in males **13**

3   Concavity between eyes in males semi-circular, with one central erect process and one pair of baso-lateral processes (Fig. 13A, B), Philippines **4**

–   Concavity between eyes in males transverse, anterior margin narrowly rounded, with one central erect process in some species but without baso-lateral processes, Southeast Asia except Philippines **5**

4   Large species, 7.0-7.2 mm long; reddish brown dorsum; without lateral process at apex of antennomere I in males.. ***P. costata* (Allard)**

–   Small species, 5.0-5.7 mm long; metallic blue dorsum; with lateral process at apex of antennomere I in males (Fig. 14A).................................. ***P. gressitti* sp. nov.**

5   General body color reddish brown, but elytra metallic blue (Fig. 5A–C)............
     ....***P. aeneipennis* (Gressitt & Kimoto)**

–   Body metallic green, blue, or purple **6**

6 Body color golden green (Figs 8A–F; 15A–F) **7**
– Body color metallic blue or purple **10**
7 Ridges on elytra distinct and convex (Fig. 8D, 8F); concavity between eyes anteriorly narrowed (Fig. 9C, D), Vietnam.......................... *P. clypealis* **(Medvedev)**
– Ridges on elytra indistinct (Figs 8A, C; 15A, B, D–E); concavity between eyes transverse (Figs 9A, B; 16A–D) **8**
8 Presence of convex area surrounding scutellum in males (Fig. 8A); concavity between eyes wide, but without erect processes (Fig. 9A, B), India ....
....*P. boreri* **sp. nov.**
– Lacking convex area surrounding scutellum in males (Fig. 15A, D); concavity between eyes wide and with one erect process (Fig. 16C, D) or narrow (Fig. 16A, B)..**9**
9 Concavity between eyes wide and with one erect process (Fig. 16C, D), China...
....*P. smaragdina* **(Gressitt & Kimoto)**
– Concavity between eyes narrow (Fig. 16A, B), Laos .... *P. hsingtzungi* **sp. nov.**
10 Ridges on elytra distinct and convex (Fig. 15A, C, F, H) **11**
– Ridges on elytra indistinct (Fig. 5D, F, H) **12**
11 All ridges on elytra distinct and convex .... *P. kimotoi* **sp. nov.**
– Distinct convex ridges intertwined with indistinct ridges... *P. leehsuehae* **sp. nov.**
12 Concavity between eyes with one pair of erect processes......................................
....*P. azurea* **(Gressitt & Kimoto)**
– Concavity between eyes with median longitudinal ridge ....
....*P. sufangae* **sp. nov.**
13 Longitudinal ridges on elytra distinct..**14**
– Longitudinal ridges on elytra indistinct or reduced **21**
14 Elytra with extremely coarse punctures, space between punctures narrower than diameters of punctures; head and prothorax yellow except vertex and pronotum; Taiwan ....*P. collaris* **(Kimoto)**
– Elytra with coarse punctures, space between punctures broader than diameters of punctures; head and prothorax metallic blue or green except mouth parts.......**15**
15 Body color metallic green; longitudinal ridges on elytra apically abbreviated from apical 1/3; antennomeres III-VII straight in males; Taiwan ....
....*P. cheni* **(Lee & Bezděk)**
– Body color metallic blue; longitudinal ridges on elytra not apically abbreviated; antennomeres III-VII more or less curved .... **(***P. sauteri* **species group) 16**
16 Males with longitudinal ridges on the elytra more or less reduced **17**
– Males with longitudinal ridges on the elytra prominent **20**
17 Aedeagus asymmetrical, curved to the right..**18**
– Aedeagus symmetrical **19**
18 Aedeagus relatively slender, 10.0× longer than wide; dorsal sclerite of endophallus extremely elongate, 3.6× longer than basal piece; Laos....*P. sekerkai* **(Lee & Bezděk)**
– Aedeagus relatively broad, 9.0× longer than wide; dorsal sclerite of endophallus less elongate, 1.6× longer than basal piece; China..... *P. coerulea* **(Gressitt & Kimoto)**

19   Triangular sclerites of endophallus elongate; ventral sclerites absent; basal piece longer than apical piece, with longitudinal row of tiny teeth along lateral margin; India .... *P. geiseri* (**Lee & Bezděk**)
–   Triangular sclerites of endophallus small; ventral sclerites present; basal piece shorter than apical piece, without tiny teeth; China, Laos, Vietnam.................... ....*P. laosensis* (**Lee & Bezděk**)
20   Males with antennomeres III–X moderately curved; swollen tarsomeres I of front legs not apically narrowed; Taiwan ....*P. sauteri* (**Chûjô**)
–   Males with antennomeres III–X straight; swollen tarsomeres I of front legs apically narrowed; China .... *P. hainanensis* (**Lee & Bezděk**)
21   Elytra with dense, short, erect setae................................... (*P. similis* **group**) 24
–   Elytra with sparse, short, erect setae **22**
22   Elytra with extremely coarse punctures, space between punctures narrower than diameters of punctures; Japan ....*P. aureoviridis* (**Chûjô**)
–   Elytra with moderately coarse punctures, space between punctures broader than diameters of punctures **23**
23   Body color sexually dimorphic, elytra yellowish brown with metallic green sides, pronotum and vertex metallic green in males; elytra entirely metallic green, prothorax and head yellow in females; hypomeron yellowish brown; antenna in males relatively shorter, antennomeres V–IX less than six times longer than wide; Taiwan .... *P. kanmiyai* (**Kimoto**)
–   Body color not sexually dimorphic, elytra, pronotum, and vertex metallic green or blue in both sexes; hypomeron dark or blackish brown; antenna in males more slender, antennomeres V-IX more than six times longer than wide; Taiwan .... *P. irregularis* (**Takizawa**)
24   Body color black (Fig. 18E, F) ....*P. nigrita* (**Medvedev**)
–   Body color metallic green (Fig. 12D–F) .... *P. similis* (**Kimoto**)
25   Ridges on elytra distinct (Fig. 26E); ventral surface yellowish brown (Fig. 26F) .. .. *B. kalimantanensis* **sp. nov.**
–   Ridges on elytra indistinct (Figs 26A, C, D); ventral surface metallic green (Fig. 26B)...*B. jakli* **sp. nov.**

Acknowledgements

055-002), and National Chung Hsing University and Agricultural Research Institute, Council of Agriculture, Executive of Yuan, ROC.（NCHU-TARI-10806）Taichung, Taiwan, Republic of China. Finally, we are grateful to Tomas Wagner and Viswajyothi Keezhpattillam for reviewing the manuscript.

References

Aston P (2009) Chrysomelidae of Hong Kong Part 3, Subfamily Galerucinae. Hong Kong Entomological Bulletin 1: 6–25.

Baly JS (1864) Descriptions of uncharacterised genera and species of Phytophaga. The Transactions of the Entomological Society of London (3)2[1864–1866]: 223–243.

Bezděk J (2012) Taxonomic and faunistic notes on Oriental and Palaearctic Galerucinae and Cryptocephalinae (Coleoptera: Chrysomelidae). Genus 23: 375–418.

Beenen R (2010) Galerucinae. In: Löbl I, Smetana A (Eds) Catalogue of Palaearctic Coleoptera, Volume 6. Chrysomeloidea. Apollo Books, Stenstrup, 443–491.

Chûjô M (1935a) H. Sauter's Formosa-Ausbeute: Subfamily Galerucinae (Coleoptera: Chrysomelidae). Arbeiten über Morphologische und Taxonomische Entomologie 2: 160–174.

Chûjô M (1935b) Chrysomelidae of Loo-Choo Archipelago (I). Transactions of the Natural History Society of Formosa 25: 69–90.

Chûjô M (1962) A taxaonomic study on the Chrysomelidae (Insecta: Coleoptera) from Formosa Part XI. Subfamily Galerucinae. The Philippine Journal of Science 91: 1–239.

Gressitt JL, Kimoto S (1963) The Chrysomelidae (Coleopt.) of China and Korea Part 2. Pacific Insects Monograph 1B: 301–1026.

Kimoto S (1984) Notes on the Chrysomelidae from Taiwan, China, XI. Entomological Review of Japan 39: 39–58.

Kimoto S (1989) Chrysomelidae (Coleoptera) of Thailand, Cambodia, Laos, and Vietnam. IV. Gallerucinaea. Esakia 27: 1–241.

Lee C-F, Bezděk J (2018) Revision the genus *Theopea* Baly (Coleoptera: Chrysomelidae: Galerucinae) of East Asia: species lacking modified clypeus in males and the *T. sauteri* species group. Zootaxa 4508: 334–376. https://doi.org/10.11646/zootaxa.4508.3.2

Lee CF, Bezděk J (2019) Revision of the genus *Theopea* Baly (Coleoptera: Chrysomelidae: Galerucinae): Redefinition of the genus. Zootaxa 4683: 451–507. https://doi.org/10.11646/zootaxa.4683.4.1

Medvedev LN (2000) Chrysomelidae (Coleoptera) of Laos from the collection of the Hungarian Natural History Museum. Annales Historico-Naturales Musei Nationalis Hungarici 92: 161–182.

Medvedev LN (2007) New and poorly known Oriental Chrysomelidae of the Staatliches Museum für Naturkunde, Stuttgart. Stuttgarter Beiträge zur Naturkunde, Serie A (Biologie) 702: 1–19.

Medvedev LN (2012) New species of Chrysomelidae (Coleoptera) from Indochina. Euroasian Entomological Journal 11: 63–69. https://doi.org/10.15298/rusentj.24.1.06

Medvedev LN (2015) New taxa of Chrysomelidae (Coleoptera) from Vietnam. Russian Entomological Journal 24: 67–72.

Mohamedsaid MS, Costant J (2007) Chrysomelid beetles of the subfamily Galerucinae from Thailand and Cambodia in the collections of the Royal Belgian Institute of Natural Sciences (Coleoptera: Chrysomelidae). Bulletin de l'Institut Royal des Sciences Naturelles de Belgique, Entomologie 77: 163–177.

Nie RE, Bezděk J, Yang XK (2017) How many genera and species of Galerucinae s. str. do we know? Updated statistics (Coleoptera, Chrysomelidae). ZooKeys 720: 91–102. https://doi.org/10.3897/zookeys.720.13517

Staines CL, Staines SL (1999) Joseph Sugar Baly: The man and his entomological works. Beiträge zur Entomologie 49: 489–530.

Takizawa H (1978) Notes on Taiwanese Chrysomelidae, I. Kontyû 46: 123–134.

Wang J, Yang X, Wang S, Wu Y, Yao J, Li W (1998) Fauna of Chrysomelidae of Wuyishan Nature Reserve in China. China Forestry Publishing House, Beijing, 213 pp (in Chinese).

Wilcox JA (1973) Chrysomelidae: Galerucinae (Luperini: Luperina). In: Wilcox JA (Ed.) Coleopterorum Catalogus Supplementa. Pars 78 (3), Second edition. W. Junk, 's-Gravenhage, 433–664.

Yang XK (2002) Chrysomelidae: Galerucinae. In: Huang, P.-K. (Ed.), Fauna of Insects of Fujian Privince of China Vol. 6. Fujian Science and Technology Press, Fuzhou, 621–633. [in Chinese with English summary]

Yang X-K, Yao J (2002) Coleoptera: Chrysomelidae: Galerucinae. In: Huang FS, Yin H, Zeng R, Lin M, Gu M (Eds) Forest insects of Hainan. National Natural Science Foundation of China, Beijing, 439–448. [in Chinese with English summary]

RESEARCH ARTICLE

A new species of *Ithome* Chambers (Lepidoptera, Cosmopterigidae, Chrysopeleiinae) from the Atacama Desert revealed by morphology and DNA barcodes

Sebastián Espinoza-Donoso[1], Dante Bobadilla[1], Wilson Huanca-Mamani[2], Marcelo Vargas-Ortiz[3], Héctor A. Vargas[1]

1 *Departamento de Recursos Ambientales, Facultad de Ciencias Agronómicas, Universidad de Tarapacá, Casilla 6-D, Arica, Chile* **2** *Departamento de Producción Agrícola, Facultad de Ciencias Agronómicas, Universidad de Tarapacá, Casilla 6-D, Arica, Chile* **3** *Programa de Doctorado en Sistemática y Biodiversidad, Departamento de Zoología, Facultad de Ciencias Naturales y Oceanográficas, Universidad de Concepción, Concepción, Chile*

Corresponding author: *Héctor A. Vargas* (havargas@uta.cl; lepvargas@gmail.com)

Abstract

Morphology and DNA barcode sequences were used to assess the taxonomic status of a micro-moth of the genus *Ithome* Chambers, 1875 (Lepidoptera, Cosmopterigidae, Chrysopeleiinae), whose larvae feed on inflorescences of *Prosopis tamarugo* Phil. (Fabaceae), a tree native to the Pampa del Tamarugal, Atacama Desert, northern Chile. As a result, *Ithome tamarugensis* Vargas, **sp. nov.** is described and illustrated. Its genitalia are remarkably similar to those of *Ithome tiaynai* Vargas, 2004 from coastal valleys of the Atacama Desert. However, the two species can be recognized by the shape of the phallus in males and the shape of the antrum and ductus bursae in females. The genetic distance between DNA barcodes of *I. tamarugensis* and *I. tiaynai* was 3.0–3.3% (K2P), and a maximum likelihood analysis indicated that they are in reciprocally monophyletic clusters, providing additional support for the heterospecific status suggested by morphology.

Keywords

Introduction

The Atacama Desert harbors a distinctive biota characterized by some endemic plants and animals (e.g. Saldivia and Faúndez 2014; Valladares-Faúndez et al. 2018) despite being the most arid desert in the world (Clarke 2006). Among its singular and amazing environments is the Pampa del Tamarugal, a plain at about 1000 m elevation in the Tarapacá Region, northern Chile, whose name is due to the presence of the endemic *Prosopis tamarugo* Phil. (Fabaceae), a tree locally known as Tamarugo. This tree is key in most of the regular ecological processes in the Pampa del Tamarugal, providing food, refuge, and other services to other species (Lopez-Calleja and Estades 1996; Vargas 2007; Carevic et al. 2013). In addition, humans have used this tree in several ways, such as for livestock feed (Zelada 1986). As fruits and leaves are the main organs consumed, serious problems can be triggered by outbreaks of phytophagous insects, among which florivorous lepidopterans are especially important (Vargas and Bobadilla 2000).

Ithome Chambers, 1875 (Lepidoptera, Cosmopterigidae, Chrysopeleiinae) is a New World genus of micro-moth with 19 species currently described. Eighteen species of *Ithome* have their type locality on mainland America and one in the Galápagos Islands (Hodges 1961, 1978, 1997; Becker 1984; Landry 2001; Vargas 2004). Although the biology of many species of *Ithome* remains unknown, when the host plants are known, the larvae mainly feed on inflorescences of trees of the family Fabaceae (Hodges 1978).

Two of the species of *Ithome* originally described from the southern United States have expanded their ranges outside of mainland America and are pests of Fabaceae. *Ithome concolorella* (Chambers, 1875), described from Texas, became a pest of *Acacia farnesiana* (L.) Willd. and *Prosopis chilensis* (Mol.) Stuntz in the Hawaiian Islands because feeding by its larvae reduces the flower production of these trees, which are important nectar sources for honey bees (Namba 1956). *Ithome lassula* Hodges, 1962, with its type locality in Florida, is currently established in Australia and Cuba, where its larvae feed on inflorescences of *Leucaena leucocephala* (Lam.) de Wit (Common and Beattie 1982; Alonso et al. 2015).

Ithome tiaynai Vargas, 2004 is the only representative of the genus currently described from Chile. Its larvae feed on inflorescences of *Acacia macracantha* Willd. (Fabaceae) in coastal valleys of the Atacama Desert (Vargas 2004), reaching higher densities on trees growing in well-preserved habitats than in highly human-modified ones (Vargas and Parra 2009). In addition, an unidentified species of *Ithome* was mentioned by Hodges (1978) from central Chile, and another, pest species, is known from the Pampa del Tamarugal, where its larvae feed on inflorescences of *P. tamarugo*, affecting the fruit production (Vargas et al. 1986). This last species was referred to as *I. concolorella* in the agricultural literature (Artigas 1994). However, because *I. concolorella* is a Northern Hemisphere species (Hodges 1978), the identity of the *Ithome* from the Pampa del Tamarugal has remained doubtful.

We used morphology and DNA barcode sequences (sensu Hebert et al. 2003) to assess the taxonomic status of the *Ithome* from the Pampa del Tamarugal. The two character sources revealed that this micro-moth represents a new species whose formal description is provided here.

Materials and methods

Sampling and rearing

Larvae of *Ithome* were collected on inflorescences of *P. tamarugo* in La Tirana village, at about 1000 m elevation in Tamarugal Province, Tarapacá Region, northern Chile, in August 2018 and September 2019. The inflorescences with larvae were placed in plastic vials with paper towel at the bottom and brought to the laboratory, where additional inflorescences were provided until the larvae finished feeding and pupated. The vials were observed daily until adult emergence. The adults were mounted and their abdomens were removed and placed in hot KOH 10% for a few minutes for dissection of their genitalia, which were stained with Chlorazol black and Eosin Y and slide mounted with Euparal. Description of genitalia follows Hodges (1978). Pupae of *I. tiaynai* were reared from larvae collected in March 2016 on inflorescences of *A. macracantha* in the type locality of this micro-moth. Three pupae of the each of the two *Ithome* species were placed in ethanol 95% at –20 °C until DNA extraction.

DNA extraction, sequencing and analysis

Genomic DNA was extracted following the procedures described by Huanca-Mamani et al. (2015) from pupae of the *Ithome* pest of *P. tamarugo* and *I. tiaynai*. Genomic DNA was sent to Macrogen Inc., South Korea, for purification, PCR amplification, and sequencing of the DNA barcode fragment with the primers LCO-1490 and HCO-2198 (Folmer et al. 1994) using the PCR program described in Escobar-Suárez et al. (2017). The software MEGA7 (Kumar et al. 2016) was used to perform the sequence alignment by the ClustalW method, to estimate the sequence divergence by the Kimura 2-Parameter (K2P) method, and to calculate the phylogenetic tree using the maximum likelihood (ML) approach with 1000 bootstrap replications. The nucleotide substitution model was chosen using the lowest Bayesian information criterion (BIC) value. The sequence used as outgroup belongs to *Ithome curvipunctella* (Walsingham, 1892), the only congeneric with barcode sequences available in BOLD (Ratnasingham and Hebert 2007). To detect the presence of phylogenetic signal, substitution saturation analysis was previously performed using the Xia test (Xia et al. 2003) in the Dambe 7.2.1 program (Xia 2018).

Abbreviations of institutional collections

MNNC   Museo Nacional de Historia Natural de Santiago, Santiago, Chile
IDEA   Colección Entomológica de la Universidad de Tarapacá, Arica, Chile

Results

Molecular analysis

Six DNA barcode sequences were obtained (Table 1), three of *Ithome* from the Pampa del Tamarugal and three of *I. tiaynai*, each representing a different haplotype. Intra- and interspecific genetic divergence was 0.2–0.3 and 3.0–3.3% (K2P), respectively. The sequence alignment length was 657 bp. Codon stops were not detected and substitution saturation was not found, indicating that the data set was suitable for phylogenetic analysis. The substitution model used was TN92 + G (with the lowest BIC value). A maximum likelihood analysis separated the haplotypes of the two species into reciprocally monophyletic clusters (Fig. 1).

Table 1. Sequences used in the analyses.

Species	BOLD accession	GenBank accession	Country
Ithome curvipunctella (Walsingham, 1892)	BBLOB1350-11		USA
Ithome tamarugensis Vargas, sp. nov.		MN586873	Chile
I. tamarugensis		MN586874	Chile
I. tamarugensis		MN586875	Chile
Ithome tiaynai Vargas, 2004		MN586876	Chile
I. tiaynai		MN586877	Chile
I. tiaynai		MN586878	Chile
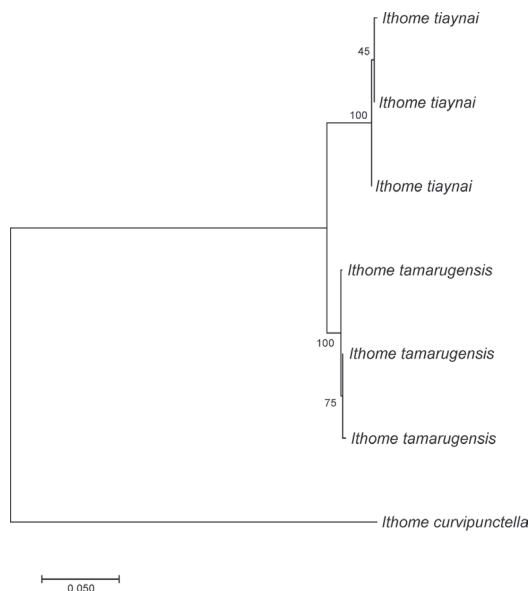
Figure 1. Maximum likelihood tree of the haplotypes of the DNA barcode fragment of *Ithome tamarugensis* Vargas, sp. nov. and *Ithome tiaynai*. Numbers indicate bootstrap percentages (1000 replicates). One sequence of *Ithome curvipunctella* was used as outgroup.

Taxonomy

Ithome tamarugensis **Vargas, sp. nov.**
http://zoobank.org/43BEAA78-9AA8-43BB-BD05-6BC197292B7F
Figures 2–4

Ithome sp. (Vargas et al. 1986; Vargas and Bobadilla 2000)
Ithome concolorella; misidentification (Artigas 1994)

Type locality. Chile, Tarapacá Region, Tamarugal Province, La Tirana village, 20°20'S, 69°39'W.

Type material. Holotype male, pinned, genitalia slide HAV-1307. Original labels: "Chile, Tamarugal, La Tirana, emerged October, 2019, H.A. Vargas coll.", "ex-larva inflorescence *Prosopis tamarugo*, collected September, 2019", "Holotype / *Ithome* / *tamarugensis* / Vargas" [red handwritten label] (MNNC).

Other material. Paratypes (Five males, five females). One male (genitalia slide HAV-1309), two females (genitalia slides HAV-1308, 1310), same data as for holotype (MNNC). Four males (genitalia slides HAV-1311, 1313, 1315, 1317), three females (genitalia slides HAV-1312, 1314, 1316), same data as for holotype (IDEA).

Figure 2. Holotype of *Ithome tamarugensis* Vargas sp. nov. in dorsal view. Scale bar: 1 mm.
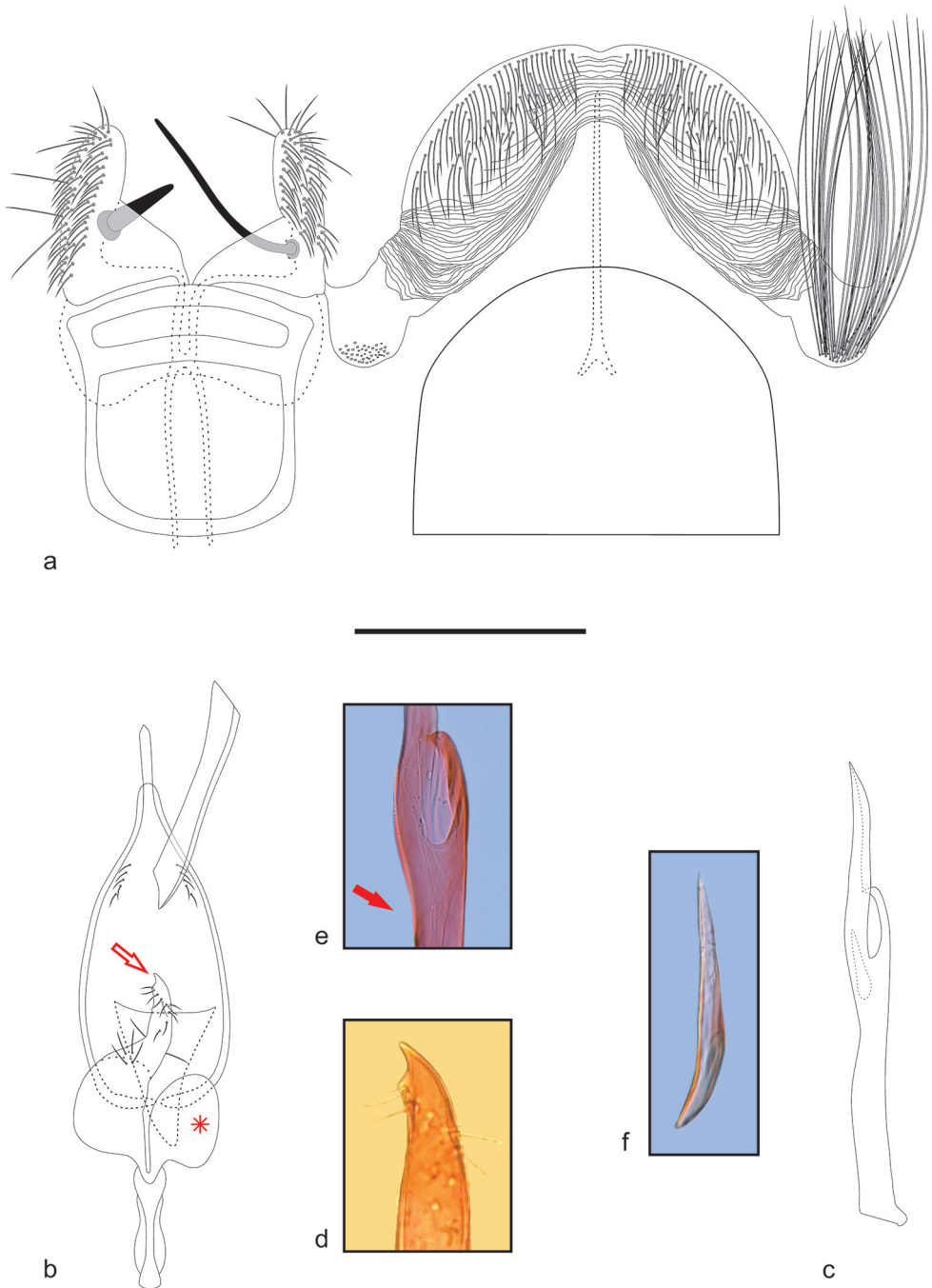
Figure 3. Male genitalia and pregenital abdominal segments of *Ithome tamarugensis* Vargas, sp. nov. **A** Abdominal segments VII and VIII **B** genitalia in ventral view, phallus removed, asterisk shows the right valva **C** phallus in lateral view **D** apex of the hook of the left valva (marked with arrow in **B**) **E** apex of phallus, arrow shows the dorsal excavation **F** cornutus. Scale bar: 0.1 mm.
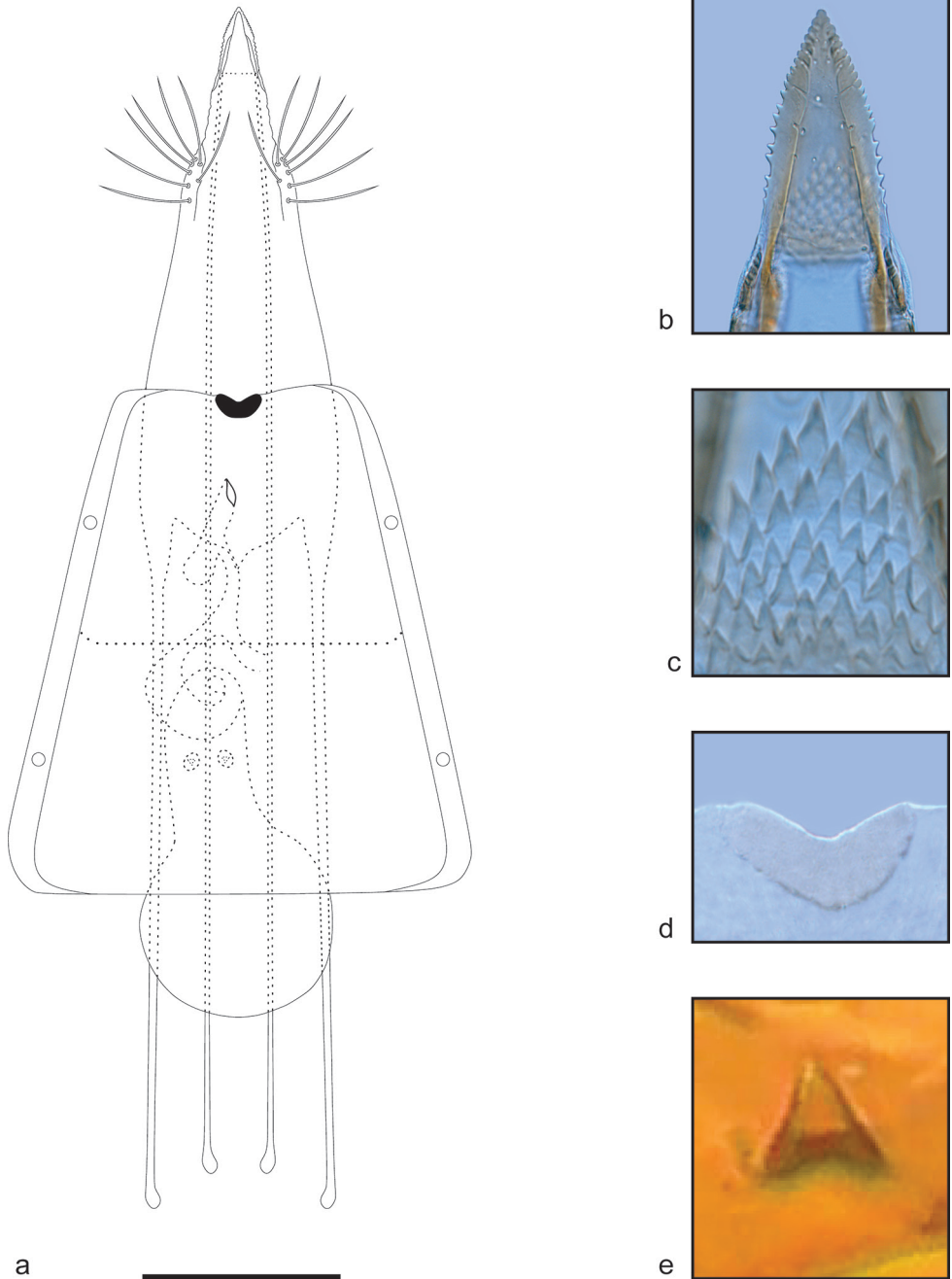
Figure 4. Female genitalia of *Ithome tamarugensis* Vargas, sp. nov. **A** Female genitalia in ventral view **B** papillae analis **C** ornamentation of intersegmental membrane between papillae and segment VIII **D** lamella postvaginalis **E** signum. Scale bar: 0.1 mm.

Diagnosis. The mainly shiny black adults of *I. tamarugensis* resemble those of *I. tiaynai*, the only other Chilean congeneric. In addition, the genitalia of the two species are outstandingly similar. However, the male of *I. tamarugensis* has the phallus dorsally excavated in the middle, slightly broadened subapically, and with a deep cleft apically. In contrast, the phallus of *I. tiaynai* is parallel sided in the middle, slightly straightening subapically, and with a small cleft apically. The female of *I. tamarugensis* has a short cylindrical antrum and coiled ductus bursae. In contrast, the female of *I. tiaynai* has a mainly undifferentiated antrum and conic ductus bursae. Although signa were not mentioned in the original description of *I. tiaynai*, recent observations have revealed the presence of two signa similar to those found in *I. tamarugensis*.

Description. Male (Fig. 2). Forewing length 4.4–4.6 mm.

Head. Shiny dark grey on face, shiny black dorsally. Haustellum shiny dark grey. Labial palpus shiny black. Antenna shiny black, filiform, about 3/4 wing length; pecten formed by a dark brown scale placed near base of scape.

Thorax. Shiny black dorsally, brownish grey laterally. Foreleg mainly shiny black; coxa brownish grey laterally; brownish grey at middle and apex of tibia and apex of tarsomeres. Midleg mainly shiny black; two brownish grey tibial spurs; brownish grey at apex of tarsomeres. Hindleg mainly shiny black laterally, brownish grey medially; tibia with longitudinal stripe of short, hair-like, yellowish-grey scales dorsally; four brownish-grey tibial spurs; tarsomeres mainly brownish grey with a few darker areas. Forewing shiny black with slightly differentiated (or sometimes absent) brownish-grey transverse stripe subapically; fringe brownish grey. Hindwing shiny black on basal half, brownish grey on distal half; fringe brownish grey.

Abdomen (Fig. 3a). Mainly brownish grey; shiny black on terga I–IV; lateral membrane of segment VII with a pocket of yellowish-brown, hair-like scales exceeding slightly the posterior margin of tergum VIII. Tergum VII mainly not modified, posterior margin broadly convex. Sternum VII modified, well-sclerotized margins, a transverse stripe close to the posterior margin divides the sternum into a square-shaped anterior part and a posterior transverse band; anterolateral margin slightly convex; posterior part of lateral margin laterally projected, posterior margin slightly convex. Tergum VIII hood-shaped; anterior margin broadly concave, posterior margin broadly convex, slightly excavated in the middle; narrow, sclerotized rod medially, anterior end bifurcated. Sternum VIII strongly modified, partially overlapped with sternum VII; longitudinally divided by a sharp posterior excavation that reaches the anterior margin; two narrow sclerotized rods medially in the middle of anterior margin, length similar to rod of tergum VIII; two finger-like posterior projections of similar length, with right one slightly narrower; both projections with an inward spine of differing length; the left projection with a short, robust, and tapering spine medially near middle, the right projection with a long, narrow, and straight spine medially, bent near base.

Male genitalia (Fig. 3b–f). Uncus short, slightly shorter than the left spine on sternum VII, narrow, parallel sided, apex suddenly pointed. Tegumen narrow, somewhat forceps-like, slightly broadened ventrally. Saccus about 1.5 times length of uncus, with a longitudinal ventral carina and a pair of convex lateral projections. Subscaphium as a narrow stripe, slightly sclerotized, and with a few small setae on the membrane near

base of subscaphium. Valvae asymmetrical; left valva lobular (Fig. 3b, arrow), a slightly curved pointed hook distally (Fig. 3d), a few short setae near apex of hook; right valva lobular without hook. Phallus (Fig. 3c) cylindrical, dorsally excavated at middle (Fig. 3e, arrow), slightly broadened subapically; apex with a deep cleft and a knife-like projection. Vesica with a conic cornutus (Fig. 3f), similar in size to apical cleft of phallus.

Female. Similar to male in size and coloration. Hindwing brownish grey; fenulum with three acanthae. Abdomen brownish grey. Separation between VI and VII segments slightly differentiated.

Female genitalia (Fig. 4a–e). Papillae analis well sclerotized, fused medially, forming a triangular plate with serrated lateral margin (Fig. 4b). Intersegmental membrane between papillae and segment VIII with triangular spinules (Fig. 4c). Posterior apophysis rod-shaped, narrow, elongated, about three times length of tergum VIII. Anterior apophysis rod-shaped, about 2/3 length of posterior apophysis. Tergum VIII slightly more sclerotized and with a few long setae posterolaterally. Lamella postvaginalis as a small semicircular plate in middle of posterior margin of sternum VII (Fig. 4d). Ostium bursae as a narrow longitudinal slit on middle of sternum VII. Antrum cylindrical, apex rounded. Ductus bursae arising subapically on antrum, membranous, coiled. Corpus bursae pear-shaped, membranous, with two small conical signa close to the base (Fig. 4e).

Geographic distribution. *Ithome tamarugensis* is known from the Pampa del Tamarugal (Fig. 5a), Atacama Desert of northern Chile.

Host plants. All the specimens of *I. tamarugensis* examined in this study were reared from larvae collected on *P. tamarugo* (Fig. 5b, c). This tree is the main host plant of *I. tamarugensis*, although its larvae also feed on inflorescences of at least two other species of *Prosopis*, *P. alba* Griseb. var. *alba* and *P. strombulifera* (Lam.) Benth. var. *strombulifera* (Vargas and Bobadilla 2000).

Etymology. The specific epithet is derived from the Pampa del Tamarugal, where the type locality of *I. tamarugensis*, La Tirana village, is located.

Discussion

Despite the extreme aridity of the Atacama Desert, some reports in the last decades suggest that it harbors a distinctive micro-moth fauna associated with native plants (e.g. Clarke 1987; Pereira et al. 2017; Vargas-Ortiz et al. 2019), which is reinforced by this study in which the taxonomic status of the *Ithome* pest of *P. tamarugo* in the Pampa del Tamarugal was assessed using morphology and DNA barcodes. The two character sources revealed that this micro-moth represents a previously undescribed species, here named *I. tamarugensis*. This discovery allows us to conclude that the previous record of *I. concolorella* in Chile (Artigas 1994) was based on a misidentification of *I. tamarugensis*. These two species can be clearly separated by the morphology of the asymmetrical posterior projections of the male sternum VIII. In *I. concolorella*, the left projection has an apical spine and the right projection is unarmed (Hodges 1961, 1978). In *I. tamarugensis*, each of the two projections has a medial spine, which is short in the left projection and long in the right one (Fig. 3a).

Figure 5. Habitat and host plant of *Ithome tamarugensis* Vargas, sp. nov. in the Atacama Desert. **A** Habitat near La Tirana village, Pampa del Tamarugal, northern Chile **B** a tree of tamarugo, *Prosopis tamarugo* (Fabaceae) **C** inflorescences of *P. tamarugo* at bud and flowering stages.

Although there are no previous studies dealing with phylogenetic relationships of the species of *Ithome*, the morphology suggests that *I. tamarugensis* and *I. tiaynai* are closely related. First, the highly specialized sternum VIII of the male abdomen is

indistinguishable among them, but clearly different from this structure in the remaining species of the genus (Hodges 1961, 1978; Landry 2001). Second, the remarkably similar genitalia of *I. tamarugensis* and *I. tiaynai* are distinguishable only after a careful examination of very fine morphological traits. In addition, although the ML analysis included sequences of only three species of *Ithome*, the clusters in which the sequences of *I. tamarugensis* and *I. tiaynai* were reciprocally grouped were highly supported by bootstrap (Fig. 1), and the genetic distance between the two species using the COI marker is comparable to those reported for other morphologically close species of Lepidoptera (e.g. Hausmann et al. 2009; Matson and Wagner 2017; Ullah et al. 2017; Müller 2018; Pfeiler et al. 2018). Accordingly, although very preliminarily, the genetic analysis also provides evidence in support of a close evolutionary relationship between the two Chilean species of *Ithome*.

The current data suggest that the geographic ranges of the two species of *Ithome* of northern Chile are restricted to different ecological zones of the Atacama Desert, the coastal valleys in the case of *I. tiaynai*, and the Pampa del Tamarugal in the case of *I. tamarugensis*. A similar geographic pattern has been described for two morphologically close micro-moths of the genus *Cryptophlebia* Walsingham (Tortricidae), with *C. cortesi* Clarke, 1987 restricted to the coastal valleys and *C. saileri* Clarke, 1987 to the Pampa del Tamarugal (Clarke 1987). This coincident pattern in two distantly related families suggests that allopatry could have been an important mechanism underlying diversification in some groups of micro moths in these arid environments. Genetic differentiation between isolated populations has been shown in at least two other micro-moths of the Atacama Desert (Escobar-Suárez et al. 2017; Vargas-Ortiz et al. 2018), which agrees with a scenario of allopatric speciation. However, further comprehensive phylogenetic studies, including a detailed taxon sampling and analyses of morphological characters and biparental (or male-linked) molecular markers, will be needed to reconstruct the diversification process in the genus *Ithome* and to assess the close evolutionary relationship between *I. tamarugensis* and *I. tiaynai* that is here suggested.

Acknowledgements

References

Alonso O, Núñez R, Lezcano JC, Suris M (2015) *Ithome lassula* Hodges (Lepidoptera: Cosmopterigidae), una nueva especie para Cuba asociada a *Leucaena leucocephala* (Lam.) de Wit. Pastos y Forrajes 38: 182–184.

Artigas JN (1994) Entomología Económica. Insectos de Interés Agrícola, Forestal, Médico y Veterinario. Volumen II. Ediciones Universidad de Concepción, Concepción, Chile, 943 pp.

Becker VO (1984) Cosmopterigidae. In: Heppner JB (Ed.) Atlas of Neotropical Lepidoptera, Micropterigoidea–Immoidea. Dr. W. Junk Publishers, The Hague, 43–44.

Carevic FS, Carmona ER, Muñoz-Pedreros A (2013) Seasonal diet of the burrowing owl *Athene cunicularia* Molina, 1782 (Strigidae) in a hyperarid ecosystem of the Atacama desert in northern Chile. Journal of Arid Environments 97: 237–241.

Clarke JDA (2006) Antiquity of aridity in the Chilean Atacama Desert. Geomorphology 73: 101–114.

Clarke JFG (1987) Two new *Cryptophlebia* Walsingham from Chile (Lepidoptera: Tortricidae). Acta Entomológica Chilena 14: 7–12.

Common IFB, Beattie WM (1982) An introduced moth, *Ithome lassula* (Cosmopterigidae), attacking *Leucaena* in northern Queenslans. Journal of the Australian Entomological Society 21: 195–197.

Escobar-Suárez S, Huanca-Mamani W, Vargas HA (2017) Genetic divergence of a newly documented population of the cecidogenous micromoth *Eugnosta azapaensis* Vargas & Moreira (Lepidoptera: Tortricidae) in the Atacama Desert of northern Chile. Revista Brasileira de Entomologia 61: 266–270.

Folmer O, Black M, Hoeh W, Lutz R, Vrijenhoek R (1994) DNA primers for amplification of mitochondrial cytochrome c oxidase subunit I from diverse metazoan invertebrates. Molecular Marine Biology and Biotechnology 3: 294–299.

Hausmann A, Hebert PDN, Mitchell A, Rougerie R, Sommerer M, Edwards T, Young CJ (2009) Revision of the Australian *Oenochroma vinaria* Guenée, 1858 species-complex (Lepidoptera: Geometridae, Oenochrominae): DNA barcoding reveals cryptic diversity and assesses status of type specimen without dissection. Zootaxa 2239: 1–21.

Hebert PDN, Cywinska A, Ball SL, deWaard JR (2003) Biological identifications through DNA barcode. Proceedings of the Royal Society B-Biological Sciences 270: 313–321.

Hodges RW (1961) The genus *Ithome* in North America north of Mexico (Walshiidae). Journal of the Lepidopterists' Society 15: 81–90.

Hodges RW (1978) Cosmopterigidae. In: Dominick RB, Dominick T, Ferguson DC, Franclemont JG, Hodges RW, Munroe EG (Eds) The Moths of America North of Mexico, Fascicle 6.1, Gelechioidea (Part). E.W. Classey Ltd and the Wedge Entomological Research Foundation, London, 166 pp.

Hodges RW (1997) A new agonoxenine moth damaging *Araucaria araucana* needles in western Argentina and notes on the Neotropical agonoxenine fauna (Lepidoptera: Gelechioidea: Elachistidae). Proceedings of the Entomological Society of Washington 99: 267–278.

Huanca-Mamani W, Rivera-Cabello D, Maita-Maita J (2015) A simple, fast, and inexpensive CTAB-PVP-Silica based method for genomic DNA isolation from single, small insect larvae and pupae. Genetics and Molecular Research 14: 7990–8000.

Kumar S, Stecher G, Tamura K (2016) MEGA7: Molecular Evolutionary Genetics Analysis Version 7.0 for Bigger Datasets. Molecular Biology and Evolution 33:1870–1874.

Landry B (2001) The Cosmopterigidae (Lepidoptera) of the Galapagos Islands, Ecuador. Revue Suisse de Zoologie 108: 513–539.

Lopez-Calleja MV, Estades CF (1996) Natural history of the Tamarugo cone bill (*Conirostrum tamarugense*) during the breeding period: diet and habitat preferences. Revista Chilena de Historia Natural 69: 351–356.

Matson T, Wagner DL (2017) A new cryptic *Lactura* from Texas (Lepidoptera, Zygaenoidea, Lacturidae). ZooKeys 711: 141–150.

Müller B (2018) *Biston rosenbaueri* sp. n. (Lepidoptera, Geometridae, Ennominae) from the Balkan Peninsula. Nota Lepidopterologica 41: 207–213.

Namba R (1956) Descriptions of the immature stages and notes on the biology of *Ithome concolorella* (Chambers) (Lepidoptera: Cosmopterigidae), a pest of Kiawe in the Hawaiian Islands. Proceedings of the Hawaiian Entomological Society 16: 95–100.

Pereira CM, Silva DS, Gonçalves GL, Vargas HA, Moreira GRP (2017) A new species of *Leurocephala* Davis & McKay (Lepidoptera, Gracillariidae) from the Azapa Valley, northern Chilean Atacama Desert, with notes on life history. Revista Brasileira de Entomologia 61: 6–15. http://doi.org/10.1016/j.rbe.2016.11.003

Pfeiler E, Nazario-Yepiz NO, Vargas CC, Laclette MRL (2018) DNA barcodes suggest possible new cryptic species in the *Codatractus melon* species group (Hesperiidae: Eudaminae) in North America. Journal of the Lepidopterists' Society 72: 203–211.

Ratnasingham S, Hebert PDN (2007) BOLD: the barcode of life data system. Molecular Ecology Notes 7: 355–367. www.barcodinglife.org

Saldivia P, Faúndez L (2014) *Weberbauerella chilensis* (Fabaceae: Papilionoideae), a new species from the Atacama Desert, Chile. Phytotaxa 156: 41–46. https://doi.org/10.11646/phytotaxa.156.1.2

Tamura K, Stecher G, Peterson D, Filipski A, Kumar S (2013) MEGA6: molecular evolutionary genetics analysis version 6.0. Molecular Biology and Evolution 30: 2725–2729. https://doi.org/10.1093/molbev/mst197

Ullah M, Yang Z, Qiao P, Zhang Y (2017) A new cryptic species of *Nagiella* Munroe from China revealed by DNA barcodes and morphological evidence (Lepidoptera, Crambidae, Spilomelinae). ZooKeys 679: 65–76. https://doi.org/10.3897/zookeys.679.11960

Valladares-Faúndez P, Etheridge R, Abdala CS (2018) Resurrection and redescription of *Liolaemus reichei*, proposal of a neotype to stabilize its taxonomy. Revista Mexicana de Biodiversidad 89: 393–401. https://doi.org/10.22201/ib.20078706e.2018.2.2086

Vargas H, Bobadilla D (2000) Insectos asociados al bosque de tamarugo. In: Baldini A, Pancel L (Eds) Agentes de daño en el bosque nativo. Editorial Universitaria, Santiago, Chile, 283–318.

Vargas H, Bobadilla D, Aguilera A (1986) Adaptación morfológica y hábito de oviposición de la polilla del botón floral del tamarugo, *Ithome* sp. (Lepidoptera: Walshiidae). Idesia 10: 39–44.

Vargas HA (2004) Una nueva especie de *Ithome* Chambers (Lepidoptera: Cosmopterigidae: Chrysopeleiinae) del norte de Chile. Revista Chilena de Historia Natural 77: 285–292.

Vargas HA (2007) Dos nuevas especies de *Iridopsis* Warren (Lepidoptera, Geometridae) del norte de Chile. Revista Brasileira de Entomologia 51: 138–141. https://doi.org/10.1590/S0085-56262007000200003

Vargas HA, Parra LE (2009) Prospección de lepidópteros antófagos asociados a *Acacia macracantha* Willd. (Fabaceae) en el norte de Chile. Revista Brasileira de Entomologia 53: 291–293. https://doi.org/10.1590/S0085-56262009000200012

Vargas-Ortiz M, Bobadilla D, Huanca-Mamani W, Vargas HA (2018) Genetic divergence of isolated populations of the native micromoth *Bucculatrix mirnae* (Lepidoptera: Bucculatricidae) in the arid environments of Northern Chile. Mitochondrial DNA Part A 29: 1139–1147. https://doi.org/10.1080/24701394.2017.1419215

Vargas-Ortiz M, Gonçalves GL, Huanca-Mamani W, Vargas HA, Moreira GRP (2019) Taxonomic description, natural history and genetic structure of *Caloptilia guacanivora* sp. nov. (Lepidoptera: Gracillariidae) in the Atacama Desert. Austral Entomology 58: 171–191. https://doi.org/10.1111/aen.12351

Xia X (2018) DAMBE7: New and improved tools for data analysis in molecular biology and evolution. Molecular Biology and Evolution 35: 1550–1552. https://doi.org/10.1093/molbev/msy073

Xia X, Xie Z, Salemi M, Chen L, Wang Y (2003) An index of substitution saturation and its application. Molecular Phylogenetics and Evolution 26: 1–7. https://doi.org/10.1016/S1055-7903(02)00326-3

Zelada L (1986) The influence of the productivity of *Prosopis tamarugo* on livestock production in the Pampa del Tamarugal – a review. Forest Ecology and Management 16: 15–31.

DATA PAPER

The FrogID dataset: expert-validated occurrence records of Australia's frogs collected by citizen scientists

Jodi J.L. Rowley[1,2], Corey T. Callaghan[2]

1 *Australian Museum Research Institute, Australian Museum, 1 William Street, Sydney, New South Wales 2010, Australia* **2** *Centre for Ecosystem Science, School of Biological, Earth and Environmental Sciences, University of New South Wales, Sydney, New South Wales 2052, Australia*

Corresponding author: *Jodi J. L. Rowley* (jodi.rowley@austmus.gov.au)

Citation: Rowley JJL, Callaghan CT (2020) The FrogID dataset: expert-validated occurrence records of Australia's frogs collected by citizen scientists. ZooKeys 912: 139–151. https://doi.org/10.3897/zookeys.912.38253

Abstract

This dataset represents expert-validated occurrence records of calling frogs across Australia collected via the national citizen science project FrogID (http://www.frogid.net.au). FrogID relies on participants recording calling frogs using smartphone technology, after which point the frogs are identified by expert validators, resulting in a database of georeferenced frog species records. This dataset represents one full year of the project (10 November 2017–9 November 2018), including 54,864 records of 172 species, 71% of the known frog species in Australia. This is the first instalment of the dataset, and we anticipate providing updated datasets on an annual basis.

Keywords

amphibians, bioacoustics, biodiversity data, citizen science, smartphone

Introduction

Citizen science biodiversity data

Biodiversity monitoring is critical for conservation, useful in warning of impending extinction crises, and has direct implications for management practices for improved biodiversity targets (Noss 1990; Pereira and Cooper 2006; Lindenmayer et al. 2012). The loss of funding, logistical constraints (e.g., time and spatial scale), and lack of in-

terest by some government authorities in fully monitoring biodiversity make it important for other methods of biodiversity monitoring to be explored. For instance, citizen science (Silvertown 2009; Dickinson et al. 2012) is currently recognized as a method for achieving broad-scale biodiversity monitoring (Pocock et al. 2018; Callaghan et al. 2019). Citizen scientists are helping to assess various ecological and biodiversity aspects of birds (Sullivan et al. 2009), coral (Marshall et al. 2012), sharks (Vianna et al. 2014), and bees (Domroese and Johnson 2017), among other taxa. Additionally, some large-scale programs, such as iNaturalist (iNaturalist.org 2018) span various taxa.

Frogs as sentinels of environmental change

Frogs and other amphibians are sensitive to changes in their environment due to their biphasic lifestyle (with most species having an aquatic larval stage and a terrestrial adult), semi-permeable skin, and reliance on specific environmental conditions for reproduction (Hopkins 2007; Lemckert and Penman 2012). Almost one-third of the 7,000 frog species known are at risk of extinction (Stuart et al. 2014; IUCN 2019), largely due to anthropogenic threats such as habitat loss and modification, disease, and invasive species. The implications are far-reaching, with frog populations declines shown to have large-scale, long-term ecosystem-level effects (e.g., Whiles et al. 2013).

Despite the need for biodiversity data on frogs, frogs are inherently difficult to survey, leaving a lack of detailed knowledge of broad-scale distributions, occurrences, and habitat associations. This is largely a result of logistical constraints, including a lack of funding available for surveys and access to often remote sites, and the fact that many frog species are difficult to detect, having activity patterns highly reliant on weather. Many frog species are also small and camouflaged, rendering them difficult to visually locate.

Frog acoustic data

The frog advertisement call serves as a premating isolation mechanism (Blair 1964; Littlejohn 1969) and is therefore typically highly species-specific. As a result, advertisement calls are often used for frog species identification during surveys (Heyer et al. 2014) and in delineating species, including the description of new species (Littlejohn 1969; Rowley et al. 2016; Köhler et al. 2017). The identification of frog species via their advertisement calls may also minimise disturbances to the frog and its habitat.

All known frog species in Australia have audible advertisement calls and only a few are difficult to identify to species via their calls alone (e.g., several species of the genus *Pseudophryne* Fitzinger, 1843 in the places where they co-occur; Pengilley 1971). Further, several Australian frog species that are morphologically indistinguishable from related species can be identified to species by their calls (e.g., *Litoria jungguy* Donnellan & Mahony, 2004 and *Litoria myola* Hoskin, 2007). Although female frogs have been demonstrated to call in a handful of species (e.g., Goyes Vallejos et al. 2017), only male frogs are known to produce advertisement calls in Australia.

Acoustic monitoring of frogs in Australia

Launched on 10 November 2017 and led by the Australian Museum, FrogID is the first citizen science initiative aimed at capturing validated biodiversity data on Australian frogs on a national scale (Rowley et al. 2019). The FrogID project collects data via a smartphone application allowing participants to submit recordings of calling frogs, which are then identified to species by experts (Rowley et al. 2019). If no frogs are heard calling (i.e., a FrogID user recorded an insect), submissions are identified as "Not a Frog". If the recording is not sufficient to identify species (i.e., too short in duration, too much other noise in the recording), or there is an otherwise high level of uncertainty, the submission is identified as "Unidentified Frog".

Publishing biodiversity data advances our collective knowledge on global biodiversity (Costello et al. 2013) and our ability to make informed conservation decisions. We hope that by making these occurrence data openly accessible (Michener 2015), others will find it useful, ultimately contributing to increased knowledge of Australia's frogs and translating into increased conservation action. In this data paper, we detail the associated dataset.

Project details

Project title: FrogID
Sponsoring institution: Australian Museum, 1 William Street, Sydney, NSW 2010
Data published through GBIF: https://doi.org/10.15468/wazqft
Data published through a self-hosted Zenodo repository: https://zenodo.org/record/3612700

Funding

Data sensitivity

While effective conservation relies on accurate knowledge of where species occur, releasing the locations of observation records may have inadvertent negative impacts (Lindenmayer and Scheele 2017). Open locality information has resulted in the poaching of wildlife (Stuart et al. 2006), and particularly in the age of social media, access to precise locality data for certain species may also drive enthusiasts or wildlife photographers to locate, photograph or even remove species, sometimes resulting in habitat disturbance (Lindenmayer and Scheele 2017; Pike et al. 2010; Tulloch et al. 2018). A considera-

tion of the potential impacts of publishing exact locality information is likely to be particularly important for FrogID records for three reasons: (1) FrogID occurrence data are derived from recordings of male frogs calling at breeding habitats, and habitat disturbance at these vital locations may influence breeding success; (2) visually locating or photographing frogs may disturb both the frog and breeding habitat, particularly for species that call from concealed microhabitats such as burrows (e.g. *Pseudophryne* and *Philoria* species); and (3) one of the major threats to frog species is disease, and pathogens may be transferred between individual frogs and between sites by people, representing a real risk to many frog species. For threatened frog species, or frog species with highly restricted distributions, revealing exact FrogID localities may therefore have serious, unintended negative consequences. Revealing exact localities for such species on private land may also result in trespassing (Lindenmayer and Scheele 2017).

We therefore follow ethical data publication guidelines (e.g., Chapman and Grafton 2008) and consider certain records as sensitive, thereby reducing geolocation accuracy in our publicly available dataset. We implement three geoprivacy options (Table 1) that take into account the state and national (DEE 2019) threat listings of the species, whether the species is range-restricted (i.e., has a geographic range or extent of occurrence of <20,000 km^2), and whether the record falls within the known geographic range of these species (Table 2; Suppl. material 1). Further, because we provide the user id, the call id, and the time of every submission, for any submission which included either an obscured or private species, all species recorded in that submission also received the higher geoprivacy options. This means, for example, that some records of common and 'open' species are obscured. A total of 1,504 records' coordinates for 74 species were therefore rounded to 0.1 degrees in this dataset. The complete dataset including sensitive information will be made available under licence to specific organisations and can be requested from the FrogID project.

Taxonomic coverage

Throughout the first year of the FrogID project, 179 species of six families and 23 genera were recorded and are represented in the database, accumulating to 55,003 biodiversity records. The top-six most recorded species were: *Crinia signifera* Girard, 1853, *Limnodynastes peronii* (Duméril & Bibron, 1841), *Litoria peronii* (Tschudi, 1838), *Litoria fallax* (Peters, 1880), *Limnodynastes tasmaniensis* Günther, 1858, and *Litoria ewingii* (Duméril & Bibron, 1841) (Fig. 1). The number of records per species varied considerably, with the six most commonly recorded species accounting for almost half of all records (Fig. 2).

The openly accessible published dataset – after applying our aforementioned rules on sensitive species and records – hosts 172 species of the 179. A total of 139 submissions of 11 species were deemed private (Table 1), and as such, these records are removed from the published dataset. The seven species recorded by the FrogID project in the first year, but not published here are as all records were allocated a private geoprivacy status are: *Cophixalus aenigma* Hoskin, 2004, *Cophixalus concinnus* Tyler, 1979, *Cophixalus hosmeri* Zweifel, 1985, *Cophixalus monticola* Richards, Dennis, Trenery & Werren, 1994, *Geocrinia alba* Wardell-Johnson & Roberts, 1989, *Geocrinia vitellina*

Table 1. Geoprivacy options, which dictate whether or not the exact latitude and longitude coordinates are provided in our published dataset.

Geoprivacy option	Action
Open	No buffering of coordinates.
Obscured	Decimal coordinates rounded to nearest 0.1 degree. Actual coordinates are available upon special request.
Private	Record is not included in our published dataset but is available upon special request.

Table 2. Associated frog species threat categories and associated geoprivacy options (Table 1).

| Frog species threat category	Geoprivacy
Not listed	Species is generally open, but may be obscured or private (if range-restricted or no confirmed recent records of the species).
Vulnerable	Species is generally open but may be obscured (with individual records outside of known range private), or private (if range-restricted or no confirmed recent records of the species).
Endangered	Species is generally obscured (with individual records outside of known range private) but may be private (if range-restricted or no confirmed recent records of the species).
Critically Endangered	Private.
Extinct	Private.
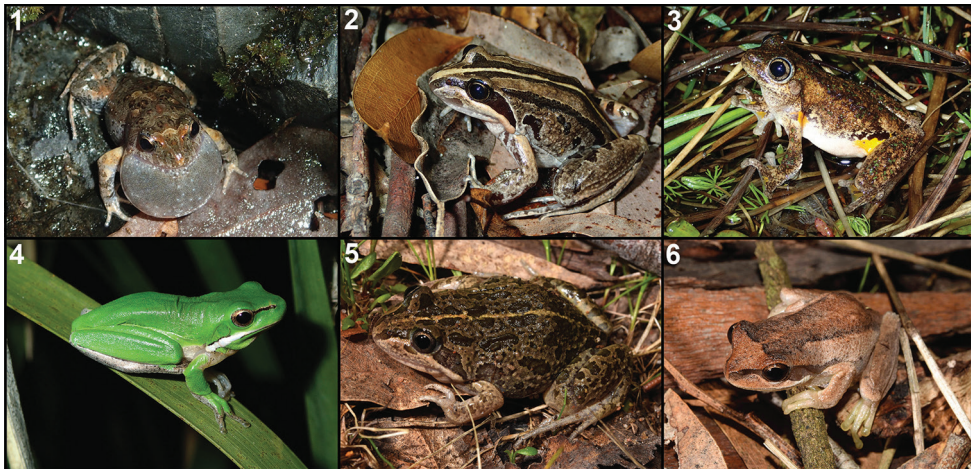
Figure 1. Photographs of the top six species recorded in the first year FrogID. **1** *Crinia signifera* **2** *Limnodynastes peronii* **3** *Litoria peronii* **4** *Litoria fallax* **5** *Limnodynastes tasmaniensis* **6** *Litoria ewingii*.

Wardell-Johnson & Roberts, 1989, and *Litoria myola* Hoskin, 2007. The published openly accessible dataset consists of 54,864 records.

The frog fauna of Australia remains incompletely known. The database will be updated on an ongoing process, incorporating taxonomic changes, including any new species described. Annual releases will reflect these changes. The date of each data release will be critical for users to track.
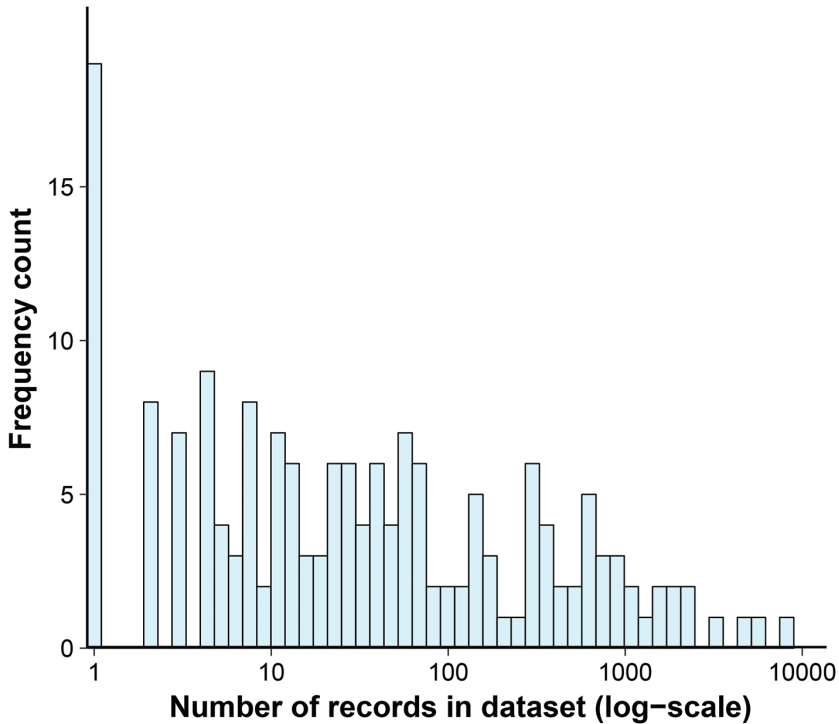
Figure 2. Frequency histogram for the 172 species published in our openly accessible dataset, showing the number of records (on a log-scale) and how many species have that associated number of records.

Taxonomic ranks

Kingdom: Animal
Phylum: Chordata
Class: Amphibia
Order: Anura
Families: Bufonidae, Limnodynastidae, Microhylidae, Myobatrachidae, Pelodryadidae, Ranidae
Genera: *Adelotus, Assa, Austrochaperina, Cophixalus, Crinia, Cyclorana, Geocrinia, Heleioporus, Lechriodus, Limnodynastes, Litoria, Metacrinia, Mixophyes, Myobatrachus, Neobatrachus, Notaden, Papurana, Paracrinia, Philoria, Platyplectrum, Pseudophryne, Rhinella, Uperoleia*
Species: *Adelotus brevis, Assa darlingtoni, Austrochaperina adelphe, Austrochaperina fryi, Austrochaperina gracilipes, Austrochaperina pluvialis, Austrochaperina robusta, Cophixalus australis, Cophixalus bombiens, Cophixalus infacetus, Cophixalus ornatus, Cophixalus saxatilis, Crinia bilingua, Crinia deserticola, Crinia flindersensis, Crinia georgiana, Crinia glauerti, Crinia insignifera, Crinia parinsignifera, Crinia pseudinsignifera, Crinia remota, Crinia signifera, Crinia sloanei, Crinia subinsignifera, Crinia tasmaniensis, Crinia tinnula, Cyclorana alboguttata, Cyclorana australis, Cyclorana brevipes,*

Cyclorana cultripes, Cyclorana longipes, Cyclorana maculosa, Cyclorana maini, Cyclorana novaehollandiae, Cyclorana occidentalis, Cyclorana platycephala, Cyclorana verrucosa, Geocrinia laevis, Geocrinia leai, Geocrinia rosea, Geocrinia victoriana, Heleioporus albopunctatus, Heleioporus australiacus, Heleioporus barycragus, Heleioporus eyrei, Heleioporus inornatus, Heleioporus psammophilus, Lechriodus fletcheri, Limnodynastes convexiusculus, Limnodynastes depressus, Limnodynastes dorsalis, Limnodynastes dumerilii, Limnodynastes fletcheri, Limnodynastes interioris, Limnodynastes peronii, Limnodynastes salmini, Limnodynastes tasmaniensis, Limnodynastes terraereginae, Litoria adelaidensis, Litoria aurea, Litoria barringtonensis, Litoria bicolor, Litoria brevipalmata, Litoria burrowsae, Litoria caerulea, Litoria chloris, Litoria citropa, Litoria cooloolensis, Litoria coplandi, Litoria cyclorhyncha, Litoria daviesae, Litoria dayi, Litoria dentata, Litoria electrica, Litoria eucnemis, Litoria ewingii, Litoria fallax, Litoria freycineti, Litoria gilleni, Litoria gracilenta, Litoria inermis, Litoria infrafrenata, Litoria jervisiensis, Litoria jungguy, Litoria latopalmata, Litoria lesueuri, Litoria littlejohni, Litoria meiriana, Litoria microbelos, Litoria moorei, Litoria nasuta, Litoria nigrofrenata, Litoria nudidigitus, Litoria olongburensis, Litoria pallida, Litoria paraewingi, Litoria pearsoniana, Litoria peronii, Litoria personata, Litoria phyllochroa, Litoria raniformis, Litoria revelata, Litoria rheocola, Litoria rothii, Litoria rubella, Litoria serrata, Litoria subglandulosa, Litoria tornieri, Litoria tyleri, Litoria verreauxii, Litoria watjulumensis, Litoria wilcoxii, Litoria xanthomera, Metacrinia nichollsi, Mixophyes balbus, Mixophyes carbinensis, Mixophyes coggeri, Mixophyes fasciolatus, Mixophyes fleayi, Mixophyes iteratus, Mixophyes schevilli, Myobatrachus gouldii, Neobatrachus aquilonius, Neobatrachus kunapalari, Neobatrachus pelobatoides, Neobatrachus pictus, Neobatrachus sudellae, Neobatrachus sutor, Neobatrachus wilsmorei, Notaden bennettii, Notaden melanoscaphus, Notaden nichollsi, Papurana daemeli, Paracrinia haswelli, Philoria kundagungan, Philoria loveridgei, Philoria pughi, Philoria richmondensis, Philoria sphagnicola, Platyplectrum ornatum, Platyplectrum spenceri, Pseudophryne australis, Pseudophryne bibronii, Pseudophryne coriacea, Pseudophryne dendyi, Pseudophryne douglasi, Pseudophryne guentheri, Pseudophryne major, Pseudophryne occidentalis, Pseudophryne raveni, Pseudophryne semimarmorata, Rhinella marina, Uperoleia altissima, Uperoleia arenicola, Uperoleia aspera, Uperoleia borealis, Uperoleia crassa, Uperoleia daviesae, Uperoleia fusca, Uperoleia inundata, Uperoleia laevigata, Uperoleia lithomoda, Uperoleia littlejohni, Uperoleia mahonyi, Uperoleia mimula, Uperoleia minima, Uperoleia mjobergii, Uperoleia rugosa, Uperoleia saxatilis, Uperoleia talpa, Uperoleia trachyderma, Uperoleia tyleri.

Methods

Spatial coverage: FrogID submissions have come from across Australia but, not surprisingly, are biased towards populated areas, with large areas of Australia, particularly in remote areas, lacking FrogID records. Despite this bias, the spatial coverage of this project encompasses the continent of Australia (Fig. 3), with frog records from 7,635,905 km² (99%) of Australia's landmass (measured as a minimum convex polygon enclosing all occurrences, excluding ocean).
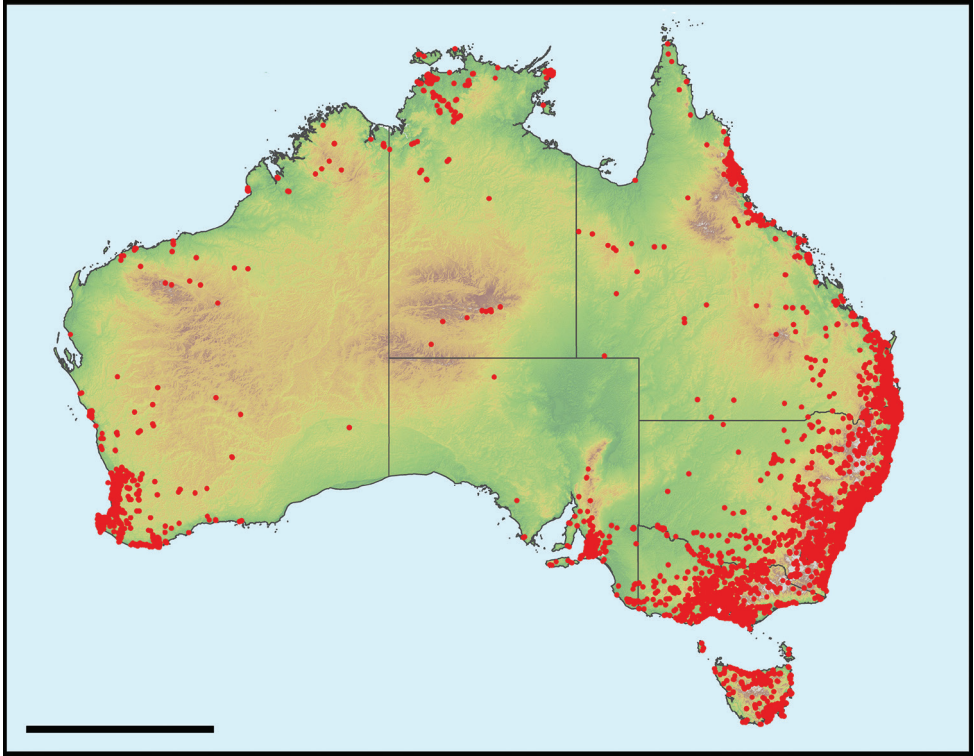
Figure 3. Occurrence records of calling frogs across Australia during year 1 of the FrogID project.

Temporal coverage: FrogID is an ongoing data collection project, and this dataset (version 1.0) makes the first year of data collection available, 10 November 2017–9 November 2018. Data was exported from the FrogID database on 14 January 2020. We anticipate releasing an updated dataset annually.

Validated frog records: FrogID collects data via a free smartphone app (iOS and Android). Recordings are 20–60 seconds in MPEG AAC audio (mp4a) files. The time, date, and geographic location (latitude, longitude, and an estimate of precision of geographic location) are automatically added by the app at the time of recording. Each recording has an estimate of precision and, depending on the question, these records may influence results. As such, for records that rely heavily on geographic precision, we recommend filtering to records which have an estimate of geographic uncertainty of <3000 m. After recordings are submitted, they are stored in a cloud-based Content Management System (CMS), before being validated. FrogID validators, experts in identifying frog species by their calls, then use the audio and associated information, plus a reference call library, to identify the frog species calling in the recording. One submission can have multiple frog species calling within it. After these processes, we are left with a presence-only dataset of frog species in Australia. For a more detailed overview of methodology and design aspects, see Rowley et al. (2019).

Dataset description

Dataset specifications

Object name: FrogID dataset
Character encoding: UTF-8
Format name: Darwin Core Archive Format
Format version: 1.0
Distribution: https://doi.org/10.15468/wazqft; https://zenodo.org/record/3612700
Publication date of data: 22 January 2020
Language: English
Licenses of use: Creative Commons Attribution (CC-BY) 4.0 License
Metadata language: English
Date of metadata creation: 19 January 2020
Hierarchy level: Dataset

Dataset description

The dataset includes basic biodiversity occurrence data, with Darwin Core terms (http://rs.tdwg.org/dwc/terms/), and is summarized in Table 3.

Table 3. Description of the data fields.

Data field	Description
datasetName	FrogID
basisOfRecord	Occurrence
dataGeneralizations	Highlights the geoprivacy options that were implemented
occurrenceID	Unique ID for each record in the dataset
sex	Male frogs are being recorded
lifestage	Adult frogs are recorded in FrogID
behavior	Only calling frogs are entered into the FrogID database
samplingProtocol	Call recording
country	Australia
machineObservation	An occurrence record based on an audio recording
eventID	Refers to the submission id – one submission can have more than one record
decimalLatitude	Latitude
decimalLongitude	Longitude
scientificName	Species name (*Genus species*).
eventDate	Date in year-month-day format
eventTime	Time the recording was taken
coordinateUncertaintyInMeters	A measure of the gps accuracy, measured in meters. See notes in methods
geoprivacy	Indicates whether the record is included and/or coordinates are buffered
recordedBy	Unique user id
stateProvince	Australian state of the record
modified	The date the record was last updated: useful for updating taxonomy or correcting errors in future dataset uploads

Discussion

The FrogID database of expert-validated records of frogs across Australia represents a significant and growing contribution to our understanding of frogs in Australia. The first year of FrogID has resulted in the collection of over 55,000 expert-validated records of frogs across Australia. As frogs call almost exclusively from breeding sites, localities of calling frogs also provide vital information on their breeding habitats and times.

FrogID data provides a valuable resource aimed to help enhance our knowledge of frog distribution and occurrence in Australia. So far, the data have (1) shown new knowledge of distribution and breeding seasons for several species, (2) detected native frogs outside their native range, likely transported by humans, (3) collected data on invasive Cane Toads (*Rhinella marina*) in Australia, (4) and detected breeding populations of rare and threatened species (Rowley et al. 2019). We hope that by making these data available, researchers will capitalize on this unique dataset. There are growing statistical techniques to model presence-only data (Pearce and Boyce 2006), making it possible to assess species distribution models, phenology, diversity, and potentially abundance (Soroye et al. 2018) as statistical techniques relating to citizen science data continue to be developed.

Acknowledgements

References

Blair WF (1964) Isolating mechanisms and interspecies interactions in anuran amphibians. Quarterly Review of Biology 39: 334–344. https://doi.org/10.1086/404324

Callaghan CT, Rowley JJL, Cornwell WK, Poore AGB, Major RE (2019) Improving big citizen science data: moving beyond haphazard sampling. PLoS Biology 17(6): e3000357. https://doi.org/10.1371/journal.pbio.3000357

Chapman AD, Grafton O (2008) Guide to Best Practices for Generalising Sensitive Species-Occurrence Data, version 1.0. Global Biodiversity Information Facility, Copenhagen, 27 pp. https://doi.org/10.25607/OBP-168

Costello MJ, Michener WK, Gahegan M, Zhang Z, Bourne PE (2013) Biodiversity data should be published, cited, and peer reviewed. Trends in Ecology & Evolution 28 (8): 454–461. https://doi.org/10.1016/j.tree.2013.05.002

DEE [Department of the Environment and Energy] (2019) Environment Protection and Biodiversity Conservation Act 1999 List of Threatened Fauna. http://www.environment.gov.au/cgi-bin/sprat/public/publicthreatenedlist.pl [Accessed on: 2019-10-1]

Dickinson JL, Shirk J, Bonter D, Bonney R, Crain RL, Martin J, Phillips T, Purcell K (2012) The current state of citizen science as a tool for ecological research and public engagement. Frontiers in Ecology and the Environment 10: 291–297. https://doi.org/10.1890/110236

Domroese MC, Johnson EA (2017) Why watch bees? Motivations of citizen science volunteers in the Great Pollinator Project. Biological Conservation 208: 40–47. https://doi.org/10.1016/j.biocon.2016.08.020

Donnellan SC, Mahony MJ (2004) Allozyme, chromosomal and morphological variability in the *Litoria lesueuri* species group (Anura: Hylidae), including a description of a new species. Australian Journal of Zoology 52: 1–28. https://doi.org/10.1071/ZO02069

Goyes Vallejos J, Grafe TU, Ahmad Sah HH, Wells K (2017) Calling behavior of males and females of a Bornean frog with male parental care and possible sex-role reversal. Behavioural Ecology and Sociobiology 71: 95. https://doi.org/10.1007/s00265-017-2323-3

Heyer R, Donnelly MA, Foster M, McDiarmid R (2014) Measuring and Monitoring Biological Diversity: Standard Methods for Amphibians. Smithsonian Institution Press, Washington.

Hopkins WA (2007) Amphibians as models for studying environmental change. ILAR Journal 48: 270–277. https://doi.org/10.1093/ilar.48.3.270

Hoskin CJ (2007) Description, biology and conservation of a new species of Australian tree frog (Amphibia: Anura: Hylidae: *Litoria*) and an assessment of the remaining populations of *Litoria genimaculata* Horst, 1883: systematic and conservation implications of an unusual speciation event. Biological Journal of the Linnean Society 91: 549–563. https://doi.org/10.1111/j.1095-8312.2007.00805.x

iNaturalist.org (2018) iNaturalist Research-grade Observations. Occurrence Dataset.

IUCN (2019) The IUCN Red List of Threatened Species. Version 2019-2. http://www.iucn-redlist.org [Accessed on: 2019-7-18]

Köhler J, Jansen M, Rodríguez A, Kok PJR, Toledo LF, Emmrich M, Glaw F, Haddad CFB, Rödel MO, Vences M (2017) The use of bioacoustics in anuran taxonomy: theory, terminology, methods and recommendations for best practice. Zootaxa 4251: 1–124. https://doi.org/10.11646/zootaxa.4251.1.1

Lemckert F, Penman T (2012) Climate change and Australia's frogs: how much do we need to worry? In: Lunney D, Hutching P (Eds) Wildlife and Climate Change: Towards Robust Conservation Strategies for Australian Fauna. Royal Zoological Society of NSW, Mosman, Australia, 92–98. https://doi.org/10.7882/FS.2012.015

Lindenmayer DB, Gibbons P, Bourke M, Burgman M, Dickman CR, Ferrier S, Fitzsimons J, Freudenberger D, Garnett ST, Groves C, Hobbs RJ, Kingsford RT, Krebs C, Legge S, Lowe AJ, McLean R, Montambault J, Possingham H, Radford J, Robinson D, Smallbone L, Thomas D, Varcoe T, Vardon M, Wardle G, Woinarski J, Zerger A (2012) Improving biodiversity monitoring. Austral Ecology 37(3): 285–294. https://doi.org/10.1111/j.1442-9993.2011.02314.x

Lindenmayer D, Scheele B (2017) Do not publish. Science 356: 800–801. https://doi.org/10.1126/science.aan1362

Littlejohn MJ (1969) The systematic significance of isolating mechanisms. In: National Research Council (Ed.) Systematic Biology: Proceedings of an International Conference. National Academies Press, Washington, DC, 459–482. https://doi.org/10.17226/21293

Marshall NJ, Kleine DA, Dean AJ (2012) CoralWatch: education, monitoring, and sustainability through citizen science. Frontiers in Ecology and the Environment 10(6): 332–334. https://doi.org/10.1890/110266

Michener WK (2015) Ecological data sharing. Ecological Informatics 29(1) 33–44. https://doi.org/10.1016/j.ecoinf.2015.06.010

Noss RF (1990) Indicators for monitoring biodiversity: A hierarchical approach. Conservation Biology 4(4): 355–364. https://doi.org/10.1111/j.1523-1739.1990.tb00309.x

Pearce JL, Boyce MS (2006) Modelling distribution and abundance with presence-only data. Journal of Applied Ecology 43(3): 405–412. https://doi.org/10.1111/j.1365-2664.2005.01112.x

Pengilley RK (1971) Calling and associated behaviour of some species of *Pseudophryne* (Anura: Leptodactylidae). Journal of Zoology 163: 73–92. https://doi.org/10.1111/j.1469-7998.1971.tb04525.x

Pereira HM, Cooper DH (2006) Towards the global monitoring of biodiversity change. Trends in Ecology & Evolution 21(3): 123–129. https://doi.org/10.1016/j.tree.2005.10.015

Pike DA, Croak BM, Webb JK, Shine R (2010) Subtle – but easily reversible – anthropogenic disturbance seriously degrades habitat quality for rock-dwelling reptiles. Animal Conservation 13: 411–418. https://doi.org/10.1111/j.1469-1795.2010.00356.x

Pocock MJO, Chandler M, Bonney R, Thornhill I, Albin A, August T, Bachman S, Brown PMJ, Cunha DGF, Grez A, Jackson C, Peters M, Rabarijaon NR, Roy HE, Zaviezo T, Danielsen F (2018) A vision for global biodiversity monitoring with citizen science. Advances in Ecological Research 59: 169–223. https://doi.org/10.1016/bs.aecr.2018.06.003

Rowley JJL, Callaghan CT, Cutajar T, Portway C, Potter K, Mahony S, Trembath DF, Flemons P, Woods A (2019) FrogID: citizen scientists provide validated biodiversity data on frogs of Australia. Herpetological Conservation and Biology 14: 155–170.

Rowley JJL, Tran DT, Le TTD, Dau VQ, Peloso PL, Nguyen TQ, Hoang HD, Nguyen TT, Ziegler T (2016) Five new, microendemic Asian leaf-litter frogs (*Leptolalax*) from the southern Annamite mountains, Vietnam. Zootaxa 4085: 63–102. https://doi.org/10.11646/zootaxa.4085.1.3

Silvertown J (2009) A new dawn for citizen science. Trends in Ecology & Evolution 24: 467–471. https://doi.org/10.1016/j.tree.2009.03.017

Soroye P, Ahmed N, Kerr JT (2018) Opportunistic citizen science data transform understanding of species distributions, phenology, and diversity gradients for global change research. Global Change Biology 24(11): 5281–5291. https://doi.org/10.1111/gcb.14358

Stuart SN, Chanson JS, Cox NA, Young BE, Rodrigues AS, Fischman DL, Waller RW (2004) Status and trends of amphibian declines and extinctions worldwide. Science 306: 1783–1786. https://doi.org/10.1126/science.1103538

Stuart BL, Rhodin AGJ, Grismer LL, Hansel T (2006) Scientific description can imperil species. Science 312: 1137. https://doi.org/10.1126/science.312.5777.1137b

Sullivan BL, Wood CL, Iliff MJ, Bonney RE, Fink D, Kelling S (2009) eBird: a citizen-based bird observation network in the biological sciences. Biological Conservation 142(10): 2282–2292. https://doi.org/10.1016/j.biocon.2009.05.006

Tulloch AI, Auerbach N, Avery-Gomm S, Bayraktarov E, Butt N, Dickman CR, Ehmke G, Fisher DO, Grantham H, Holden MH, Lavery TH (2018) A decision tree for assessing the risks and benefits of publishing biodiversity data. Nature Ecology & Evolution 2: 1209. https://doi.org/10.1038/s41559-018-0608-1

Vianna GMS, Meekan MG, Bornovski TH, Meeuwig JJ (2014) Acoustic telemetry validated a citizen science approach for monitoring sharks on coral reefs. PLoS One 9(4): e95565. https://doi.org/10.1371/journal.pone.0095565

Whiles MR, Hall RO, Dodds WK, Verburg P, Huryn AD, Pringle CM, Lips KR, Kilham SS, Colon-Gaud C, Rugenski AT, Peterson S (2013) Disease-driven amphibian declines alter ecosystem processes in a tropical stream. Ecosystems 16: 146–157. https://doi.org/10.1007/s10021-012-9602-7

Supplementary material 1

The 241 frog species known from Australia (including the introduced Cane Toad), taxonomic authority and geoprivacy category used

Authors: Jodi J. L. Rowley, Corey T. Callaghan

Data type: Species data

Link: https://doi.org/10.3897/zookeys.912.38253.suppl1

CORRIGENDA

ZooKeys
A peer-reviewed open-access journal
Launched to accelerate biodiversity research

Corrigendum: A new genus and species of Staphylininae rove beetle from the Peruvian Amazon (Coleoptera, Staphylinidae). https://doi.org/10.3897/zookeys.904.48592

Josh Jenkins Shaw[1], Igor Orlov[2], Alexey Solodovnikov[2]

1 *Institute of Zoology, Chinese Academy of Sciences, Beijing, China* **2** *Natural History Museum of Denmark, Copenhagen, Denmark*

Corresponding author: *Josh Jenkins Shaw* (joshjenkins@btinternet.com)

Citation: Jenkins Shaw J, Orlov I, Solodovnikov A (2020) Corrigendum: A new genus and species of Staphylininae rove beetle from the Peruvian Amazon (Coleoptera, Staphylinidae). https://doi.org/10.3897/zookeys.904.48592. ZooKeys 912: 153–153. https://doi.org/10.3897/zookeys.912.50592

In a recent paper (Jenkins Shaw et al. 2020) we stated that the holotype of *Amazonothops aslaki* would be deposited in the Natural History Museum of Denmark (NHMD). According to the conditions of the permit RDG 0328-2017-SERFOR-DGGSPFFS/ RDG 356-2017-SERFOR-DGGSPFFS, the holotype and one paratype (SEM coated male with same data as holotype but from 4°53.210'S, 73°38.921'W, 7–10.IX.2017, rainforest, FIT near creek (PER 17-22l) of *Amazonothops aslaki* described in Jenkins Shaw et al. (2020) were sent for the permanent deposition to the Museo de Historia Natural de la Universidad Nacional Mayor de San Marcos in Peru (MHN-UNMSM).

References

Jenkins Shaw J, Orlov I, Solodovnikov A (2020) A new genus and species of Staphylininae rove beetle from the Peruvian Amazon (Coleoptera, Staphylinidae). ZooKeys 904: 103–115. https://doi.org/10.3897/zookeys.904.48592